

UNIVERSITY OF SOUTHERN QUEENSLAND

Faculty of Engineering and Surveying



**Modelling the Change in Conductivity of Soil Associated
with the Application of Saline –Sodic Water**

A dissertation submitted by

YOUNES DAW EZLIT

BSc. (Hons)

M.Sc. (Hons)

FOR THE AWARD OF

DOCTOR OF PHILOSOPHY

2009

I dedicate this work to my mother Fatima, my brothers Ali, Abdol-Fattah, Nor-Addhin, sisters Salmeen, Mabroka, Amal, my wife Safia, my children Hibba, Joud-Addhin, Juriya, and to the spirits of my father Daw and my best friend Abdu-Razaq.

YOUNES DAW ZIDE EMBARAK EZLIT

USQ, Queensland, Australia, 2009-07-02

Abstract

Scarcity of fresh water has led to use of low quality waters (high sodicity and salinity) that were considered unsuitable for irrigation in the past. Mismanagement of irrigation using this water can increase the potential for soil degradation and limit crop production in the long term. Irrigation using highly saline-sodic water requires appropriate management to avoid long term development of sodicity and salinity problems. The main factors that control the sodicity and salinity problems are maintenance of sufficient leaching and avoidance of soil structure degradation due to sodicity. The management options are determined by complex factors such as soil type and condition, water quality, irrigation practice and crop type.

Investigating the management options for using highly saline-sodic water in irrigation experimentally is costly and time consuming. However, it could be done using an appropriate modelling tool that can handle the degradation of soil structure due to sodicity along with the chemical reaction system within the soil profile. UNSATCHEM has been widely used to model sodicity and salinity effects under irrigation. It has a feature to deal with soil structure degradation along with water and solute movement, major ion chemistry, CO₂ production and movement and heat transfer under sodic conditions. It uses a hydraulic conductivity reduction function to relate the change of chemical properties to the change in hydraulic properties of the soil. However, the evaluation of the hydraulic conductivity reduction function under high sodicity during simulation has not been done. Hence, the core of this research project has been to improve quantification of soil structure degradation under sodic conditions and enhance the modelling of water and solute movement under sodic conditions. The hydraulic conductivity reduction function incorporated in UNSATCHEM was evaluated using data obtained from soil column experiments.

Columns of two local soils were used in an experiment to investigate the effect on soil structural stability of different amendments to highly saline-sodic water rich with bicarbonates (EC = 4.6 dS/m and SAR = 117). The column experiments were used to examine the effect of reducing water pH to different levels using sulphuric acid and combined gypsum and dilution treatments. It was found that reducing the pH of highly saline-sodic water did not enhance soil structural stability as the water applied has

naturally high relative sodium concentrations. However, the application of diluted highly saline-sodic water amended with gypsum showed no significant effect on soil structure and permeability. It is concluded that different amendments associated with appropriate irrigation management can be applied to sustain irrigation and prevent long term salinity and sodicity problems.

The data from the column experiments was used to evaluate the quantification of the soil structure degradation in UNSATCHEM. The resultant simulations for the soil columns showed that the estimated outflow and hydraulic conductivity were less than the experimental measurements, which suggested that the soil structure degradation was not accounted for properly. The sodicity effect was accounted for in UNSATCHEM by a reduction function, which is a combined function of the McNeal (1968) clay swelling model and the Simunek et al. (1996) pH effect equations. The empirical pH effect equation accounts for the reduction of the conductivity due to increasing pH and clay swelling. The evaluation of UNSATCHEM under highly sodic conditions suggests that the hydraulic conductivity reduction function is limiting the UNSATCHEM performance.

Consideration of the first term of the hydraulic conductivity reduction function (i.e. the McNeal (1968) clay swelling model) has highlighted the weaknesses of the McNeal model and led to develop a generic clay swelling model (GCSM). Calibration of the GCSM using the data of McNeal showed good agreement between the estimated and measured relative conductivity data. Further calibration of the GCSM using relative conductivity data obtained for five local soils also showed good agreement between the model estimation and the measured data.

Coding of the generic clay swelling model into UNSATCHEM and re-simulating the column experiments showed that the modelling process is improved compared with the UNSATCHEM version containing the McNeal (1968) clay swelling model. However, the outflow and conductivity values produced were still less than measured values. This result suggested that further investigations are required to identify the effect of pH on the change of hydraulic conductivity, cation exchange capacity, and the exchangeable sodium percentage. Further research is also required regarding bicarbonate chemistry during application of highly saline-sodic water.

Certification of Dissertation

I certify that the ideas, experimental work, analyses, results, and conclusions reported in this dissertation are my own work, except where otherwise specified. I further certify that this work is original and has not been previously submitted for any another award, except where otherwise acknowledged.

Endorsement:

_____	_____
Younes Daw Ezlit, candidate	Date
_____	_____
Professor Rod Smith, Principal supervisor	Date
_____	_____
Professor Steven Raine, Co- Supervisor	Date

Acknowledgment

This research has been completed with the support and assistance of a large number of people. I wish to express my gratitude to some of those who have helped and inspired me during my candidature.

Firstly, my sincere thanks to my supervisors and mentors Prof. Rod Smith and Prof. Steven Raine for their guidance and patience during my study. I sincerely thank them for their encouragement, expert advice, technical assistance and patience. Their effort in creating an active and inclusive research environment is appreciated.

I wish to greatly acknowledge the support of Al-Fateh University and Libyan Arab Jamahiriya government, for the full scholarship funding and the CRC for Irrigation Futures for providing additional funding to support operation costs associated with the research.

A special thanks to the CRCIF staff for their support during my study, I am grateful to Dr. Richard Stirzaker and Dr. Tapas Biswas for their valuable discussions and advice and to Dr. Malcolm Gillies for his help in the MATLAB programming. I also appreciate the support provided by Prof. Jirka Simunek at the University of California, Riverside for his valuable advice and support with the modelling aspects of this research. I also thank the staff at the NCEA at USQ for their support during the experimental work of this study.

I am grateful also to the lovely staff in the Faculty of Engineering and Surveying, USQ. I consider them my wonderful family in Australia. Also, a special thanks to my friends and colleagues at USQ especially Dev Raj Paudyal for their support and encouragement.

Finally I would like to thank my family and friends in Libya for their continued support and encouragement throughout my studies. To my family, my mother Fatima, my brothers and sisters, my wife, my friends, and my little Hibba I say *“my name is written on the first page but your names are written on every page because there was no one moment of this journey you were not with me”*.

Table of Contents

Abstract	I
Certification of Dissertation.....	III
Acknowledgment	IV
Table of Contents	V
List of Figures	X
List of Tables.....	XVI
List of Symbols	XVIII
List of Abbreviations.....	XXIII
CHAPTER 1: Introduction.....	1
1.1 Background	1
1.1.1 Salinity and sodicity problems in irrigation	1
1.1.2 Sodicity and salinity control	5
1.1.3 Sodicity and salinity management options	6
1.1.4 Modelling the effect of sodicity and salinity in irrigation	7
1.1.5 Conclusion	9
1.2 Overview of research	10
1.2.1 Research hypotheses	10
1.2.2 Specific objectives of research	10
1.3 Structure of dissertation	11
CHAPTER 2: Review of Salinity and Sodicity under Irrigation	12
2.1 Introduction	12
2.2 Salts in the root zone	12
2.2.1 Salinity.....	12
2.2.2 Sodicity	16
2.2.3 Relationships between SAR and ESP.....	16
2.2.4 The distribution of salts within the root zone	20
2.2.5 Crop responses to saline conditions.....	21
2.2.6 Leaching of salts from the root zone	24
2.3 The effect of salinity and sodicity on soil and water movement.....	28
2.3.1 Clay minerals and dispersion.....	28
2.3.2 Clay dispersion and hydraulic conductivity	32

2.3.3 Factors affecting dispersion and hydraulic conductivity	35
2.3.4 Relationships between sodicity, salinity and saturated hydraulic conductivity	40
2.3.5 Quantifying the change in saturated hydraulic conductivity due to sodicity.....	46
2.3.6 Relationships between sodicity, salinity and unsaturated hydraulic conductivity	49
2.4 Sodicity management under irrigation water	53
2.5 Soil hydraulic changes due to sodicity in modelling water- solute movement.	56
2.6 Conclusions	57
CHAPTER 3: Long Column Laboratory Experiment to Evaluate the Change in Hydraulic Conductivity with the application of Saline-Sodic Water	59
3.1 Introduction	59
3.2 Materials and methods	59
3.2.1 Soil collection and preparation	59
3.2.2 Soil columns	61
3.2.3 Measurement of saturated hydraulic conductivity.....	62
3.2.4 Experimental design and water quality treatments.....	63
3.2.5 Data collection.....	65
3.2.6 Bulk density measurements	65
3.2.7 Soil-water characteristic curve determination	66
3.3 Results and discussion.....	67
3.3.1 Saturated hydraulic conductivity	67
3.3.2 Effect of saline-sodic water on selected soil physical properties	72
3.4 Conclusion.....	74
CHAPTER 4: Validation of the Hydraulic Reduction Function in the UNSATCHEM Model	75
4.1 Introduction	75
4.2 Overview of the UNSATCHEM model	76
4.3 Methodology	77
4.3.1 Soil hydraulic parameters	78
4.3.2 Dispersion coefficient and longitudinal dispersivity	79
4.3.3 Chemical reaction parameters	79

4.3.4 Operation of the UNSATCHEM model	80
4.3 Results	82
4.5 Discussion	95
4.6 Conclusion.....	98
CHAPTER 5: Development of a Generic Clay Swelling Model.....	99
5.1 Introduction	99
5.2 Review of the McNeal clay swelling model	100
5.2.1 Background.....	100
5.2.2 The McNeal approach	100
5.2.3 Later modification to the McNeal model	104
5.3 Assumptions underpinning the McNeal (1968) clay swelling model	106
5.3.1 Clay swelling distance calculation	106
5.3.2 Threshold levels in the clay swelling model	109
5.3.3 Swelling and dispersion in the clay swelling model.....	111
5.4 Evaluation of the McNeal (1968) model of clay swelling	112
5.4.1 Evaluation methodology.....	112
5.4.2 Results and discussion.....	113
5.5 Towards a generic clay swelling model	116
5.5.1 RK_{sat} data.....	116
5.5.2 Calculation of ESP_T	118
5.5.3 Effect of ESP_T on swelling factor and RK_{sat}	120
5.5.4 Determination of n and c functions	121
5.5.5 Structure of the generic clay swelling model	124
5.6 Calibration of the generic clay swelling model.....	125
5.6.1 Calibration methodology	125
5.6.2 Non-linear regression results and discussion.....	126
5.7 Conclusion.....	131
CHAPTER 6: Applicability of the Generic Clay Swelling Model for a Broader	
Range of Soils	132
6.1 Introduction	132
6.2 RK_{sat} data for the Sodosol and Vertosol soils.....	133
6.2.1 Sodosol and Vertosol soils characteristics.....	133
6.2.2 Experimental design	134

6.2.3 Saturated K_{sat} apparatus and soil packing.....	134
6.2.4 Water treatments.....	135
6.2.5 The RK_{sat} for different sodicity and salinity levels for the Sodosol and Vertosol soils	137
6.3 Red brown and Alluvial soils	140
6.3.1 Characterisation of the soils	140
6.3.2 RK_{sat} data	141
6.4 Evaluation of the GCSM using the non-linear regression analysis.....	143
6.5 Results and Discussion.....	143
6.6 Conclusion.....	155
CHAPTER 7: Evaluation of the UNSATCHEM with the Generic Clay Swelling Model Incorporated.....	
7.1 Introduction	156
7.2 Methodology	157
7.2.1 Incorporating the generic clay swelling model in the UNSATCHEM..	157
7.2.2 The UNSATCHEM parameters for the Sodosol and Vertosol soils	157
7.3 Results	158
7.4 Discussion	166
7.5 Conclusion.....	168
CHAPTER 8: Conclusion and Recommendations.....	
8.1 Introduction	169
8.2 Review of research	169
8.3 General conclusions	170
8.3.1 Characterise the soil structural degradation associated with the application of highly saline and sodic water	170
8.3.2 Evaluation of modelling water and solute movement within soil profile under sodic conditions and diagnosis of the limitations.....	171
8.3.3 Evaluation of McNeal (1968) model and proposing a new generic form....	172
8.3.4 Improved modelling of water and solute movement within soil profiles under sodic conditions and diagnosis of the problem.....	172
8.4 Recommendations and further research	173
List of References	174
Appendix A: Standard Chemical Analysis for HSS Water.....	190
Appendix B: Data Obtained From Long Columns Experiments	191

B.1 Introduction	191
B.2 Part I: Sodosol columns experiment results	194
B.3 Part II: Vertosol columns experiment results	216
Appendix C: the UNSATCHEM Sub-Models	241
Appendix D: Determination of the Dispersivity Coefficient and Longitudinal Dispersivity for the Sodosol and Vertosol Soils	252
Appendix E: Evaluation of the SAR-ESP Relationship and Calculating the Gapon Selectivity Coefficients Values for the Sodosol and Vertosol	255
Appendix F: The MATLAB Code to Demonstrate the Three Surface of McNeal (1968) Function	265
Appendix G: Calibration of the Generic Clay Swelling Model Using the Non-linear Regression (TableCurve 3D package)	267
G.1 The McNeal et al. (1968) RK_{sat} Data	267
G.2. The Sodosol, Vertosols, Red brown, and Alluvial soils	270
Appendix H: Results of Non-linear Regression for Soils (a), (b), and (c) from McNeal et al. (1968)	271
Appendix I: Calculations of EC and SAR for the Standard Solutions Used in Soil Stability Indicator Experiments	277
Appendix J: The Results of Non-linear Regression for Local Soils	278
Appendix K: The new GCSM Function Code Incorporated Manually into UNSATCHEM	288

List of Figures

Figure 1.1 Development of soil problems under saline-sodic conditions.....	4
Figure 2.1 Comparison of different SAR- ESP relationships published in literature as presented in Qadir and Schubert (2002) at wide range of SAR (0-169) for different type of soils	19
Figure 2.2 Root zone salt distribution under different irrigation systems.....	20
Figure 2.3 Effects of salinity and sodicity on plants.....	22
Figure 2.4 Basic molecular and structural components of silicate clays	29
Figure 2.5 A simple 3-plane model to describe the arrangement of clay crystals in a clay domain.....	31
Figure 2.6 Change of suction head produced by leaching a column of soil dominated by Montmorillonite (15% clay, ESP =30) with 0.01N, SAR 30 solution and pure water added.....	34
Figure 2.7 Variation in charge with pH and electrolyte concentration of the ambient solution for permanent, variable and mixed charge systems.....	38
Figure 2.8 Relationship between soil pH at saturated paste and ESP of Alluvial alkali soil.....	39
Figure 2.9 The general guideline adopted for relative infiltration as affected by salinity and sodium adsorption ratio.....	41
Figure 2.10 Concentration of electrolyte required to maintain permeability (10-15% reduction) in Sawyers I soil for varying degrees of sodium saturation	43
Figure 2.11 Combinations of salt concentration and SAR at which a 25% reduction in hydraulic conductivity occurred	45
Figure 2.12 Combinations of salt concentration and ESP at which a 25% reduction in hydraulic conductivity occurred	45
Figure 2.13 Relative hydraulic conductivity of the soil as a function of solution concentration and composition (solution concentration > 0.01N)	48
Figure 2.14 Soil-water suction head (h) as a function of volumetric soil-water content and solution concentration, for three SAR values (i.e. 0, 20, and 50) .	51
Figure 2.15 Unsaturated hydraulic conductivity values as a function of volumetric soil-water content and the solution concentrations for three values of SAR (i.e. 0, 20, and 50)	51

Figure 2.16 Solubility of gypsum in aqueous solutions of different NaCl concentrations at 25° C, and 1 atmospheric pressure	55
Figure 3.1 Diagram of system used to apply the water treatments and measure the saturated hydraulic conductivity (constant head method)	62
Figure 3.2 Change in pH for a saline-sodic water containing carbonates where the pH has previously been adjusted to either 5 or 7 using H ₂ SO ₄ acid.....	64
Figure 3.3 The positions of soil samples taken from the soil columns to determine the SWCC and bulk density after applying the water quality treatments.....	66
Figure 3.4 The change in K_{sat} with water applications for the Sodosol.....	68
Figure 3.5 The change in K_{sat} with water applications for the Vertosol.....	69
Figure 3.6 Changes in saturated hydraulic conductivity for the Sodosol when 0.4 dS/m water is applied following the application of 700 mm of the HSS water	70
Figure 3.7 Changes in saturated hydraulic conductivity for the Vertosol when 0.4 dS/m water is applied following the application of 700 mm of the HSS water	71
Figure 3.8 Average relationship between gravimetric water content and suction applied for the Sodosol samples treated with HSS water and normal tap water amended with gypsum	73
Figure 3.9 Average relationship between gravimetric water content and suction applied for the Vertosol samples treated with HSS water and normal tap water amended with gypsum	74
Figure 4.1 Sodicty-salinity effects in water and solute movement model (UNSATCHEM) under isothermic conditions	77
Figure 4.2 Comparison of measured and simulated outflow when HSS water applied for the Sodosol, (a) replicate 1, (b) replicate 2, and (c) replicate 3	83
Figure 4.3 Comparison of measured and simulated outflow for the Sodosol soil column when diluted HSS water amended with gypsum was applied	84
Figure 4.4 Simulated hydraulic conductivity with depth at different simulation time, for the Sodosol (a) replicate 1, (b) replicate 2, and (c) replicate 3	85
Figure 4.5 Example of the estimated change in SAR of the soil solution with depth at final time for the Sodosol soil (replicate 1)	86
Figure 4.6 Example of the estimated change in pH of the soil solution with depth at final time for the Sodosol soil (replicate 1)	86

Figure 4.7 Comparison of measured and simulated outflow for the Vertosol when HSS water applied (a) replicate 1, (b) replicate 2, and (c) replicate 3.....	87
Figure 4.8 Comparison of measured and simulated outflow for the Vertosol soil column when diluted HSS water amended with gypsum was applied	88
Figure 4.9 Simulated hydraulic conductivity with depth at different simulation time for the Vertosol (a) replicate 1, (b) replicate 2, and (c) replicate 3	89
Figure 4.10 Example of the estimated change in SAR of the soil solution with depth at final time for the Vertosol soil (replicate 1)	90
Figure 4.11 Example of the estimated change in pH of the soil solution with depth at final time for the Vertosol soil (replicate 1)	90
Figure 4.12 Comparison of measured and estimated saturated hydraulic conductivity for HSS water in the Sodosol (a) replicate 1, (b) replicate 2, and (c) replicate 3	92
Figure 4.13 Comparison of measured and estimated saturated hydraulic conductivity for the Sodosol (when diluted HSS water amended with gypsum was applied)	93
Figure 4.14 Comparison of measured and estimated saturated hydraulic conductivity for HSS water in the Vertosol (a) replicate 1, (b) replicate 2, and (c) replicate 3	94
Figure 4.15 Comparison of measured and estimated saturated hydraulic conductivity for the Vertosol when diluted HSS water amended with gypsum was applied	95
Figure 5.1 Graphical method for estimating the swelling factor as a function of ESP^* and salt concentration in soil-water	101
Figure 5.2 The effect of soil solution concentration on montmorillonite swelling ($ESP = 100\%$) as described by Norrish (1954).....	106
Figure 5.3 Lattice expansion up to 2 nm and more than 40 nm) of montmorillonite under two Na-solutions (i.e. \times NaCl, \circ Na_2SO_4 , and --- fitted line) with the square root of different concentrations	107
Figure 5.4 Demonstration of d^* equation under sodic condition ($ESP = 100\%$) and its adjustment as described by McNeal (1968).....	108
Figure 5.5 Three dimensional representation of the McNeal function (RK_{Sat} versus ESP and C_o)	113

Figure 5.6 Three dimensional plot of the McNeal function with RK_{Sat} limited to 100%	114
Figure 5.7 McNeal (1968) n values with ESP	115
Figure 5.8 McNeal (1968) c values with ESP	115
Figure 5.9 Change of ESP and electrolyte concentration at threshold level (i.e. $RK_{Sat} = 0.9$) for soil group (a) having clay content of 5.7%	118
Figure 5.10 Change of ESP and electrolyte concentration at threshold level (i.e. $RK_{Sat} = 0.9$) for soil group (b) having average clay content of 16.2%	119
Figure 5.11 Change of ESP and electrolyte concentration at threshold level (i.e. $RK_{Sat} = 0.9$) for soil group (c) having average clay content of 48.5 %	119
Figure 5.12 Proposed threshold level by McNeal (1968) compared with threshold levels at 10% RK_{Sat} reduction for three soils group obtained from McNeal et al. (1968)	120
Figure 5.13 Change of n parameter obtained (by best fit) with different levels of exchangeable sodium percentage (ESP) for soils group (b) of McNeal data (1968)	122
Figure 5.14 Change of n parameter obtained (by best fit) with different levels of exchangeable sodium percentage (ESP) for soils group (c) of McNeal data (1968)	122
Figure 5.15 Change of c parameter obtained (by best fit) with different levels of ESP for soils group (b) of McNeal data (1968)	123
Figure 5.16 Change of c parameter obtained (by best fit) with different levels of ESP for soils group (c) of McNeal et al. (1968) data	123
Figure 5.17 Three dimensional surface of best fit and the residuals of RK_{Sat} (i.e. between predicted and measured) for the for the group (a) soils	128
Figure 5.18 Three dimensional surface of best fit and the residuals of RK_{Sat} (i.e. between predicted and measured) for the group (b) soils	129
Figure 5.19 Three dimensional surface of best fit and the residuals of RK_{Sat} (i.e. between predicted and measured) for the group (c) soils	130
Figure 6.1 Electrolyte concentration and SAR of the water quality treatments applied to the Sodosol and Brown Vertosol	136

Figure 6.2 Electrolyte concentration and SAR of the water quality treatments applied to the Grey Vertosol.....	136
Figure 6.3 Three dimensional surface of best fit and the residuals of RK_{Sat} (i.e. between predicted and measured) for the Sodosol soil	146
Figure 6.4 Three dimensional surface of best fit and the residuals of RK_{Sat} (i.e. between predicted and measured) for the Brown Vertosol soil.....	147
Figure 6.5 Three dimensional surface of best fit and the residuals of RK_{Sat} (i.e. between predicted and measured) for the Grey Vertosol soil.....	148
Figure 6.6 Three dimensional surface of best fit and the residuals of RK_{Sat} (i.e. between predicted and measured) for the Red brown soil.....	149
Figure 6.7 Three dimensional surface of best fit and the residuals of RK_{Sat} (i.e. between predicted and measured) for the Alluvial soil	150
Figure 6.8 Change of RK_{Sat} with electrolyte concentration and SAR for the Sodosol as produced using the GCSM	152
Figure 6.9 Change of RK_{Sat} with electrolyte concentration and SAR for the Brown Vertosol as produced using the GCSM	152
Figure 6.10 Change of RK_{Sat} with electrolyte concentration and SAR for the Grey Vertosol as produced using the GCSM	153
Figure 6.11 Change of RK_{Sat} with electrolyte concentration and SAR for the Red brown soil as produced using the GCSM	153
Figure 6.12 Change of RK_{Sat} with electrolyte concentration and SAR for the Alluvial soil as produced using the GCSM	154
Figure 6.13 Change of RK_{Sat} with electrolyte concentration and SAR as produced from the McNeal (1968) clay swelling model using the parameters incorporated in the UNSATCHEM model for any soil.....	154
Figure 7.1 DOS window to enter the GCSM parameters into UNSATCHEM (i.e. HYDRUS 1D).....	157
Figure 7.2 The estimated outflow by the UNSATCHEM when the GCSM was used compared with the estimated outflow using the UNSATCHEM that incorporated the McNeal model for the Sodosol soil column during application of HSS water (a) replicate 1, (b) replicate (2), and (c) replicate 3	159

Figure 7.3 The estimated K_{sat} by the UNSATCHEM when the GCSM was used compared with the estimated K_{sat} produced using the UNSATCHEM that incorporated the McNeal model for the Sodosol soil column during application of the HSS water (a) replicate 1, (b) replicate (2), and (c) replicate 3.....	160
Figure 7.4 The estimated outflow by the UNSATCHEM when the GCSM was used compared with the estimated outflow using the UNSATCHEM that incorporated the McNeal model for the Sodosol soil column during application of diluted HSS water.....	161
Figure 7.5 The estimated K_{sat} by the UNSATCHEM when the GCSM was used compared with the estimated K_{sat} produced using the UNSATCHEM that incorporated the McNeal model for the Sodosol soil column during the applications of diluted HSS water	161
Figure 7.6 The estimated outflow by the UNSATCHEM when the GCSM was used compared with the estimated outflow using the UNSATCHEM that incorporated the McNeal model for the Vertosol soil columns during application of the HSS water (a) replicate 1, (b) replicate (2), and (c) replicate 3	163
Figure 7.7 The estimated K_{sat} by the UNSATCHEM when the GCSM was used compared with the estimated K_{sat} produced using the UNSATCHEM that incorporated the McNeal model for the Vertosol soil columns during application of the HSS water (a) replicate 1, (b) replicate (2), and (c) replicate 3	164
Figure 7.8 The estimated outflow by the UNSATCHEM when the GCSM was used compared with the estimated outflow using the UNSATCHEM that incorporated the McNeal model for the Vertosol soil column during application of diluted HSS water.....	165
Figure 7.9 The estimated K_{sat} by the UNSATCHEM when the GCSM was used compared with the estimated K_{sat} produced using the UNSATCHEM that incorporated the McNeal model for the Vertosol soil column during the applications of diluted HSS water	165

List of Tables

Table 3.1 Field description of the Vertosol soil profile	60
Table 3.2 Field description of the Sodosol soil profile	60
Table 3.3 Selected chemical properties for the soils used in the experiment	61
Table 3.4 Selected chemical properties of the highly saline-sodic (HSS) water	63
Table 3.5 The mean K_{sat} of the Sodosol and Vertosol soils after infiltrating 700 mm of the various water quality treatments.....	67
Table 3.6 The K_{sat} of the Sodosol and Vertosol when 0.4 and 0.1 dS/m water was applied after various HSS water pre-treatments	70
Table 3.7 Bulk density of the soil (5-10cm below surface) after application of either tap water amended with gypsum or HSS water.....	72
Table 4.1 van Genuchten (1980) hydraulic function parameters obtained for the Sodosol and Vertosol soils	79
Table 4.2 The UNSATCHEM input parameters for simulation of the HSS water and diluted HSS water amended with gypsum application for both the Sodosol and Vertosol soils	80
Table 5.1 Relative saturated hydraulic conductivity of Imperial Valley soils in the presence of mixed NaCl-CaCl ₂ solutions	117
Table 5.2 The n and c parameters obtained from non-linear regression analysis for soil groups (b) and (c) at different levels of ESP.....	121
Table 5.3. Summary of the surface fit output for three group of soils from McNeal (1968).....	127
Table 6.1 Selected chemical properties for the Grey Vertosol soil.....	133
Table 6.2 Saturated hydraulic conductivity RK_{sat} measurements for the Sodosol soil columns at different mixed NaCl-CaCl ₂ solutions with different electrolyte concentration.....	137
Table 6.3 Saturated hydraulic conductivity RK_{sat} measurements for the Brown Vertosol soil columns at different mixed NaCl-CaCl ₂ solutions with different electrolyte concentration.....	138

Table 6.4 Saturated hydraulic conductivity RK_{sat} measurements for the Grey Vertosol soil columns at different mixed NaCl-CaCl ₂ solutions with different electrolyte concentration.....	139
Table 6.5 Selected physical and chemical properties of the Alluvial and Red brown soils.....	140
Table 6.6 Relative saturated hydraulic conductivity of the Red brown soil for water quality treatments. Bulk density 1.22 g/cm ³	141
Table 6.7 Relative saturated hydraulic conductivity of the Alluvial soil for different water quality treatments. Bulk density 1.22 g/cm ³	142
Table 6.8 Summary of the GCSM surface fit output for the five soils	144

List of Symbols

a	empirical parameter in generic clay swelling model
\grave{a}	empirical parameter which is varying with different mixed solutions
a_i	fitted parameters
A0	parameters a in n function as defined in the user function in TableCurve program
A1	parameter b in n function as defined in the user function in TableCurve program
A2	parameter g in c function as defined in the user function in TableCurve program
A3	parameter m in c function as defined in the user function in TableCurve program
A4	parameter s for ESP_T function as defined in the user function in TableCurve program
A5	parameter l for ESP_T function as defined in the user function in TableCurve program
A6	parameter f
b	empirical parameter in generic clay swelling model
B	water flow geometry term
b_i	fitted parameters
b_z	proportion of applied water moving as bypass flow past z
c	empirical parameter in clay swelling model
C	an ion concentration in soil solution
c'	adjusted c parameter for different montmorillonite contents
\overline{C}	linearly averaged salt concentration of the root zone
C_o	salt or electrolyte concentration
\overline{C}_{Cl}	depth weighted mean soil-water chloride concentration at saturation above z
Ca_{CO_2}	volumetric concentration of CO_2 in the soil air
C_d	concentration in the drainage water
CEC	cation exchangeable capacity
C_{ir}	salt concentration in the irrigation water
C_{IW}	chloride concentration of soil-water at z
C_k	total dissolved concentration of the soil solution species k
\hat{C}_k	total solid phase concentration of aqueous component
\overline{C}_k	total surface species concentration of the aqueous component k
$Cp(\theta)$	volumetric heat capacities of the soil system
C_w	volumetric heat capacities of water

Cw_{CO_2}	CO ₂ concentration in soil solution
C_{ws}	an average salt concentration in the soil solution,
\overline{C}_z	chloride concentration of soil-water at z at field saturation water content,
\hat{d}	interlayer distance of the montmorillonite due to increasing of relative sodium concentration
D	dispersion coefficient
D_{ij}	generic component of the dispersion coefficient
d^*	adjusted interlayer spacing
D^*	distance between the montmorillonite platelets
D_a	diffusivity of the CO ₂ in soil air
D_d	depth of drained water
D_L	longitudinal dispersivity
D_{irr}	depth of irrigated water
dL	leaching rate
dV	increase of volume (expansion) within Smectite soils
D_{wCO_2}	CO ₂ diffusivity in soil solution
Dw	molecular diffusion coefficient in free water
EC_d	electrical conductivity of the drainage water
EC_{irr}	electrical conductivity of the irrigation water
ESP^*	adjusted ESP in McNeal clay swelling model
ESP_T	critical average ESP at which K_{sat} began to decline for given salinity
$ESP_{T\ Mont.}$	montmorillonite threshold of sodicity
EXN	adsorbed concentration of any cation
$EXCa^{2+}$	amounts of calcium involved in balancing the charge of the soil's exchange complex
$EXNa^+$	amounts of sodium involved in balancing the charge of the soil's exchange complex in units
f	empirical parameter related to weighted fraction of montmorillonite
f_{amount}	weight fraction of montmorillonite in the soil
$f(C_{O_2})$	reduction coefficient of oxygen (O ₂) gas concentration
$f(h)$	reduction coefficient of pressure head (soil-water content)
$f(h_\phi)$	reduction coefficient of osmotic effect
$f(T)$	temperature coefficient which could be more than one at temperature above 20°C

F_w	weighting function
f_z	proportion of flow at the concentration of the soil matrix
$f(z)$	reduction coefficient of the soil depth
G	water potential gradient from the soil to the root
g	empirical parameter in generic clay swelling model
H	soil-water potential
h	soil-water pressure head
h_0	osmotic potential
h_m	matric potential
h_r	root water potential
h_{rs}	water potential at the root- bulk soil solution interface
i_i	rate of irrigation water application
I_{ir}	depth of irrigation water
K	hydraulic conductivity
k''	linear adsorption coefficient
$K^!$	conductivity term (including the root and soil conductivities)
K_{CO2}	Henty law constant
K_G	Gapon selectivity coefficient
K_{Gij}	Gapon selectivity coefficient for species i and j
$K_{(h)}$	unsaturated hydraulic conductivity function
K_{ij}^A	generic component of the dimensionless anisotropy tensor for the unsaturated conductivity
K_r	root hydraulic conductivity
κ_s	empirical constant
K_{Sat}	saturated hydraulic conductivity
K_{Sat}^{Max}	maximum saturated hydraulic conductivity achieved when the soil is stable
K_{Unsat}	unsaturated hydraulic conductivity
l	empirical parameter, which depend on soil type and soil condition
L_f	leaching fraction
m	empirical parameter in generic clay swelling model
m_i	empirical parameter dependent on the soil type
m_i	an empirical parameter depends on the soil type

List of Symbols

n	empirical parameter
N_c	number of primary aqueous species
q_r	rate of root water uptake
q_{wj}	Darcy water flux density component in the i direction
$ q_w $	absolute value of the Darcian water flux density
q_w	Darcy water flux density
r	hydraulic conductivity reduction function
R_f	retardation factor
R	universal gas constant which is $8.314 \text{ (kg}\times\text{m}^2 / \text{s.} \times \text{K}\times\text{mol)}$
r_1	reduction of K_{Sat} due to the clay swelling
r_2	reduction of K_{Sat} due to an increase in the net negative charges on the clay colloids associated with the increase in soil solution pH
RK_{Sat}	relative saturated hydraulic conductivity
r_p	root activity function
S	water sink term (root water uptake)
s	empirical parameter, which depend on soil type and soil condition
Sa_{start}	initial amount of the salt in the root zone
SCW	dissolved CO_2 removed from soil by root water uptake
S'	plant salt uptake
t	time
T	absolute temperature
T_r	transpiration rate per unit soil surface area
v	average soil pore velocity
x	valence of species i and j , respectively
x	swelling factor (i.e. the calculated interlayer swelling of soil Montmorillonite)
X	electrolyte concentration (mmol _c /litre) in TableCurve program
x_o	adjusted effective swelling factor
$x+$	valence of a cation i
x_i	spatial coordinate and $i, j = 1, 2, 3$
$y+$	valence of species a cation j
Y	exchangeable sodium percentage (ESP) in user function in TableCurve program
Z	RK_{Sat} in user function in TableCurve program

z	soil depth
z_r	depth of the root zone
\bar{z}	relative soil depth according to the entire soil column length
$\lambda(\theta)$	coefficient of the apparent thermal conductivity of the soil
ΔSa	change of salt storage within the root zone
Δz	thickness of the layer of soil
γ_s	sum of the production of CO ₂ by the soil micro-organisms
γ_r	sum of the production of CO ₂ by plant roots
γ_{r0}	optimum CO ₂ production from plant roots
γ_{s0}	optimum CO ₂ production from micro-organisms
β	empirical parameter depends on soil type and clay mineralogy
$\bar{\alpha}$	depth weighted mean anion exclusion volume as a proportion of the volumetric water content above z
δ	empirical constant set to 0.2 z
μ	production coefficient
ρ	soil bulk density
ζ	equivalent Pore Neck Radius
θ_a	soil air content
θ_{fc}	volumetric soil-water content at field capacity
$\bar{\theta}_s$	depth weighted mean volumetric soil-water content at field above z
θ_w	volumetric soil-water content
τ_w	tortuosity factor in the liquid phase
ϖ	empirical parameter which varies with different mixed solutions

List of Abbreviations

BC	Boundary Conditions
CDE	Convection Dispersion Equation
CEC	Cation Exchange Capacity
DDL	Diffuse Double Layer theory
EC	Electrical Conductivity
ECe	Electrical conductivity of saturated extract
ESC	Exchangeable Sodium Content
ESP	Exchangeable Sodium Percentage
ESP _T	Exchangeable Sodium Percentage Threshold
ESR	Exchangeable Sodium Ratio
FC	Flocculation Concentration
Fit Std Error	Standard Error Coefficient
GCSM	Generic Clay Swelling Model
HSS water	Highly Saline-Sodic water
<i>k</i>	Soil Permeability
LR	Leaching Requirements
M	Solute Molarities
P _A	Attractive Pressure
PSI	Pore Size Index
P _R	Repulsive Pressure
PZNC	Point of Zero Net Charge
R ²	Coefficient of Determination
RCBD	Randomized Complete Block Designs
RSC	Residual Sodium Concentration
SAG	Sulphuric Acid Generator
SAR	Sodium Adsorption Ratio
SAR _{1:5}	Sodium Adsorption Ratio in soil-water extract 1: 5
SE. Coeff.	Standard Error Coefficient
SWCC	Soil-Water Characteristic Curve
TDR	Time Domain Reflectometry
TDS	Total Dissolved Solids
TEC	Threshold Electrolyte Concentration
TC	Turbidity Concentration

CHAPTER 1: Introduction

1.1 Background

World growth in population demands more food and fibre. The need for food and fibre production necessitates water to be used more efficiently in irrigated agriculture. However, the scarcity of fresh water is limiting irrigation development. One of the more feasible solutions is to use marginal water for irrigation purposes. Marginal water is generally saline and/or sodic water that has been considered unsuitable for agriculture in the past. Using marginal waters for irrigation requires further consideration of the possible negative effects of salinity and sodicity.

World-wide, most irrigation systems have inherently low efficiencies. In arid and semi arid areas, significant amounts of water are allocated for irrigation. In these areas, water use efficiency can be improved by increasing the spatial and temporal precision of irrigation applications. However, as irrigation efficiency is increased, salts from the irrigation water are not leached out of the root zone. Consequently increasing salinity and sodicity in the root zone may become a major concern (Raine et al. 2005). Under these conditions, using marginal water for irrigation without appropriate management can compound salinity and sodicity problems.

1.1.1 Salinity and sodicity problems in irrigation

The term salinity refers to the concentration of ions in water (Burger & Celkova 2003). The salinity level for water to be considered as saline depends on the purpose of the water use. Guidelines have been provided for different water uses including drinking, agriculture and industry. Agriculturally, salinity is the concentration of dissolved mineral salts in water and soil-water as a unit of volume or weight basis (Ghassemi et al. 1995).

Salinity problems become visible when salt concentrations in the soil solution exceed crop threshold levels. Crops can tolerate low concentrations of salt throughout the root zone. Productivity declines above the threshold concentration. The salt tolerance thresholds for crops vary between species. Maas and Hoffman (1977) summarised previous published work and carried out a comprehensive review of crop salt tolerance data, which was subsequently updated by Maas (1990). However, the data indicate that some crops can tolerate a high level of salinity (e.g. 7 dS /m for barley). In addition, the decline of crop yield occurs gradually above the salinity threshold level. Such crop behaviour allows for crop selection and management for irrigation with different water qualities. However, salt tolerance data has inherent uncertainties concerning plant responses to spatial and temporal variations in root zone salinity (Hopmans & Bristow 2002; Meiri & Plaut 1985).

Sodicity describes the relative concentration of sodium (Na^+) compared with the divalent cations mainly calcium (Ca^{2+}) and magnesium (Mg^{2+}) in the soil solution. Sodicity problems manifest at higher relative Na^+ concentration and lead to degradation of soil structure. Sodicity problems are usually inherent with salinity in irrigated clayey soils having significant sodium content. Sodicity is common also in soils irrigated with water containing considerable bicarbonate concentrations. That is because bicarbonate anions raise soil pH and can result in precipitation of divalent cations and an increase in the relative sodium concentration. High levels of sodium in irrigation water typically result in an increase of soil sodium levels, which affect soil structural stability, infiltration rates, drainage rates, and crop growth potential.

The interrelation between sodicity and salinity levels in irrigation water introduces a dual problem in term of crop response, soil structure degradation, and irrigation management. An increase of water salinity is shown to have a positive consequence on the sodicity effect. Sodicity has less impact at higher electrolyte concentrations at any particular level. Nevertheless, continuous use of saline irrigation water might lead to accumulation of salt above the threshold level of crops. On the other hand, low water salinity and high levels of sodicity can cause soil degradation and reduction in soil permeability. Such degradation results in aeration and waterlogging problems which negatively affect the crop yield. Consequently, waterlogging and low permeability might also induce salt accumulation within the root zone. Clearly rising salinity associated with an increase of Na^+ relative concentration presents two

thresholds values to be considered. The lower level is the salinity threshold above which the soil structure remains stable, and the higher salinity threshold level is the salt tolerance threshold of the grown crop.

Sodicity-salinity effects on the physical and hydraulic properties of the soil are very complicated processes that can be influenced by many factors. The main factors that control sodicity problems are soil type (Felhendler et al. 1974; Quirk & Schofield 1955), clay type and content (Goldberg et al. 1991), pH of the soil solution (Suarez et al. 1984; Sumner 1993), the manner of application of irrigation water, the initial water content in the soil (Dehayr & Gordon 2005), and organic matter. Therefore, the soil structure degradation due to rising sodicity is unique for a given soil and its condition (Evangelou & McDonald Jr 1999). The mechanisms of developing sodicity and related salinity problems under irrigation is conceptualised in Figure 1.1. Determining the sodicity effect within a given soil requires a comprehensive knowledge of the mineralogy, structure and chemistry of that soil.

In Figure 1.1, it is assumed that the source of total salt and sodium concentration is the irrigation water. The time required to develop sodicity and salinity problems can be determined by the sodicity and salinity levels in irrigation water, along with management practices under this condition. The management options include leaching for salinity control, amelioration to manage the increase of sodicity level, along with crop selection.

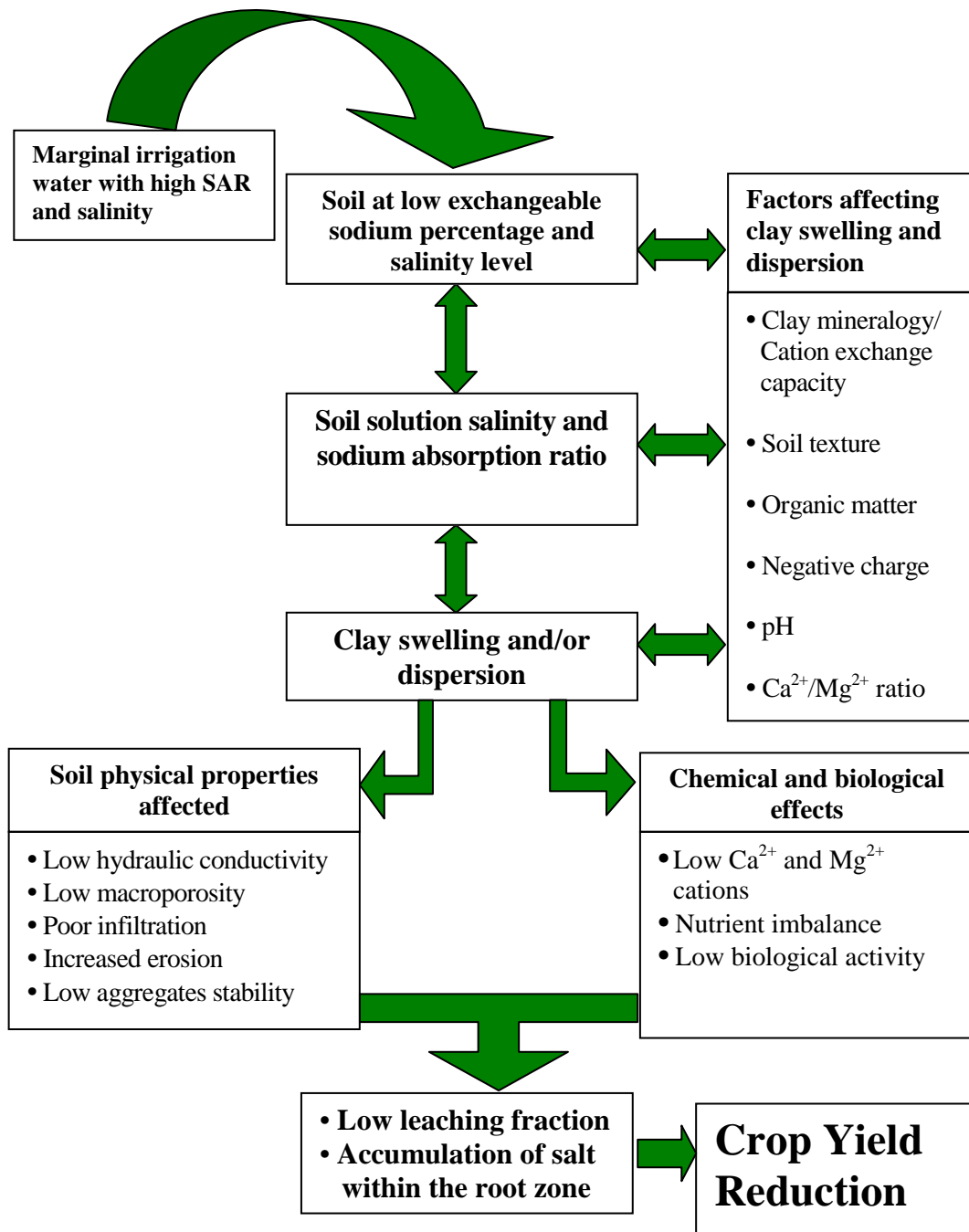


Figure 1.1 Development of soil problems under saline-sodic conditions

Modified from Surapaneni and Olsson (2002)

1.1.2 Sodicity and salinity control

Sodicity and salinity problems are usually controlled by leaching (Rhoades 1982). Leaching is the process of applying extra irrigation water to prevent the build up of salt including sodium within the soil profile. It is imperative to maintain and accurately determine the leaching requirements to minimise water and nutrient loss out of the root zone. Efficient leaching depends on the hydraulic properties and structural stability of the soil.

An appropriate leaching requirement is determined by many factors such as crop type and growth stage, root depth, climate, irrigation system and irrigation management, and interrelated change of physical and chemical soil properties as affected by water quality.

Traditional methods for determining the leaching requirements of irrigated soils assume that a steady state condition applies from one season to the next (Rhoades 1974, USSL Staff 1954). This steady state approach ignores the variation with time of the input and output salinity and the salt distribution within the root zone. This approach has appeared to be reasonable and acceptable in the past due to the low efficiency of the irrigation systems and the availability of good quality water (Meiri 1984). However, under new irrigation systems that have uniform distribution and high efficiency, the salt movement and accumulation needs to be more precisely described by an unsteady state approach.

Soil profile salinity is in an unsteady state during single irrigation event and within a season. The input salt with irrigation water into the root zone is often different to the output salt load with drainage water. Furthermore, there may be a temporal and spatial variation of salt concentration within the root zone. The unsteady state condition becomes more pronounced in the short term when associated with an increase in irrigation efficiency and inefficient salt leaching. In addition, the presence of high sodium concentrations in irrigation water (which has a significant effect on soil physical properties) reduces the leaching efficiency, and makes the unsteady state condition more pronounced. The salt distribution within the root zone under different

irrigation systems is dynamic. The variation of salt distribution might result in different responses of the crop. Therefore, appropriate leaching management should account for these variations to flush undesired salt out of the root zone. Such leaching management depends on soil hydraulic properties. The leaching will be conducted properly as long as the permeability of the soil is maintained (Rhoades 1982).

Determining the precise leaching requirement and plant response under efficient irrigation systems require a better understanding and quantification of salt movement within the soil profile. Salt movement and accumulation is highly affected by the process of temporal and spatial interrelated change of the soil chemical and physical properties in the soil water plant system (Mmolawa & Or 2000). However, monitoring water and solute movement and accumulation associated with crop response is costly and time consuming.

1.1.3 Sodicity and salinity management options

Salinity control is mainly determined by the salinity of the irrigation water and the amount of that water applied. It also depends on irrigation type and its management. Furthermore, it has a direct effect in plant growth. However, the sodicity problem is more complicated than salinity as it could result in the degradation of soil structure which makes the management options more complex. Sodicity management options usually involve some amendments to prevent any soil degradation occurring. These amendments can be added either to the irrigation water or directly to the soil surface.

These amendments generally work either by reducing the relative concentration of the sodium in the soil solution (i.e. by raising the Ca^{2+} concentration in the soil solution) or by preventing the precipitation of the divalent cations (i.e. Ca^{2+} and Mg^{2+}). Among these amendments, gypsum has been widely used to treat irrigation water or directly applied to soil because of its availability and low cost. Gypsum has low solubility and offers a relatively long term source of calcium cations in the soil. Irrigation water with high concentrations of bicarbonates is usually treated by sulphuric acid to reduce the loss of calcium and magnesium concentrations in the soil solution. Recently, sulphuric acid (H_2SO_4) generators (SAGs) have been introduced to

treat water with high bicarbonates. The SAG is a sulphur burner which produces sulphur dioxide (SO_2) that forms sulphuric acid in water. The sulphuric acid goes through a series of reactions to convert bicarbonates to carbon dioxide gas. These reactions reduce the bicarbonate concentration and the water pH. However, this treatment neither reduces the original sodium concentration nor the total water salinity. The SAG treatment will be more effective in water having higher bicarbonate and lower sodium concentrations, especially if it is combined with other amendments such as gypsum.

Blending with good quality water could be used to reduce salinity and sodicity in sodic-saline water. However, blending depends on the availability of the good quality water.

The flexible management options of sodicity and salinity problems such as using amendments, crop selection, climate condition, and type of irrigation system can make saline-sodic water usable for irrigation. The management options for marginal water can be readily investigated using suitable modelling tools.

1.1.4 Modelling the effect of sodicity and salinity in irrigation

Modelling is an efficient tool to investigate water and solute movement and salt accumulation under irrigation. Modelling could be also used to evaluate the appropriate management for irrigation under sodic conditions. However, in most available models, continuing degradation of soil hydraulic properties as a result of rising Na^+ concentrations is ignored. Disregarding the soil hydraulic degradation due to sodicity level in some cases makes modelling water and solute movement within the soil profile questionable. The UNSATCHEM (Simunek et al. 1996), in which the interactions between chemical and physical properties have been considered, has been widely used. Recently, the UNSATCHEM has been incorporated in HYDRUS 1 D model, version 3 and 4 (Simunek et al. 2005).

UNSATCHEM is a combined one dimensional flow model of chemical reaction, water-solute movement, and carbon dioxide production and movement. It uses the

Richards equation (Richards 1931) and convection dispersion type equations (CDE) for solute and carbon dioxide movements. In this model, the effect of sodicity on soil hydraulic properties is incorporated using the clay swelling model of McNeal (1968; 1974). Simunek and Suarez (1997) indicated that this clay swelling model was used in the UNSATCHEM because of its simplicity. The effect of the pH in soil solution has also been accommodated with the clay swelling model to provide a general reduction function of K_{sat} . An empirical pH- K_{sat} relationship was incorporated based on results by Suarez et al. (1984) to improve the accuracy of the model.

The sodicity impact is usually evaluated in terms of the reduction in saturated hydraulic conductivity (K_{sat}) or infiltration rate. The reduction in K_{sat} under sodic conditions can be interpreted basically as a result of the relative effect between both swelling and dispersion processes (Quirk & Schofield 1955). At relatively high electrolyte concentrations, the swelling process is most likely to be responsible for reducing K_{sat} . At lower electrolyte concentrations the K_{sat} reduction is attributed mainly to the dispersion process. The dispersion at low electrolyte concentration depends on the osmotic gradient generated between added water and soil solution within the micro-pores (i.e. diffuse double layer) within the clay crystalline structure (Emerson & Bakker 1973).

In the UNSATCHEM, the interaction between sodicity and permeability were introduced based on the reduction of K_{sat} . In this model, it is assumed that the sodicity effect acts in the same manner at low water content. The reduction of unsaturated hydraulic conductivity is assumed to be similar to the reduction of K_{sat} . Therefore, if the physical reduction of K_{sat} is known, it would be possible to accommodate the sodicity impact on soil hydraulic properties. In addition, an unsaturated hydraulic conductivity (K_{Unsat}) function can be described at corresponding combined levels of sodicity and salinity simultaneously.

It should be noted that the UNSATCHEM uses the chemical basis for calculating K_{sat} reduction (i.e. individual and total concentrations of the major cations). Modelling the chemical reaction during water and solute movement provides a

temporal and spatial quantitative prediction of major cation concentrations (i.e. Ca^{2+} , Mg^{2+} , and Na^{+}). The predicted cation concentrations are used to calculate the chemical parameters required to quantify sodicity (e.g. exchangeable sodium percentage (ESP) and electrolyte concentration (C_o)).

1.1.5 Conclusion

It is clear that the interrelated effects between sodicity and salinity are important to determine the fate of the salt within the root zone in sodic saline affected areas. Therefore, these interrelated effects are essential to determine crop response and appropriate management of sodicity and salinity under irrigation. The effect of sodicity clearly appears in soil hydraulic properties. Hydraulic properties of the soil are the main characteristics that are responsible for the conveyance of water and salt during irrigation and plant water uptake. Thus, it is crucial to determine the change of hydraulic properties during irrigation.

Modelling is an appropriate way to develop suitable management of sodicity and salinity problems under irrigation. However, sodicity is ignored in most available models. However, the effect of sodicity was addressed in UNSATCHEM using a reduction function that includes the McNeal clay swelling function and the influence of the pH on the soil conductivity. However, the evaluation of this model is still limited under highly sodic conditions. Improving the quantification of the negative sodium effect on soil structure can improve modelling of water- solute movement in the water soil and plant systems. Subsequently, it helps to investigate different management options in an efficient way.

1.2 Overview of research

1.2.1 Research hypotheses

The hypotheses to be addressed in this PhD thesis are:

- 1) Highly saline-sodic water can be used in irrigation using appropriate irrigation management including amendments.**
- 2) The interaction between physical and chemical soil properties can be quantified more precisely, taking into account the factors that influence soil degradation due to sodicity.**
- 3) Modelling water and solute movement under sodic conditions can be improved if the interrelationship between the physical and chemical properties is quantified precisely.**

1.2.2 Specific objectives of research

This project aims to improve modelling of water and solute movement by taking into account the change of soil hydraulic properties under sodic-saline conditions. The main objectives of this research are to:

- 1) Characterise the soil structural degradation associated with the application of saline sodic water.
- 2) Evaluate the current models which adjust most hydraulic properties in respect to soil chemical changes.
- 3) Identify strategies to improve the ability to model soil structural change associated with the application of saline-sodic waters.

1.3 Structure of dissertation

This dissertation contains eight chapters addressing the importance of the processes involved in soil structure degradation due to sodicity and salinity. Chapter 2 serves as a general review of salinity and sodicity problems in the soil-water-plant system and the methods used to quantify these problems. Clay reactions under sodic conditions are also reviewed along with the current soil-water and solute models.

Chapter 3 reports on a laboratory study conducted to evaluate the effect of applied water quality on soil physical degradation. This study also evaluated the benefits associated with the use of gypsum and pH amendments. Chapter 4 reports on a preliminary evaluation of the UNSATCHEM soil-water and solute model using data obtained from the laboratory study (chapter 3). Limitations in the UNSATCHEM are identified, and provide the basis for subsequent studies.

Chapter 5 reviews clay swelling theory, and provides a justification for the development of a generic clay swelling model. The generic clay swelling model is developed in chapter 5 and validated in chapter 6 using laboratory data measured on three local soils and published data for two soils from Tasmania. Chapter 7 reports on an evaluation of the UNSATCHEM model after the new generic clay swelling model was implemented. Chapter 8 presents the conclusions arising from this research and provides suggestions for future research.

CHAPTER 2: Review of Salinity and Sodicity under Irrigation

2.1 Introduction

The aim of this chapter is to describe the problems related to salinity and sodicity in the soil-water-plant system and the methods used to quantify these problems. It also provides a justification for this research. This chapter contains six sections. Section 2.2 starts with the definitions of salinity and sodicity and their interrelationships. It also discusses the mechanisms of developing salinity and sodicity problems and their relationships in the soil-water and plant system. Section 2.3 discusses the effect of salinity and sodicity on soil and water movement under irrigation. Furthermore, it discusses the clay reactions under sodic conditions along with the main factors that influence sodicity problems. Section 2.4 is a brief overview of sodicity-salinity management. Section 2.5 provides a discussion about modelling soil-water and solute movement within the root zone. The current soil-water and solute modelling is reviewed along with the models most widely used to quantify the sodicity effect. Finally, the review is concluded in section 2.6.

2.2 Salts in the root zone

2.2.1 Salinity

Salinity is the concentration of dissolved mineral salts in water and soil-water as a unit of volume or weight basis (Ghassemi et al. 1995). Different qualities of water usually contain nearly the same ions of the elements. The major ions present in water are the anions of chloride (Cl^-), sulphate (SO_4^{2-}), bicarbonate (HCO_3^-), carbonate (CO_3^{2-}) and nitrate (NO_3^-), and the cations of sodium (Na^+), calcium (Ca^{2+}), magnesium (Mg^{2+}), and potassium (K^+). In hyper saline water, other constituents can be present, such as barium (Ba), strontium (Sr), lithium (Li), silicon dioxide (SiO_2),

rubidium (Rb), iron (Fe), molybdenum (Mo), manganese (Mn), and aluminium (Al^{3+}) (Tanji 1990). Soil solutions have the same components of elements that are in water. The ratios of the constituents in soil-water depend on the chemical reactions that take place in soil-water-plant systems under different conditions.

Chemical analyses provide full details of water salinity (i.e. pure water or soil-water extract) and specific ion concentration. However, as a general predictor, salinity usually is described in irrigation as total salts irrespective of its constituents.

The total dissolved solids (TDS) can be determined simply by evaporating a known amount of water to dryness, and weighing the quantity of dissolved materials contained in that amount. The TDS has historically been expressed in parts per million (ppm), which is a unit of measurement of the weight of salt per unit weight of solution. This unit can be used for more diluted solution such as water encountered in irrigation. However, ppm might not be accurate in high salinity. A more appropriate unit is mg/litre (Bresler et al. 1982). It should be noted that the TDS method might contain some errors because various salts exist in water in different hydration states, which depend on the drying condition (Bresler et al. 1982). In addition, measuring TDS is tedious and time consuming.

Electrical conductivity (EC) is used as a fast method to evaluate water salinity. EC measurements are based on the fact that the electrical current transmitted between two electrodes (i.e. with standardised solution, temperature and electrodes areas that usually equal to unity) increases with an increase of soluble ionic salts and vice versa. The basic SI unit of EC is Siemens per metre (S/m). In agriculture EC is often low. Thus deciSiemens per metre (dS/m) has been widely used. The unit (mmhos / cm) used in the past is numerically equal to dS/m.

EC can be related to electrolyte concentration as in equation 2.1 for different solution conditions:

$$\log C_o = a + b \log EC \quad (2.1)$$

where C_o is the salt concentration expressed in mmol/litre, ϖ and λ are empirical parameters which vary with different mixed solutions, and have values of about 1.

Bresler et al. (1982) and Smith and Hancock (1986) reported that such a relationship might not always hold, especially at higher solute concentrations. A simplified version of equation 2.1, which can be used to calculate salt concentration presented in mmol/litre for a range of EC between 0.1 and 10 dS/m can be written as (Bresler et al. 1982; Dudley 1994; USSL Staff 1954):

$$C_o \approx 10 \times EC \quad (2.2)$$

Bresler et al. (1982) have indicated that the EC in equation 2.2 increases less rapidly with increase of salt concentration. At higher salt concentration, equivalent to that in sea water (about 33 g/litre), equation 2.2 underestimates the actual salinity by nearly 20%.

Soil-water salinity depends on the water content at which the salinity needs to be determined. Separating the soil solution from the soil sample is difficult and the extracted water is usually insufficient to conduct chemical analyses. Therefore, an extra known volume of water can be added to the soil sample before extracting the soil solution. The extraction process can be performed after mixing a given weight of soil with certain volume of water. Different soil-water extract ratios have been used to predict soil salinity such as 1_{soil}:5_{water}, 1_{soil}: 2.5_{water} and 1_{soil}:1_{water} extract. A good approximation of soil-water salinity is that measured in a saturated soil paste extract. Saturated soil paste extract can be prepared in which a given weight of soil sample is saturated and then the soil solution extracted. Since the water content at saturation is nearly twice that of field capacity (Rhoades 1982), the salinity measurement of the saturated extract is approximately half of the salinity at field capacity (Rhoades 1982). The salinity predicted in soil solution at field capacity is usually used as a standard value for comparison of salinity data.

Soil salinity in the field can be monitored using various instruments. Examples of these instruments are a salinity sensor based on electronic conductivity, time domain reflectometry (TDR), and inductive electromagnetic meter (Dudley 1994). More

details about the instruments used to predict field soil salinity were reported by Rhoades et al. (1999).

Soluble salt is usually added to the root zone with irrigation water. The suitability of water for irrigation is evaluated by the amount of soluble salt included, its constituents and the crop response. Ayers and Westcot (1976) concluded that water quality problems occur in four general categories, which are salinity, soil permeability, toxicity, and miscellaneous. Assessment of water salinity is highly dependent on crop salt thresholds. Soil permeability has a strong impact on water and solute movement. Degradation of soil permeability can produce complex problems related to water logging and aeration. In addition, declining soil permeability might compound the salinity problems. Toxicity occurs when certain ions exceed the crop tolerance level. Salinity problems might also result in miscellaneous problems such as delaying of crop maturity and excessive vegetative growth because of excessive nitrogen in irrigated water (Ayers & Westcot 1976).

Hoffman (1986) determined three main factors to evaluate water for irrigation which are salinity, sodicity and specific ion toxicities. Pratt and Suarez (1990) pointed out that water suitability for irrigation might be influenced by chemical reactions of dissolved salts in water, chemical and physical properties of soils, climatic conditions, and irrigation management practices. Bar-Yosef (1999) added two further factors in the case where municipal or recycled water is used for irrigation. These factors are biochemical oxygen demand, which is the quantity of oxygen required for microbial degradation of organic compounds in water at 20° C and total suspended solids in water. Many guidelines have been provided for irrigation water quality, which depend on these components (e.g. ANZECC & ARMCANZ 2000; Ayers & Westcot 1985; USSSL Staff 1954). These factors should be evaluated concurrently before using the water in irrigation.

2.2.2 Sodicity

The level of sodium present in a water or soil is important as it influences the structural stability of clay minerals and the potential for dispersion, erosion and drainage problems. The sodicity of water or soil is usually described in terms of the relative proportion of sodium cations compared to the divalent cations (i.e. calcium and magnesium) in solution. The sodium adsorption ratio (SAR) of water (including soil solutions) is calculated as:

$$SAR = \frac{Na^+}{\sqrt{\frac{Ca^{2+} + Mg^{2+}}{2}}} \quad (2.3)$$

where the cation concentrations are expressed in mmol/litre. However, sodicity in soils is expressed by the exchangeable sodium percentage (ESP) and calculated as:

$$ESP = \frac{\text{Exchangeable Na}}{CEC} \times 100 \quad (2.4)$$

where CEC is the cation exchange capacity. The CEC is the sum of exchangeable cations such as Na^+ , Ca^{2+} , Mg^{2+} and K^+ (as well as Al^{3+} in low pH soils) expressed in mmol/100 g.

2.2.3 Relationships between SAR and ESP

Using the measured ESP as an indicator of the level of sodium on soil exchange surfaces may have errors due to the difficulties in determining the CEC. Qadir and Schubert (2002) concluded the reasons for deficiency of ESP in three points: (a) the extraction of exchangeable Ca^{2+} and Mg^{2+} during the chemical analysis process might cause some $CaCO_3$ and $MgCO_3$ to dissolve, erroneously leading to an increase of apparent CEC especially in calcareous soils; (b) the CEC in variable charge soils depends on pH, solute concentration and buffering capacity of soil-water extract; (c) the removal of Na^+ by extraction from a source that does not contain a true form of exchangeable Na^+ such as sodium zeolites. Furthermore, determining the CEC is time consuming.

So and Aylmore (1993) showed that the exchangeable sodium content (ESC) (in which the level of sodium are expressed on an oven-dried soil basis rather than relative to the cation exchange capacity (Cook & Muller 1997)), which is closely related to SAR is a better indicator to evaluate sodicity. Likewise, Cook and Muller (1997) compared using ESP and ESC to evaluate sodicity, and concluded that ESC or SAR were more the appropriate indices to evaluate the negative Na^+ effect. However, using the ESC as an indicator of the level of sodicity instead of ESP is still limited in the literature.

SAR is thermodynamically more appropriate because it approximates the activities of various cations in solution (Chartres 1993). In addition, SAR requires less parameters (the concentration of Na^+ , Ca^{2+} and Mg^{2+}), and can be determined from the same soil-water extract used to evaluate the EC in soil solution (Qadir & Schubert 2002).

SAR, however, does not take into account the change of calcium concentration in soil solution as a result of change of solubility of the Ca^{2+} (Ayers & Westcot 1985; Qadir & Schubert 2002). Sodium remains soluble and in equilibrium with exchangeable soil sodium all the time. Conversely, Ca^{2+} does not remain completely soluble. Ca^{2+} might be raised in soil solution because of dissolution of soil minerals. Ca^{2+} usually precipitates in the presence of carbonates, bicarbonates and/or sulphates in solution. This process follows the irrigation which might lead to error in the calculation of SAR of soil-water. In brief, the presence of carbonates and bicarbonates in the water contribute to soil structural degradation in the long term because the precipitation of calcium carbonate will further increase the relative concentration of sodium ions or the values of SAR in soil-water. Adjusting the SAR to account for the increase of carbonate and bicarbonate concentrations in irrigation water has been reported by Ayers and Westcot (1985), Rhoades (1982) and Suarez (1981).

Furthermore, averaging the concentrations of Ca^{2+} and Mg^{2+} in equation 2.3 assumes that both cations contribute equally to overcome the adverse effect of Na^+ cations. However, many researchers (e.g. Brady 1990; Emerson & Chi 1977; Keren 1991; Rengasamy 1983) pointed out that Mg^{2+} has a low tendency to flocculate the soil colloid compared with Ca^{2+} especially where Mg^{2+} is presented in significant proportion. Conversely, a high concentration of Mg^{2+} might induce clay dispersion.

Therefore, equal weight should not be given to Mg^{2+} and Ca^{2+} while calculating SAR (Qadir & Schubert 2002). In general, SAR evaluation procedures were widely used for most waters encountered in irrigation (Ayers & Westcot 1985).

The ESP is closely related to the SAR of the applied water. USSL Staff (1954) indicated that if the exchange reactions between soil solution and the soil colloid reach an equilibrium state, the ESP is closely equal to SAR in the range of 0 - 40. The SAR-ESP relationship provides an easy way to estimate the ESP (Qadir & Schubert 2002). Empirical relationships between SAR and ESP have been established for different soil types. For example, Rengasamy et al. (1984) established a linear relationship between SAR in soil-water extract (1:5) and ESP with R^2 about 0.82 for 138 samples of Australian soils. The linear relationship can be written as:

$$ESP = 1.95 SAR_{1:5} + 1.8 \quad (2.5)$$

However, equation 2.5 was obtained for relatively low values of $SAR_{1:5}$ (0.38-12.4) and ESP (0.42-22.2).

The SAR-ESP relationship developed by SSSL Staff (1954) was based on a linear correlation between experimental measurements of soil exchangeable sodium ratio (i.e. $ESR = EXNa/(CEC-EXNa)$) and ESP for 51 American soils. The linear relationships produced ($R^2=0.923$) was:

$$ESR = -0.0126 + 0.01475SAR \quad (2.6)$$

where EXNa is the exchangeable sodium concentration. Since the ESP can be calculated from ESR as:

$$ESP = 100 \times \left(\frac{ESR}{1 + ESR} \right) \quad (2.7)$$

The relationship can also be written as:

$$ESP = \frac{100(-0.0126 + 0.01475SAR)}{1 + (-0.0126 + 0.01475SAR)} \quad (2.8)$$

It is noteworthy that the SAR-ESP relationship varies from one soil type to another due to differences in clay minerals content and texture in soils. Figure 2.1 shows the comparison of different empirical parameters for equation 2.8 over a wide range of SAR. It can be observed from Figure 2.1 that at low SAR values some equations produce negative values of ESP. The equation developed by USSL Staff (1954) gives negative values of ESP below SAR (0.5). The equations from Ghafoor et al. (1988) also produced negative values of ESP for SAR values less than 3. The results indicate that SAR= 0 at ESP higher than zero, while at ESP is zero, negative values of SAR were produced. These results indicate that the minimum value of ESP of zero (Dudley 1994) was ignored during the regression analyses between SAR and ESR. The negative predictions for ESP values produced from these equations indicate that these models should be corrected at the lower range of SAR-ESP (i.e. SAR approaching zero). However, equation 2.8 has been approved for values of SAR and ESP up to 65 and 50, respectively, for a wide range of soils including Australian soils (Department of Natural Resources 1997; Skene 1965).

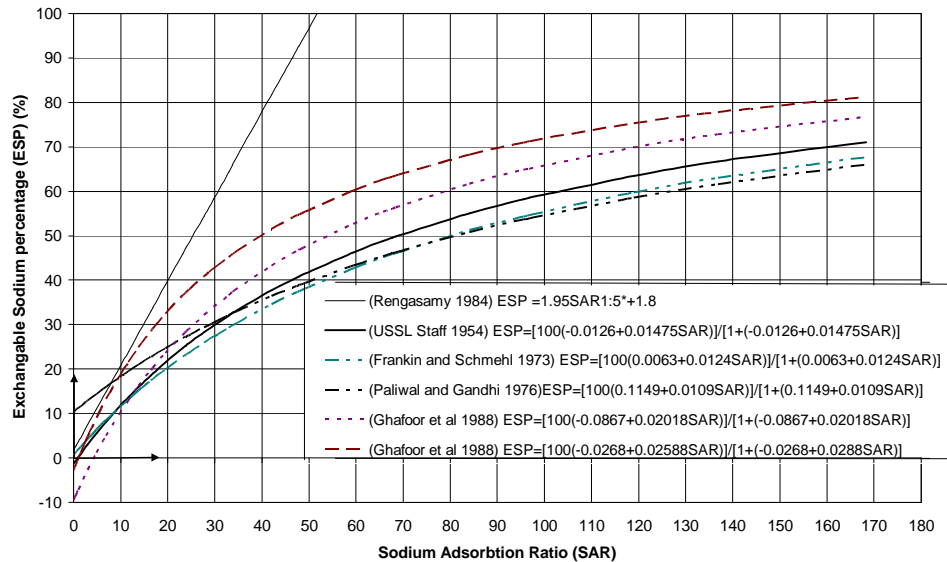


Figure 2.1 Comparison of different SAR- ESP relationships published in literature as presented in Qadir and Schubert (2002) at wide range of SAR (0-169) for different type of soils

Note that SAR1:5 designated to Sodium Adsorption Ratio of soil to water extract 1:5, and SAR is Sodium Adsorption Ratio of saturated soil paste extract

2.2.4 The distribution of salts within the root zone

The salt movement and accumulation within the root zone varies with different irrigation systems. Salt distribution profiles depend on the irrigation system and its management, climate, and the soil condition. Sprinkler, flood or border check, and level basin irrigation systems produce one dimensional vertical flow. Thus, for these systems most of the salts are expected to accumulate in the lower parts of the root zone (Burt 1995). The upper parts are leached by the applied irrigation water. Root water extraction results in salts increasing in concentration as water flows downward through the soil profile (Tanji & Kielen 2002). Reduced water flow at depth also leads to a reduced capacity to flush salts from deeper parts of the root zone (Burt 1995; Tanji & Kielen 2002). Furrow and trickle (i.e. line source) irrigation systems produce two dimensional water flow. The salt may accumulate in the upper part of the root zone between the adjacent rows (Figure 2.2). A semi-spherical water flow is inherent with drip (i.e. point source) irrigation, allowing the salt to accumulate away from the water source.

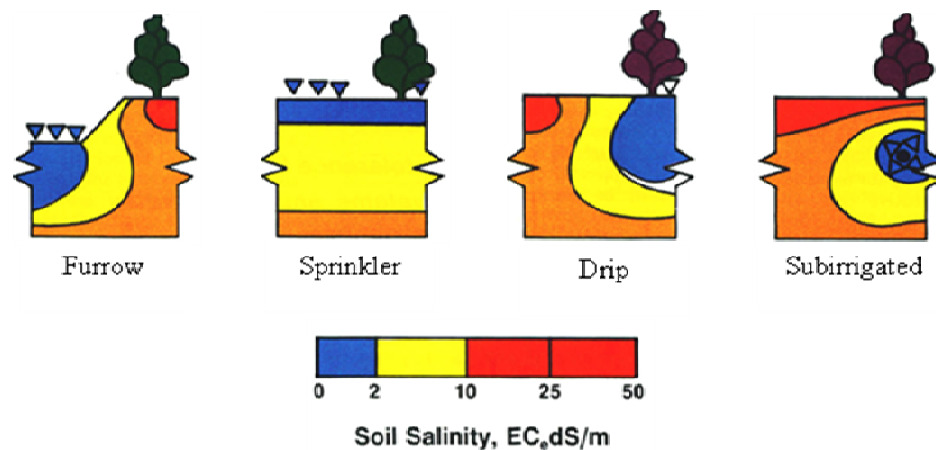


Figure 2.2 Root zone salt distribution under different irrigation systems

Source: (Oster et al. 1984)

A more complicated situation can be found under sub-irrigation systems. In these systems, water and solute flow in spherical dimensions. The main complexity in this system is water moves upward to soil surface. Such water movement allows salt to accumulate in

the surface soil. However, rainfall can flush downward the salt accumulated near the soil surface, which makes controlling salinity under this system difficult.

Furthermore, root zone salt distribution is different in the presence of a shallow water table as capillary rise plays a major role in redistributing the accumulated salt within the root zone (Burt 1995; Scherer et al. 1996).

Smith and Raine (2000) divided the historical hierarchy of irrigation practices into three stages; traditional irrigation, precise irrigation and prescription irrigation. The past practise of irrigation was simply applying water to crops. Current practise is more precise irrigation which ensures the efficient and uniform application of water to meet the spatial average requirements of crop. Future prospects include prescription irrigation which is the accurate precise and possibly spatially variable application of water to meet the specific requirements of individual plants. Clearly, new developments in both design and management can provide differential delivery of optimal irrigation water quantities over an entire field (Perry 2006), which is not uniform and has a variation in soil type, soil-water capacity, yield potential and topography (Dennis 2006). Precision irrigation as a current practise can be defined as *the accurate and precise application of water to meet the specific requirement of individual plants or management units and minimise adverse environmental impact* (Raine et al. 2005). Under these systems more attention should be paid to salinity and sodicity effects.

2.2.5 Crop responses to saline conditions

The responses to saline conditions vary among crops but the reaction can be similar. Two kinds of salinity effects can be distinguished. First is the osmotic effect, which can induce losses of the plant energies that are needed for other physiological processes. If the osmotic potential of the soil becomes low, the root tissues suffer osmotic desiccation (Katerji et al. 2003; Tanji 1990). Second is the toxicity effect, as a result of a certain ion level rising above its threshold (Katerji et al. 2003; Tanji 1990), which makes determining the general thresholds for crops more complicated (Patel et al. 2002). The situation can be more severe at the lower water contents, where the plant is expected to reach wilting point at higher levels of moisture than when less saline water is used (Burt 1995). In addition, the salinity has a strong

impact on the chemical properties of the soil in a way that can hamper the absorption processes of the vital nutrient elements (Lauchli & Epstein 1990). Figure 2.3 shows the main effects of salinity on crop growth.

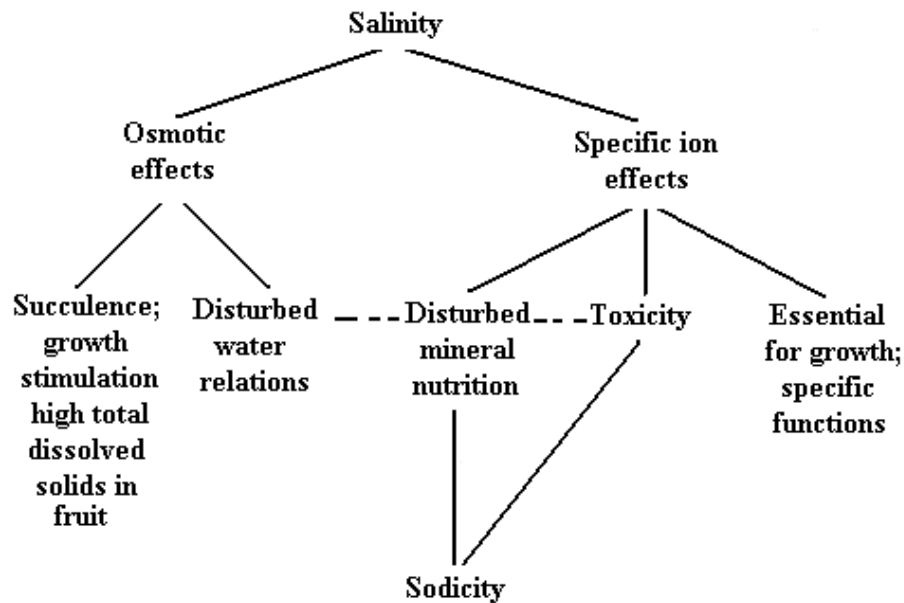


Figure 2.3 Effects of salinity and sodicty on plants

Source: (Tanji 1990)

During last century, many researchers conducted experiments to determine the salt tolerance of crops. Maas and Hoffman (1977) have summarised these data and carried out a comprehensive analysis of salt tolerance data, which was updated by Maas (1990). The assumption is made that the plant responds to uniform root zone salinity. Crop tolerance is described as functions of the yield reduction across a range of soil salinity (Maas & Hoffman 1977; van Genuchten & Hoffman 1984).

There are substantial difficulties in determining a soil solution parameter that can be readily measured in the field and is related to plant response (Smith & Hancock 1986). Many empirical methods have been proposed to determine root zone salinity that can be used as an indicator of plant response. Bernstein (1961; 1964) assumed that salinity in the drained water can be equal to the plant salinity thresholds at which the yield in the salt tolerance experiments decreased to 50% for forage, field, and vegetable crops, and 10 % for fruit crops. Bernstein and Francois (1973) suggested that the leaching requirement of Bernstein (1961; 1964) can be reduced to one fourth as crop growth is

comparatively insensitive to salt concentration in the lower part of the root zone. Van Schilfgaarde et al. (1974) recommended that the thresholds should equal the salinity at which the roots cannot extract the water from the root zone. However, Hoffman and van Genuchten (1983), and Rhoades (1974) concluded that experimental evidence indicates that the Bernstein (1961; 1964) method overestimates the plant salt threshold, while the van Schilfgaarde et al. (1974) method underestimates the plant salt threshold.

A logical assumption for the root zone salinity is that the salinity in the soil-water will be between the irrigation salinity and salt concentration in the drainage water C_d (Bernstein & Francois 1973; Cavazza 1989; Rhoades 1974). Rhoades (1974) suggested that the crop responds to an average salt concentration in the soil solution C_{ws} , which will lie between the salt concentration in the irrigation water C_{ir} and C_d , which can be shown as:

$$C_{ws} = \frac{\kappa_s}{2}(C_d + C_{ir}) \quad (2.9)$$

where κ_s is an empirical constant.

Hoffman and van Genuchten (1983) related crop response to the linearly averaged salt concentration of the root zone. The relationship was expressed as a ratio of the salt concentration of the irrigation water. An exponential root water uptake pattern function was assumed giving:

$$\frac{\bar{C}}{C_{ir}} = \frac{1}{L_f} + \frac{\delta}{z_r L_f} + \ln \left[L_f + (1 - L_f) e^{-z_r / \delta} \right] \quad (2.10)$$

where \bar{C} is the linearly averaged salt concentration of the root zone, δ is an empirical constant set to $0.2z_r$, z_r is the depth of the root zone, and L_f is the leaching fraction.

The effect of the variation of salinity on the plant response is involved through the weighted average root zone salinity.

The spatial variation of the salt concentrations might have a significant effect on the crop response. Bernstein and Francois (1973) recommended using the weighted average root zone salinity. Minhas et al. (1990) related crop performance to the weighted average root zone salinity. Maas (1990) reported that crop growth is closely related to the soil-water salinity in that part of the root zone where most water uptake takes place. Therefore, plant tolerance to salt could be related to the time- integrated salinity of the part of the root zone contributing the most root uptake. Furthermore, Rhoades (1982) mentioned that crop yields are better correlated with the water-uptake weighted root zone salinity for crops irrigated on a daily or near daily basis (localized or drip irrigation). Moreover, Ayers and Westcot (1985) commented that the differences are not great but may become important with higher salinity.

However, many researchers indicated that the plant responds to average root zone salinity irrespective of root water extraction. For example, Meiri (1984) concluded that there is a stronger relationship between crop yield and average root zone salinity, compared with weighted average root zone salinity. Hoffman (2006) mentioned that *“the plant response is better correlated with average root zone salinity, but the problem is determining that average”*. Evidently, clarifying the effect of the variation of salinity within the root zone requires a better prediction of spatial distribution of soil profile salinity.

2.2.6 Leaching of salts from the root zone

Leaching is associated with water flow in soil. Most solute transport is by the convection process (Raine et al. 2005). The main leaching occurs during irrigation when the irrigated water infiltrates and redistributes in the soil. This infiltrated water does not mix readily with the soil-water. Miyazaki et al. (1993) concluded that the infiltrated water pushes the soil solution away from the infiltrating source during the infiltration. However, the displacement of the soil solution might not happen in blocked pores or in the inner pores of clayey aggregates. Furthermore, an early study by van Genuchten (1976) indicated that a part of the solute might remain in these spaces.

During the irrigation, two paths of the infiltrated water into the soil can be distinguished, which are bypass water flow, and soil matrix water flow. Bypass flow is the part of the infiltrated water that passes quickly into the cracks or larger pores and out of the root zone (Tanji & Kielen 2002). This part of the infiltrated water does not significantly participate in the leaching process. The second part passes through the pores, which are filled by soil solution, and convey a high part of the soluble salt (Miyazaki et al. 1993).

The main strategy that should be used for efficient leaching is to reduce bypass flow and the proportion of soil pores that do not contribute in matrix flow (Miyazaki et al. 1993). The bypass flow can be controlled by the infiltration rate or application rate during the irrigation to assure that unsaturated flow processes dominate (Khosla 1979; Rycroft & Amer 1995). Reducing the application rate might also allow the solute in the remaining soil solution to diffuse to the drained water (Rhoades 1982). Furthermore, rising sodicity levels might lead to an increase of micro-pores that retain soil solution. This might affect the leaching processes negatively. Under such conditions, using the pulse irrigation technique could improve the leaching process (Hamdy 2002).

Leaching under steady state conditions

Traditional methods for determining the leaching requirement of an irrigated soil assume steady state conditions. There are four fundamental assumptions associated with this approach. Firstly, irrigation water mixes completely with the soil solution. Secondly, the exchange processes and chemical reactions which take place in soil are not taken into consideration, which means there are no salts precipitated or dissolved. Thirdly, the amount of salt supplied by fertilisers and exported by crops is negligible. Finally, the drained water carries the same mass of salt as applied in the irrigation water. Soil salinity is assumed constant from one season to the next (Rhoades 1974; Tanji & Kielen 2002; USSL Staff 1954). The simple formula to calculate the leaching requirements (LR) based on steady state conditions can be expressed as (USSL Staff 1954):

$$LR = \frac{D_d}{D_{ir}} \cong \frac{EC_{ir}}{EC_d} \quad (2.11)$$

where D_d is the depth of drained water, D_{ir} is the depth of irrigated water, EC_{ir} is the electrical conductivity of the irrigation water (dS/m), and EC_d is the electrical conductivity of the drainage water (dS/m).

The steady state assumptions have been made to simplify the leaching calculation. However, weathering of the soil matrix and dissolution of fertilisers may be a significant source of salts in the long term (Rhoades 1982). Similarly, salts may precipitate out of solution or be taken up by the crop. In addition, mixing of the irrigation water with soil solution is not always complete and is influenced by the presence of the preferential flow paths (Miyazaki et al. 1993). The term leaching efficiency has been used to indicate that there is a fraction of irrigated water which passes through the large pores within the root zone (i.e. with little increase in the salt content) (Stevens 2002), while the remaining water mixes with soil solution in the smaller pores to convey the salt out of the root zone. However, fine-textured soils (where cracks and large pores may abound, and significant micro-pores retain water) have lower leaching efficiency (Bouwer 1969).

The steady state leaching might be achieved under a few cases, particularly in the long term. However, steady state conditions are difficult to achieve due to variations in the applied water quality, solute movement within the soil, root water uptake dynamics and the physical and chemical changes within the soil profile. Therefore, salt concentration and distribution is expected to vary during the cropping season (Mmolawa & Or 2000). Van Hoorn et al. (1997) conducted experiments in lysimeters using different crops and concluded that complete mixing and homogeneous salt distributions do not exist in reality. However, the steady state model might be useful for estimating long-term average salinity of the soil profile.

Leaching under unsteady state conditions

The main criterion of unsteady state conditions is that some of the salt added by the irrigation water remains in the root zone or vice versa. The unsteady state conditions are dominant especially in the field where the leaching fractions are low (Hamdy 2002). The salt stored in the root zone can be predicted as (Tanji & Kielen 2002; van Hoorn & van Alphen 1994):

$$\Delta Sa = \frac{I_{ir} EC_{ir} - \frac{D_d Sa_{start}}{\theta_{fc}}}{1 + \frac{D_d}{2\theta_{fc}}} \quad (2.12)$$

where I_{ir} is depth of irrigation water, ΔSa is the change of salt storage within the root zone, Sa_{start} is the initial amount of the salt in the root zone, and θ_{fc} is the moisture content at field capacity.

An alternative model which has been used in heavy soils is the chloride mass balance model (Rose et al. 1979). Chloride is a toxic element moving readily with water within the soil and into the plants (Ayers & Westcot 1985). In this model, the deep percolation is predicted by assuming that the irrigation water is the sole source of input of chloride within the root zone. Taking into consideration the preferential flow, the equation can be written (Slavich & Yang 1990):

$$z_r \bar{\theta}_s (1 - \bar{\alpha}) \frac{d\bar{C}_{Cl}}{dt} = i_{ir} C_{ir} - dL [f_z C_z + (1 - f_z) C_{IW}] - b_z i_{ir} C_{SW} \quad (2.13)$$

where z_r is the root zone depth, $\bar{\theta}_s$ is the depth weighted mean volumetric soil-water content at field above z_r , $\bar{\alpha}$ is the depth weighted mean anion exclusion volume as a proportion of the volumetric soil-water content above z_r , \bar{C}_{Cl} is the depth weighted mean soil-water chloride concentration at saturation above z_r , f_z is the proportion of the matrix flow that has the concentration of the soil matrix, \bar{C}_z is the chloride concentration of soil-water at z_r at field saturation water content, C_{SW} is the chloride concentration of soil-water at z_r , b_z is the proportion of applied water moving as bypass flow past z_r , t is the time, i_{ir} is the rate of irrigation water application, and dL is the leaching rate.

2.3 The effect of salinity and sodicity on soil and water movement

2.3.1 Clay minerals and dispersion

Brady (1990) categorised clay types in four major groups of colloids present in soils; layer silicate clays, iron and aluminium oxide clays, allophone and associated amorphous clays, and humus. All the groups have general colloidal characteristics; however each group has some specific characteristics. Silicate clay minerals are the most prominent clay minerals in soils of temperate areas and tropical soils (Brady 1990). The most important property of this group is the clarity of their crystallines, which are layer-like structured. The silicate clay fraction in general consists of many plate-like minerals. Crystalline particles are made up of two basic units which are tetrahedral silica and octahedral aluminium hydroxide in alternating layers as shown in Figure 2.4. Due to imperfections in the crystals the Si^{4+} is substituted with aluminium (Al^{3+}) ions and some Al^{3+} ions are replaced by magnesium (Mg^{2+}) ions. Silicate clays commonly have permanent negative charges which enable clay fractions to attract cations.

The silicate clays fall into three subcategories, which are 1:1, 2:1, and 2:1:1 type minerals. The layers of 1:1 types are made up of one sheet tetrahedral silica and an octahedral aluminium hydroxide sheet. The 2:1 types are comprised by an octahedral sheet between two tetrahedral layers to form a sandwich like shape. The crystals of 2:1:1 type minerals consist of two slides of silica tetrahedral and two octahedral. In general, only the 2:1 clay minerals exhibit swelling during the wetting process. Most swelling clay minerals for this group are smectite minerals such as montmorillonite (Churchman et al. 1993).

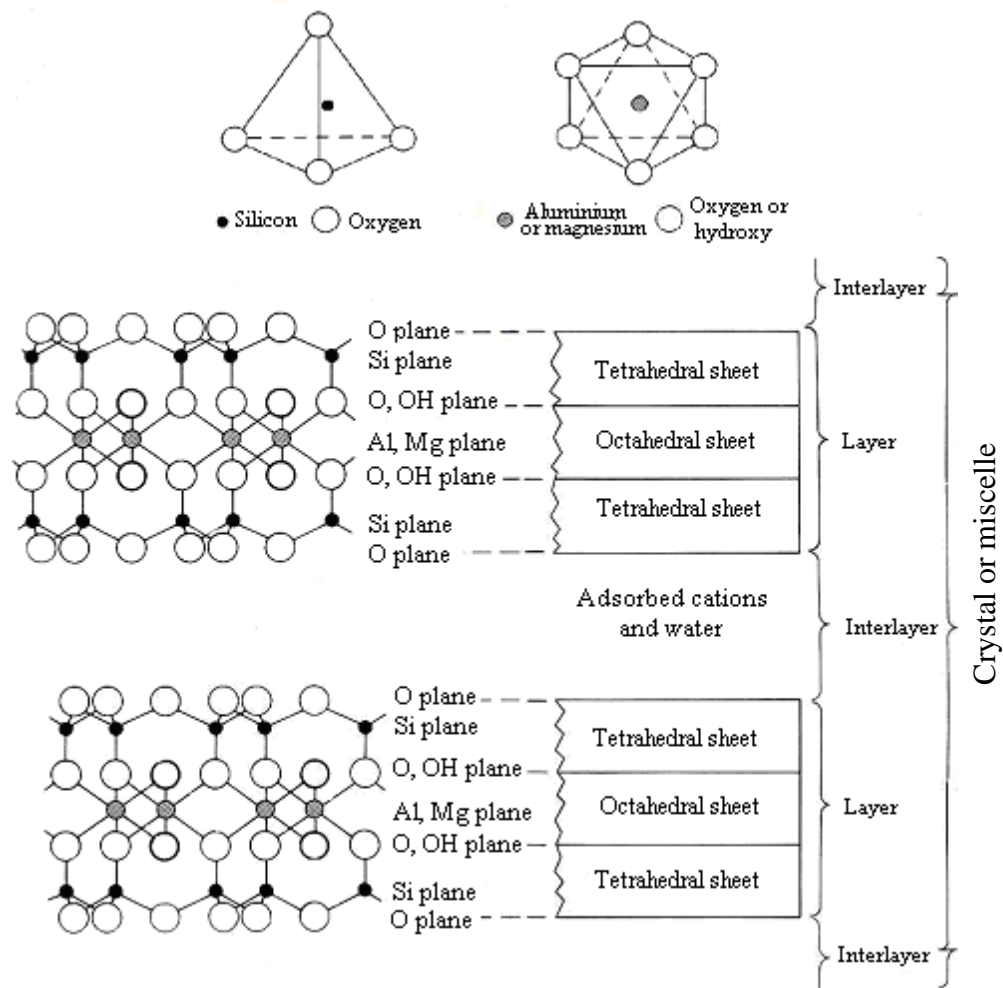


Figure 2.4 Basic molecular and structural components of silicate clays

Source: (Brady 1990)

The increase of relative concentration of a specific cation in the soil solution can increase the adsorption ratio of that cation on the colloid surface. The order of strength of adsorption on the clay surface, when the cations are present in equivalent quantities in the soil solution is Aluminium (Al^{3+}) > Calcium (Ca^{2+}) > Magnesium (Mg^{2+}) > Potassium (K^{2+}) = Ammonium (NH_4^+) > Sodium (Na^+) (Brady 1990). Clay particles do not have a very strong preference for which cations are adsorbed to compensate for their built-in negative charges (van de Graaff & Patterson 2001). The relative concentration of the cations in the soil solution might determine which is the dominant cation being adsorbed. For example, increasing the Na^+ cations in the soil solution will replace gradually the Ca^{2+} and Mg^{2+} cations. However, it is easy to replace Na^+ on the exchange complex by increasing the divalent cations such as

Ca^{2+} , because Na^{+} is less effective in neutralising the negative charges, and clay fractions have preference for cations with more than one positive charge (van de Graaff & Patterson 2001). Therefore, when excessive irrigation water is applied, it is most likely that the cations adsorbed on the negative charges are closely related to the relative concentrations of cations in the added water.

Sodicty is manifested when the sodium concentration in the soil solution increases and the structural stability of soil aggregates degrades significantly. Quirk and Schofield (1955) explained that soil structural degradation caused by sodicty in soils is due to swelling and dispersion processes. Swelling is the increase of aggregate size as a result of water and sodium cations entered between the platelike structure, while dispersion describes the process of separating and moving the clay layers with percolated water. According to the diffuse double layer theory (DDL), both swelling and dispersion processes stem from the balance between repulsive forces (as a result of osmotic pressure) in diffuse double layer and Van Der Waals forces of attraction on clay fraction surfaces (Sumner 1993). Swelling is a reversible and continuing process and depends on the threshold concentration of ambient solution and the degree of sodicty. Dispersion is not a continuing process and may occur even at low SAR as long as soil salinity can not prevent dispersion. Dispersion is an irreversible process because flocculation by increasing concentration above the threshold level does not restore the original particle associations and orientations (Levy 2000).

The clay mineral crystal layers in soils are closely associated with each other to form structures known as “*domains*” or “*tactoids*” (Quirk 2001). In such systems, dispersion can only occur if the individual mineral layers separate. Quirk (2001) described this system using a simple “three plate model” in which individual clay crystals overlap as shown in Figure 2.5.

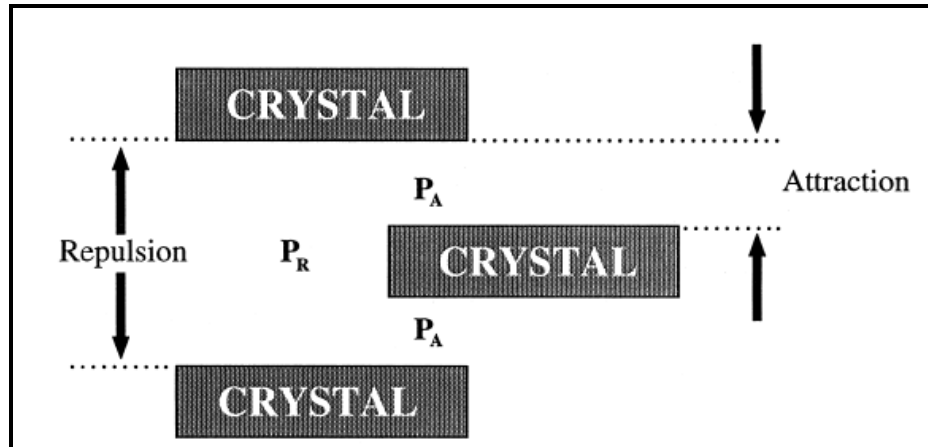


Figure 2.5 A simple 3-plane model to describe the arrangement of clay crystals in a clay domain

Source: (Quirk 2001)

This model is useful for illustrating the swelling and dispersion processes and the effect of exchangeable sodium on dispersion. When water or an electrolyte solution is added to soil, repulsive pressure (P_R), associated with osmotic effects and the change in the diffuse double layer develop over the surface area of the larger slit-shaped pores. While an attractive pressure (P_A) associated with Van Der Waals forces operates over the surface area of the closely aligned crystals (Kjellander et al. 1988; Raine & Loch 2003). Dispersive cations mainly sodium tend to concentrate in the slit shaped pores (Sumner 1993) and form extensive double layers (compared to smaller double layers for cations of higher valence), particularly if the salt concentration of the soil solution is low. Thus, the repulsive force can more readily exceed the attractive force in soil systems containing sodium, resulting in “spontaneous dispersion” when the soil is exposed to excess water at low electrolyte concentration (Raine & Loch 2003). When the repulsive force is nearly equal to the attractive force, dispersion will require the input of a threshold shear stress from flowing water or raindrops (Sherard et al. 1976).

Cook et al. (2006) demonstrated that the structural stability of soils which have reactive clay content is dependent on the interaction between soil sodicity and salt concentration in the soil solution. Clays will swell and disperse spontaneously at a certain relative sodium concentration value when the salt concentration in soil-water is below a critical electrolyte concentration, defined as the threshold concentration (Quirk & Schofield 1955), and will be discussed later in this chapter.

2.3.2 Clay dispersion and hydraulic conductivity

The sodicity impact is usually evaluated in terms of the reduction in saturated hydraulic conductivity (K_{Sat}) or occasionally infiltration rate. It is worth noting that comparing the absolute K_{Sat} measurements for a given soil is difficult and may lead to erroneous results. The K_{Sat} values for a given soil can vary substantially and depend on soil condition. The measurement of K_{Sat} in the laboratory depends on the length of the soil columns and the way they are packed. Therefore, the use of relative K_{Sat} could eliminate these variations (Ayers and Westcot 1985; McNeal 1968; Quirk 2001; Quirk and Schofield 1955; Simunek and Suarez 1997; Simunek et al. 2005). The relative K_{Sat} requires having a measurement of K_{Sat} under conditions at which there is no reduction of K_{Sat} due to the sodicity effect.

The potential for reduction of infiltration or K_{Sat} is evaluated on the basis of the salinity and relative Na^+ content of the applied water. It has been shown by many researchers (e.g. Quirk and Schofield 1955, Levy et al. 2005) that the aggregates slaking, clay swelling and dispersion are the main processes resulting in K_{Sat} decrease. Slaking is a physical process in which soil aggregates disintegrate. Aggregates break down either by explosion of entrapped air or by differential swelling into smaller size aggregates or micro aggregates during wetting of a dried soil (Ruiz-Vera & Wu 2006). Slaking causes a reduction in K_{Sat} as a result of disintegrating the soil aggregates when water is added to dried clayey soils. Auerswald (1995) concluded that the air entrapped within the soil pores was the main reason of aggregate disintegration of pre-wetted aggregates of 113 arable top soils during percolation tests, while shear force of the percolating water, swelling, and clay dispersion had insignificant effect on aggregate disintegration. Furthermore, Abu-Sharar et al. (1987) stated that the extent of slaking depends on relative concentration of Na^+ , and for soils with lower salinity levels, dispersion can be noted at the final stages of the slaking process. However, the K_{Sat} reduction is mainly attributed to the interrelated phenomena of swelling and dispersion (Levy et al. 2005). Swelling reduces soil pore sizes, and dispersion clogs soil pores (Frenkel et al. 1978). Drastic changes in

K_{Sat} due to dispersion and particle movement are irreversible, while K_{Sat} change because swelling is a reversible process. Therefore, determining which process is predominant is important (Frenkel et al. 1978).

The K_{Sat} reduction at high salt concentration and SAR of water added seems to be attributed mainly to the swelling process. McNeal and Coleman (1966), Quirk and Schofield (1955), and Russo and Bresler (1977a) suggested that swelling of clay particles associated with an increase in SAR could result in total or partial blockage of the conducting pores. McNeal et al. (1966) found a linear relationship between reduction of K_{Sat} and macroscopic swelling of the extracted soil clay. In swelling clay during soil wetting, the swelling process under sodic condition can be highly dispersive because ion hydration and osmotic swelling forces pull water into interlayer spaces between the clay platelets. The swelling forces are pushing clay particles apart and causing the breakdown of the aggregates of swelling soils (Quirk 2001). Furthermore, many of the bonds between particles can be broken at the shear plane of the wetting front during the initial stage of water infiltration into dried soil (Quirk 2001).

Clay swelling due to sodicity has not been noted at ESP less than 15 % (Oster et al. 1980). However, Smith and McShane (1981) and Ayers and Westcot (1985) reported that low salinity irrigation water, especially below 0.2 dS/m, can cause severe infiltration problems regardless of the level of sodicity as a result of an excessive leaching of Ca^{2+} cations in the soil. Frenkel et al. (1978) investigated the change of the water suction along soil columns dominated by montmorillonite, vermiculite and kaolinite at low SAR and electrolyte concentrations of the water applied. The results showed that the hydraulic gradient was increased with depth before decreasing again (Figure 2.6). The increase in suction was higher when diluted water was applied. The results indicate that the upper parts of the soil columns were clogged as a result of clay fraction movement or dispersion.

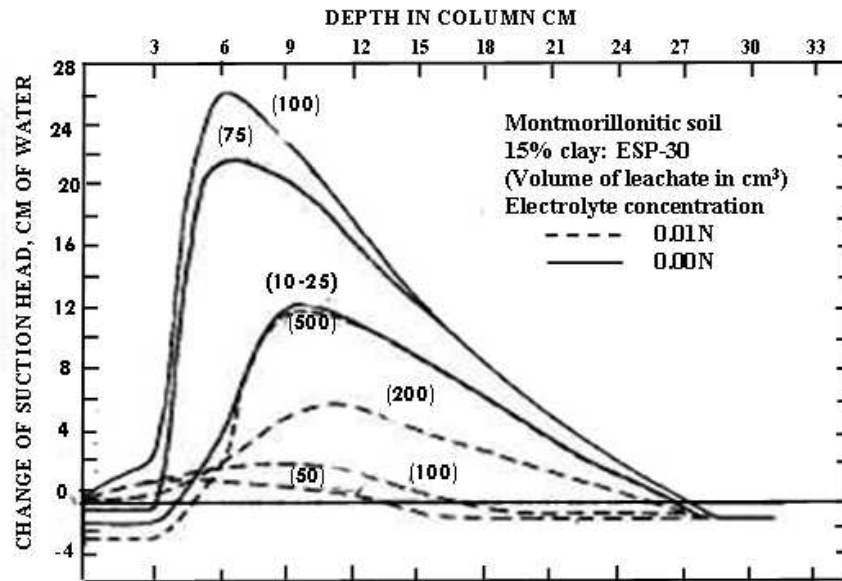


Figure 2.6 Change of suction head produced by leaching a column of soil dominated by Montmorillonite (15% clay, ESP =30) with 0.01N, SAR 30 solution and pure water added

Source: (Frenkel et al. 1978)

Emerson and Bakker (1973) explained that when water with a low electrolyte concentration and SAR was added to the soil, the solute concentration in macro-pores dropped to levels below the critical concentration. As a result, a sharp osmotic gradient will be created between the water solution in micro-pores (i.e. inner pores in clay aggregate between clay layers) and the water in the macro-pores. This osmotic gradient at critical concentration of added water (at which the shear stress on the clay particles exceeds a critical value) will pull the water into the inner pores between the platelets. This in turn leads to clay dispersion of the outer layers of the aggregates and is followed by a decreasing osmotic gradient. A lower osmotic gradient below the critical concentration may cause swelling in the remaining clay aggregates. Although the aggregates do not break down, swelling of the soil aggregates into the inner-aggregate pores occurred (Jayawardane & Beattie 1978). This explanation was experimentally emphasised by Pupisky and Shainberg (1979) in which a wide range of SAR and electrolyte concentration were added to red brown soil columns. In addition, Pupisky and Shainberg (1979) concluded that at low ESP and electrolyte concentration the main process causing degradation of K_{sat} is clay dispersion while swelling is the main reason at higher ESP and soil-water salinity.

The dispersion process might be highly dependent on the osmotic gradient, initiated between the added water solution percolating in macro-pores and water solution in the micro-pores. Keren and Singer (1988) showed that adding deionised water to soil columns after a leaching by 10 mmol_c/litre solutions with SAR 5, 10 and 20 resulted in a sharp decrease in K_{Sat} and the appearance of clay fraction in the outflow. Nevertheless, no clay fraction was noted in the outflow and the reduction of K_{Sat} was less and gradual when applying 10 mmol_c/litre solution and was followed by incrementally lower concentrations before applying deionised water.

The reduction in K_{Sat} under sodic conditions can be interpreted basically as a result of the relative effect between both swelling and dispersion processes. The K_{Sat} reduction is a result of many factors inherent with soil itself and soil condition. Dominant clay types may be a major factor that determines which process prevails. The threshold concentrations concept discussed later in section 2.4.2 is useful to distinguish between the processes of clay swelling and dispersion within the soil. The K_{Sat} reduction within soil might be the result of total effect of clay types within the soil, which may disperse or swell by different manners as affected by many factors associated with soil conditions.

2.3.3 Factors affecting dispersion and hydraulic conductivity

Temporal changes in soil-water content

The effect of temporal changes in soil-water such as the initial water content, rate and ageing of wetting under sodic conditions might have a significant effect on K_{Sat} reduction. Panabokke and Quirk (1957) concluded that the rate of wetting is the main factor causing the breakdown of aggregates or slaking. This result from Panabokke and Quirk (1957) suggests that slaking will result in a further decrease of K_{Sat} . Key and Angers (2000) mentioned that slaking at different initial water content (i.e. result in different initial wetting rates) might shift the pore size distribution toward smaller pores.

Moutier et al. (1998) examined the addition of water at two sodicity levels (i.e. ESP = 0 and 10) to columns of two clayey soils. The K_{Sat} was measured in the soil columns under two different hydraulic gradients (2.9-12 cm) and different ageing durations, which produced different leaching times. For both sodicity levels, the results showed that the lower hydraulic gradient (20 h leaching) maintained significantly higher K_{Sat} compared with leaching under a higher hydraulic gradient (a short period leaching of 3h). In addition, Moutier et al. (2000) evaluated the effect of the rate of leaching with Ca-solutions below a threshold concentration and with distilled water. The results showed that when the soil samples were leached with Ca-solutions, K_{Sat} depends highly on the rate of wetting (i.e. the higher wetting rate the lower K_{Sat} produced). However, leaching with distilled water led to a notable decrease in K_{Sat} irrespective of the wetting rate.

Shainberg et al. (2001) studied the K_{Sat} of five soils, varying in texture with a range of ESP (i.e. 2, 6, 10%) leached with distilled water, as a function of wetting rate. The results indicated that K_{Sat} values at the beginning of the leaching were larger for slow wetting compared with fast wetting. Furthermore, Shainberg et al. (2001) observed that the K_{Sat} of sodic soils decreased more steeply and to lower values with the increase in the rate of wetting. Levy et al. (2005) studied the combined effect of water quality, ESP, and the rate of wetting on the initial, steady state, and relative K_{Sat} of four semiarid soil types varying in texture. They concluded that the wetting rate effect increased with increasing clay content in the soils especially when distilled water was applied. Levy et al. (2005) suggested the wetting rate, sodicity and salinity should not be considered independently but simultaneously to better simulate possible conditions that may prevail in the field.

Clay mineralogy and content

The imperative factor that has been related to soil deflocculation or the reduction of the hydraulic conductivity is the type and the amount of clay mineral content in soil (Goldberg et al. 1991). For example, McNeal and Coleman (1966) found that soils containing high proportions of kaolinite were more stable compared with soils containing montmorillonite. In addition, they noted that dispersion increases with

increase of montmorillonite in soils. Alperovitch et al. (1985) and Oster et al. (1980) found that illite clay was more sensitive to sodicity than montmorillonite. Oster et al (1980) explained that the selectivity for exchangeable Na^+ is greater for illite compared with montmorillonite. McNeal et al. (1968) showed that the K_{Sat} further decreases under sodic conditions when clay content increases in the soil. McIntyre (1979) showed that for soils containing illite clay K_{Sat} decreased linearly with increasing clay content. However, the decrease of K_{Sat} with increasing clay content was not significant for soils containing montmorillonite.

Reduction in K_{Sat} seems to be more complicated in soils of different texture and mixed clay mineralogy. Surprisingly, the change of K_{Sat} can occur in coarser texture soils. For example, Felhendler et al. (1974) found that clay dispersion increased and K_{Sat} decreased in soils with higher silt content compared with other soils that had the same SAR, clay mineralogy, and electrolyte concentration. Pupisky and Shainberg (1979) found that the K_{Sat} in sandy soil with low clay (mixed montmorillonite and kaolinite) content increased because of deflocculation and clay movement out of the soil column. The clay type mixture and soil texture is one of the main factors for determining the soil flocculation condition.

Soil pH

Sumner (1993) explained that soils are composed of a wide range of clay minerals that exhibit both permanent and variable charges of both polarities. He presented the following discussion. *“The change of pH in soil solution has no effect on the flocculation of permanent charge minerals. Conversely, in case of variable charge minerals, the increase of pH above pH_0 (i.e. the pH value at which there is equal numbers of positive and negative charges on the particle surface) increases negative charges. Whereas below it, positive charges increase and soil water solution oppositely charged surfaces would interact owing to the soil system to be flocculated”*. Figure 2.7 illustrates the effect of pH in three soil systems that have permanent charge minerals, variable charge minerals and a mixed soil system that have both types of the clay minerals. The point of zero net charge (PZNC) (Figure 2.7) is defined as the soil pH at which the positive and negative charges in the whole permanent and variable

charges surfaces are equal. A detailed description of the effect of pH on clay charges can be also found in Brady (1990), and Brady and Weil (2008).

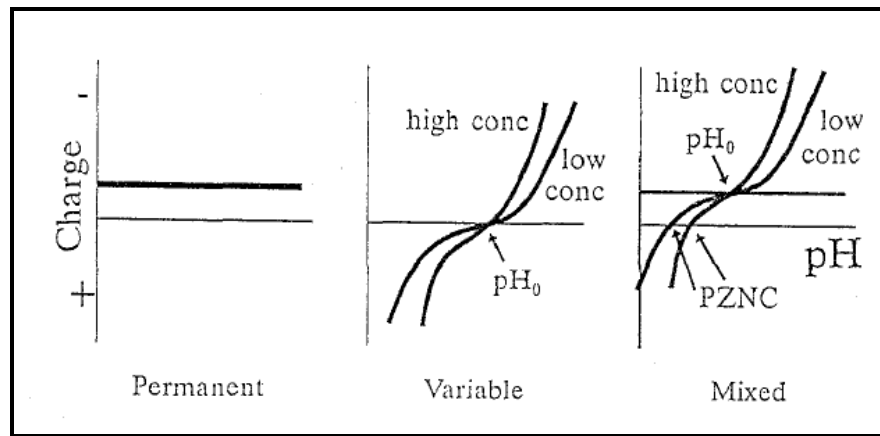


Figure 2.7 Variation in charge with pH and electrolyte concentration of the ambient solution for permanent, variable and mixed charge systems

Source: (Sumner 1992)

The pH of the soil solution is shown to have a significant effect on clay dispersability at a given salinity and sodicity level for most soils. Suarez et al. (1984) examined the effect of a range of pH values including 6, 7, 8, and 9 on K_{sat} for three different soils at constant SAR and electrolyte concentrations. The results showed that the K_{sat} decreased and clay dispersion increased with increase of pH in two clayey soils dominated by montmorillonite and kaolinite respectively. The reason given for this result is differences in the quantities of variable-charge minerals and organic matter. Gupta et al. (1984) found that increasing pH from 6 to 10.8 for a Na saturated soil with a high percentage of illite resulted in an increase in clay dispersion.

It is worth noting that the increase of pH could cause a significant increase of ESP. Khajanchi and Meena (2008) mentioned that there is a linear relationship between ESP and pH of the soil saturated paste. Figure 2.8 shows clearly that a small increase in the pH could result in a large increase of the ESP values. This suggests that the increase of the pH enhances the preference of Na^+ to be adsorbed on clay colloids. It also indicates that the increase of ESP with pH is the main factor that determines the clay deflocculation at given sodicity and salinity levels. Thus, the negative effect of pH on soil deflocculation may be due to the increase of the ESP.

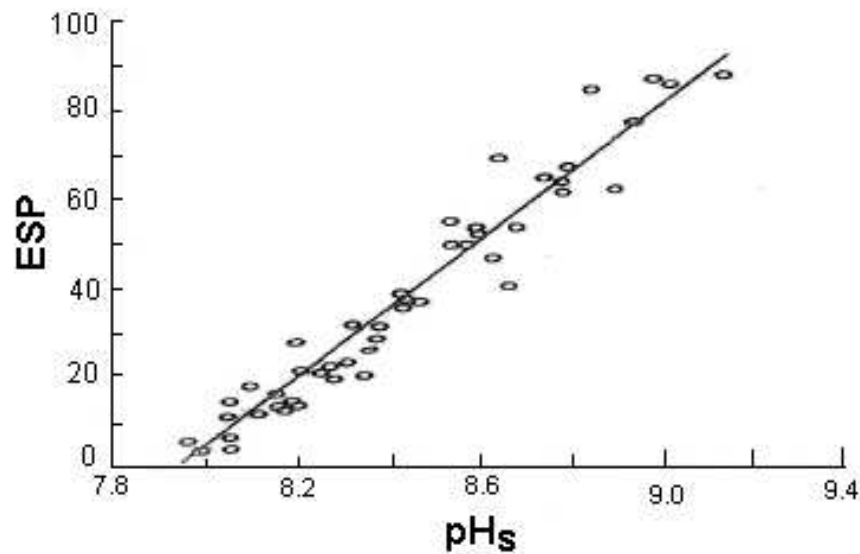


Figure 2.8 Relationship between soil pH at saturated paste and ESP of Alluvial alkali soil

Source: (Khajanchi & Meena 2008)

Organic matter

Quirk (1994) mentioned that organic matter, which can stabilise soil aggregates against slaking, can also induce clay dispersion. He referred to this behaviour as the organic matter paradox. The negative effect of the organic matter has been reported by many researchers. For example Gupta et al. (1984) demonstrated that increasing soil organic matter under moderate to highly sodic conditions (i.e. ESP between 10 and 30) encouraged clay dispersion in soils. They noted that the dispersion is more pronounced in non-calcareous than calcareous soils. Goldberg et al. (1988) showed that organic matter in arid zone soils in which the organic carbon content was below 1% appears to promote clay dispersion. Sumner (1993) concluded that organic matter which has a greater preference for Ca^{2+} over Na^{+} than the clay minerals (Black 1968) may be causing the inorganic clay fraction to become relatively enriched in Na^{+} which then would promote dispersion. Nelson et al. (1999) stated that organic anions enhance dispersion by increasing the negative charge on clay particles and by complexing Ca^{2+} and other polyvalent cations such as those of Al^{3+} , thereby reducing their activity in solution.

However, organic materials such as fungal hyphae and fine roots can help prevent dispersion by stabilising macro aggregates and thereby reducing the surface area from which clay can disperse (Tisdall 1996). Barzegar et al. (1997) concluded that the role of organic matter on clay dispersion is controlled mainly by (a) the degree of sodicity, (b) the nature of the organic matter, (d) the degree of mechanical disturbance and, (e) other characteristics of the soils, such as clay content and type. Barzegar et al. (1997) also investigated the effect of organic matter (i.e. 50 g/kg of Pea- *Pisum sativum* L. straw) added to two different soil types at different levels of sodicity (i.e. SAR 0, 5, 15, and 30) and concluded that organic matter has at least as great a role in aggregation in sodic soils as in non-sodic soils.

2.3.4 Relationships between sodicity, salinity and saturated hydraulic conductivity

Guidelines for evaluating the negative impact of sodicity in terms of K_{sat} according to SAR and irrigation water salinity were developed by Quirk and Schofield (1955). Figure 2.9 shows an example of the guidelines in which the effect of salinity and SAR determine the degradation of soil physical properties and permeability rates.

The division between the deflocculation and the flocculation conditions in a given soil are some what arbitrary because of the change occurs gradually and no clear cut break point exists between the two phases. Quirk and Schofield (1955) and Quirk (1994) proposed two terms to determine the transition phase between the flocculation and deflocculation, and deflocculation to dispersion. These are the Threshold Electrolyte Concentration (TEC) and Turbidity Concentration (TC).

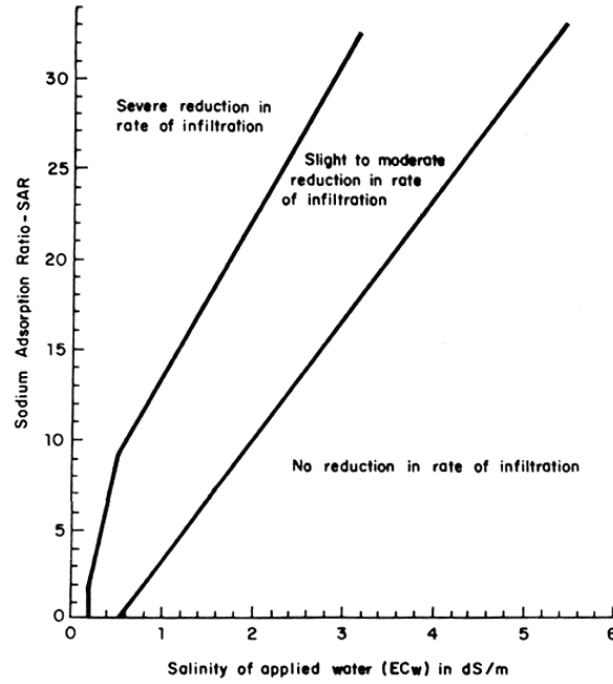


Figure 2.9 The general guideline adopted for relative infiltration as affected by salinity and sodium adsorption ratio

Source: (Ayers & Westcot 1985)

Definitions of the threshold values

Various researchers have identified the boundary between soil flocculation and deflocculation in relation to the total salinity concentration and the SAR of the water applied. The threshold electrolyte concentration (TEC) and turbidity concentration (TC) are the main parameters used to identify the boundary between the flocculation and the spontaneous clay dispersion of the stable soils. Both terms were introduced by Quirk and Schofield (1955) as indicators to identify the degree of soil degradation under sodic conditions. Quirk and Schofield (1955) measured the K_{Sat} in relation to water sodicity and salinity using soil columns equilibrated with solutions at given SAR values and different electrolyte concentrations. The process of Na-Ca exchange equilibrium between soil solution and soil surfaces can be described theoretically by the Gapon equation, which can be expressed as:

$$\frac{EXNa^+}{EXCa^{2+}} = K_G \frac{[Na^+]}{[Ca^{2+}]^{\frac{1}{2}}} \quad (2.14)$$

where $EXNa^+$ and $EXCa^{2+}$ are the amounts Na^+ and Ca^{2+} balancing the charge of the soil's exchange complex in units (mmol/100g_{soil}), K_G is the Gapon selectivity coefficient in units (mmol/litre)^{0.5}. Quirk (2001) explained that if more dilute solutions than the original one are applied while the ratio of $EXNa / EXCa$ is maintained on the exchange complex, then dilution has to be accompanied by a reduction of the Ca^{2+} by the square of the dilution factor for Na^+ .

The Threshold Electrolyte Concentration (TEC)

TEC is defined as the salt concentration at which the soil permeability starts decreasing for a certain sodicity level (Quirk and Schofield 1955). Some level of K_{Sat} reduction might happen because of pore clogging as a natural process of water movement. Water flow can convey fine particles which may plug some of the fine effective pores. Thus, Quirk and Schofield (1955) determined the critical reduction of K_{Sat} at 10 to 15 % of the optimal K_{Sat} value. On the other hand, McNeal and Colman (1966) proposed using 25% reduction as critical values of TEC for some American soils tested. Similarly, Cook et al. (2006) introduced the 20% reduction of K_{Sat} as a critical value to determine TEC. Irrespective of the reduction percentage selected as threshold, it is clear that the usefulness of TEC is to determine practical values of K_{Sat} reduction, which may vary with different soil types.

The Turbidity Concentration (TC)

TC was defined as the salt concentration at which clay fractions appear in the percolated water (Quirk & Schofield 1955). Quirk (2001) explained that the turbidity concentration indicates that soil microstructure is becoming unstable and increasingly so as the amount of turbidity increases as ESP increases and as the salinity concentration of the percolated solution decreases. The reduction of K_{Sat} may occur before the fragments of the clays appear in the outflow (Figure 2.10).

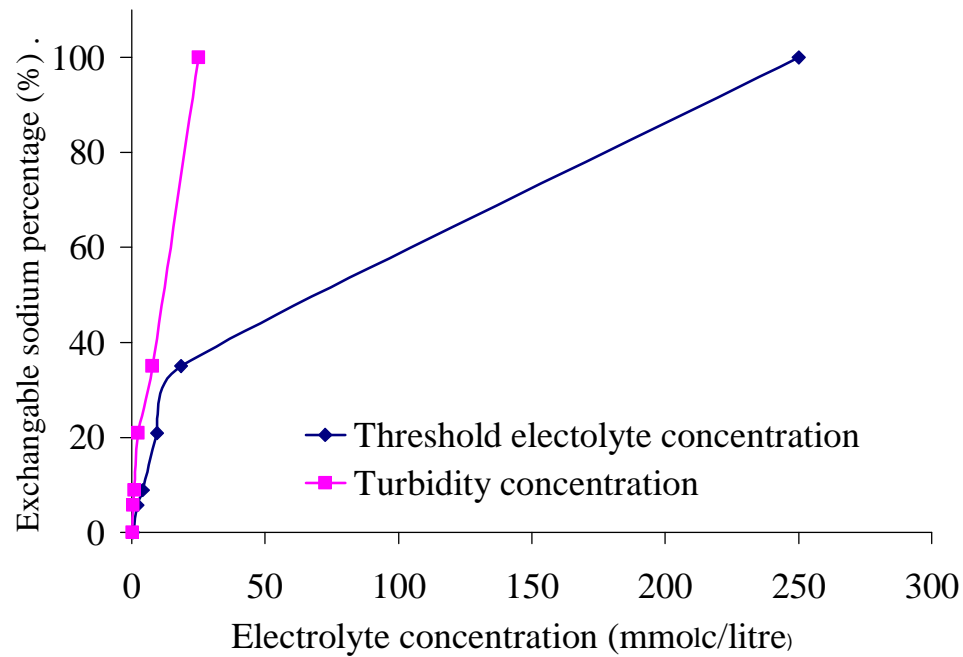


Figure 2.10 Concentration of electrolyte required to maintain permeability (10-15% reduction) in Sawyers I soil for varying degrees of sodium saturation

Based on data from Quirk and Schofield (1955)

It should be noted that the misperception of the threshold electrolyte concentration reported in the literature rises essentially from the mystification of a difference between the clay flocculation to dispersion transition and dispersion to flocculation transition conditions. Quirk (2001) has observed the widely held misconception of the definition of the threshold electrolyte concentration (required to maintain a stable permeability) as that electrolyte concentration required to flocculate a dispersed suspension of the soil. He has drawn attention to the difference between the transition condition from flocculation to deflocculation condition and the flocculation of dispersed clay suspensions. The flocculation to dispersion transition condition involves face to face interaction and requires lower electrolyte concentration at a given level of sodicity to deflocculate. However, the dispersion to flocculation transition involves edge to face interaction for clay suspension and occurs at higher electrolyte concentration. Wearing (2004) indicated that the smaller turbidity concentration is because the particles have to be removed from a potential well where the clay crystals overlap.

At a given sodicity level the flocculation concentration (FC) in the dispersion to flocculation transition is much greater than both the TEC and TC. Rowell et al. (1969) found that at ESP values of 21, the ratio of TC to TEC to FC was 1: 3.5: 7. This result shows that soil-water having salinity below FC and above TEC will have no effect on soil structural stability when the flocculation to dispersion is the case. In addition, Wearing (2004) recommended that FC should not be used as an estimate of threshold concentration because of the effect of the peptising agents. In the case of the dispersion to flocculation transition condition, the dispersing of the peptising agents such as organic matter could affect clay flocculation and eventually raise the FC values.

The TEC and TC are determined by the soil type and vary with other soil properties (Rengasamy et al. 1984). The variation of TEC is mainly caused by the differences of the clay mineral contents and soil texture (Frenkel et al. 1978; McNeal & Coleman 1966). Various researchers have developed soil stability indicators for different soils in relation to the total salinity concentration and SAR of the water applied as shown in Figure 2.9 (Ayers & Westcot 1985; Quirk & Schofield 1955; Rengasamy et al. 1984).

It is worth noting that substituting SAR by ESP can improve the visual graphs for a set of soil types. McNeal and Coleman (1966) found that using estimated ESP from SAR of added water to express sodicity further reduces the variation among TEC curves. This improvement can be noted from Figures 2.11 and 2.12. This is because ESP is a percentage limited between 0 and 100% which compresses the curves. ESP may be an appropriate way to evaluate the sodicity problem for a set of soil types. Therefore, for a family of soils that has similar general characteristics, expressing the sodicity as ESP values could generalise the soil stability indicators.

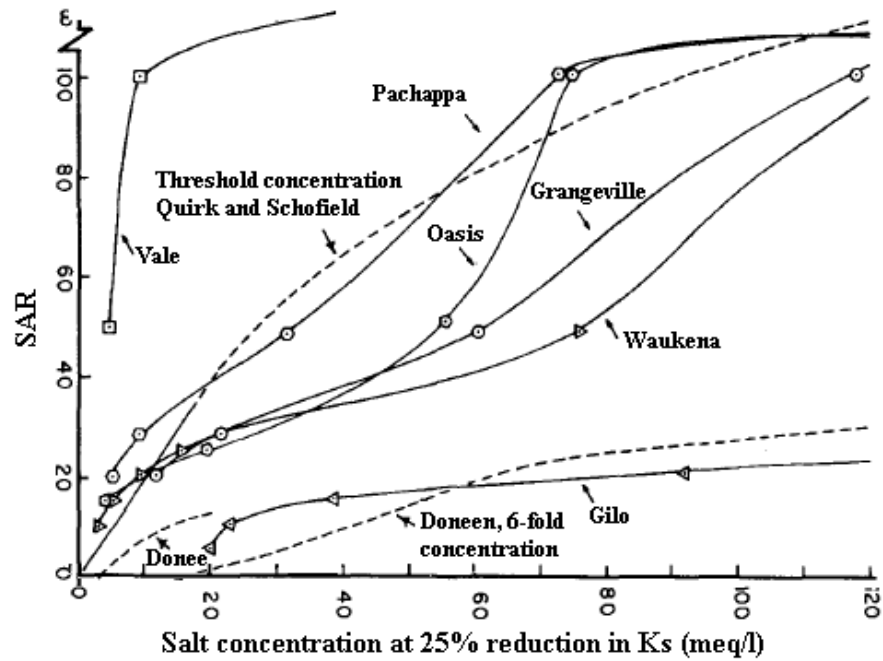


Figure 2.11 Combinations of salt concentration and SAR at which a 25% reduction in hydraulic conductivity occurred

Source: (McNeal & Coleman1966)

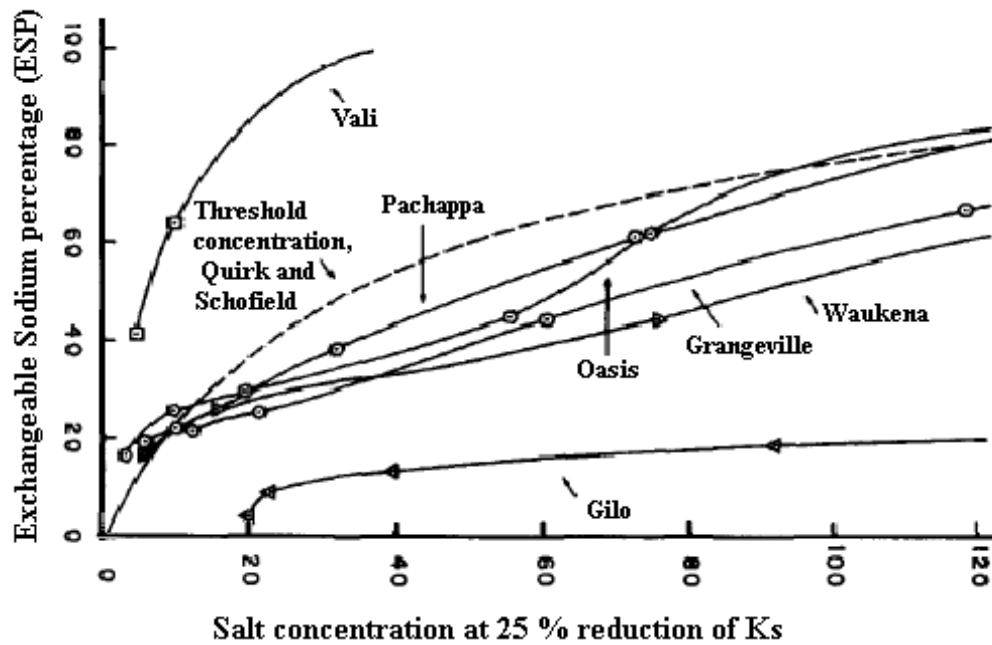


Figure 2.12 Combinations of salt concentration and ESP at which a 25% reduction in hydraulic conductivity occurred

Source: (McNeal & Coleman1966)

2.3.5 Quantifying the change in saturated hydraulic conductivity due to sodicty

The preceding discussion regarding the factors that affect K_{Sat} suggested that the main processes of the K_{Sat} reduction in soils containing expanding clay are swelling followed by dispersion. McNeal and Coleman (1966) and later on Jayawardane and Beattie (1978) showed that there is a sigmoidal relationship between the reduction of K_{Sat} and the logarithm of electrolyte concentrations at a given SAR. McNeal (1968) proposed a semi-empirical approach based on a clay-swelling model. In his model, the effect of salinity and sodicty in soils is evaluated using a swelling factor. The swelling factor is used to predict whether the sodium and solute concentration will induce soil physical degradation or flocculation (Warrence et al. 2003). Furthermore, McNeal (1968) used a semi-empirical equation to fit experimental data of the relative K_{Sat} at different combinations of SAR (converted to ESP) and the electrolyte concentration to the swelling factor calculated. The predictive interlayer swelling (i.e. swelling factor) was estimated by an empirical relationship generated from a demixed-ion distribution model for Na-Ca clay systems as:

$$1 - RK_{Sat} = \frac{cx^n}{(1 + cx^n)} \quad (2.15)$$

where RK_{Sat} is the relative saturated hydraulic conductivity, x is swelling factor (i.e. the calculated interlayer swelling of soil Montmorillonite), and c and n are constants for a given soil within a specified range of ESP.

Likewise, Lagerwerff et al. (1969) proposed a physical model in which the reduction of K_{Sat} was predicted by the Kozeny-Carmen equation (Carman 1937, 1948) after an empirical correction was made to the change of effective porosity based on clay swelling (i.e. the conducting porosity that conveys the water into the soil). Clay swelling was calculated based on diffuse double layer theory.

Mustafa and Hamid (1977) compared both the aforementioned models for two clay soils from Sudan. It was concluded that the McNeal model produced a better

prediction of clay swelling. The Lagerwerff model failed to predict the swelling. However, both models were able to demonstrate the decrease of K_{Sat} due to sodicity for both soils especially at higher values of electrolyte concentration and SAR. The failing of the Lagerwerff model might be as a result of limitations inherent with diffuse double layer and Kozeny theories as described by Lagerwerff et al. (1969). In addition, Russo and Bresler (1977b) stated that the Lagerwerff model can not always be applied to the soil material with its wide range of pore size distribution and the complex geometry of the flow paths.

Yaron and Thomas (1968) found that the relative hydraulic conductivity can be related linearly to average ESP of soil columns at a given C_o as:

$$\frac{K_{Sat}}{K_{Sat}^{Max}} = 1 - \beta(ESP - ESP_T), \text{ when } ESP > ESP_T \quad (2.16)$$

where β is an empirical parameter which depends on soil type and clay mineralogy, ESP_T is the critical average ESP at which K_{Sat} began to decline for given salinity, K_{Sat}^{Max} is the maximum saturated hydraulic conductivity under normal condition, and K_{Sat} is the measured saturated hydraulic conductivity under given level of average ESP.

Results from Yaron and Thomas (1968) showed that the parameter β is not consistent over different C_o values which indicate that this empirical equation might not be applicable at a certain level of salinity. In addition, Yaron and Thomas (1968) derived equation 2.16 using water with low electrolyte concentration (i.e. 11.3 to 34.5 mmol_e/litre) and a range of water sodicity added to the soil columns having SAR values between 2.8 to 28.5. However, Pupisky and Shainberg (1979) showed that the reduction in relative saturated hydraulic conductivity (RK_{Sat}) with increase of SAR at certain C_o is sigmoidal in shape as in Figure 2.13. Thus, equation 2.16 was derived over a narrow range of SAR in which the K_{Sat} reduction usually exhibits a linear decrease. Therefore, using such a model for water having higher SAR values is questionable.

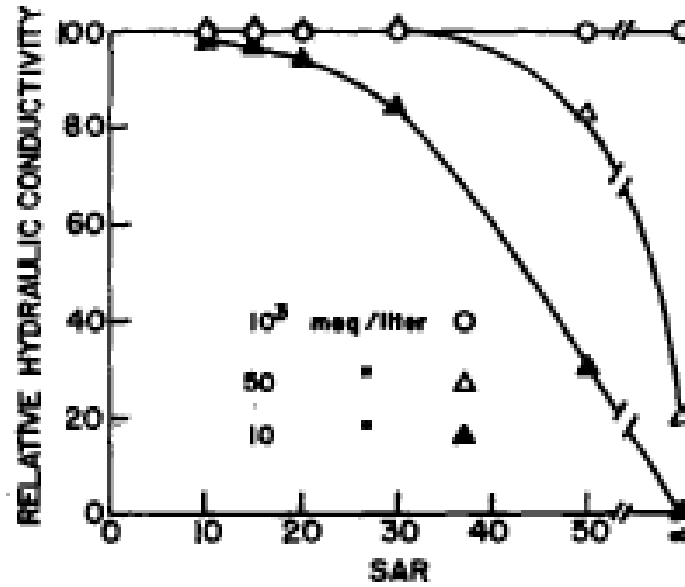


Figure 2.13 Relative hydraulic conductivity of the soil as a function of solution concentration and composition (solution concentration > 0.01N)

Source: (Pupisky & Shainberg 1979)

Jayawardane (1979) proposed a different approach to predict the reduction in K_{Sat} due to raising sodicity using the equivalent salt solutions method. The equivalent salt solutions are defined as solutions with combinations of SAR and C_o producing the same extent of clay swelling in a given soil (Jayawardane 1979). Thus, the K_{Sat} reduction for this set of added solutions should be equal. Furthermore, the increase of sodicity level will be reducing the pore size for a given soil. Thereby, the assumption was made that the equivalent salt solutions should produce identical soil-water characteristic curves or the same pore size distributions. The equivalent salt solutions which produce the same reduction of K_{Sat} were assigned to the value produced of the pore size index (PSI) under this condition. The PSI is similar to that described by (Childs 1940) and redefined in Jayawardane & Beattie (1978) as the ratio between the equivalent pore neck radius (ζ) produced in the soil when solutions of lower electrolyte concentration are added (i.e. where the K_{Sat} reduction is notable) to β for the soil when solution of the highest electrolyte concentration (i.e. insignificant change in K_{Sat}) at given level of SAR. The PSI has values between 0 and 1. The ζ can be obtained by differentiating soil-water characteristic curves and using the relationship between the radius of a capillary tube and the matric potential.

The pore size index was used as a quantitative evaluation of the effect of C_o and SAR on K_{sat} . However, Jayawardane (1983) used the clay swelling factor as described by McNeal (1968) instead of the PSI. Furthermore, Jayawardane (1992) extended the equivalent salt concentrations concept to predict the unsaturated hydraulic conductivity (K_{Unsat}) based on swelling factor as described by McNeal (1968).

2.3.6 Relationships between sodicity, salinity and unsaturated hydraulic conductivity

Water flow in soil at moisture contents below saturation moves through a part of pores. If a steady state is reached, the Darcy equation can be applied under unsaturated conditions by involving matric potential instead of pressure head in the hydraulic gradient. In addition, the unsaturated hydraulic conductivity (K_{Unsat}) (as a function of water content or matric potential) replaces the K_{sat} . This version of the Darcy law is known as the Buckingham- Darcy law (Buckingham 1907). K_{Unsat} depends on the proportion of pores that are filled by water and can convey it. K_{Unsat} decreases with decrease of water content and matric potential. K_{Unsat} can be predicted from the soil-water characteristic curve (SWCC) as described by many researchers (e.g. Kosugi 1996; van Genuchten 1980; Vogel & Cislerova 1988). Furthermore, the SWCC is highly depended on the pore size distribution within the soil. A higher proportion of smaller pores increases the residual water content at a given matric potential, resulting in rising of K_{Unsat} at that level. However, the water content at a given matric potential comprises the amount of water retained in soil micro-pores below that matric potential. Thus, water in micro-pores might be below the limitation of laminar flow equation (Darcy law). Therefore, as the micro-pore water proportion increases the actual unsaturated water flow within the soils might be decreased, which is expected in higher clay content soils.

Sodicity results in a dual change in soil structure (Gonçalves et al. 2007). Whilst the ratio of macroscopic pores is reduced as a result of clay swelling and dispersion, the soil pores are expected to shift to smaller size with applying sodic water (Levy 2000). As it

generally thought that this process leads to an opposite change in K_{Sat} and K_{Unsat} . K_{Sat} is decreased while K_{Unsat} is significantly increased at a moderate to low range of water contents. Goncalves et al. (2007) measured the K_{Unsat} using the instantaneous profile method in a soil profile irrigated with sodic treated sewage effluent. The soil has generally low clay percentage. The result showed that the K_{Unsat} increased under sodic conditions especially at a low and intermediate range of water contents, while a lower increase was noted in K_{Unsat} at higher water content.

However, the magnitude of K_{Unsat} change seems to be highly affected by the increase in the proportion of micro-pores that retain water. Early results from Russo and Bresler (1977a) over the range of suction of 0 to 1 bar in loamy soil showed that the K_{Unsat} and the diffusivity are dramatically decreased with the increase of the SAR in solutions applied to loamy soil columns. The reduction was higher at low electrolyte concentration. The findings from Russo and Bresler (1977a) showed that while the water content at a given suction increased with rising sodicity, the actual K_{Unsat} decreased. Figures 2.14 and 2.15 show the change of soil water characteristic curves and corresponding measurements of K_{Unsat} at different SAR and solution concentrations.

The interpretation given is that the swelling or the space between platelets increases. This, in turn, raises the amount of water held in the soil micro-pores in which the water is retained in-between the clay layer, this water does not participate in the water flow. These synthesis results from literature indicate that the clay percentage or soil texture may determine the magnitude of the K_{Unsat} change, especially at moderate to lower water contents. In other words, despite higher water content, the effective porosity at which water flow occurs might be reduced or increased significantly.

Russo and Bresler (1977b) proposed a model to predict the unsaturated hydraulic conductivity under sodic conditions involving the porous nature and electrical properties of the soils (Diffuse Double Layer model (DDL)). However, the model was found to be sensitive to the number of clay platelets in clay particles at a given level of ESP.

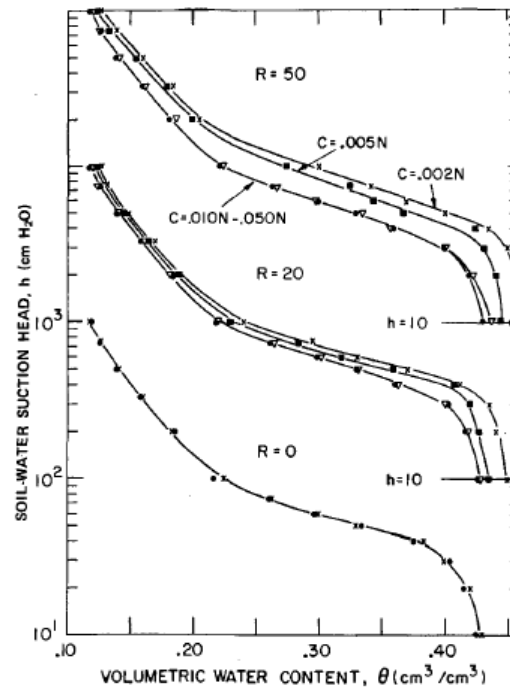


Figure 2.14 Soil-water suction head (h) as a function of volumetric soil-water content and solution concentration, for three SAR values (i.e. 0, 20, and 50)

Source: (Russo & Bresler 1977a). Note that $h=10$ (indicated by the arrows) is shifted and the data are translated along the h -axis.

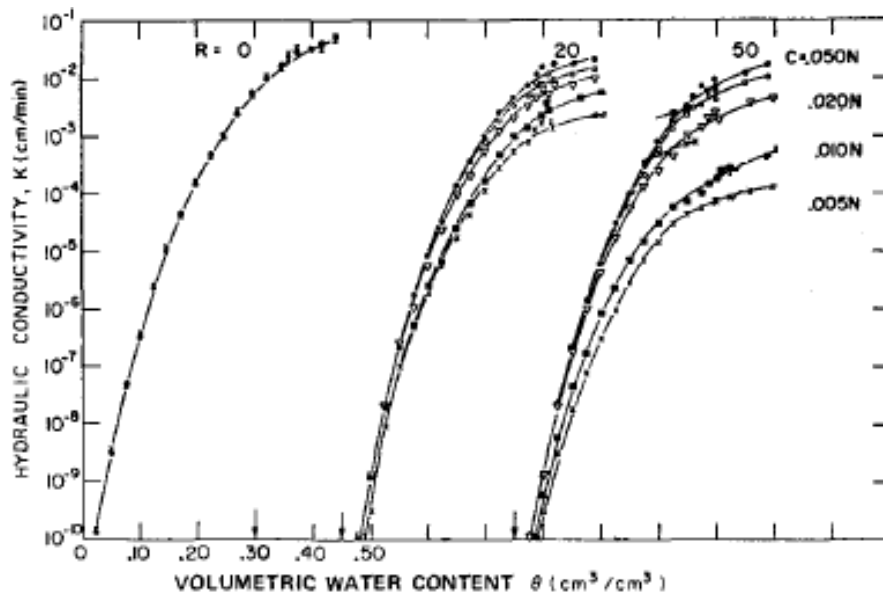


Figure 2.15 Unsaturated hydraulic conductivity values as a function of volumetric soil-water content and the solution concentrations for three values of SAR (i.e. 0, 20, and 50)

Source: Modified from Russo and Bresler (1977a). Note that the curves corresponding to other values of SAR in the original graph have been removed to facilitate the comparison with Figure 2.14

Simunek et al. (1996) concluded that the reduction of K_{Unsat} can be determined from K_{Unsat} function derived from the SWCC. The method assumes that the sodicity effect acts in the same manner at low water content. Since the K_{Unsat} as a function of (h) can be determined from the SWCC as:

$$K_{Sat} = r K_{Sat}^{Max} \quad (2.17)$$

where r is a general reduction function account for the sodicity effect and K_{Unsat} can be calculated as (van Genuchten 1980):

$$K_{unsat} = K_{sat} K_{(h)} \quad (2.18)$$

where $K_{(h)}$ is the relative hydraulic conductivity, which might be determined as described by (van Genuchten 1980) as:

$$K_{(h)} = S_e^{1/2} \left[1 - (-S_e^{1/m_i})^{m_i} \right]^2 \quad (2.19)$$

where S_e is the relative water saturation in the soil, and m_i is an empirical parameter depending on the soil type. By substituting equations 2.17 and 2.19 into equation 2.18, the resultant relationship is (Simunek et al. 1996):

$$K = r K_{Sat}^{Max} S_e^{1/2} \left[1 - (-S_e^{1/m_i})^{m_i} \right]^2 \quad (2.20)$$

Equation 2.20 is useful to predict the reduction of K_{Unsat} at higher water content, particularly in clayey soils. However, equation 2.20 does not account for the rapid increase or decrease of K_{Unsat} at moderate and low water content, especially in more coarse or fine textures. Nonetheless, under irrigation, water is usually applied to maintain the soil-water content at a relatively high level. Hence, equation 2.20 satisfies the needs to quantify solute and water movement.

2.4 Sodicity management under irrigation water

Improvements observed in the soil physical properties under sodic condition during the amelioration process have been attributed mainly to an increase in Ca^{2+} levels, both in the soil solution and on the exchange complex (Qadir et al. 2006). Maintaining sufficient levels of Ca^{2+} involves addition of amendments to either the irrigation water or soil. The amendments can be categorised in two groups. The first group are those that work as an independent source of Ca^{2+} such as gypsum ($\text{CaSO}_4 \cdot 2\text{H}_2\text{O}$) and calcium chloride ($\text{CaCl}_2 \cdot 2\text{H}_2\text{O}$). The second group are those used to promote the dissolution of domestic Ca^{2+} available within the soil (especially calcareous soils) (Hussain et al. 2001). Examples for those amendments are sulphuric acid (H_2SO_4), sulphur (S), and ferric sulphate ($\text{Fe}_2(\text{SO}_4)_3$) (Qadir et al. 2006).

Marginal water in irrigation containing relatively high sodium concentration can be managed by blending (Qadir & Oster 2004). Mixing saline-sodic water by the ratio of 1:1 with good quality water reduces the water salinity to 50% and the SAR to about 71%. Irrigation water containing high levels of bicarbonates have been ameliorated using sulphuric acid. Applying gypsum to irrigation water is useful in terms of reducing the water sodicity and the bicarbonate concentrations (Ayers & Westcot 1985). Using blending concurrently with amelioration could provide appropriate management to saline-sodic irrigation water.

Use of Sulphuric Acid Generators (SAG_s)

SAG_s are a recently introduced technology to treat saline-sodic waters. Sulphur (S) is burnt to produce sulphur dioxide gas (SO_2) in a chamber, which is dissolved in a fraction (10-15%) of irrigation water to form sulphuric acid (H_2SO_4). H_2SO_4 neutralises carbonate (CO_3^{2-}) and bicarbonate (HCO_3^-) ions in water resulting in a decrease in residual sodium concentration (RSC) of the treated water (Doneen 1975). Theoretically, this will not ameliorate water salinity and SAR (Amrhein 2000). Zia et al. (2006) evaluated using sulphuric acid generators (SAGs) and did not find any significant soil physical benefits.

Gale et al. (2001) treated the irrigation water applied with of a sulphuric acid (5%) and did not find any significant differences in the water quality, soil properties or crop (lucerne) responses. They concluded that the use of either acid injection or sulphur burners should be preceded by a thorough evaluation of irrigation water quality and soil properties in terms of economical achievement.

It should be noted that H_2SO_4 has been used to reclaim sodic soils. Gale et al. (2001) suggested that the main effect of sulphur in the treatment of a sodic soil is not through direct acidification, but rather by dissolving lime and releasing Ca^{2+} which replaces sodium and allows it to be leached from the soil. In this case, excess water must be applied to leach sodium, which is often difficult in poorly drained soils.

Use of gypsum amendment

Calcium sulphate dihydrate, which is known as gypsum ($\text{CaSO}_4 \cdot 2\text{H}_2\text{O}$) has been widely used as a Ca^{2+} source to replace sodium on the soil exchange complex. Among the other amendment materials, gypsum is comparatively cheap, generally available, and easy to apply (Qadir et al. 2006). The application of gypsum to soils will both increase the soil solution salinity and exchangeable Ca^{2+} levels in the soil. Both of these actions reduce the inter-particle swelling pressures and the potential for dispersion.

Surface application of gypsum generally increases infiltration rates and reduces dispersion but the process is sometimes slow because the gypsum solubility is low. Mixing the gypsum into the soil surface layers accelerates the reclamation process because the Ca^{2+} is physically placed where it can react. Leaching removes gypsum from the upper part of the soil profile where the major problems of dispersion and hard setting are located. Thus, periodic applications are necessary to both maintain adequate electrolyte to prevent dispersion and slumping and to slowly reduce the ESP level (Chartres et al. 1985; Greene & Ford 1985).

Gypsum has also been dissolved in irrigation water to improve water quality by increasing the electrical conductivity, reducing the SAR and reducing the RSC. Davidson and Quirk (1961) concluded that the dissolved gypsum which produces a concentration of Ca^{2+} up to 10 mmol_c/litre is sufficient to maintain flocculation of colloidal clay having ESP about 20%.

However, gypsum has low solubility (Kernebone et al. 1986). The solubility of gypsum is estimated to be about 0.30 g/ 100 ml of water at 25 C° (USSL Staff 1954). The solubility of gypsum increases to produce an additional 2-4 mmol/litre in flowing irrigation water (Ayers & Westcot 1985; Doneen 1975).

Gypsum solubility is highly affected by its particle size, temperature, and the water salinity. Fine gypsum particles are quicker to dissolve (Mater et al. 1990). The solubility of gypsum increases with increase in temperature. The optimal temperatures for maximum gypsum solubility are between 35° to 50° C (Mater et al. 1990). Furthermore, the solubility of gypsum increases with increasing electrolyte concentration.

For example, the solubility of gypsum sharply increases with an increase in NaCl concentration at low salinity concentrations (Figure 2.16). Furthermore, the solubility of gypsum tends to further increase in the presence of bicarbonates. This is because bicarbonates in water have a tendency to increase water pH and decrease the solubility of calcite (CaCO_3) (Mater et al. 1990). Wallace (2003) explained that if soil or irrigation water contains bicarbonate ions, the soluble Ca^{2+} in gypsum reacts with bicarbonates to form insoluble Ca^{2+} carbonate. Subsequently, the pH decreases to the range of 7.5 to 7.8. Chorom and Rengasamy (1997) found that the direct application of gypsum to alkali soil in laboratory plots reduced the soil pH from 9.38 to 7.89.

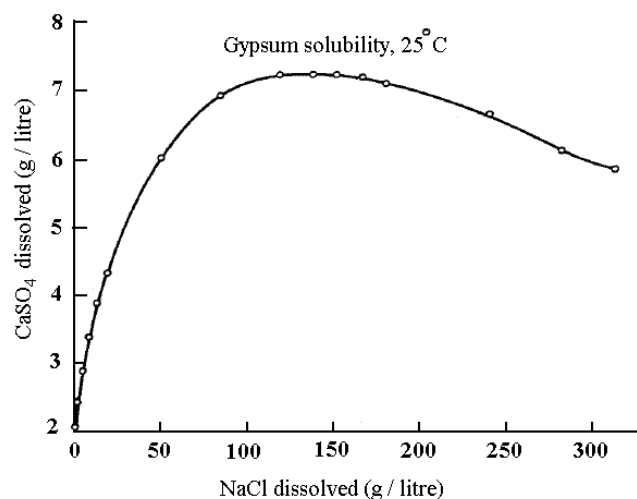


Figure 2.16 Solubility of gypsum in aqueous solutions of different NaCl concentrations at 25° C, and 1 atmospheric pressure

Source: (Shternina 1960)

2.5 Soil hydraulic changes due to sodicity in modelling water- solute movement

There are limitations of the models that can handle water and solute movement associated with soil chemical reactions under sodic conditions (Qadir et al. 2006). Simulation of soil-water flow and chemical processes under highly sodic conditions requires a consideration of the effect of soil structural degradation on water and solute transport under variable water content conditions. Modelling of unsaturated water and solute flow coupled to equilibrium major ion chemistry has been carried out by a number of researchers (e.g. Robbins et al. 1980a; Russo 1986; Seetharam et al. 2007; Wagenet & Hutson 1987; Yeh & Tripathi 1991). In most of these models, the main assumptions are; a) the chemical reactions are in equilibrium state, and b) the pH with soil depth is either assumed constant or related to fixed concentrations of CO₂ with soil depth. Simunek and Suarez (1994) developed a two-dimensional model (UNSATCHEM 2D) with unsaturated water flow and major ion chemistry in which CO₂ production and transport is considered. However, the change of soil structure was ignored in all aforementioned models. Furthermore, evaluation of these models in either laboratory or in field conditions is limited (Suarez & Simunek 1997).

Simunek et al. (1996) developed a model (UNSATCHEM) that takes into consideration the change of physical properties as a result of the chemical conditions of the soil-water. The reduction of K_{Sat} has been used as an indicator of soil degradation due to sodicity. The magnitude of reduction of K_{Sat} has been related mathematically to sodicity and salinity levels in soil solution. Simunek et al. (1996) assumed a relationship between the reduction of K_{Unsat} and reduction of K_{Sat} ; the reduction of K_{Unsat} can be described at corresponding combined levels of sodicity and salinity. The soil chemical reactions model provides a temporal and spatial quantitative prediction of major cation concentrations (i.e. Ca⁺², Mg⁺², and Na⁺) during water and solute movement. The cation concentrations predicted are used to calculate the chemical parameters required such as SAR or ESP and electrolyte concentration, which allow predicting both soil sodicity and salinity. This, in turn, can be used to determine the reduction of K_{Unsat} using the reduction function.

2.6 Conclusions

Degradation of soil permeability can produce complex problems related to waterlogging and aeration along with the potential to develop salinity problems. It is necessary to maintain a sufficient soil permeability to leach the salt out of the root zone. High relative sodium concentrations result in adverse effects. The structural stability of soils which have reactive clay is dependent on the interaction between the sodicity and salt concentration in the soil solution. The primary processes responsible for soil structural degradation are clay swelling and dispersion.

The processes of spontaneous swelling and dispersion that affect the saturated hydraulic conductivity can be explained using both TEC and TC concepts. The reduction of K_{Sat} at the values below the TEC occurs mainly due to swelling, while dispersion is the main cause below the TC. However, each soil has specific relationship for TEC and TC due to differences in clay mineralogy, pH, soil texture, climatic conditions, and organic matter. Irrigation practices also affect temporal changes in soil-water (e.g. initial water content, rate and ageing of wetting) under sodic conditions which also have a significant effect on K_{Sat} .

The effect of sodicity is more complicated in unsaturated soils. Sodicity results in a change in soil pore size distribution. The number of macroscopic pores is reduced as a result of clay swelling and dispersion. However, the number of smaller soil pores increases. Hence, K_{Sat} is decreased while K_{Unsat} may increase at moderate to low water contents.

The management of soil sodicity is usually carried out using amendments. The amendments may be added to either the irrigation water or directly to the soil. Amendments may either counter the effect of rising sodium levels or stabilise soil structure. The use of soil amendments such as gypsum is often necessary for successful management. Blending with better quality water is also common in irrigation systems utilising saline-sodic water.

Modelling may be used to evaluate management strategies for the use of saline-sodic water. The effect of sodicity on soil physical properties has been presented in the UNSATCHEM model in which the soil chemical conditions are related to the physical conditions. The effect of sodicity was incorporated into the UNSATCHEM using a hydraulic conductivity reduction function that includes clay swelling (McNeal 1968) and pH (Simunek et al. 1996). However, there has been limited research using this model and the assumption underpinning the reduction function parameters have not been evaluated for different soils. Therefore, there is a need to validate this model and approach before it can be used to investigate different water quality and irrigation management options.

CHAPTER 3: Long Column Laboratory Experiment to Evaluate the Change in Hydraulic Conductivity with the application of Saline-Sodic Water

3.1 Introduction

Soil structure and permeability will change with the application of saline-sodic water (chapter 2). The degree of reduction in hydraulic conductivity will depend on the level of sodium in the soil-water. However, the effect of sodicity varies and is highly dependent on factors such as soil condition, soil solution pH, method of adding the water, quality of irrigation water and management practices.

This chapter reports on a laboratory experiment conducted using soil columns to investigate the reduction in the saturated hydraulic conductivity (K_{sat}) with decreasing concentrations of applied saline-sodic irrigation water. The experiment also investigated the effect on K_{sat} of reducing the pH of the applied water, and of diluting the saline-sodic water and adding a gypsum amendment. In addition, good quality water (i.e. 0.4 and 0.1 dS/m respectively) was applied to the soil columns after the application of water treatments. The data from these experiments is also used to validate the UNSATCHEM model in chapter 4.


3.2 Materials and methods

3.2.1 Soil collection and preparation

Disturbed samples of two virgin soils were collected from Windibri station, Chinchilla, QLD. Approximately 200 kg of each soil was collected from < 20 cm depth in the soil profile. The soils were classified as a Sodosol and a Vertosol (Isbell 2002). The Field


description of the Sodosol and Vertosol soil profiles are shown in Table 3.1 and 3.2. Selected chemical properties for both soils are presented in Table 3.3.

Table 3.1 Field description of the Vertosol soil profile

	0 to 20 cm Black medium heavy clay with strong grade of polyhedral structure and ped size of 3 cm breaking to 1 cm. Soil is not dispersive, completely slakes, has a poor to moderate SOILpak score and has an average number of roots present.
	20 to 50 cm Black medium heavy clay with strong grade of prismatic structure and ped size of 2 cm breaking to 1 cm. Soil is slightly dispersive, completely slakes, has a poor SOILpak score and has an average number of roots present.
	50 to 130 cm Black medium heavy clay with strong grade of polyhedral structure and ped size of 10 cm breaking to 1 cm. Soil is moderately dispersive, completely slakes, has a moderate SOILpak score and has few roots present.

Source: (QGC 2009)

Table 3.2 Field description of the Sodosol soil profile

	0 to 10 cm Black sandy clay loam with moderate grade of subangular blocky structure and ped size of 2 cm breaking to 0.5 cm. Soil is slightly dispersive, partially slakes, has a moderate SOILpak score and has many roots present.
	10 to 45 cm Brown sandy clay loam with moderate grade of columnar structure and ped size of 20 cm breaking to 0.5 cm. Soil is moderately dispersive, completely slakes, has a moderate SOILpak score and has few roots present.
	45 to 60 cm Grey sandy clay with strong grade of polyhedral structure and ped size of 5 cm breaking to 0.5 cm. Soil is slightly dispersive, completely slakes, has a moderate SOILpak score and has few roots present.
	60 to 140 cm Grey sandy clay with strong grade of polyhedral structure and ped size of 5 cm breaking to 0.5 cm. Soil is moderately dispersive, partially slakes, has a poor to moderate SOILpak score and has no roots present.

Source: (QGC 2009)

Table 3.3 Selected chemical properties for the soils used in the experiment

Chemical analysis	Soil type	
	Sodosol	Vertisol
ECe (dS/m)*	0.18	0.52
pH	7	8.3
CEC (mmol _c /kg)	99	270
ESP %	3.5	10.9
Exch. Na ⁺ (mmol _c /kg)	4	29
Exch. Ca ⁺² (mmol _c /kg)	60	154
Exch. Mg ⁺² (mmol _c /kg)	31	83
Exch. K ⁺² (mmol _c /kg)	4	4
SO ₄ ²⁻ (mg/kg)	21	-
Cl ⁻ (mg/kg)	10	39

(Source: Sustainable, Soils & Management 2005)

*Electrical conductivity of saturated extract estimated from $EC_{1:5\text{soil:5water}}$

The soils were spread on plastic sheets and left to air dry for a minimum of 5 days. Thereafter, the soils were crushed using an iron hammer and passed through a 9.5 mm sieve. Each soil was also thoroughly mixed to ensure that the samples were uniform.

3.2.2 Soil columns

Plastic pipes 300 mm height and 90 mm inner diameter were used to form the soil columns. The pipes were closed at the bottom using a rigid plastic net which was fixed using tape and reinforced by a rubber band. A filter paper (whatman No. 4) was placed at the bottom of each column and 200 mm of soil added to the column. The soil was loosely poured into the columns in increments of 50 mm height and dropped 5 times from height of 20 mm to ensure uniform packing. The density of the Sodosol and Vertisol soil columns was $1.14 \pm 0.01 \text{ g/cm}^3$ and $1.32 \pm 0.02 \text{ g/cm}^3$, respectively. The remaining space above the soil was left for the water head. Finally, a filter paper was placed on the top of each soil column to avoid soil disturbance when the solutions were being added to the column.

3.2.3 Measurement of saturated hydraulic conductivity

The constant head method (Klute 1965) was used to measure the K_{sat} . When the K_{sat} was less than 2 mm/h, the falling head method (Klute 1965) was used to more accurately determine the K_{sat} . The bench system allowed measurement of up to ten soil columns simultaneously (Figure 3.1). One litre plastic bottles were used to apply the constant head (≈ 80 mm) of each water treatment to the top of each column. The outflow was collected in beakers at the bottom of the column. Measurements of outflow were tabled in increments of not less than 10 minutes where the discharge (flux) was > 100 ml/h. The period was incremented up to a maximum of 12 hours for smaller discharge. The plastic bottles were refilled and maintained until at least four litres (i.e. 7 pore volume) of the water treatment had been applied.

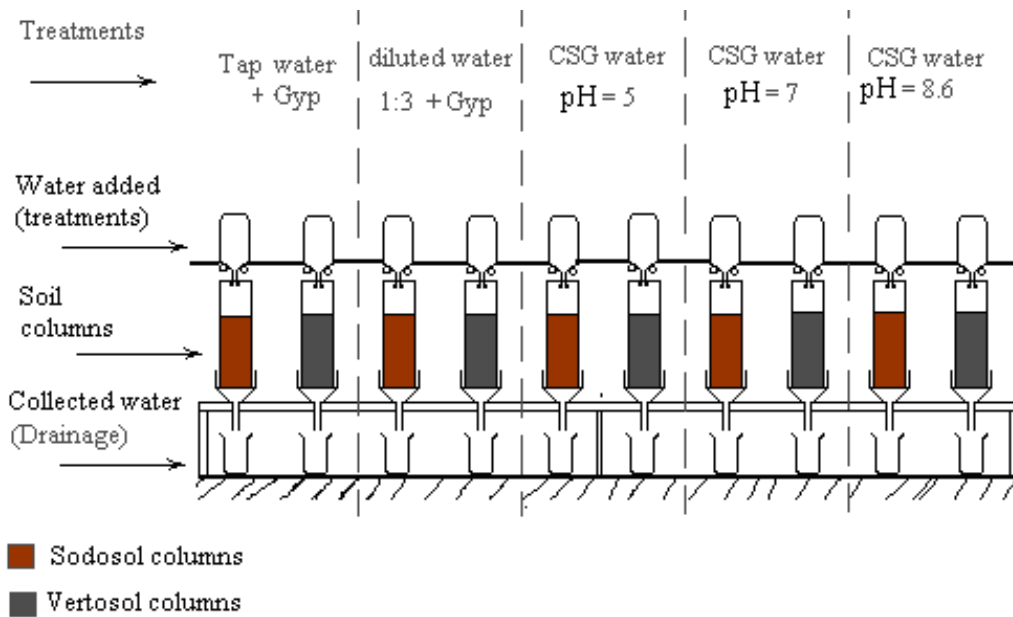


Figure 3.1 Diagram of system used to apply the water treatments and measure the saturated hydraulic conductivity (constant head method)

3.2.4 Experimental design and water quality treatments

Five water quality treatments were applied to each soil. Four replicates of each soil and water quality treatment were conducted (i.e. 40 columns). The treatments were:

- 1) Tap water + gypsum
- 2) Highly saline-sodic water (pH=8.6)
- 3) Highly saline-sodic water (pH = 7)
- 4) Highly saline-sodic water (pH = 5)
- 5) Diluted Highly saline-sodic water + gypsum (1:3)

The water treatments are categorised in three major groups as:

1) Highly saline-sodic water treatments:

The water was obtained from a natural coal seam gas bore located at Windibri station, Chinchilla, QLD. This treatment represents water with high salinity and SAR of 117. In addition, this water has a high concentration of bicarbonates and $\text{pH} \approx 8.6$. Table 3.4 shows selected chemical properties of the HSS water. A full chemical analysis is provided in appendix A.

Table 3.4 Selected chemical properties of the highly saline-sodic (HSS) water

EC ds/m	pH	Cl ⁻ (mmol _e /litre)	HCO ₃ ⁻ (mmol _e /litre)	Na ⁺ (mmol _e /litre)	K ⁺ (mmol _e /litre)	Ca ⁺² (mmol _e /litre)	Mg ⁺² (mmol _e /litre)
4.62	8.6	16.47	24.58	47.85	0.128	0.2295	0.107

Two bore water treatments in which the pH values were reduced using H₂SO₄ were: (a) HSS water with pH adjusted to 7, (b) HSS water with pH reduced to 5. The third treatment was the HSS water having naturally $\text{pH} \approx 8.6$. It should be noted that the EC for the HSS water treatments were about 4.62 dS/m.

The pH values in the adjusted pH treatments showed some increase with time when the water was exposed to the atmosphere. This change of pH was observed for two samples of pH = 5 and 7. The water samples were left in open beakers in the laboratory for three days and the pH values were found to increase linearly with time (Figure 3.2).

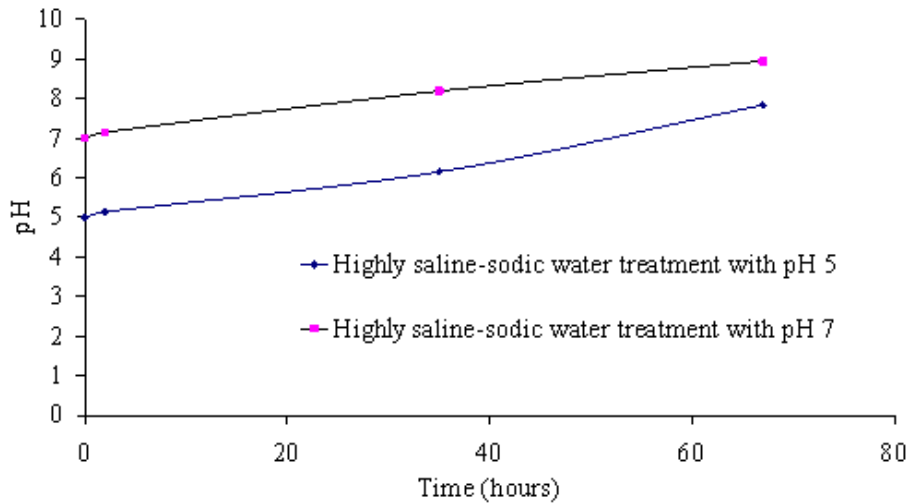


Figure 3.2 Change in pH for a saline-sodic water containing carbonates where the pH has previously been adjusted to either 5 or 7 using H_2SO_4 acid

Thus, pH was checked at the beginning of each replicate. Where the water was stored in closed plastic containers there was an insignificant change in pH. However, where it was necessary, extra H_2SO_4 was added to achieve the intended pH.

2) Diluted highly saline-sodic water + gypsum:

This water treatment was obtained by mixing HSS water with deionised water in the ratio 1:3, respectively, and amended with gypsum to provide an electrical conductivity of between 1.6 and 2 dS/m and SAR of 10 to 15.

3) Reference water treatment:

Tap water (EC less than 0.65 dS/m) was amended with gypsum to provide an electrical conductivity less than 1.5 dS/m. This treatment represents the grower practices where these soils exist and serves to provide the maximum measurements of K_{sat} .

The water treatments were prepared and stored in 20 litre plastic containers. The proposal was to apply two low saline- sodic waters having $EC = 0.4$ and then 0.1 dS/m followed after the treatments. However, waters having $EC = 0.1 \text{ dS/m}$ were not applied in soil columns with highly saline-sodic waters treatments as a result of sharp decreases in K_{Sat} .

It should be noted that each replicate was conducted separately. Therefore, the uniformity of the replicates at the time of soil column preparation and water treatments has not been achieved. In addition, the period between the conduct of one replicate and another could be a number of weeks, which might have exposed the soils and waters applied to a wide range of atmospheric conditions. Thus the randomized complete block design (RCBD) was preferred for statistical analysis.

3.2.5 Data collection

Applying the water treatments and measuring the outflow volume and its EC were conducted simultaneously. The outflow volumes were collected at the intended time increments. EC measurements were conducted using a MC-84 EC-Meter in each outflow collected. In the MC-84 EC-Meter, the EC reading is temperature compensated to automatically adjust the EC reading at 25° C . Record of the change of EC and outflow volume with time was obtained for each soil column. In addition the head of water was recorded at the beginning and after replacing each empty bottle. The outflow volume and water head and geometry information were transferred to spread sheets to calculate the saturated hydraulic conductivity (K_{Sat}). The K_{Sat} data obtained are presented in Appendix B.

3.2.6 Bulk density measurements

Bulk densities were measured in selected samples after completion of the experiment. Bulk density was measured in samples from three replicates (i.e. tap water amended with gypsum and highly saline-sodic treatments with $\text{pH} > 8.6$). The bulk density samples were taken from 5 to 10 cm from the top of the soil columns at saturated water content (Figure 3.3). Samples were prepared using rings with 5 cm inner diameter and 5 cm heights. The samples were weighed before being oven dried. The

density values were obtained by dividing the net oven dried soil weight by the inner volume of the ring.

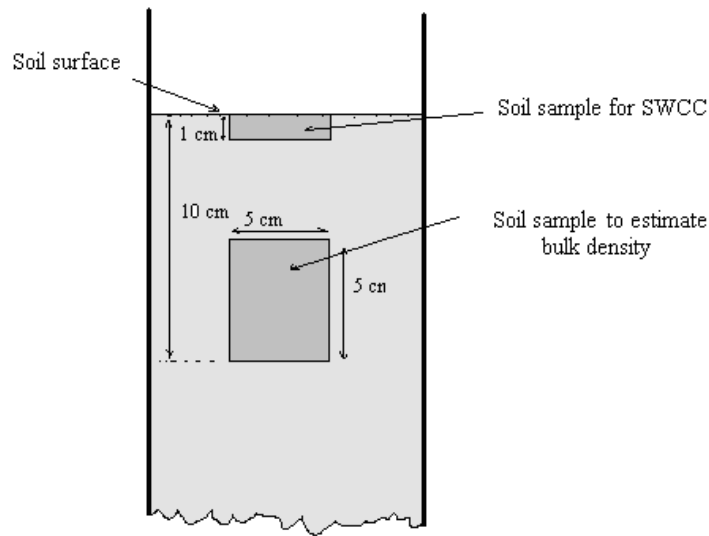


Figure 3.3 The positions of soil samples taken from the soil columns to determine the SWCC and bulk density after applying the water quality treatments

3.2.7 Soil-water characteristic curve determination

Soil-water characteristic curves (SWCC) were determined after finishing the K_{Sat} experiments. The SWCC were measured in the same soil columns in which the after treatment bulk density was measured (Figure 3.3). About 1 cm depth samples were taken from the soil surface at the top of each column where the greatest dispersion was expected. The replicates of gypsum and tap water treatment soil represented the maximum soil stability condition, while the replicates of saline-sodic water with pH >8.6 represent the sodicity impact on the soil structure.

Two methods were used to establish the SWCC. The hanging columns method (Dane & Hopmans 2002) was used to establish the relationship between matric potential and gravimetric water content every -20 cm suction in the range from -60 to -200 cm_{water}. The gravimetric water content at -250, -500, -1000, -2000, -3000, -5000, -10000 and -15000 cm_{water} were obtained using the pressure plate method (Dane & Hopmans 2002). The combined curves were plotted for the entire gravimetric water content-matric potential range from 0 to -15000 cm_{water}.

3.3 Results and discussion

3.3.1 Saturated hydraulic conductivity

The application of the HSS water was found to have a significant impact on the K_{Sat} in both soil types. The K_{Sat} for the stable condition treatments (i.e. tap water + gypsum) remained high. The K_{Sat} of the Sodosol under stable conditions ranged from 12.8 to 27.1 mm/h. However, applying the HSS water to the Sodosol columns produced K_{Sat} values between 0.04 to 0.78 mm/h after 700 mm of water had been applied. The K_{Sat} for the Vertosol under stable conditions ranged from 25.9 to 38.4 mm/h. Conversely, applying the HSS waters produced conductivity values between 0.09 to 2.86 mm/h after 700 mm of water had been applied. Table 3.5 shows the final K_{Sat} values obtained under the various treatments for both soils.

It is clearly evident that the application of the HSS water resulted in spontaneous deflocculation in both soils. Moreover, there is no significant difference between the hydraulic conductivities of HSS waters at the three pH values. Therefore, there is no evidence that amending HSS waters with sulphuric acid or reducing the pH would have any significant effect on soil structural stability. In fact, the low pH of the applied water does not mean that the pH in the soil-water and the relative Na^+ concentration will also be reduced. However, the interaction between added water and soil colloids is very complex, especially in the short term.

Table 3.5 The mean K_{Sat} of the Sodosol and Vertosol soils after infiltrating 700 mm of the various water quality treatments

Water Applied	Final K_{Sat} (mm/h)	
	Sodosol	Vertosol
Tap water + gypsum	32.73 (± 5.51) ^a	22.71 (± 5.51) ^a
Diluted HSS water +gypsum	30.57 (± 4.21) ^a	18.88 (± 4.21) ^a
HSS water pH=5	1.42 (± 1.07) ^b	0.35 (± 1.07) ^b
HSS water pH =7	0.83 (± 0.53) ^b	0.22 (± 0.53) ^b
HSS water pH>8.6	1.71 (± 0.81) ^b	0.27 (± 0.81) ^b

Superscripts indicate significant differences ($P < 0.05$) within columns

The K_{sat} of both soils decreased with increasing applications of HSS water (Figures 3.5 and 3.6). For both soils, the decrease was apparent after only small application volumes. For the Sodosol, a 50% decrease in conductivity was observed after about 150 mm of drainage had occurred and was less than 2 mm/h after approximately 350 mm had drained. For the Vertosol, a 50% decrease in conductivity was observed after about 100 mm had been drained but was < 2 mm/h after 150 to 280 mm had drained. It should be noted that for both soils approximately 100 mm of water had infiltrated through the surface before any drainage from the bottom of the columns occurred.

The behaviour of the decrease in K_{sat} with drained water in HSS water treatments was varied but the final K_{sat} approached similar values. For example, comparing the replicates of a given water treatment for both soils show that the K_{sat} behaviour varies during application of the water treatments. The results suggested that the K_{sat} decrease is governed by a complex and highly dynamic system associated with geometry, clay particle orientations, tortuosities in the soil matrix and water movement condition. Thus, the variation in K_{sat} after a certain amount of drained water might be a result of the effect of clay swelling and dispersion.

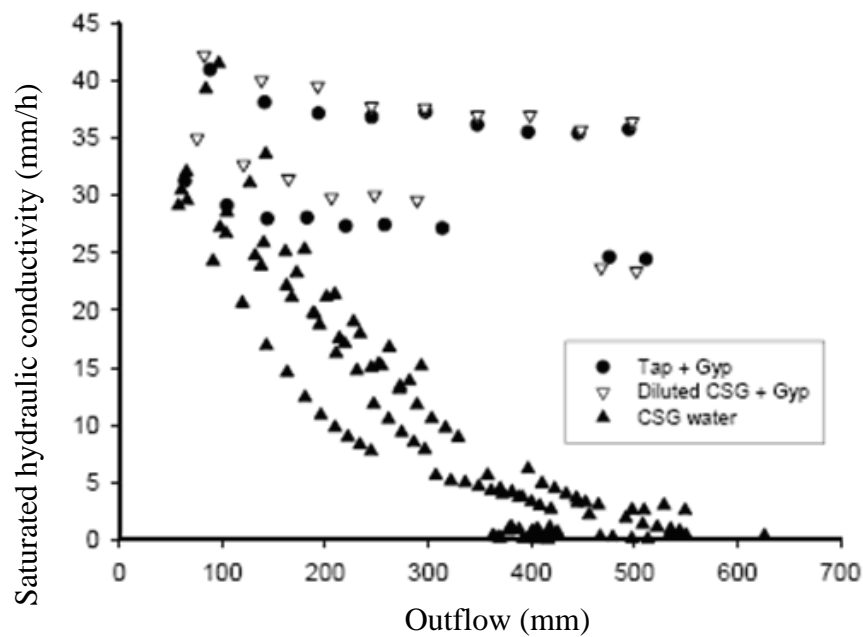


Figure 3.4 The change in K_{sat} with water applications for the Sodosol

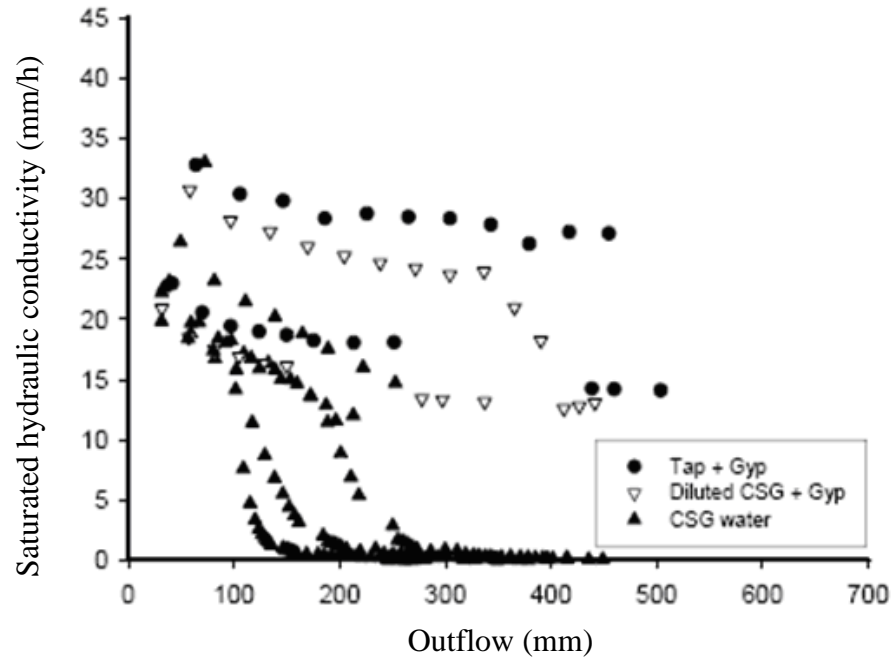


Figure 3.5 The change in K_{sat} with water applications for the Vertosol

Application of 0.4 dS/m water

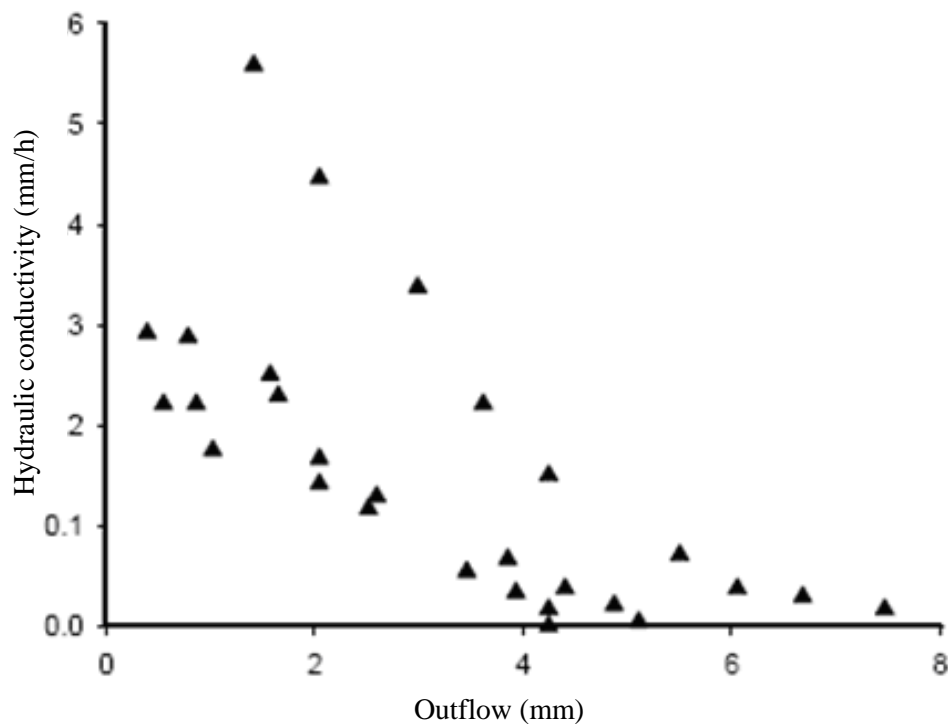
The application of the 0.4 dS/m water to the soils was conducted immediately after applying the water treatments. As shown in Table 3.6, it was found that the K_{sat} values of the soils were further reduced especially in the soil columns of the HSS water treatments. The K_{sat} of the soil previously treated with HSS waters declined sharply to less than 0.01 mm/h, which was observed after less than 0.1 mm had drained from the Vertosol and after about 4 mm of drainage had occurred in the Sodosol (Figures 3.7 and 3.8). However, applying 0.4 dS/m water to either the Sodosol and Vertosol previously treated with gypsum amended water produced a K_{sat} that was approximately 65 - 75 % of the pre-treatment K_{sat} . Applying 0.2 dS/m water to the soil columns of tap water + gypsum and diluted HSS water+ gypsum treatments did not produce a significant decrease in K_{sat} compared to when the 0.4 dS/m water was used.

Table 3.6 The K_{Sat} of the Sodosol and Vertosol when 0.4 and 0.1 dS/m water was applied after various HSS water pre-treatments

Water applied	Soil Pre-treatment	Final K_{Sat} (mm/hr)	
		Sodosol	Vertosol
0.4 dS/m	Tap water + gypsum	21.62 (± 8.01) ^a	15.81 (± 3.18) ^a
	Diluted HSS water + gypsum	23.45 (± 9.97) ^a	13.32 (± 4.02) ^a
	HSS water	0.02 (± 0.01) ^b	0.04 (± 0.03) ^b
0.1 dS/m	Tap water + gypsum	18.51 (8.05 ^a)	13.23 (± 3.30) ^a
	Diluted HSS water + gypsum	20.66 (± 8.92) ^a	12.67 (± 3.76) ^a
	HSS water	na	na

Superscripts indicate significant differences ($P < 0.05$)

Diluting the HSS water by deionised water amended with gypsum produced high values of K_{Sat} for both soils. Insignificant differences between the stable condition and diluted treatments indicate that diluting the HSS water with good quality water once accompanied with gypsum amendment might provide an alternative management to use HSS water in irrigation.

**Figure 3.6 Changes in saturated hydraulic conductivity for the Sodosol when 0.4 dS/m water is applied following the application of 700 mm of the HSS water**

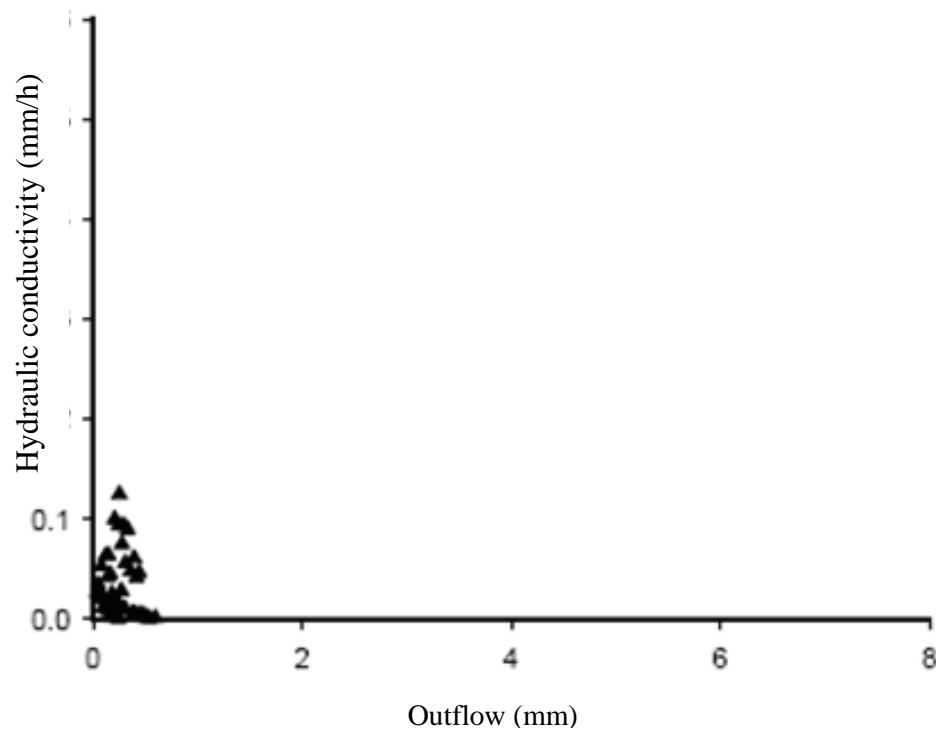


Figure 3.7 Changes in saturated hydraulic conductivity for the Vertosol when 0.4 dS/m water is applied following the application of 700 mm of the HSS water

The fast decrease of K_{Sat} in HSS water treatments indicates that dispersion likely plays the main role to clog the soil. The reduction in K_{Sat} is due to lower EC of the soil-water and the flushing out of Ca^{2+} cations. This, in turn, raises the relative concentration of Na^{+} cations in both soil solution and exchange colloids and encourages the dispersion process. The sharp difference between osmotic pressure in the interlayer spacing and the ambient solution in larger pores as described by Emerson and Bakker (1973) can increase the repulsive pressure resulting in clay fraction dispersion. This result demonstrates that under field conditions, the application of rainfall drops or other low salinity water to soil which had previously been treated with HSS waters would result in almost complete sealing of the soil. Soil in this condition would be expected to have very low infiltration and low internal drainage rates resulting in excessive surface runoff and erosion as well as difficulties with crop establishment and irrigation.

3.3.2 Effect of saline-sodic water on selected soil physical properties

Bulk density

Table 3.7 shows the bulk densities for the 12 columns after application of the water treatments. The variation between the values was small and there was no significant difference between the two treatments for each soil. This result is not consistent with the literature (e.g. Shakir et al. 2002) where the bulk density is often increased under sodic conditions. The lack of change in bulk density observed here may be due to sampling issues (i.e. the effect may have been more noticeable if the 0-5 cm layer was sampled) or because the columns had not been exposed to long term wetting and drying cycles.

Table 3.7 Bulk density of the soil (5-10cm below surface) after application of either tap water amended with gypsum or HSS water

Water treatments	Replicate number	Bulk density (g/cm ³)	
		Sodosol columns	Vertosol columns
Tap water + gypsum	2	1.53	1.25
	3	1.47	1.30
	4	1.52	1.30
	Average	1.50	1.28
HSS water treatments	2	1.50	1.29
	3	1.49	1.36
	4	1.53	1.28
	Average	1.51	1.31

Soil water characteristic curves

The relationships between gravimetric water content and suction applied for both soils are shown in Figures 3.8 and 3.9. It can be noted that the HSS water treatments further increase the gravimetric water content at intermediate and low suction at the soil surface, suggesting that the soil surface may be exposed to severe degradation. Results shown in Figures 3.8 and 3.9 suggest that the application of the HSS water followed by low EC water (0.4 dS/m) affected aggregate stability and resulting in dispersion, and leading to a change in the pore size distribution as shown by the increase in water holding capacity.

The effect of the dispersion on water holding capacity has been explained by Frenkel et al. (1978). They concluded that increasing clay dispersion and breakdown of the soil structure also affects clay immigration with water flow. The clay particles tend to settle at short distance to clog the fine pores and slow down water flow. In deeper depths displacement of dispersed clay occurs gradually due to slower water movement.

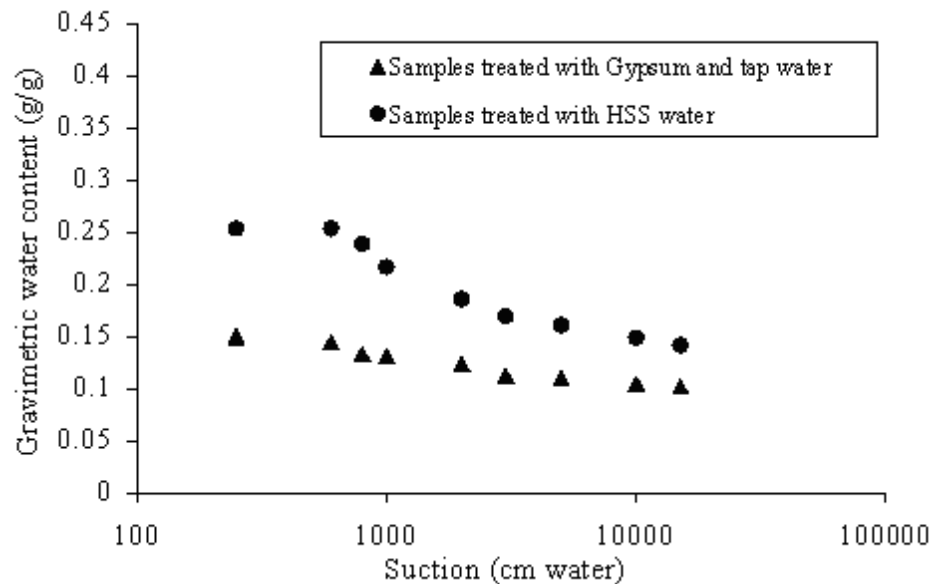


Figure 3.8 Average relationship between gravimetric water content and suction applied for the Sodosol samples treated with HSS water and normal tap water amended with gypsum

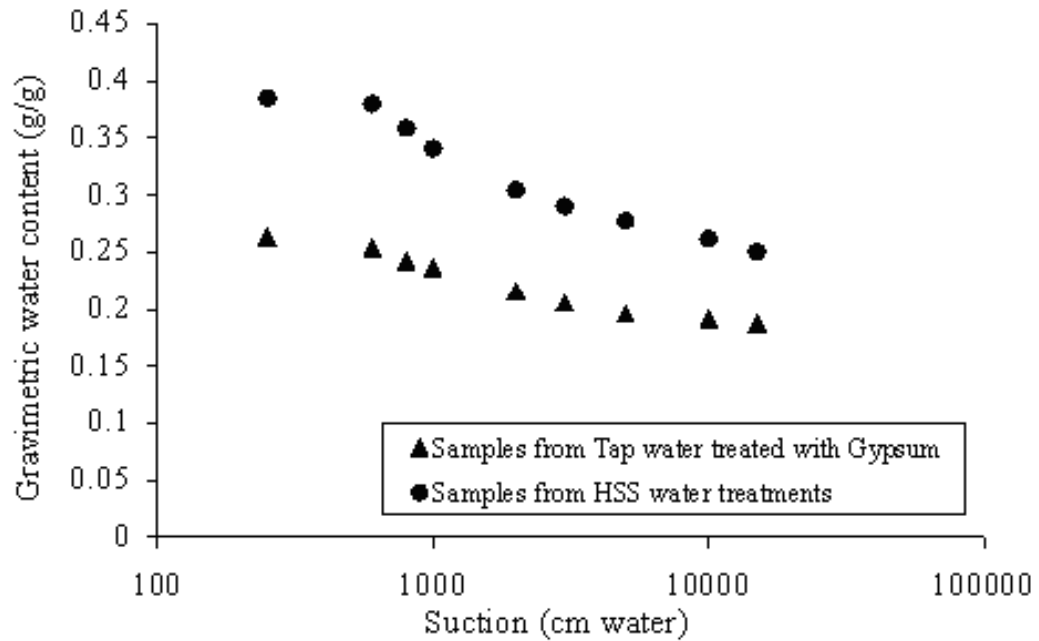


Figure 3.9 Average relationship between gravimetric water content and suction applied for the Vertosol samples treated with HSS water and normal tap water amended with gypsum

3.4 Conclusion

The uncontrolled application of the HSS water to both soils would be expected to produce substantial impacts on soil structural properties and sustainability of irrigated production systems. However, the column experiments confirmed that the pH amendment of the natural HSS water using sulphuric acid did not have any significant effect on the changes observed in soil structural stability or conductivity. The saturated hydraulic conductivity was found to decline with increasing volumes of the HSS water applied.

The HSS water which had been diluted with deionised water and amended with gypsum was found to have no adverse impact on the soil structural stability or conductivity. This suggests that the conductivity could be maintained above an acceptable target level by controlling the volume of the HSS water applied. The results suggested that it may be possible to develop feasible strategies by using gypsum and mixing the HSS water with good quality water to ensure the maintenance of the conductivity above an acceptable target level.

CHAPTER 4: Validation of the Hydraulic Reduction Function in the UNSATCHEM Model

4.1 Introduction

Soil column experiments (chapter 3) were conducted to investigate the effects of different saline-sodic water treatments on soil structural stability and hydraulic properties. Two disturbed soils were tested with different water qualities. Two water amendment options were investigated; 1) reducing the saline-sodic water pH using sulphuric acid, and 2) blending saline-sodic water with good quality water and adding gypsum. The results showed that using sulphuric acid to reduce the pH has no significant effect on the reduction of K_{sat} . However, diluting highly saline-sodic water and adding gypsum did maintain the K_{sat} . The results also showed that different management options could be implemented to improve the sustainability of irrigation with saline-sodic water.

Modelling can be an effective tool to investigate different irrigation management options. The UNSATCHEM model has been used to describe soil-water and solute movement, and dynamic soil chemical reactions under irrigation. The major ion chemistry components have recently been extracted from UNSATCHEM and incorporated into HYDRUS 1D as an independent module (Simunek et al. 2005). However, there are few evaluations reported in the literature of either the UNSATCHEM model or the UNSATCHEM module incorporated into HYDRUS 1D under sodicity levels that cause a significant reduction in hydraulic conductivity. In this chapter, the UNSATCHEM module in HYDRUS 1D is evaluated.

The chapter contains six sections. Section 4.2 provides an overview of the main UNSATCHEM sub-models. It also describes the physical basis for model use and the main chemical reactions included in the model. Section 4.3 outlines the

methodology used to prepare the soil and water parameterisation. Section 4.4 provides the results of simulation and section 4.5 presents the discussion. Section 4.6 presents the main outcomes.

4.2 Overview of the UNSATCHEM model

UNSATCHEM simulates water, heat, carbon dioxide production and movement, and solute transport in one-dimensional variably saturated soils. Major ion chemistry reactions (extracted from UNSATCHEM) have recently been incorporated into HYDRUS 1D Version 3 and 4 (Simunek et al. 2005). Hence, HYDRUS 1D is a one-dimensional numerical soil-water and solute transport model, able to simulate variably saturated flow, heat transport, CO₂ production and transport, and major ions chemistry. The major ion chemistry module considers the transport of seven major ions and their ionic chemical reactions including aqueous complexation, precipitation and dissolution of solid phases, and cation exchange. It should be noted that references to UNSATCHEM in this research refer to the UNSATCHEM module as incorporated into HYDRUS 1D.

The UNSATCHEM model also solves three different partial differential equations under isothermic conditions by a simultaneous iteration process (Figure 4.1). These partial differential equations are the Richards equation for variable soil-water movement, convection-dispersion equations (CDE) for unsteady solute species movement, and the CO₂ movement equation. The sodicity effect is incorporated via the hydraulic conductivity reduction function and impacts primarily on soil-water movement.

The simulation process under saline-sodic conditions can be illustrated as follows. The chemical reaction model provides information about the concentration of the individual chemical species in the soil solution and on adsorbing colloids, which allows calculation of the ESP at any time and space. The ESP is used to calculate the change of K_{sat} via the hydraulic conductivity reduction function. The reduction in K_{sat} reduces the water movement and solute dispersivity. In addition, the reduction of water movement will affect both solute and CO₂ movements, and influence the temporal and spatial chemical species concentrations calculated by the chemical reaction model. These processes occur simultaneously during the simulation. Hence,

the accuracy of UNSATCHEM at higher sodicity levels depends heavily on the appropriateness of the hydraulic conductivity reduction function and its validity under unsaturated conditions. Appendix C provides further details on the main sub-models incorporated.

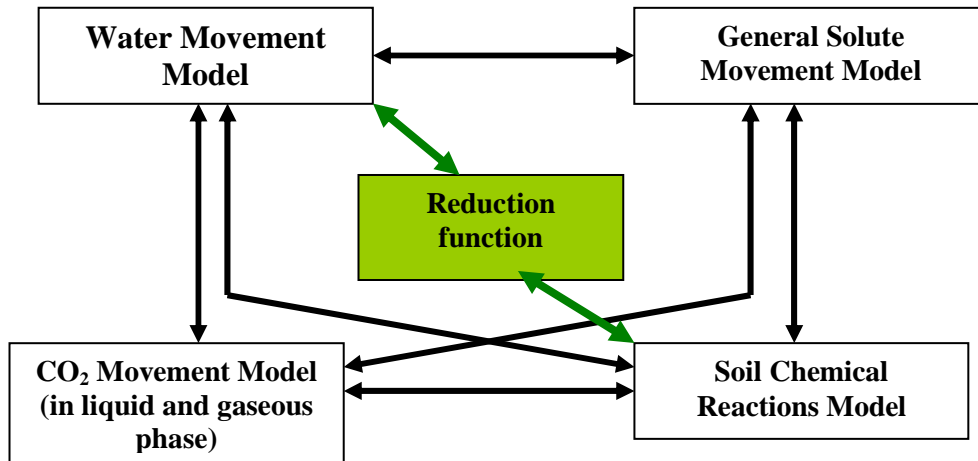


Figure 4.1 Sodicty-salinity effects in water and solute movement model (UNSATCHEM) under isothermic conditions

4.3 Methodology

UNSATCHEM was used to simulate the soil-water and solute movement data from selected column experiments reported in chapter 3 (i.e. replication 3) for two water treatments. These selected data are the three HSS water and diluted HSS water treatments. The water movement in the soil columns was assumed to be under isothermic conditions. Theoretically, changes in temperature during the experiments can affect water movement and chemical reactions within the soil columns. However, the experiments were conducted under laboratory conditions with little variation in the temperature ($\pm 2^\circ \text{C}$). Therefore, the temperature effect was not considered and heat transfer was ignored.

The model simulates CO_2 production from the biological activities. However, CO_2 production was not included in the simulation as there were no plants in the soil columns. The biological activities were also assumed to be insignificant and the root water uptake term in the water movement equation was set to zero.

The main sub-models considered during simulation were water movement, solute species movement and reactions. The hydraulic conductivity reduction function (r) was included during simulation of HSS water and diluted HSS water amended with gypsum applications. Therefore, the parameters needed to operate the model were the soil hydraulic function parameters, solute movement parameters (i.e. longitudinal dispersion and water diffusion coefficient), exchangeable reactions parameters (i.e. adsorbed species concentration, CEC, and Gapon selectivity coefficients), aqueous species concentrations, and the exchangeable cation concentrations on the exchange complex.

Data from the soil column experiments (chapter 3) were used to obtain the model parameters. The data for the tap water amended with gypsum treatment were used to obtain values of solute parameters. The flux and solute data for replicate 3 of the HSS water and diluted HSS water amended with gypsum treatments were used to evaluate the UNSATCHEM output. The process used to obtain the model parameters is summarised as following:

- 1) Hydraulic function parameters were determined for both soils.
- 2) Solute parameters (namely, dispersion coefficient and longitudinal dispersivity) were obtained by analysing EC data for discharge from the tap water amended with gypsum treatment.
- 3) The chemical reaction parameters were obtained by chemical analysis and Gapon selectivity coefficients assumed.

In the column experiments, water was added to the surface of a dry soil. Hence, the initial soil-water suction was assumed to be $-2000 \text{ cm}_{\text{water}}$ and $-5000 \text{ cm}_{\text{water}}$ for the Sodosol and Vertosol, respectively. The atmospheric CO_2 concentration was left at default values as recommended by Simunek et al. (1996).

4.3.1 Soil hydraulic parameters

The van Genuchten (1980) function was selected. The van Genuchten function parameters were estimated from the average of the SWCC data for soil samples of the tap water amended with gypsum treatment (assumption was made that hysteresis is negligible), which were reported in chapter 3. Non-linear regression analyses were performed using the RETC program to obtain these parameters. The

maximum saturated hydraulic conductivity was set as measured in the soil column for each replicate at the initial stage. The parameters obtained are shown in Table 4.1.

Table 4.1 van Genuchten (1980) hydraulic function parameters obtained for the Sodosol and Vertosol soils

Hydraulic parameters	θ_{sw}	θ_{rw}	α	I	n
Sodosol	0.43	0.18	0.0056	0.5	5.12
Vertosol	0.51	0.238	0.0619	0.5	3.20

4.3.2 Dispersion coefficient and longitudinal dispersivity

The EC with time data obtained for the tap water amended with gypsum were used to estimate the solute parameters (i.e. considering the continues change in outflow salinity with time). The outflow and EC measurement data were extracted from different replicates when 0.4 dS/m and 0.1dS /m water treatment were applied for both soils.

The CXTFIT program (Toride et al. 1999) incorporated into STANDMOD (Simunek et al. 1999) was used to estimate the solute parameters (mainly the dispersion coefficient) for both Sodosol and Vertosol soils. The solute parameters were determined by fitting the EC measurements in the outflow with time to an appropriate analytical solution (included in CXTFIT program) for CDE (i.e. steady one-dimensional flow and solute transport). A full description of the method used to determine solute parameters is presented in Appendix D.

4.3.3 Chemical reaction parameters

The concentrations of the aqueous species in water were obtained from the chemical analysis for the HSS water and diluted HSS water (Table 3.4). The CEC and concentrations of the exchangeable cations adsorbed onto the soil complex were obtained from the soil chemical analyses (Table 3.3) and entered in units of mmol_c/kg. The Gapon selectivity coefficient (K_G) describe the exchange reactions between Ca-Na, Mg-Ca, and Ca-K. The K_{GCa-K} was assumed to be 0.37 (Robbins et al. 1980b), K_{GMg-Ca} was assumed to be 0.58 (Robbins et al. 1980b), and the K_{GCa-Na} was calculated from Kopittke et al. (2004).data to be 2.59 (mol/litre)^{-0.5} and 3 (mol/litre)^{-0.5} for the Vertosol and Sodosol soils, respectively (Appendix E).

4.3.4 Operation of the UNSATCHEM model

The key soil and water parameters used in the validation simulations are summarised in Table 4.2.

Table 4.2 The UNSATCHEM input parameters for simulation of the HSS water and diluted HSS water amended with gypsum application for both the Sodosol and Vertosol soils

Parameter	Soil Type			
	Sodosol		Vertosol	
Soil Hydraulic parameters (van Genuchten- Mualem model ($m=1-1/n$))				
K_{Sat} (cm/h)	Rp1= 2.95, Rp2 = 3.92, and Rp3 = 2.91		Rp1 = 2, Rp2 = 2.22, and Rp3 = 2.26	
Qr	0.18		0.238	
Qs	0.43		0.51	
Alpha (cm ⁻¹)	0.0056		0.0069	
n	5.116		3.202	
I	0.5		0.5	
Solution Composition (mmol _e /litre)				
	HSS water	Diluted HSS Water	HSS water	Diluted HSS Water
Ca ²⁺	0.2295	0.075	0.2295	0.075
Mg ²⁺	0.107	0.027	0.107	0.027
Na ⁺	47.847	11.96	47.847	11.96
K ⁺	0.128	0.032	0.128	0.032
Alkalinity	30.63	7.66	30.63	7.66
Cl ⁻	16.473	4.12	16.473	4.12
SO ₃ ⁻	-	0.436	-	0.436
Exchangeable concentrations (mmol _e /kg)				
Ca	60		154	
Mg	31		83	
Na	4		29	
K	4		4	
other parameters				
Bulk density (g/cm ³)	1.50		1.28	
Diffusion coefficient (cm ² /s)	0.00001		0.00001	
Dispersivity (cm)	0.964		1.592	
CEC (mmol _e /kg)	99		270	
Gapon selectivity coefficient				
K(Mg/Ca) (1/√mol/litre)	0.58		0.58	
K(Ca/Na) (1/√mol/litre)	2.59		3	
K(Ca/K) (1/√mol/litre)	0.37		0.37	

The simulations of the column experiments were conducted under equilibrium precipitation/dissolution of the calcite. The period of simulation differed between replicates based on the experimental time. One replicate of the diluted water amended with gypsum for both soils was also simulated.

The water flux initial conditions were a constant head at the top and -2000 cm for Sodosol and -5000 cm for the Vertosol at the bottom of the soil column, and decreased linearly through the column with depth.

The convection-dispersion equations were solved using the Galerkin finite-element method with a Crank–Nicolson implicit scheme. Simunek et al. (2005) recommended using the Crank-Nicholson implicit scheme to achieve high precision in the values of solution concentrations. It was assumed that the precipitation/dissolution reactions were in equilibrium. It was also assumed that there was no dissolution of calcium or magnesium from the soil solid matter. The critical ionic strength was set to 0.5 mol/litre.

The maximum number of iterations for both the water movement and chemical reactions models were set to 80 to ensure convergence of the water, solute and chemical reaction models. Evaluation of the model performance was based on a comparison of the simulated and measured accumulated outflow.

It is worth noting that the simulations for the column experiments were also performed using the kinetic precipitation/dissolution of calcite operation. The kinetic precipitation/dissolution of calcite method was shown to cause a gradual change in conductivity and chemical parameters (i.e. pH and SAR). Nonetheless, the kinetic precipitation /dissolution condition did not significantly improve the fit of the discharge and hydraulic conductivity data. The data obtained during the experiments do not allow an examination of whether the kinetic or the equilibrium model was most appropriate. Therefore, the equilibrium precipitation/dissolution calcite was adopted in this study.

4.3 Results

Figure 4.2 shows the model estimates of accumulated outflow compared with time for the Sodosol soil columns. In general, the model was able to demonstrate a reduction in outflow due to the application of the HSS water. However, there is a large variation between the simulated outflow and the experimental measurements. The model underestimated the outflow for each of the three replicates. These results suggest that the simulated conductivity was small compared with the measured conductivity. The model also underestimated the outflow for the Sodosol when the diluted HSS water treatment was applied (Figure 4.3).

The Vertosol soil columns were simulated for up to 746 h. The Vertosol results show that the model underestimated the outflow when the HSS water treatments were initially applied (Figure 4.7). However, during the later stages the difference in the simulated and measured hydraulic conductivity is very small and the outflow rate approaches zero. The results for the simulation of the diluted HSS water treatment indicate that the model underestimates the outflow over the whole period of water application (Figure 4.8).

Figures 4.4 and 4.9 show the estimated change in hydraulic conductivity (K) with soil depth during the water application. It can be noted that the surface layers were severely affected by the increasing sodicity and had lowest K values. The differences in the hydraulic conductivity within the soil column are because the equilibrium model predicts a large quantity of calcite precipitation in the shallow surface soils. However, there is also an increase of the calcium concentration in the deeper depth as a result of exchangeable calcium being replaced by sodium and it moving with the water.

The model provides SAR and pH data at each depth and time step (Figures 4.5, 4.6, 4.10 and 4.11). The SAR values showed maximum reduction at the surface. However, the values of simulated SAR were less than the SAR of the applied water (i.e. 117). These results can be attributed to the soil chemical reactions and the effect of calcium buffering and the exchange reactions. Sodium cations remove the adsorbed Ca from the exchange complex. The calcium then reacts with the bicarbonate in the soil solution to form precipitated calcium carbonate. Calcium carbonate precipitation and an increase in sodium hydroxyl then increase the surface soil pH (Figure 4.6).

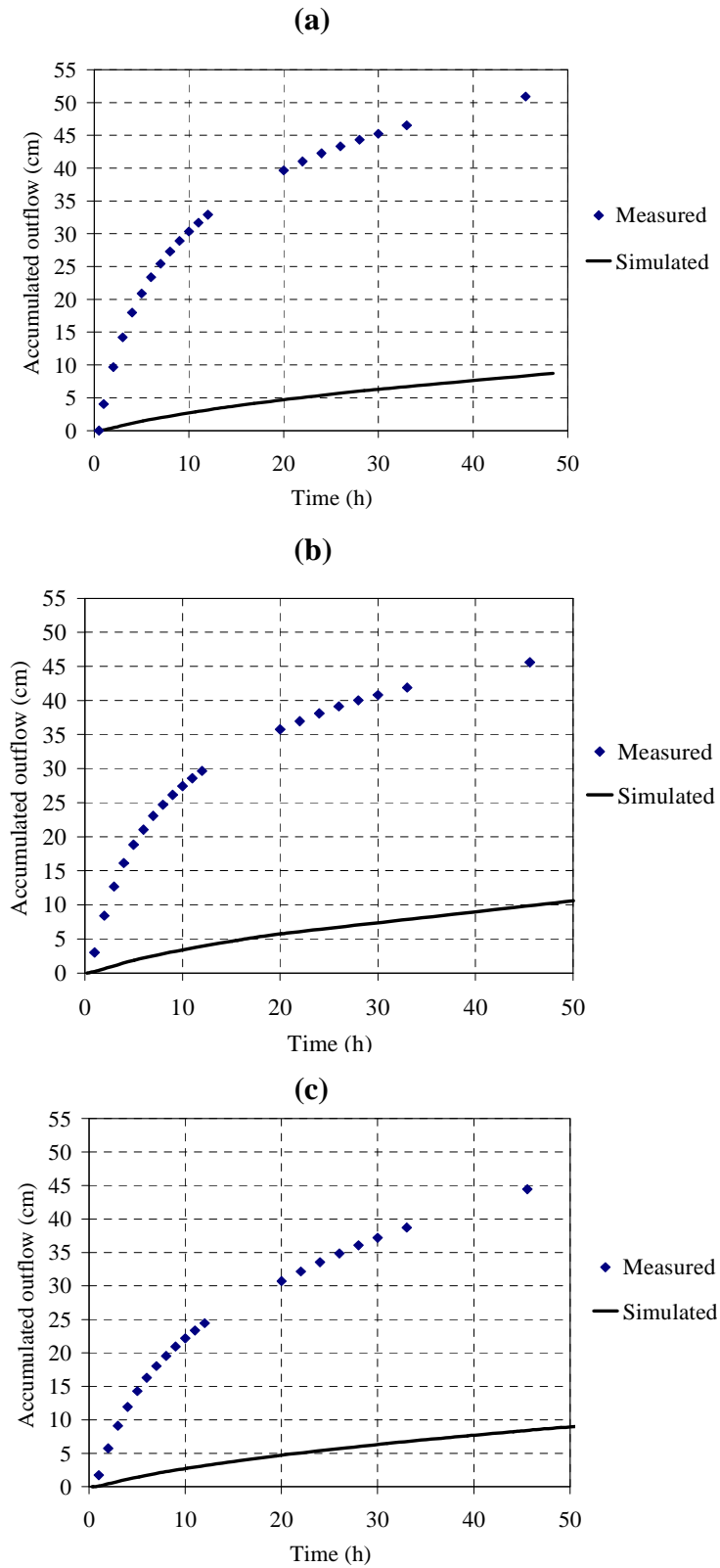


Figure 4.2 Comparison of measured and simulated outflow when HSS water applied for the Sodosol, (a) replicate 1, (b) replicate 2, and (c) replicate 3

Precipitation of the calcium carbonate in the surface soil results in an increase of the SAR of the soil solution. This increases the soil ESP, reduces the conductivity, and slows down the water movement. These reactions occur simultaneously during application of HSS water. However, the estimated SAR is still less than the initial SAR of applied solution suggested that the calcium buffering and the exchange reactions dominate the simulation of the chemical reactions.

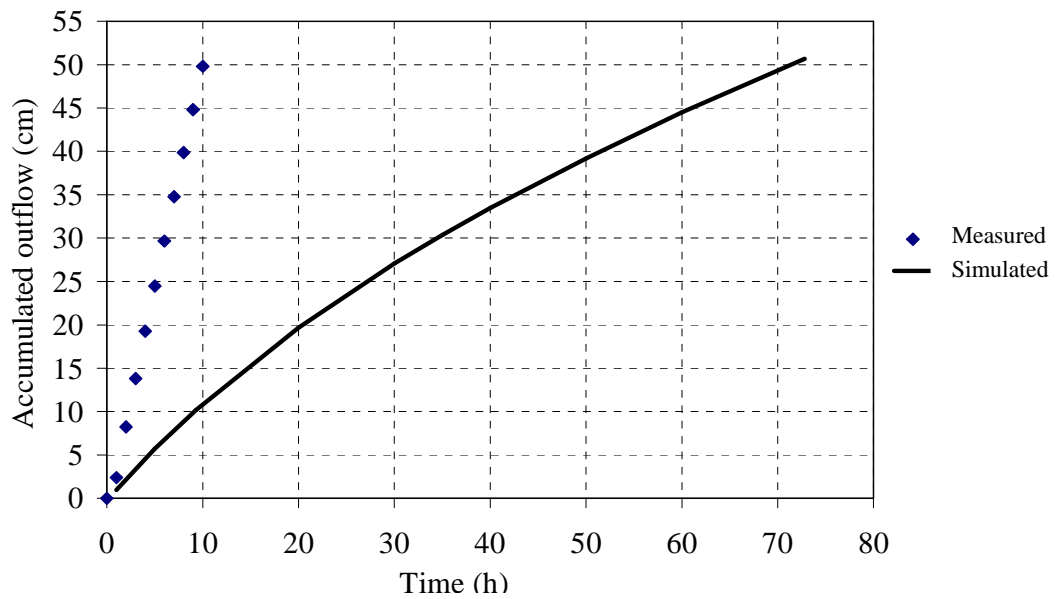


Figure 4.3 Comparison of measured and simulated outflow for the Sodosol soil column when diluted HSS water amended with gypsum was applied

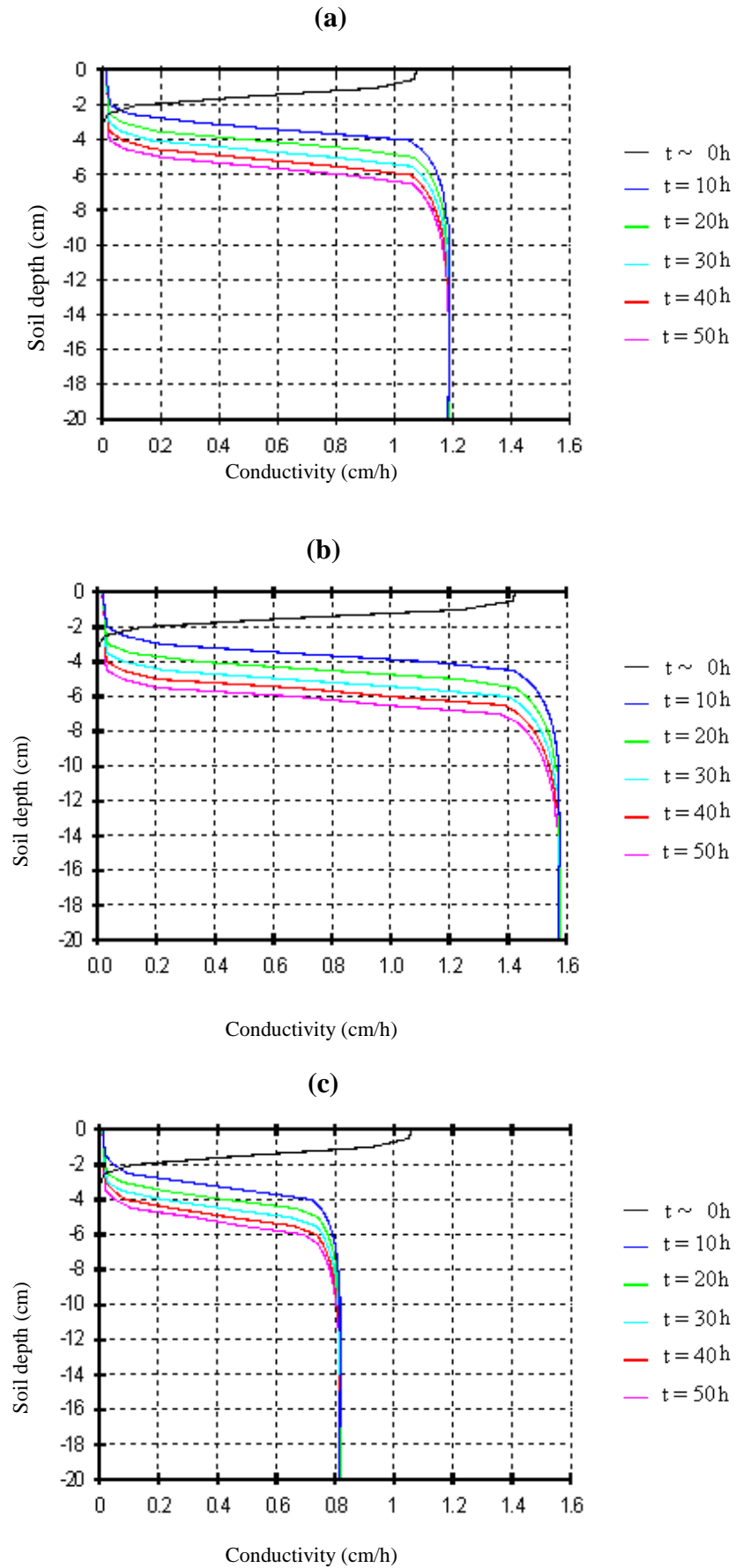


Figure 4.4 Simulated hydraulic conductivity with depth at different simulation time, for the Sodosol (a) replicate 1, (b) replicate 2, and (c) replicate 3

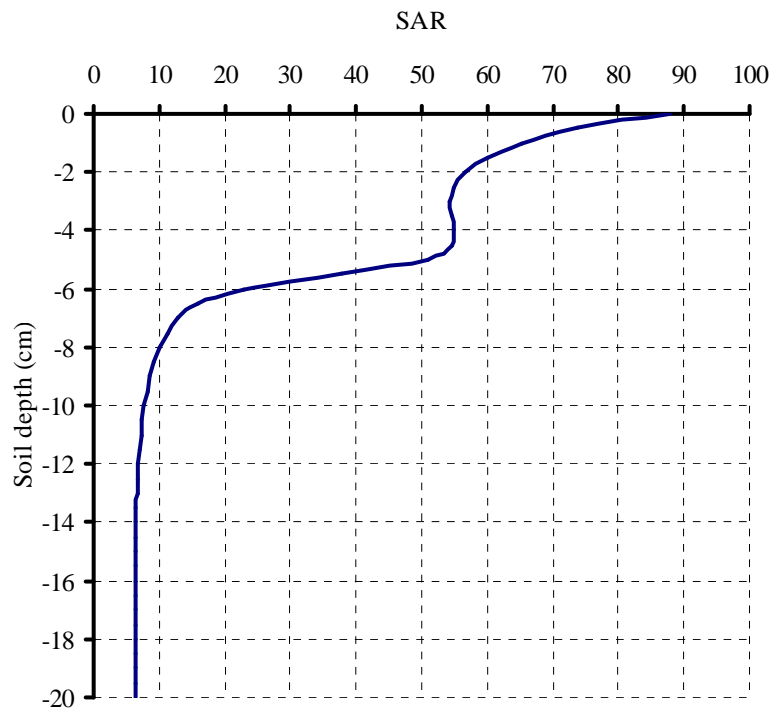


Figure 4.5 Example of the estimated change in SAR of the soil solution with depth at final time for the Sodosol soil (replicate 1)

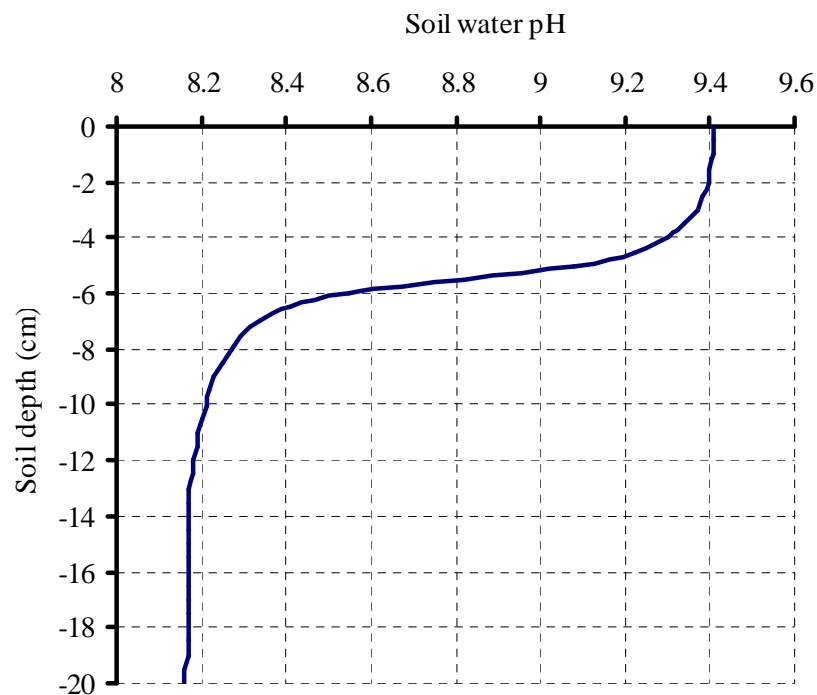


Figure 4.6 Example of the estimated change in pH of the soil solution with depth at final time for the Sodosol soil (replicate 1)

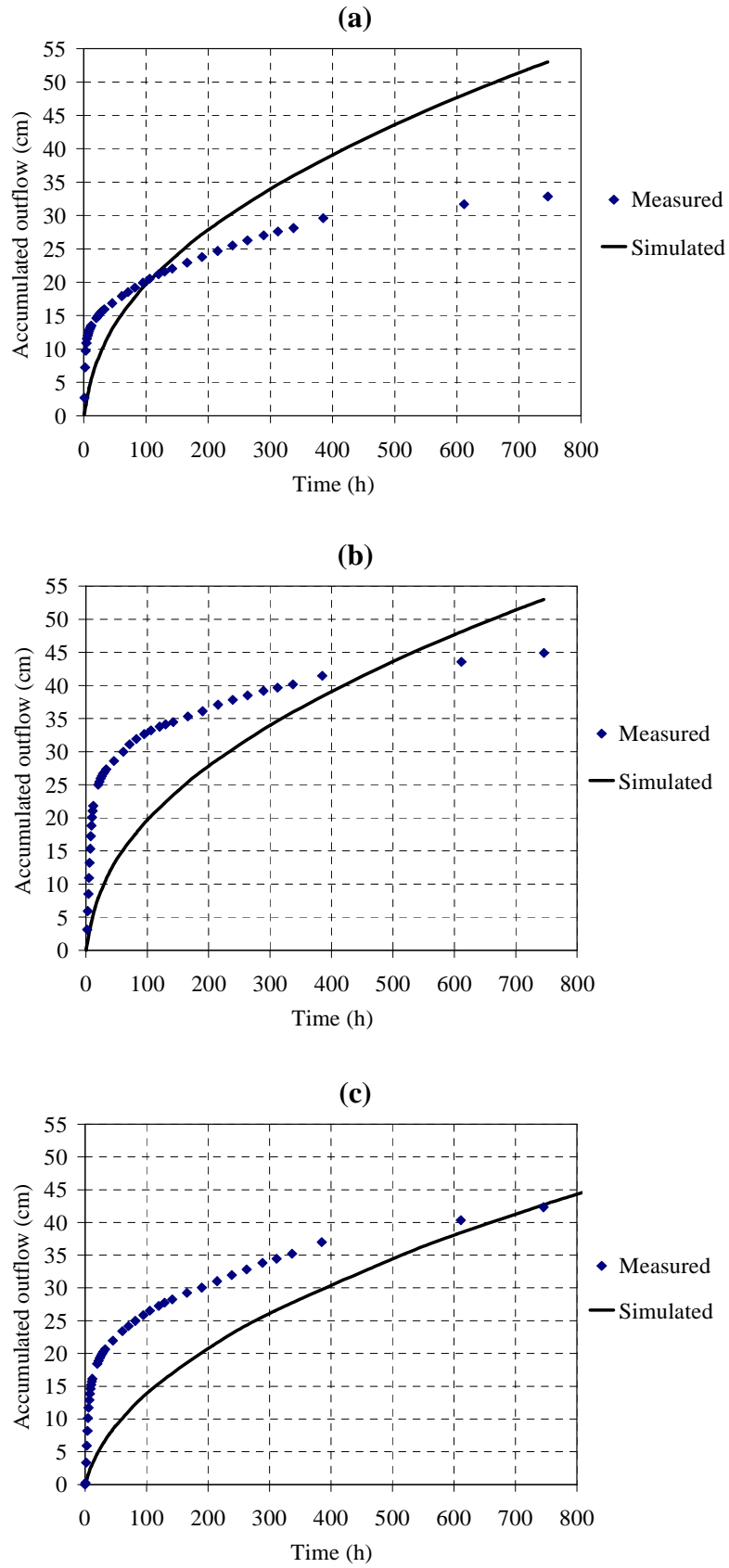


Figure 4.7 Comparison of measured and simulated outflow for the Vertosol when HSS water applied (a) replicate 1, (b) replicate 2, and (c) replicate 3

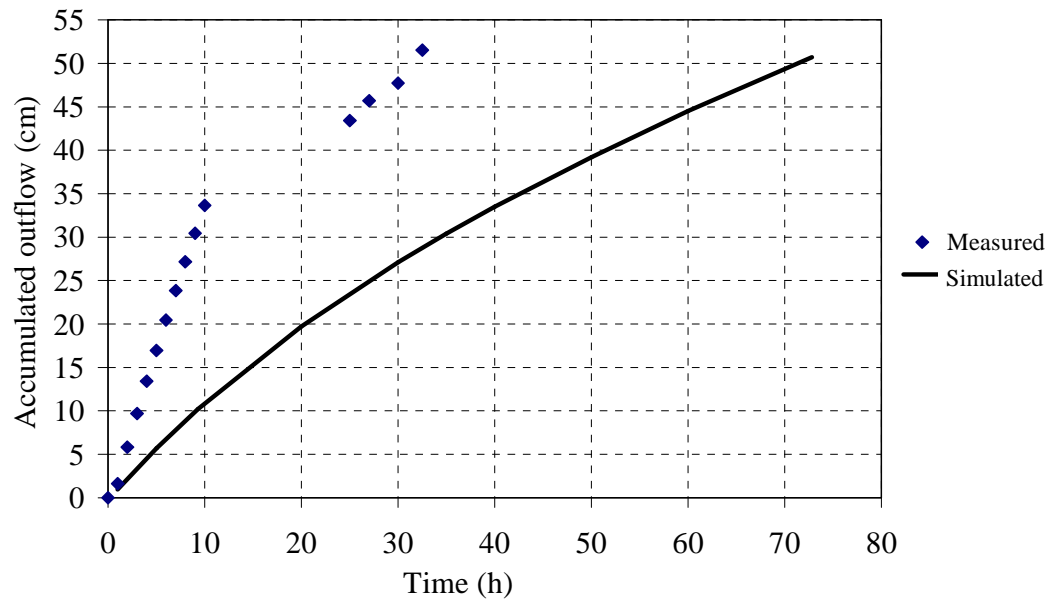


Figure 4.8 Comparison of measured and simulated outflow for the Vertosol soil column when diluted HSS water amended with gypsum was applied

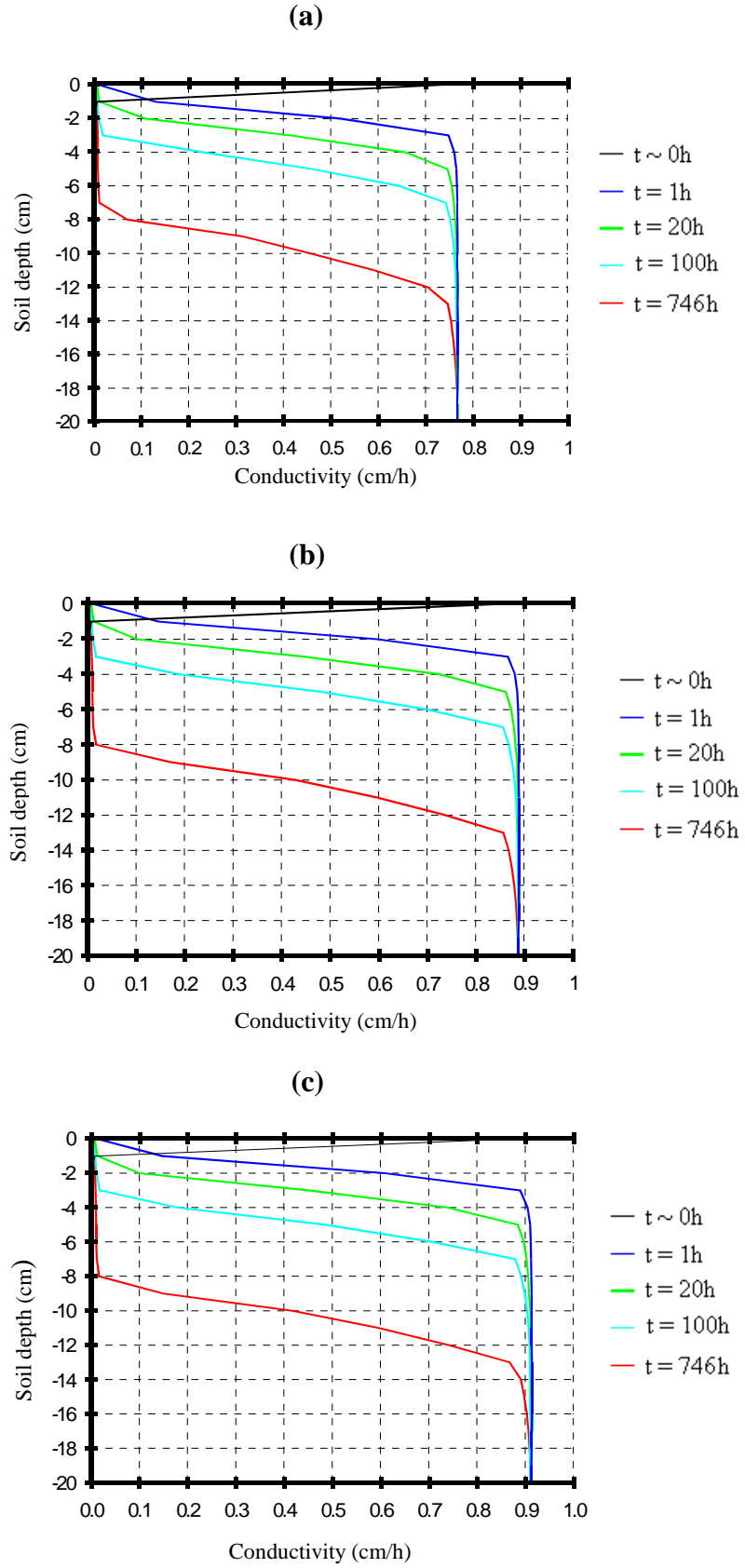


Figure 4.9 Simulated hydraulic conductivity with depth at different simulation time for the Vertosol (a) replicate 1, (b) replicate 2, and (c) replicate 3

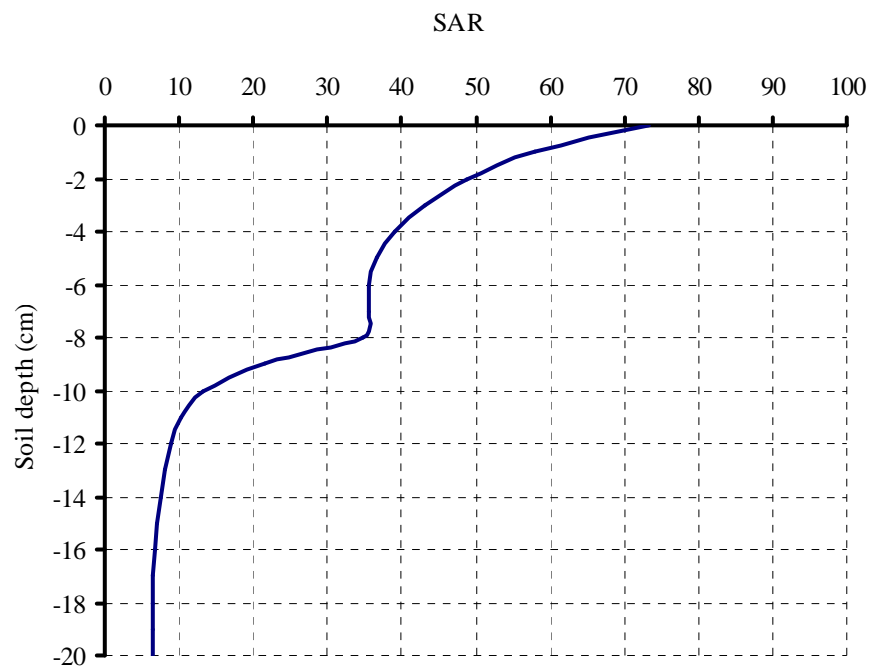


Figure 4.10 Example of the estimated change in SAR of the soil solution with depth at final time for the Vertosol soil (replicate 1)

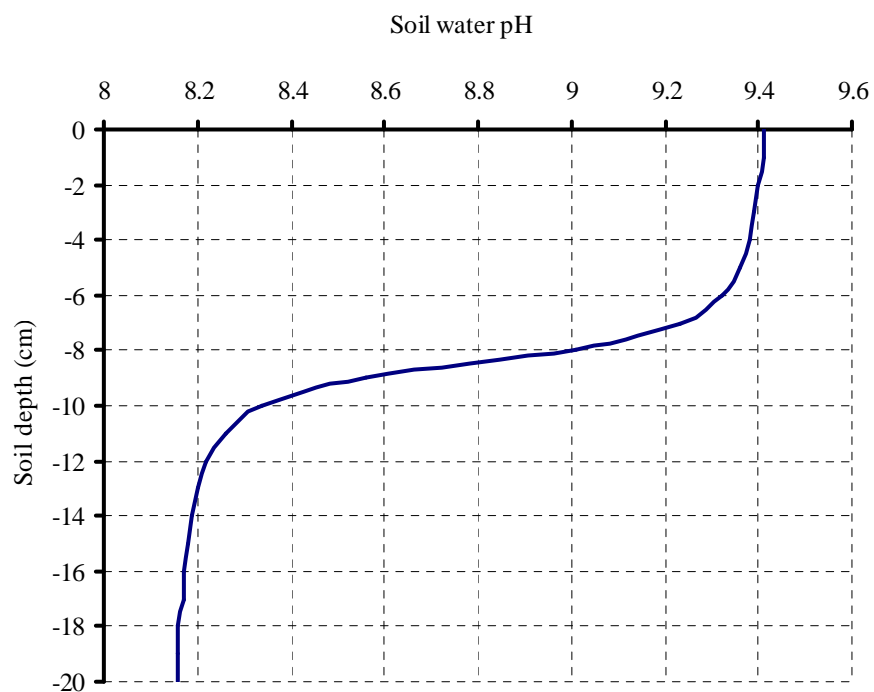


Figure 4.11 Example of the estimated change in pH of the soil solution with depth at final time for the Vertosol soil (replicate 1)

Comparisons of the measured and estimated saturated hydraulic conductivity for each soil and water quality treatment are presented in Figures 4.12, 4.13, 4.14, and 4.15. The simulation period for each soil column was extended to allow for the same volume of applied water during the experiment to percolate. The column outflow data was used to calculate hydraulic conductivity. For the Sodosol columns treated with the HSS water (Figures 4.12) the estimated K_{Sat} during the initial stages was low compared with the measured values. However, the estimated K_{Sat} approaches the measured K_{Sat} as the infiltrated volume increases and the entire soil column approaches equilibrium. This is because the sodicity level at that late stages is high and the variation between the model estimation and the measured K_{Sat} is hard to identify. Clear sight of the underestimation of the model can be noted in the simulation results for the diluted HSS water applications (Figure 4.13). The estimated K_{Sat} was lower than measured, which indicates clearly that the hydraulic conductivity reduction function does not properly account for the change in K_{Sat} in relation to the chemical conditions.

The estimated K_{Sat} with percolated HSS water for the Vertosol treatments exhibit the same response as was noted in the simulations of the Sodosol treatments. Figure 4.14 shows that the estimated K_{Sat} was very low compared with measured values in the initial stages of water application. However, the values of estimated K_{Sat} are higher than the measured K_{Sat} in the final stage as the amount of percolated water increases. However, the results from simulation diluted HSS water show clearly that the K_{Sat} estimated is lower than the measured values (Figure 4.15). It is clear that the UNSATCHEM demonstrates the change of conductivity due to high sodicity. However, it seems that there are some limitations inherent in relating the change of soil chemistry and sodicity to the hydraulic properties of the soil and the chemical model.

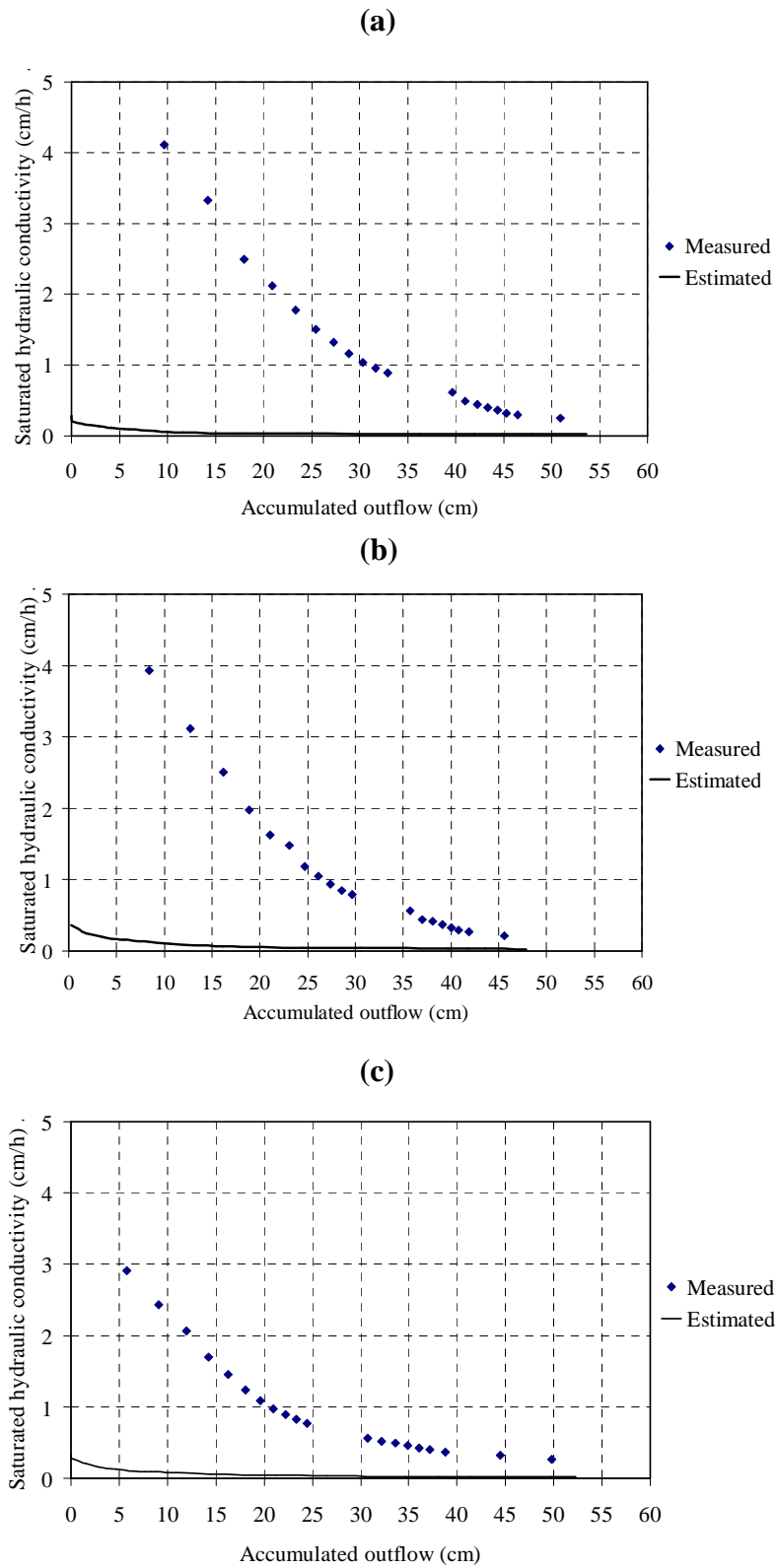


Figure 4.12 Comparison of measured and estimated saturated hydraulic conductivity for HSS water in the Sodosol (a) replicate 1, (b) replicate 2, and (c) replicate 3

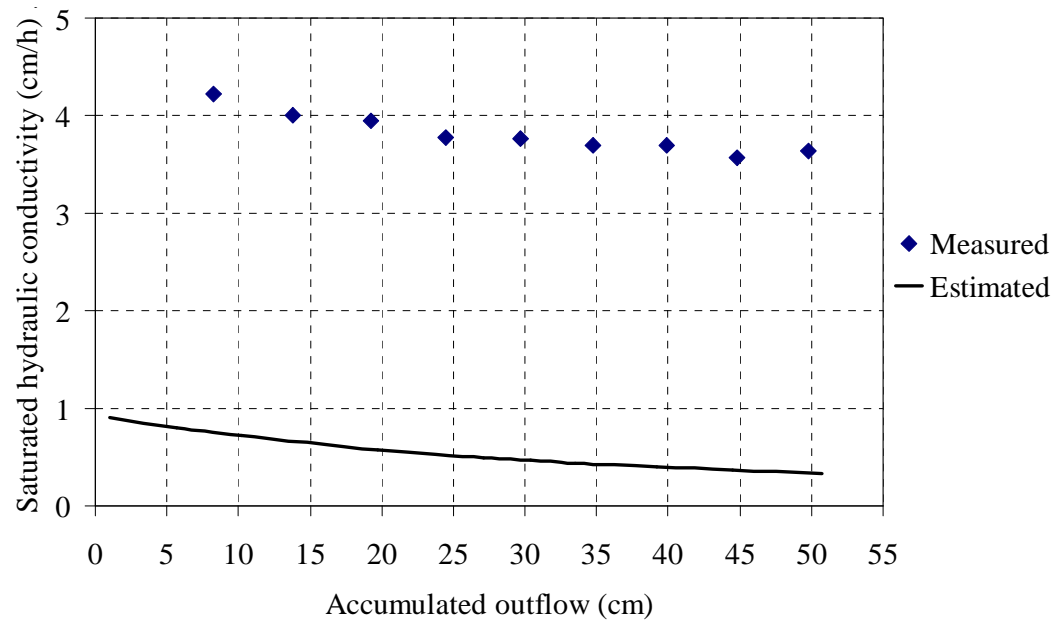


Figure 4.13 Comparison of measured and estimated saturated hydraulic conductivity for the Sodosol (when diluted HSS water amended with gypsum was applied)

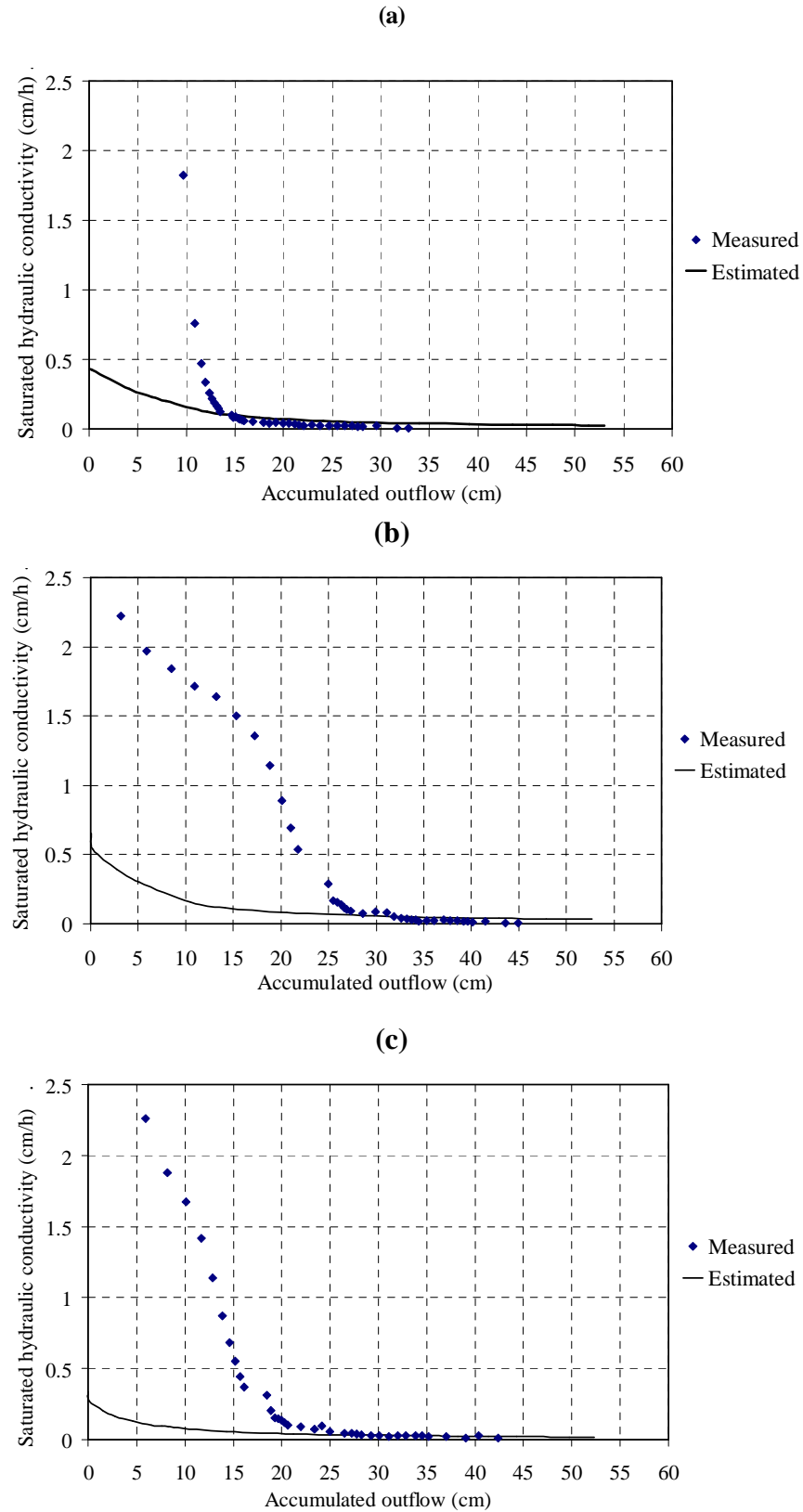


Figure 4.14 Comparison of measured and estimated saturated hydraulic conductivity for HSS water in the Vertisol (a) replicate 1, (b) replicate 2, and (c) replicate 3

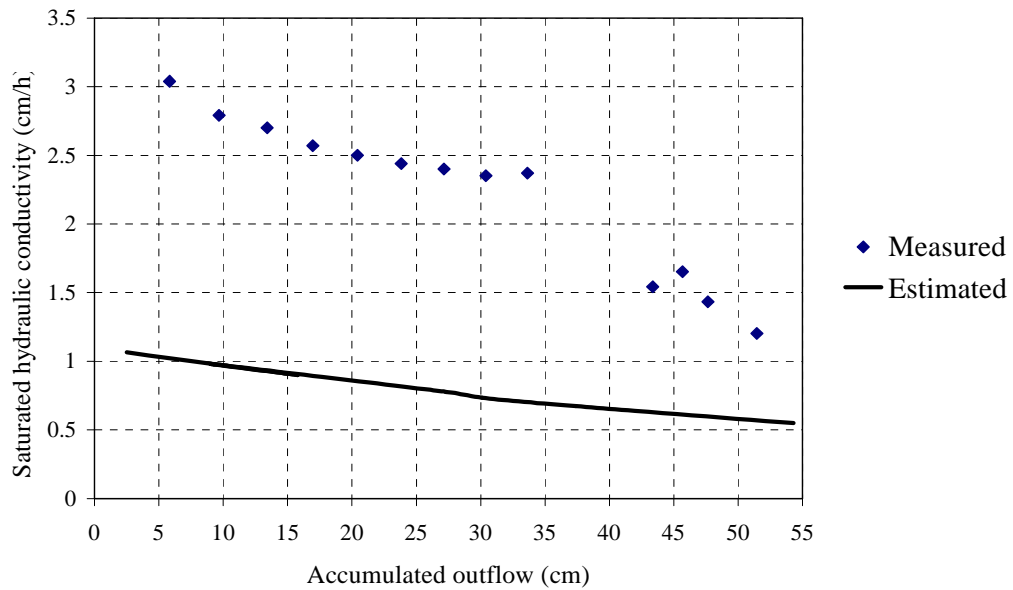


Figure 4.15 Comparison of measured and estimated saturated hydraulic conductivity for the Vertosol when diluted HSS water amended with gypsum was applied

4.5 Discussion

The simulation results for the application of HSS water to both Sodosol and Vertosol soil columns suggests that there are inherent limitations with either the chemical reaction model or the hydraulic conductivity reduction function in UNSATCHEM. However, the chemical reaction model has been used successfully in many research projects around the world (e.g. Schoups et al. 2006; Goncalves et al. 2006). Successful modelling of solute and chemical reactions using UNSATCHEM has been repeated in the literature. In most of these studies, the solute and sodium concentration levels were lower than the threshold levels likely to cause soil degradation, and the reduction of the hydraulic conductivity either was stable or assumed to be small. However, in this current study, the degradation of soil structure and the reduction in conductivity are significant.

The simulation results for the Sodosol and Vertosol soils clearly shows that the model failed to properly describe the HSS water discharged from the soil columns. Simulation of water and solute movement under sodic conditions simultaneously considers the relationships between the soil chemical reactions and hydraulic conductivity during water application treatments. The variations between the measured and simulated

outflow may be due to many factors that act together. These factors include a number of assumptions regarding water and solute movement incorporated in UNSATCHEM. For example, preferential flow pathways are not considered in the simulation. However, preferential flow could be expected to occur particularly during the early stage of infiltration (as the water was applied to disturbed soil columns) resulting in a higher measured K_{Sat} . Consolidation processes reduce preferential flow and conductivity. The reduction in the hydraulic conductivity due to consolidation was estimated from the reference treatment (i.e. Tap water amended with gypsum) to be less than 14% of the initial conductivity. However, the differences in the simulated outflow reported in Figure 4.2 and 4.6 is greater, suggesting that consolidation is not the only reason for these differences. Furthermore, the chemical and physical parameters used in the simulation were either assumed or an averaged of the values determined for three replicates. Individual replicate may slightly vary due to the packing of the soil columns. However, packing processes are not expected to be the cause of these significant variations.

The reasons behind the failure of the model to properly simulate the column experiments can be identified primarily in limitations inherent with; (a) the hydraulic conductivity reduction function, and (b) assumptions inherent within the chemical reaction model. The hydraulic conductivity function consists of two independent and multiplicative relationships that relate the chemical conditions to the change in conductivity within the soil profile. The first relationship deals with clay swelling (McNeal 1968) and relates the change in the conductivity to the clay swelling as a function of both ESP and electrolyte concentration (C_o) values. Simunek et al. (1996) incorporate the McNeal clay swelling model into UNSATCHEM using parameter values calculated by McNeal (1968) for small selections of American soils. These parameters should be characterised for local soils and were incorporated only for demonstration purposes. In addition, the clay swelling model was derived from data in which the ESP of the soils was estimated from the SAR of the soil-water using empirical USSL Staff (1954) relationship. However, the USSL Staff (1954) SAR-ESP relationship has been found to vary from soil to soil (Qadir & Schubert 2002). Hence, using this relationship might result in errors when estimating the soil ESP.

The second relationship in the hydraulic conductivity reduction function is an empirical pH- K_{Sat} relationship (Simunek et al. 1996) which is based on a limited number of soils tested by Suarez et al. (1984) and relates the reduction in K_{Sat} to soil pH. Simunek et al. (1996) incorporated the pH- K_{Sat} relationship into UNSATCHEM using parameter values obtained from a small number of soils and these could vary with different soil types. However, the manner of K_{Sat} decrease may vary from soil to soil. For example, Aydin et al. (2004) showed that the increase of pH (above 7) reduces the hydraulic conductivity in two clayey soils differing in mineralogy. However, the manner of K_{Sat} decrease was varied from the pH- K_{Sat} relationship soil of Simunek et al. (1996).

In UNSATCHEM, the hydraulic conductivity reduction function uses estimated chemical parameters (i.e. pH for pH- K_{Sat} functions, and ESP and C_o for the McNeal model) obtained by the soil chemical model at each soil depth to calculate the values of the reduction function, which will be used to calculate the hydraulic conductivity. It should be noted that the reduction of hydraulic conductivity (as shown in Figures 4.4 and 4.9) occurs at high sodicity (Figures 4.5 and 4.10) and pH values (Figures 4.6 and 4.11). This suggests that both parts of the reduction function produce lower values and cause the conductivity to be excessively decreased. Multiplication of both terms further reduces the hydraulic conductivity. However, it was difficult to identify which part of the hydraulic conductivity reduction function (r) contribute significantly in r limitations.

The main limitation in the chemical model is that the effects of pH have not been completely incorporated in the chemistry model incorporated into UNSATCHEM, as CEC and the ESP are both assumed to be independent of pH. This assumption may not be correct, as evident by many researchers (e.g. Evangelou & McDonald Jr 1999; Khajanchi & Meena 2008).

Simulation of water and solute movement under sodic conditions is complicated. Errors in assumption or calculating any component during the simulation will result in inaccurate outcomes. This is because the water and solute balance components are interrelated. Water flow conveys the ions and determines the exchangeable cation concentrations and the chemical reactions that take place at any given depth of the soil

profile. Therefore, the aforementioned limitations should be considered separately. It seems appropriate to start by investigating the appropriateness of the McNeal (1968) model and strategies to characterise its parameters.

4.6 Conclusion

The UNSATCHEM model has been evaluated using data obtained in chapter 3. The aim of this evaluation was to test the capability of the model to describe the reduction of water flow due to sodicity in the irrigation water. The model provides detailed information about the soil profile including SAR and pH and species concentrations with depth. The model shows that the hydraulic conductivity is reduced due to high sodicity in the applied water. However, it failed to properly describe the magnitude of the conductivity reduction and inconsistently predicted discharge from the soil columns. The differences between estimated and measured hydraulic conductivities were large, especially for the Sodosol columns. The possible mechanisms underlying the discrepancies were identified in the hydraulic conductivity reduction function and assumptions associated with the chemistry reaction model. It has been shown that the hydraulic conductivity reduction function overestimates the reduction of the conductivity associated with high sodicity soil chemistry reactions. In addition, as UNSATCHEM assumes that the CEC and ESP are independent of soil pH, the $\text{pH}-RK_{Sat}$ relationship may not be valid for soil with different (especially variable charge) mineralogy.

Therefore, there is a need for more research to improve the UNSATCHEM for modelling highly sodic conditions before using it for any further management investigations. The main factors identified in this chapter should be considered separately and investigate their interrelations compared with experimental data. The starting point is by investigating the McNeal (1968) model and providing a method to characterise its parameters. The following chapter investigates and describes the development of an improved clay swelling model.

CHAPTER 5: Development of a Generic Clay Swelling Model

5.1 Introduction

UNSATCHEM has been shown (chapter 4) to underestimate water and solute movement at higher sodicity levels in the Sodosol and Vertosol soils. These results suggest that there is a need to investigate the hydraulic conductivity reduction function. The reduction function incorporates the McNeal (1968) clay swelling model and has generalised parameters. Therefore, the McNeal (1968) clay swelling model may be used to an under prediction of the hydraulic conductivity. The attempt to parameterise the clay swelling model suggested that there are limitations in the model and there is a need to identify a more appropriate form of the model. Hence, the purpose of this chapter is to evaluate the clay swelling model (McNeal 1968) and to develop a strategy to estimate the model parameters for local soils.

This chapter contains seven sections. Section 5.2 starts by reviewing the mechanisms of clay dispersion and K_{sat} reduction. Section 5.3 identifies inconsistencies in the assumptions underpinning the McNeal (1968) clay swelling model. Section 5.4 provides a mathematical evaluation of the clay swelling function used in UNSATCHEM and proposes adjustments to improve the model. Section 5.5 provides a new form of clay swelling model. Section 5.6 serves as a calibration of the new generic clay swelling model using RK_{sat} data sourced from McNeal et al. (1968). Section 5.7 concludes the main findings of this chapter.

5.2 Review of the McNeal clay swelling model

5.2.1 Background

Quirk and Schofield (1955) demonstrated that the stability of clay aggregates in soils is a function of both the soil and the amount of sodium within the soil solution. These factors interact to produce both swelling and dispersion of clay particles. Swelling creates an increase in the aggregate size due to the movement of water and cations between the clay platelets while dispersion is the process of separating the clay platelets and suspending them in the soil-water. Swelling is reversible. However, dispersion is an irreversible process because re-flocculating suspended clay platelets does not recreate the original particle associations and orientations (Levy 2000).

Both swelling and dispersion can be explained by the Diffuse Double Layer theory (DDL) which involves the attraction of cations to the negatively charged clay surfaces. The clay platelets are attracted to each other by van der Waals forces while the osmotic pressure created by the increase in ion concentration in the DDL acts to repulse the platelets (Sumner 1993). The effect of the changes in the bulk solution electrolyte concentration and relative proportion of sodium ions is to change the number and mix of ions present within the diffuse double layer which affects the osmotic pressure operating to repel the platelets. Where the electrolyte concentration is low and/or the sodium level is high, both the diffuse double layer and the osmotic pressure exerted on adjoining platelets are large. Where the osmotic pressure is large enough that the adjoining platelets move beyond the influence of the van der Waals forces, the platelets move apart and become suspended (i.e. dispersed) in the soil-water. The clay swelling model has been widely used (e.g. Mustafa & Hamid 1977; Simunek & Suarez 1997; Simunek et al. 1996; Suarez & Simunek 1997) to determine and quantify the effect of sodicity on soil hydraulic properties.

5.2.2 The McNeal approach

The McNeal (1968) clay swelling model was proposed to quantify changes in saturated hydraulic conductivity (K_{Sat}) under sodic soil conditions. McNeal and Coleman (1966) found that for a given level of sodicity, the reduction in relative saturated hydraulic

conductivity (RK_{Sat}) was related by a sigmoidal function to the logarithm of the solute concentration (C_o). McNeal (1968) subsequently used the concept of a swelling factor to determine the RK_{Sat} with changes in solution concentration and sodium. The swelling factor is used to predict whether the sodium and solute concentration will induce soil physical degradation or flocculation (Warrence et al. 2003). The relationship between RK_{Sat} and swelling factor (McNeal 1968, 1974) provides a description of the RK_{Sat} at various combinations of solute concentration and exchangeable sodium percentage (ESP):

$$1 - RK_{Sat} = \frac{cx^n}{(1 + cx^n)} \quad (5.1)$$

where RK_{Sat} is relative hydraulic conductivity, x is the swelling factor (i.e. the calculated interlayer swelling of soil montmorillonite), and c and n are constants for a given soil within a specified range of ESP.

McNeal (1968) provided a graphical method (Figure 5.1) for the estimation of x based on the soil solution concentration and an adjusted ESP (i.e. ESP^*) value.

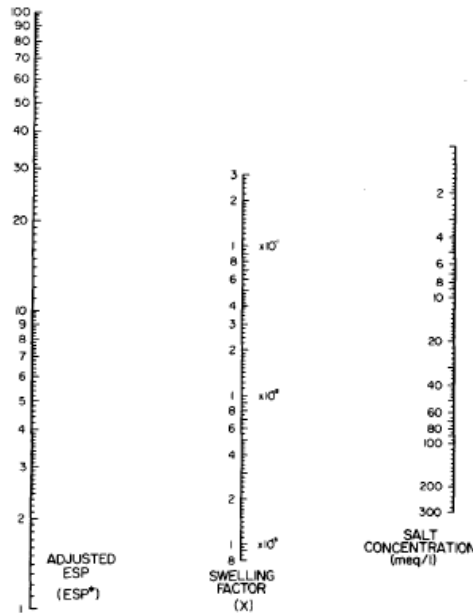


Figure 5.1 Graphical method for estimating the swelling factor as a function of ESP^* and salt concentration in soil-water

Source: (McNeal 1968)

In this case, the ESP^* value is calculated as:

$$ESP^* = ESP - ESP_T \quad (5.2)$$

where ESP_T represents the threshold ESP at which the K_{sat} starts to decline. As the reduction of K_{sat} depends on the solute concentration, the generic function for ESP_T proposed by McNeal (1968) is:

$$ESP_T = 1.24 + 11.63 \log C_o \quad (5.3)$$

where C_o is the solute concentration of the added water. It should be noted that equation 5.3 and the graphical method (Figure 5.1) provide an average threshold level for the set of soils studied by McNeal et al. (1968). The McNeal (1968) graphical method for determining the swelling factor was based on the modified domain model (Norrish 1954):

$$x = (f_{amount})(3.6 \times 10^{-4})(ESP^*)(d^*) \quad (5.4)$$

where f_{amount} is the weighted fraction of montmorillonite in the soil (i.e. mass of montmorillonite divided by the mass of the soil). McNeal (1968) assumed f_{amount} to be at the ratio 0.1. If $f_{amount} \neq 0.1$, the c parameter in equation 5.1 should be replaced by c' calculated:

$$c' = c \left(\frac{f_{amount \text{ actual}}}{f_{amount \text{ assumed}}} \right)^n \quad (5.5)$$

where c' is the adjusted c parameter for different montmorillonite contents and n is the same as in equation 5.1. McNeal (1968) identified the d^* variable in equation 5.4 as the adjusted interlayer spacing which can be predicted (Norrish 1954) as:

$$d^* = 0 \quad \text{for } C_o > 300 \text{ meq / litre} \quad (5.6I)$$

$$d^* = 356.4(C_o)^{-0.5} + 1.2 \quad \text{for } C_o \leq 300 \text{ meq / litre} \quad (5.6II)$$

The transformation constant (3.6×10^{-4}) in equation 5.4 accounts for the relative increase of the interlayer spacing volume (cm^3) due to swelling. McNeal (1968) calculated the transformation constant (i.e. 3.6×10^{-4}) as:

$$\frac{\left(800 \times 10^4 \frac{\text{cm}^2}{\text{g}_{\text{montmorillonite}}} \right) \times 0.9 \times (1 \times 10^{-8} \text{ cm} / \text{\AA})}{100 \times 2} \quad (5.7)$$

where $800 \times 10^4 \text{ cm}^2/\text{g}$ is the approximate specific surface area of montmorillonite clay. The factor 0.9 represents the ratio of inner specific surface (i.e. inner pores of clay platelets) which comprises 90% of the total specific surfaces for montmorillonite. The factor 1×10^{-8} converts the d^* from angstroms (\AA) to cm. Since the shape of montmorillonite particles is sheet-like, only one side area is used to calculate the increase of the interlayer spacing. Thus, the specific surface area is divided by 2. To facilitate the use of ESP as integer numbers, 100 is also placed in the denominator of the calculation. Note that to avoid confusion, the transform constant is reported here as angstrom units as per McNeal (1968), but when appropriate, this value is converted into SI units for calculating the swelling factor.

McNeal (1968) suggested that the value of the n parameter in equation 5.1 was fixed for a particular soil and was closely related to the ESP. The recommended n values based on ESP were:

$$n = \begin{cases} 1 & \text{ESP} < 25 \\ 2 & 25 \leq \text{ESP} \leq 50 \\ 3 & \text{ESP} > 50 \end{cases} \quad (5.8)$$

The c value in equation 5.1 is also closely related to the n parameter and McNeal (1968) suggested that c values could be assigned for each of the three ESP ranges listed above (equation 5.8). McNeal (1968) identified c values for Pachappa soils by best fit as 35, 932, and 2500 for $n = 1, 2$ and 3 , respectively. However, where the relative hydraulic conductivity is measured and the ESP is known, equation 5.1 can be directly used to calculate the value of the c parameter.

5.2.3 Later modification to the McNeal model

Simunek et al. (1996), Suarez and Simunek (1997) and Simunek et al. (2005) adopted the McNeal clay swelling function in UNSATCHEM along with the suggested n and c values:

$$n = 1 \quad c = 35 \quad \text{for } ESP^* < 25 \quad (5.9I)$$

$$n = 2 \quad c = 932 \quad \text{for } 25 \leq ESP^* \leq 50 \quad (5.9II)$$

$$n = 3 \quad c = 2500 \quad \text{for } ESP^* > 50 \quad (5.9III)$$

However, Simunek et al. (1996) and Simunek and Suarez (1997) also modified the (McNeal 1968) model to account for pH effects by incorporating a general hydraulic conductivity reduction function (r) for K_{sat} :

$$r(\text{pH}, \text{SAR}, C_o) = r_1(\text{SAR}, C_o) r_2(\text{pH}) \quad (5.10)$$

where r_1 is the reduction of K_{sat} due to the clay swelling and calculated as:

$$r_1 = 1 - \frac{cx^n}{(1 + cx^n)} \quad (5.11)$$

and r_2 is the reduction of K_{sat} due to an increase in the net negative charges on the clay colloids associated with the increase in soil solution pH. Values for r_2 have been suggested by Simunek et al. (1996) to be:

$$r_2 = \begin{cases} 1 & \text{pH} < 6.83 \\ 3.46 - 0.36\text{pH} & 6.83 \leq \text{pH} \leq 9.3 \\ 0.1 & \text{pH} > 9.3 \end{cases} \quad (5.12)$$

The general hydraulic conductivity reduction function (r) used to predict the saturated hydraulic conductivity (K_{sat}) is thus:

$$K_{sat} = r K_{sat}^{Max} \quad (5.13)$$

where K_{Sat}^{Max} is the maximum saturated hydraulic conductivity achieved when the soil is stable (i.e. no reduction noted due to sodicity or low electrolyte concentration).

The effect of sodicity on soil physical properties can be practically evaluated by observation of the K_{Sat} reduction. Simunek et al. (1996) assumed that the effect of sodicity on unsaturated hydraulic conductivity (K_{Unsat}) was the same as for K_{Sat} . Hence, K_{Unsat} can be calculated from K_{Sat} as (van Genuchten 1980):

$$K_{Unsat} = K_{Sat} K_{(h)} \quad (5.14)$$

where $K_{(h)}$ is the unsaturated hydraulic conductivity function, which can be written (van Genuchten 1980):

$$K_{(h)} = S_e^{1/2} \left[1 - \left(-S_e^{1/m_i} \right)^{m_i} \right]^2 \quad (5.15)$$

where S_e is the relative water saturation in the soil, and m_i is an empirical parameter dependent on the soil type. Hence, the reduction in K_{Unsat} can be predicted by substituting equations 5.13 and 5.15 in equation 5.14:

$$K_{Unsat} = r K_{Sat}^{Max} S_e^{1/2} \left[1 - \left(-S_e^{1/m_i} \right)^{m_i} \right]^2 \quad (5.16)$$

The complexity of parameterising the clay swelling model, however, has led workers to use general parameters developed on only a narrow range of soils. Simunek and Suarez (1997) noted that using generalised parameters for different soils was not likely to provide an accurate prediction of hydraulic conductivity, but rather serve to describe the type of changes that could occur during infiltration under various sodic conditions. To achieve accuracy in modelling solute and water movement for particular soils the parameters need to be calibrated.

5.3 Assumptions underpinning the McNeal (1968) clay swelling model

5.3.1 Clay swelling distance calculation

According to the domain model (Norrish 1954), clay swelling can be demonstrated by considering two clay platelets which are parallel (Figure 5.2). When water is added to dry montmorillonite the actual interlayer spacing (D^*) increases. When non-sodic saline water is added to dry montmorillonite, D^* increases from about 0.95 nm (9.5 Angstrom (Å)) to approximately 2 nm (20 Å) (Iwata et al. 1995; Norrish 1954; Quirk & Murray 1991). However, this distance increases according to the solution chemistry and is greater for absolute sodic solutions.

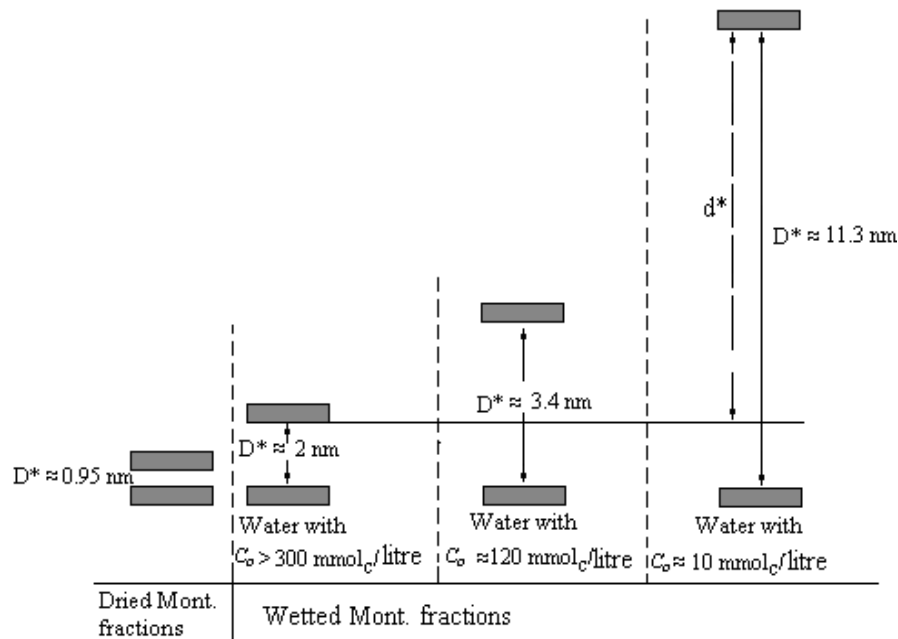


Figure 5.2 The effect of soil solution concentration on montmorillonite swelling (ESP =100%) as described by Norrish (1954)

Norrish (1954) used X-ray diffraction methods to measure D^* on samples of pure montmorillonite for two different sodic solutions (i.e. sodium chloride (NaCl) and sodium sulphate (Na_2SO_4), which were assumed to have $\text{SAR} = \infty$) at different electrolyte concentrations. The ESP of the clay samples was assumed to approach 100% as SAR approaches ∞ (Evangelou & McDonald Jr 1999). Norrish (1954) found

that the distance between the two clay platelets was high at low electrolyte concentration (i.e. electrolyte concentration approaching zero). However, with increasing electrolyte concentration (C_o), the distance between the platelets decreased dramatically. The conclusion was made that D^* increased linearly with $C_o^{-1/2}$ (Figure 5.3). McNeal (1968) later described the change in adjusted interlayer spacing (d^*) using an empirical equation based on the Norrish (1954) findings (equation 5.6).

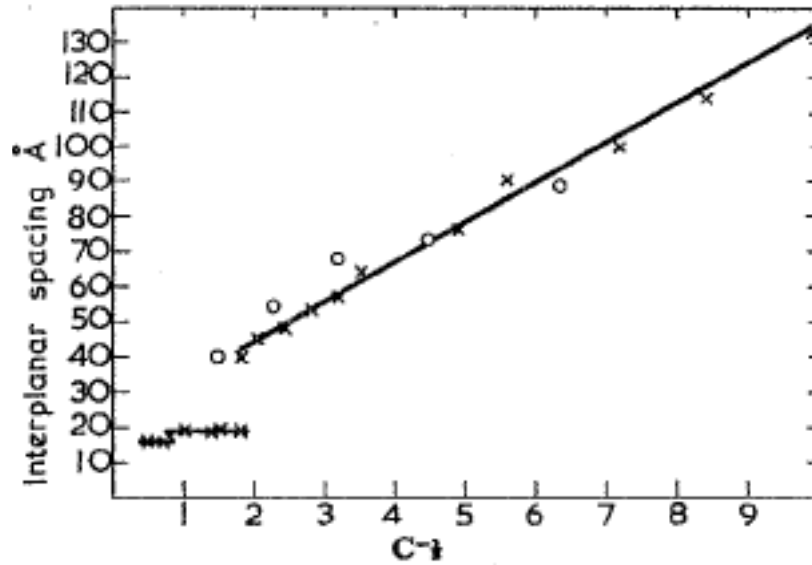


Figure 5.3 Lattice expansion up to 2 nm and more than 40 nm) of montmorillonite under two Na-solutions (i.e. x NaCl, o Na_2SO_4 , and --- fitted line) with the square root of different concentrations

Source: (Norrish 1954)

According to the McNeal (1968) approach, the adjusted interlayer spacing (d^*) is defined as the increase in the distance between the clay platelets due to the sodicity effect at a given salinity. Swelling can occur during clay wetting with low sodicity. The adjusted interlayer spacing accounts for the increase in the distance between the clay platelets due to only sodicity and varies with solute concentration. McNeal (1968) also suggests that sodicity has no significant effect on montmorillonite swelling above $C_o = 300$ mmol/litre and the adjusted interlayer spacing (d^*) should be equal to zero at higher concentrations. However, Equation 5.6(II) produces a value for d^* of 21.78 Å (2.178 nm) at an electrolyte concentration of 300 mmol/litre (Figure 5.4). This suggested that there is a disjunction in the d^* values derived using equation 5.6II and this equation may not describe the adjusted interlayer spacing properly.

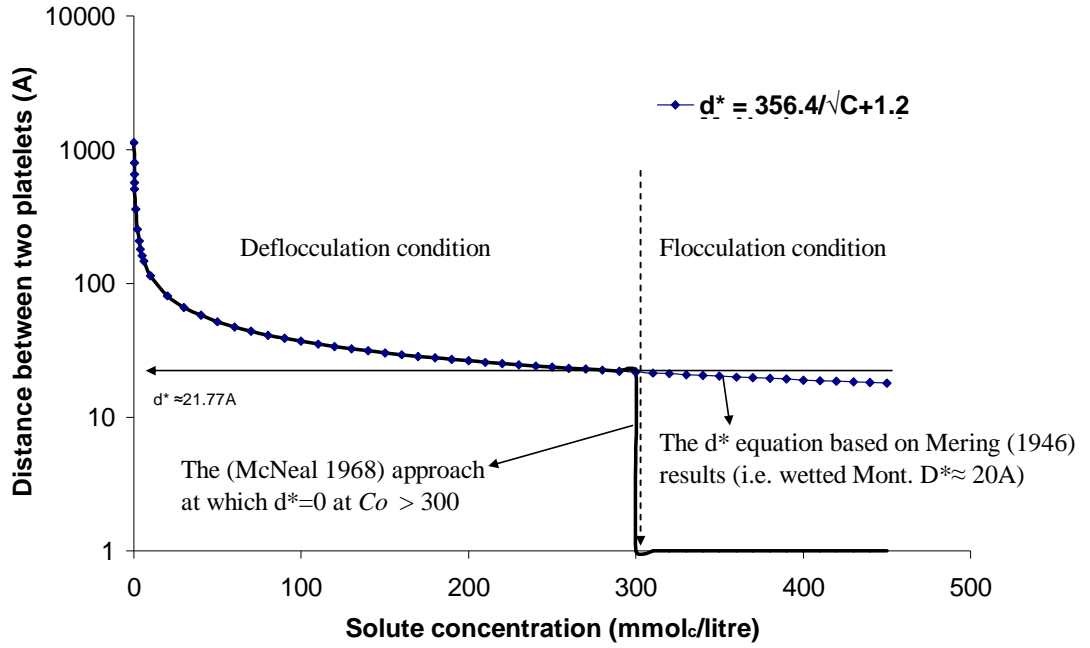


Figure 5.4 Demonstration of d^* equation under sodic condition (ESP= 100%) and its adjustment as described by McNeal (1968)

The value of d^* at 300 mmol_e/litre calculated using equation 5.6(II) approaches the normal interlayer spacing (2.178 nm) for montmorillonite swelling when wetted with low sodicity water (e.g. Norrish 1954; Iwata et al. 1995; and Mering 1946). It is clear evidently from Figure 5.4 that equation 5.6 describes the actual interlayer spacing (D^* not d^*). Therefore, equation 5.6 should be rewritten to account only for the increase of interlayer spacing due to maximum sodic conditions as:

$$d^* = 356.4(C_0)^{-0.5} - 20.58 \quad \text{for } C_0 \leq 300 \text{ meq/litre} \quad (5.17)$$

Hence, the adjusted interlayer distance produced using equation 5.17 accounts for only the effect of sodicity which approaches zero at $C_0 = 300$ mmol_e/litre. Equation 5.17 is applicable at electrolyte concentrations less than 300 mmol_e/litre. For higher C_0 , the d^* value is equal to zero.

5.3.2 Threshold levels in the clay swelling model

A major assumption in the McNeal (1968) clay swelling model is that the cation concentrations on the soil exchange surfaces and in the soil solution have reached an equilibrium with the applied water. Consequently, the ESP of the soil is estimated from the SAR of the applied water. The SAR-ESP relationship proposed by the USSS Staff (1954) has been widely used (e.g. Department of Natural Resources 1997; Skene 1965).

The d^* represents the adjusted interlayer spacing due to Na^+ cation adsorption. At $\text{ESP} = 100\%$ (or $\text{SAR} \rightarrow \infty$) (Evangelou & McDonald Jr 1999; Panabokke 1999) and $C_o < 300 \text{ mmol/L}$, the magnitude of d^* depends on C_o (Norrish 1954). For Na-Ca solutions, the expansion of the montmorillonite will be a function of the ESP. Therefore, the change in interlayer spacing of montmorillonite due to the differences in sodium concentration (\hat{d}) can be predicted if the threshold level of sodicity for montmorillonite inherent with C_o is known (i.e. at which the adjusted interlayer spacing d^* begins to increase or $d^* > 0$) as:

$$\hat{d} = \frac{(100 - \text{ESP}_{T\text{Mont.}})}{100} (d^*) \quad (5.18)$$

where 100 represents the Exchangeable Sodium Percentage (all the exchange surfaces are saturated by Na^+ cations) and $\text{ESP}_{T\text{Mont.}}$ is the threshold ESP at which the clay (i.e. montmorillonite) starts to swell.

In the clay swelling model, the effect of clay expansion depends on the proportion of expansive clay present in the soil. Assuming that the density of montmorillonite aggregates are similar to the density of other aggregates, then the ratio by weight of the montmorillonite clay (f_{amount}) to total soil amount may be used to calculate the expansion of a given volume of soil. However, it is also necessary to assume that the ESP of the montmorillonite in the soil is equal to the ESP of the bulk soil (i.e. there is no mineralogical preferences for cation adsorption). If this is the case, the expansion (i.e. increase of volume) within soils containing montmorillonite (dV) due to the effect of sodicity can be predicted as:

$$dV = (ESP - ESP_T) (d^*) (f_{amount}) \quad (5.19)$$

The clay expansion under sodic condition occurs within clay aggregates and leads to a reduction in the size of the adjacent fine pores and/or increase in the volume of the bulk aggregates. This, in turn, causes a reduction in outer pore size (large pores) and an increase in the bulk soil volume. The change of the pore size depends on both the degree of clay swelling and the initial pore size distribution. The initial pore size distribution depends on soil type and condition (e.g. tillage, or intensive vegetation). Reshaping of the pores due to clay swelling determines the magnitude of the reduction in hydraulic conductivity.

The ESP_T varies with C_o and is unique for each soil. Assuming that the water applied, soil solution, and adsorbed species on colloid surfaces are chemically equilibrated, then the ESP can be estimated from the SAR of the applied water. The ESP_T identical to the threshold electrolyte concentration (TEC) (discussed in section 2.3.4). Thus, the ESP_T can be predicted from the soil stability indicators as originally provided by Quirk and Schofield (1955). The function that relates C_o with ESP_T rather than SAR is (McNeal & Coleman 1966):

$$ESP_T = l + s \ln(C_o) \quad (5.20)$$

where, l and s are empirical parameters, which depend on the soil type and soil condition. The common logarithm (\log) herein was replaced by the natural logarithm (\ln) for simplification purpose. Therefore, the adjusted ESP (i.e. ESP^*) which is related to the adjusted interlayer spacing (d^*) is:

$$ESP^* = ESP - (l + s \ln(C_o)) \quad (5.21)$$

It should be noted that l and s are generalised in equations 5.20 and 5.21. However, the ESP_T value proposed by McNeal (1968) is based on a family of soils studied by McNeal et al. (1968). Hence, the threshold values proposed may be unsuitable for other soils.

5.3.3 Swelling and dispersion in the clay swelling model

The clay swelling model is based on measurements of montmorillonite expansion in open and pure clay systems. Under maximum (i.e. 100%) sodic conditions, the distance between two clay platelets increases rapidly with decreases in the electrolyte concentration. Practically, soil structure may constrain clay expansion (Oster & Shainberg 2001) and prevent complete expansion of platelets. On the other hand, larger repulsive forces or higher expansion of the clay reduces the attractive forces between the platelets. This, in turn, increases the probability of separating and displacing clay fractions during water movement. The probability of clay fraction separation increases with the increase in the distance between platelets. Assuming that clay dispersion can be related to d^* in the same manner as swelling behaviour, the clay swelling model will account indirectly for the process of clay dispersion and movement. Therefore, both swelling and dispersion could happen concurrently within the soil at different levels and their combined effects on K_{sat} reduction could be quantified by the clay swelling model irrespective of which process predominates.

Furthermore, the clay swelling model may also be more generally used to describe the reduction of K_{sat} in soils that have any type of swelling clay mineralogy. The parameter for the weighted fraction of montmorillonite clay in the clay swelling model (i.e. f_{amount} term in equation 5.4) can be replaced by an empirical parameter which depends on the amount of expanding clay within the soil.

In this case, the use of the traditional swelling factor (x) reflects the magnitude of clay swelling and relates it directly to RK_{sat} (equation 5.1), irrespective of soil mineralogy. In any case, estimating the actual quantity of the different clay minerals present in a soil is not routinely conducted and is subject to large errors due to the inability to measure small amounts (Sumner 1993). Therefore, it is often not appropriate to use the actual montmorillonite fraction in the x calculation (equation 5.4). Instead, it may be most appropriate to replace the weighted fraction of montmorillonite by a fitted empirical parameter f , which accounts for the effective clay swelling.

5.4 Evaluation of the McNeal (1968) model of clay swelling

The difficulty of measuring the clay swelling model parameters for specific soils has led many researchers to use the generalised parameters proposed by McNeal (1968). However, the use of these parameters is limited to only particular levels of sodicity and salinity. Validation of the clay swelling model for a broader range of ESP and C_o has not been found in the literature. The work reported in this section is a demonstration and discussion of the clay swelling model using the set of n and c parameters (equation 5.4) as proposed by McNeal (1968; 1974), and that have been hard coded in UNSATCHEM.

5.4.1 Evaluation methodology

To evaluate the generalized clay swelling model (equation 5.1), RK_{Sat} values were calculated based on the set of n and c parameters (equation 5.9I, 5.9II, and 5.9III) proposed by McNeal (1968). Numerical values for ESP and electrolyte concentration ranged from 0.1 to 100 and 1 to 120 mmol/litre, respectively. The intervals for both variables were chosen to equal unity.

A MATLAB program (Appendix F) was written (utilizing the grid fit function) to generate a three dimensional surface of the clay swelling equation. The evaluation was conducted by comparing the calculated RK_{Sat} with observations of RK_{Sat} as reported in the literature.

5.4.2 Results and discussion

The 3-D surface of the McNeal (1968) clay swelling model is illustrated in Figure 5.5.

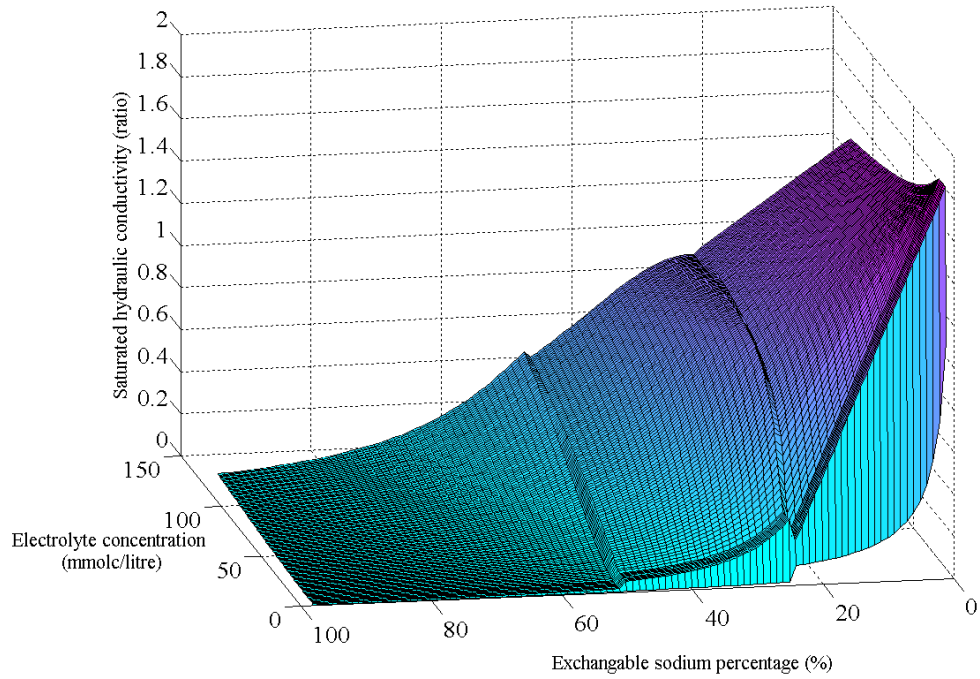


Figure 5.5 Three dimensional representation of the McNeal function (RK_{Sat} versus ESP and C_o)

The observations from the graphical surface in Figure 5.5 are twofold.

- 1) At low electrolyte concentration and ESP values below the threshold level proposed by McNeal (i.e. ESP_T), the calculated RK_{Sat} values are above 100 %. However, the increase in aggregate stability at these ESP and C_o should maintain but not increase the K_{Sat} above the stable K_{Sat} condition (i.e. $RK_{Sat} = 1$). The incorrect RK_{Sat} values produced are due to the negative values of swelling factor (x) calculated because the model uses fixed values of ESP_T and does not properly accommodate the hydraulic stability condition.
- 2) Discontinuous results for RK_{Sat} are found at the boundaries of the ESP ranges (where n changes from 1 to 2 and at n changes from 2 to 3). These results suggest that the McNeal n and c parameter values result in sharp change in the calculated RK_{Sat} around these values of ESP and C_o . In

addition, the shape of the surface indicates that considering n and c as fixed parameters might not be appropriate. A more appropriate surface would likely result if n and c were continuous functions of ESP.

To avoid the incorrect values of RK_{Sat} above 100%, Simunek et al. (2005) provided an adjustment of the ESP^* as:

$$ESP^* = \max[0, ESP - (1.24 + 11.63 \log C_0)] \quad (5.22)$$

An alternative adjustment with a similar outcome can be made to the model as:

$$\text{Flocculation condition} \quad RK_{Sat} = 1 \quad \text{when } x \leq 0, \quad (5.23I)$$

$$\text{Non-flocculation condition} \quad RK_{Sat} = 1 - \frac{cx^n}{(1 + cx^n)} \quad \text{when } x > 0, \quad (5.23II)$$

When this latter correction was implemented the resultant surface of the clay swelling model was improved (Figure 5.6).

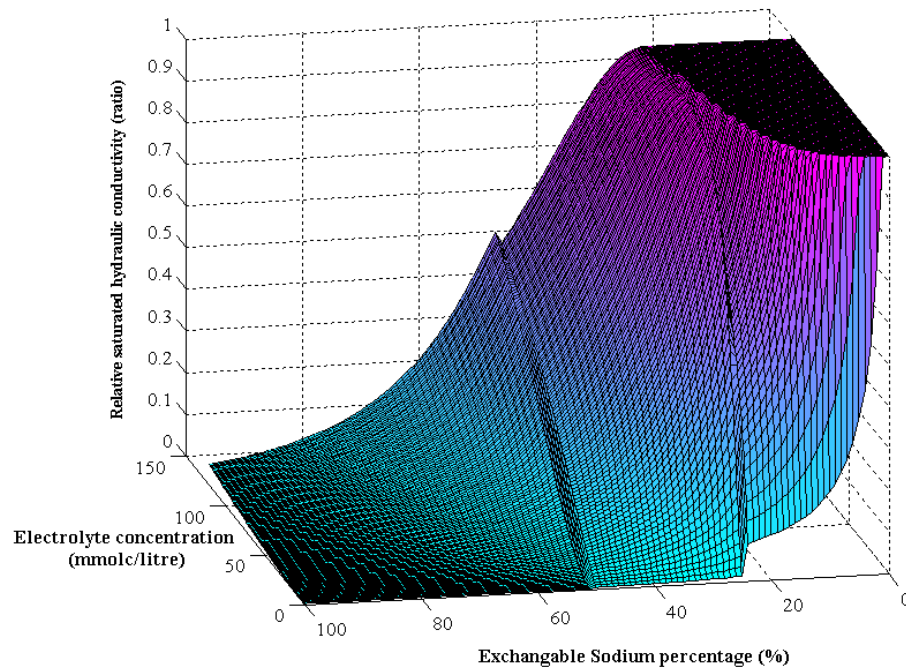


Figure 5.6 Three dimensional plot of the McNeal function with RK_{Sat} limited to 100%

The parameters n and c are functions of ESP (equation 5.9). Figures 5.8 and 5.9 diagrammatically demonstrate the set of n and c values versus ESP. Figure 5.7 suggests that the n versus ESP relationship might be close to linear. In addition, Figure 5.8 suggests that c might have an exponential relationship with ESP .

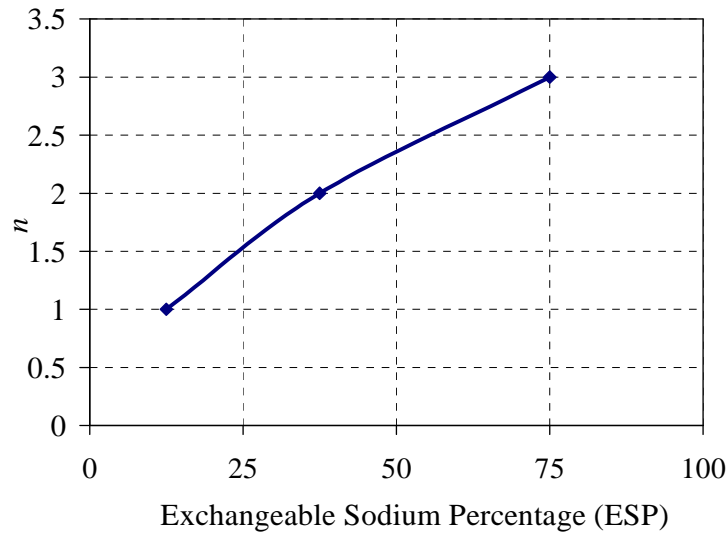


Figure 5.7 McNeal (1968) n values with ESP

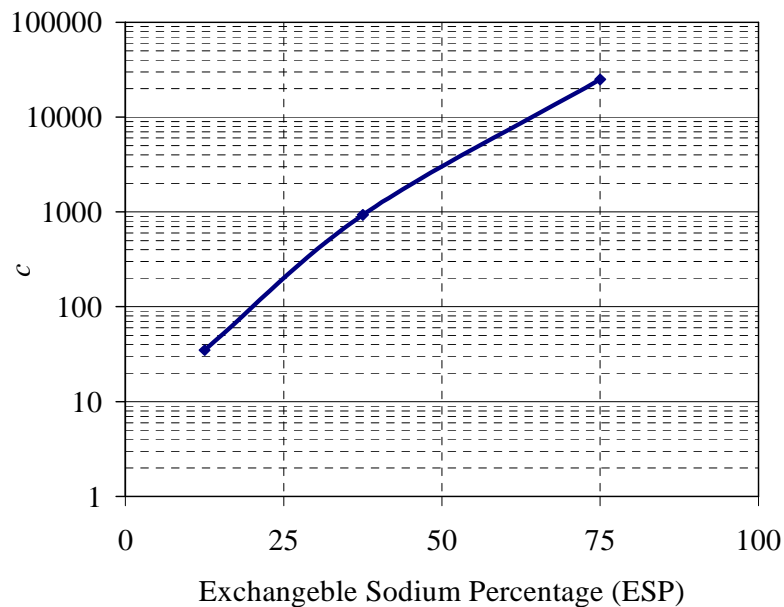


Figure 5.8 McNeal (1968) c values with ESP

5.5 Towards a generic clay swelling model

It has been shown (section 5.4) that n and c should vary continuously and are closely related to ESP. The initial demonstration using the n and c values proposed by McNeal (1968) showed that n might vary linearly with ESP and c exponentially. However, the change in both n and c with ESP may be determined precisely using experimental data of RK_{Sat} and water quality. This provides the opportunity to develop a generic clay swelling model which could be parameterised for local soils. The steps toward developing a generic clay swelling model were: (a) demonstration of ESP_T and quantifying its effect on x and RK_{Sat} , (b) determination of n and c functions empirically based on available data, and (c) validate the generic clay swelling model with the experimental data available.

5.5.1 RK_{Sat} data

Experimental data (Table 5.1) for the reduction of K_{Sat} with different mixed NaCl- $CaCl_2$ solutions applied to three groups of soils were obtained from McNeal et al. (1968). The data are averages of RK_{Sat} measurements that were obtained in a series of column experiments. Soils were classed according to clay content as: group (a) has an average clay content of 5.7%, group (b) with average clay content of 16.2%, and group (c) with higher average clay content of 48.5%. McNeal et al. (1968) indicated that all of the soils groups had an average montmorillonite content of approximately 42% of the total clay content. The RK_{Sat} data were calculated from K_{Sat} measured on a particular soil column at the specific concentration divided by the maximum K_{Sat} measured for that column (i.e. with high C_o at the same estimated ESP). The estimated ESP was calculated from the SAR of the applied water. The measurements of RK_{Sat} were reported as an average for each soil group (Table 5.1).

Table 5.1 Relative saturated hydraulic conductivity of Imperial Valley soils in the presence of mixed NaCl-CaCl₂ solutions

Source: (McNeal et al. 1968)

Soil Group	Average clay content (%)	Average maximum K_{Sat} (cm/h)	SAR	Estimated ESP (%)	Relative saturated hydraulic conductivity RK_{sat} (Ratio)				
					800 mmol _c /litre	200 mmol _c /litre	50 mmol _c /litre	12.5 mmol _c /litre	3.13 mmol _c /litre
Group (a)	5.7	7.13	0	0*	1.00	1.07	1.06	1.03	1.02
			25	26.19	1.00	0.99	0.99	0.93	0.89
			100	59.3	1.00	0.96	0.76	0.38	0.21
			∞	100	1.00	0.82	0.29	0.14	0.14
Group (b)	16.2	1.98	0	0*	1.00	1.01	1.00	0.98	0.96
			25	26.19	1.00	1.00	0.90	0.62	0.26
			100	59.3	1.00	0.75	0.10	0.00	0.00
			∞	100	1.00	0.35	0.07	0.00	0.00
Group (c)	48.5	0.523	0	0*	1.00	1.06	1.03	0.99	0.94
			25	26.19	1.00	0.84	0.66	0.20	0.01
			100	59.3	1.00	0.33	0.01	0.00	0.00
			∞	100	1.00	0.03	0.00	0.00	0.00

* The calculated values of ESP at SAR=0 produced negative values, therefore, the ESP values were assumed to be 0.

5.5.2 Calculation of ESP_T

The purpose of this step is to investigate the validity of ESP_T proposed by McNeal (1968) and subsequently, to facilitate the accurate calculation of the swelling factor (x). Determining the threshold ESP at which K_{Sat} begins to decline is arbitrary. Therefore, the approach used for TEC as defined by Quirk and Schofield (1955) and Quirk (2001) (i.e. RK_{Sat} reduction by 10-15%) was used to predict the ESP_T . The TEC is a function of SAR and ESP. The thresholds for the soils were determined by (a) simple linear interpolation of RK_{Sat} at every electrolyte concentration level to give the ESP at which RK_{Sat} reduced by 10%, and (b) fitting a logarithmic function to the interpolated ESP values. The resulting fitted ESP_T equations for the three soil groups (a), (b) and (c) are shown in Figures 5.9, 5.10, and 5.11, respectively.

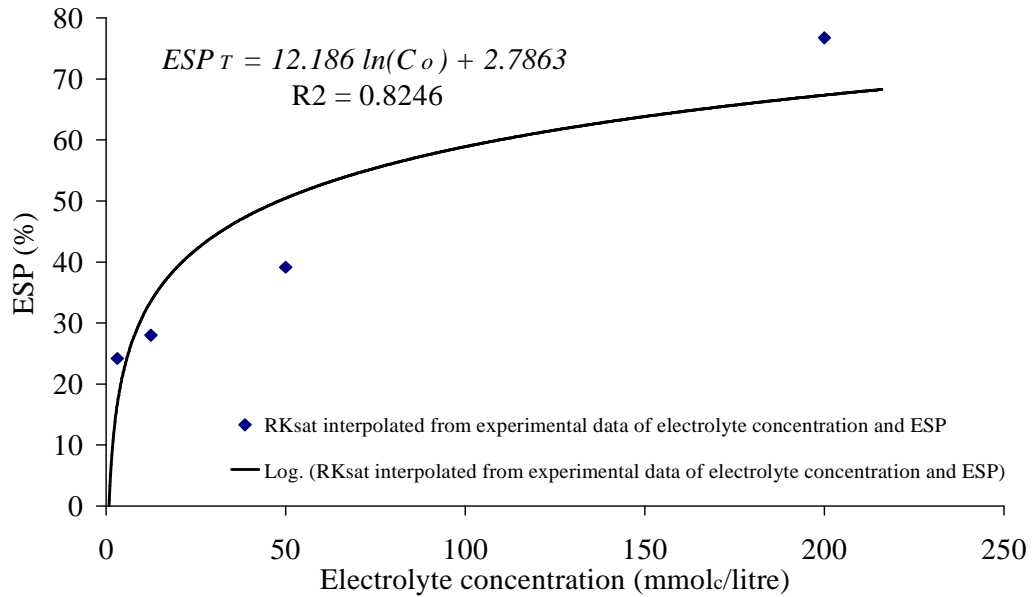


Figure 5.9 Change of ESP and electrolyte concentration at threshold level (i.e. $RK_{Sat} = 0.9$) for soil group (a) having clay content of 5.7%

Data from McNeal et al. (1968)

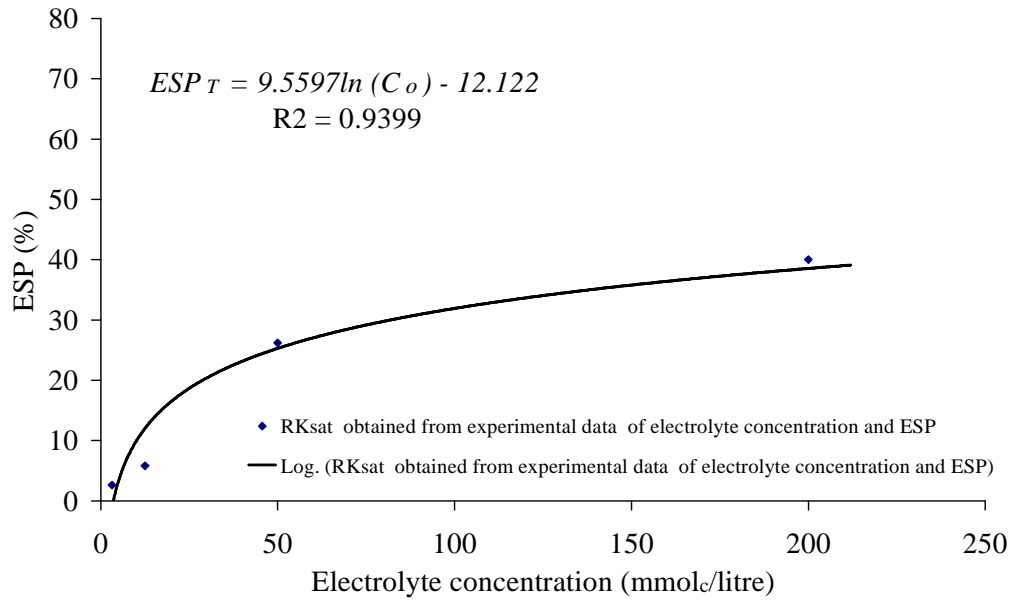


Figure 5.10 Change of ESP and electrolyte concentration at threshold level (i.e. $RK_{Sat} = 0.9$) for soil group (b) having average clay content of 16.2%

Data from McNeal et al. (1968)

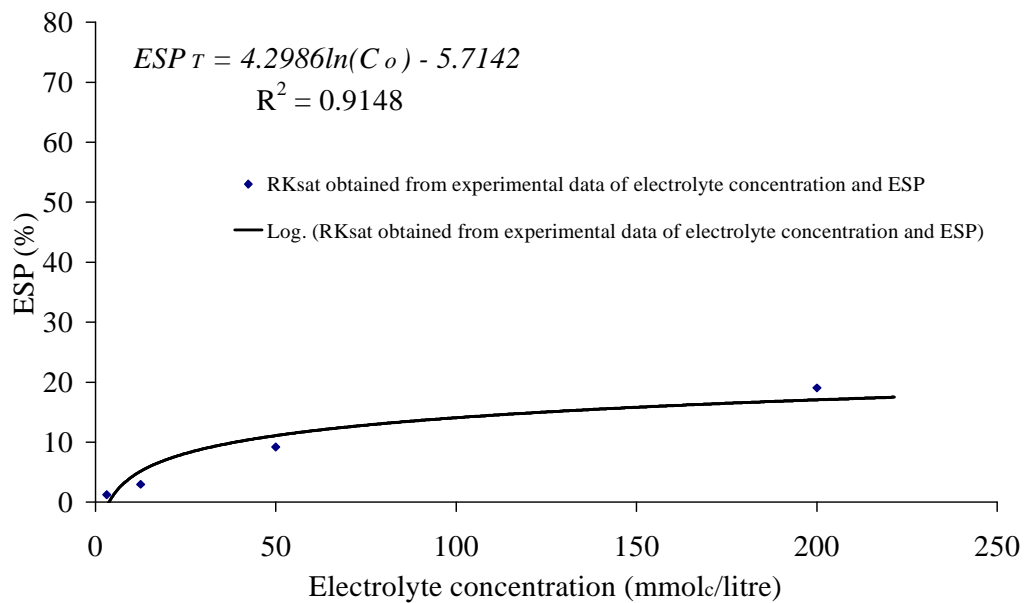


Figure 5.11 Change of ESP and electrolyte concentration at threshold level (i.e. $RK_{Sat} = 0.9$) for soil group (c) having average clay content of 48.5 %

Data from McNeal et al. (1968)

5.5.3 Effect of ESP_T on swelling factor and RK_{Sat}

It is clear that the thresholds for the different soil groups differ substantially. To demonstrate the magnitude of the differences in the threshold levels for each soil group the fitted curves are shown in Figure 5.12 along with the ESP_T proposed by McNeal (1968).

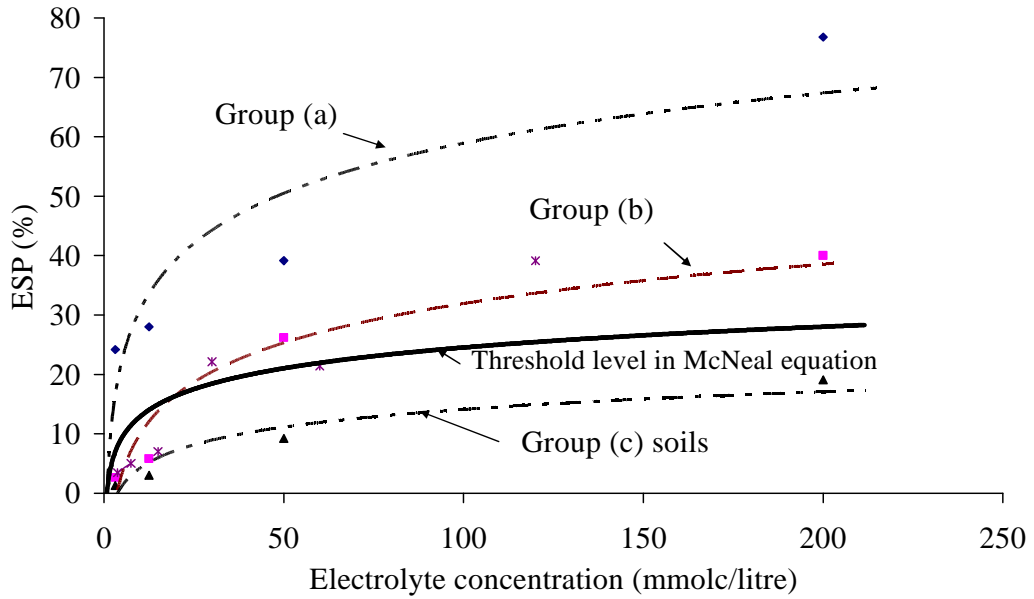


Figure 5.12 Proposed threshold level by McNeal (1968) compared with threshold levels at 10% RK_{Sat} reduction for three soils group obtained from McNeal et al. (1968)

The soils from McNeal et al. (1968) were reported to have a similar percentage of montmorillonite (approximately 42% of the clay content). However, each soil group has a different absolute montmorillonite content because each has a different clay content. The weighted fractions of montmorillonite in group (a), (b), and (c) soils are 0.024, 0.068, and 0.204, respectively. For these soils, the effect of the clay content on ESP_T is clear with ESP_T decreasing with increasing clay content in these soils.

Figure 5.12 also shows that the group (c) ESP_T is below the general ESP_T proposed by McNeal (1968). This suggests that the use of their threshold values will result in the model accuracy to describe the RK_{Sat} reduction in soils that have a ESP_T below the general ESP_T . It is clear that using the actual ESP_T for a particular soil will enhance the accuracy of the model.

5.5.4 Determination of n and c functions

The McNeal et al. (1968) data has only a limited number of ESP levels at which the reduction in RK_{sat} was measured. Amongst this data, only RK_{sat} measurements for two soils (group (b) and (c)) were able to be used to evaluate the change in n and c parameters with ESP. The rest of the data was used in section 5.6 for the calibration of the n and c functions.

For both soils (b) and (c), the x factors corresponding to the measured RK_{sat} were calculated based on the ESP_T (as described in Figures 5.9, 5.10 and 5.11), and the actual f_{amount} predicted for each soil. Graphpad software was used to conduct a non-linear regression analysis to obtain n and c parameters at each level of ESP. The results are presented in Table 5.2 for both soils at three levels of ESP.

Table 5.2 The n and c parameters obtained from non-linear regression analysis for soil groups (b) and (c) at different levels of ESP

SAR	Estimated ESP	Data for group (b)			Data for group (c)		
		n	c	R^2	n	c	R^2
25	26.19	0.9772	17.89	0.98	2.205	266.3	0.997
100	59.3	2.885	83064	0.999	15	$1.2 \times E^{+13}$	1
∞	100	4.965	16460000	0.99	30	$1.48 \times E^{+21}$	0.999

It is clear from Table 5.2 that n and c increase with the increase of ESP. While the low number of data points showing the change in n and c with ESP are not sufficient to establish significant relationships, the general trend can be depicted. The relationships between n and ESP, and c and ESP are shown in Figures 5.13, 5.14, 5.15, and 5.16. An initial evaluation of the values of n and c with different ESP levels reveals that a linear relationship can be established between n and ESP, and an exponential relationship for c .

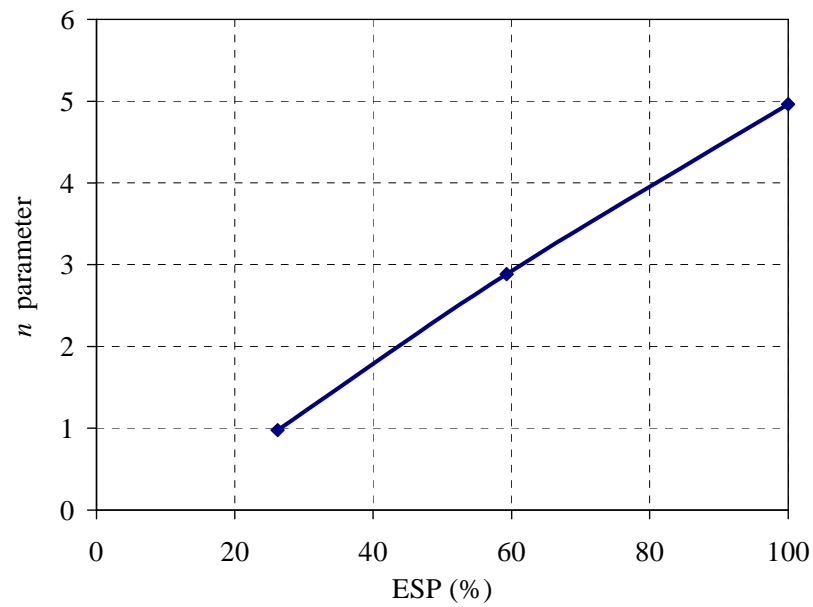


Figure 5.13 Change of n parameter obtained (by best fit) with different levels of exchangeable sodium percentage (ESP) for soils group (b) of McNeal data (1968)

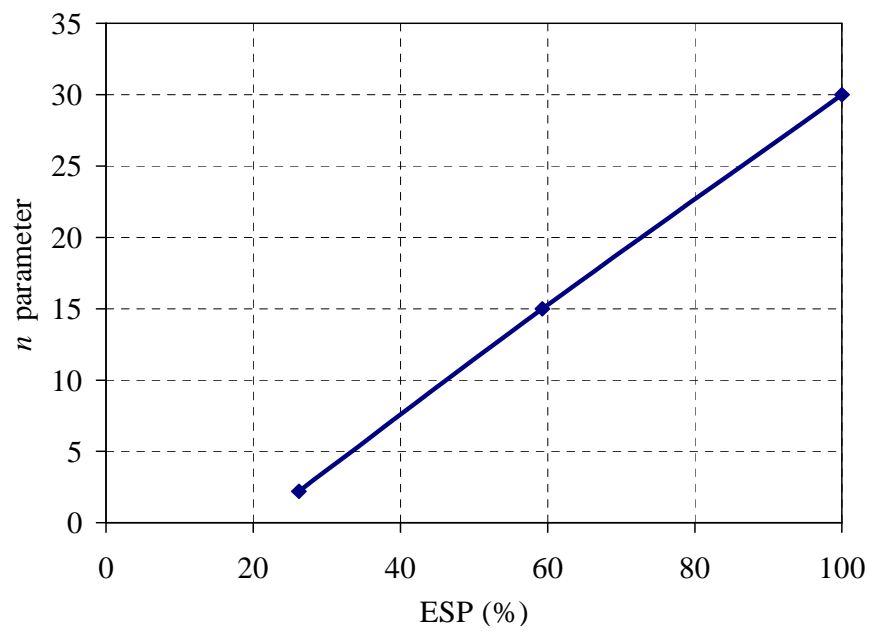


Figure 5.14 Change of n parameter obtained (by best fit) with different levels of exchangeable sodium percentage (ESP) for soils group (c) of McNeal data (1968)

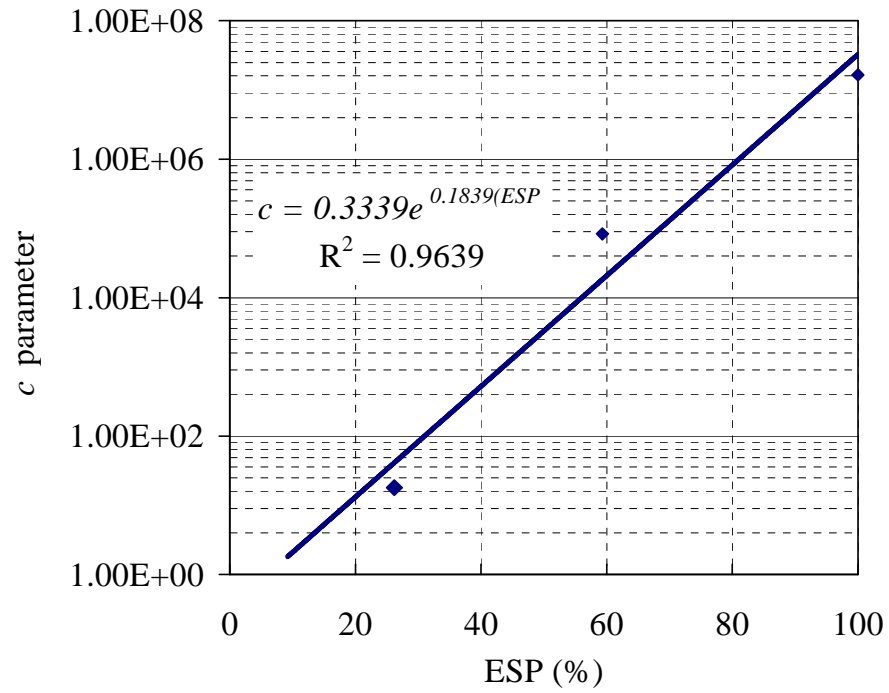


Figure 5.15 Change of c parameter obtained (by best fit) with different levels of ESP for soils group (b) of McNeal data (1968)

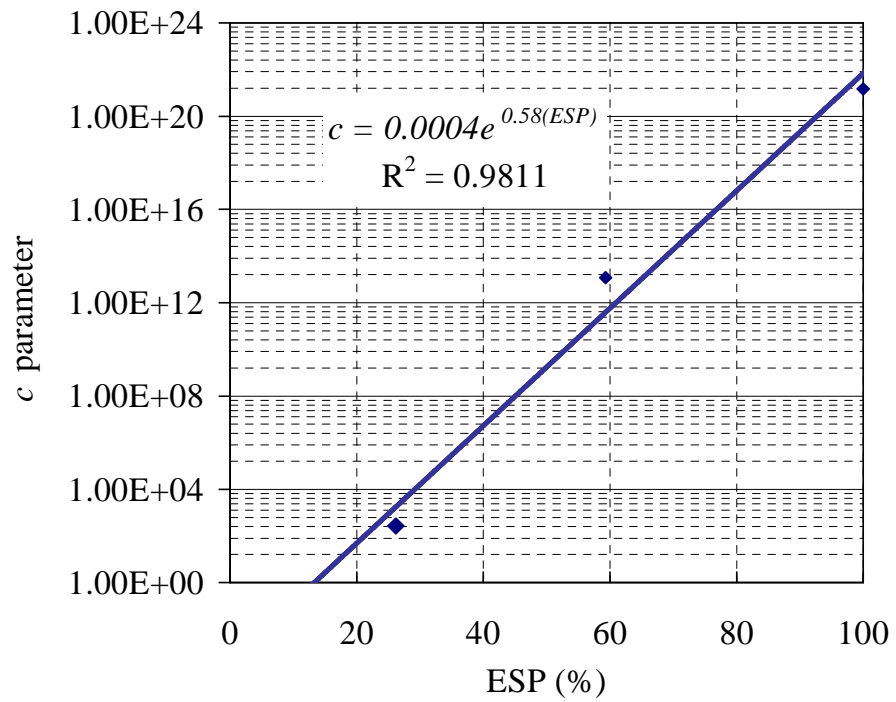


Figure 5.16 Change of c parameter obtained (by best fit) with different levels of ESP for soils group (c) of McNeal et al. (1968) data

It should be noted that both parameters n and c are interrelated at any particular ESP. Thus, any change in one parameter will result in a change in the other and both parameters should be used together. The n parameter controls the degree of curvature in the clay swelling model. The primary conclusion made is that n varies with ESP and could be described by:

$$n = (ESP)^a + b \quad (5.24)$$

where a and b are empirical fitted parameters. Furthermore, c is a function of ESP and can be written as:

$$c = ge^{m(ESP)} \quad (5.25)$$

where g and m are empirical fitted parameters.

5.5.5 Structure of the generic clay swelling model

The steps involved in developing the generic clay swelling model were as follows. The first step was to clarify the boundary between flocculation and deflocculation. This was done by considering the swelling factor (x) value. The soil is flocculated if x is equal to or less than zero, while it will deflocculate if x is greater than zero. The second step was that the constant n and c values were replaced by their functions (i.e. equation 5.24 and 5.25, respectively). The third adjustment was to use the measured ESP_T for each soil rather than the generalized McNeal ESP_T . The final adjustment involved replacing the f_{amount} by an empirical parameter which represents the effective clay swelling.

The boundary conditions for the entire range of soil sodicity in the generic clay swelling model can be concluded as:

Flocculation	$x = 0$	at	$ESP^* \leq 0$	and	$d^* = 0$
Deflocculation	$x > 0$	at	$ESP^* > 0$	and	$d^* = 356.4\sqrt{C} - 20.58$

Implementing these adjustments and incorporating the new n and c functions results in a new generic clay swelling model for describing the change in RK_{sat} within a given soil. The new model can be expressed as:

$$\text{Flocculation condition} \quad RK_{sat} = 1 \quad \text{at} \quad x \leq 0, \quad (5.26)$$

$$\text{Non-flocculation condition} \quad RK_{sat} = 1 - \left(\frac{(ge^{\frac{m(ESP)}{100}})(x_o)^{\left(\frac{ESP}{100}\right)^a + b}}{(1 + (ge^{\frac{m(ESP)}{100}})(x_o)^{\left(\frac{ESP}{100}\right)^a + b})} \right) \text{ at } x > 0 \quad (5.27)$$

where a , b , g and m are empirical parameters dependent on soil type and condition, and x_o is the adjusted effective swelling factor, which accounts for the effective swelling and dispersion that induces RK_{sat} reduction. x_o can be calculated as:

$$x_o = (f)(3.6 \times 10^{-4})(ESP^*)(d^*) \quad (5.28)$$

Where f is an empirical parameter related to effective weighted fraction of expanding clay content. The ESP^* can be calculated as:

$$ESP^* = ESP - (l + s \ln(C_o)) \quad (5.29)$$

where l and s are empirical parameters which depend on soil type and soil condition.

5.6 Calibration of the generic clay swelling model

5.6.1 Calibration methodology

The calibration of the generic clay swelling model developed in the previous section was carried out using non-linear regression (ordinary least squares method). The model was fitted to the original experimental data from McNeal et al. (1966). The data for electrolyte concentrations > 300 mmol/litre were excluded as those levels of salinity were not applicable. TableCurve 3D (version 4.0.01e) was used to fit a non-linear surface equation 5.27 to the measured RK_{sat} data for each soil. The regression analyses were performed for the three soil groups to determine the seven parameters in the generic clay swelling model (i.e. a , b , g , m , l , s , and f). A full description of the method used to perform the non-linear regression analysis is presented in Appendix G.

5.6.2 Non-linear regression results and discussion

The full results and statistical analyses from the regression analyses are shown in Appendix H. Table 5.3 shows the fitted parameters and the regression statistics. It should be noted that the R^2 values for the surface fits are greater than 0.98 and the F-test values for the three groups are between 74.75 and 157.63 (i.e. highly significant). This indicates that the model appropriately describes the experimental RK_{Sat} data. The standard error values ranged between 0.055 and 0.065 for the three soil groups. The resultant RK_{Sat} surfaces and residuals are demonstrated up to ESP = 100 (assuming that the SAR-ESP relationship is valid for the entire range of SAR and ESP) in Figures 5.17, 5.18, and 5.19. The residuals between the estimated and measured RK_{Sat} are low.

It is clear that the adjusted clay swelling model is able to describe overall the reduction of RK_{Sat} for the data available. However, the t-test values for the parameters produced are insignificant (Appendix H), which suggests that these parameters are interrelated and have no significant meaning. For example, despite the physical basis of the f parameter, it should not be given any physical meaning. The results indicate that the f_{amount} values are different from the f parameter estimated at the best fit. However, using its value estimated from the soil characterisations as initial parameters provides the best fit for the non-linear regression.

Table 5.3. Summary of the surface fit output for three group of soils from McNeal (1968)

Soil type	Model parameters							R ²	F-test	Fit Std Error
	<i>a</i>	<i>b</i>	<i>g</i>	<i>m</i>	<i>f</i>	CTEC parameters				
						<i>s</i>	<i>l</i>			
Group (a)	0.649	0.0003	8.837	4.046	0.008	6.356	30.818	0.98	74.75	0.065
Group (b)	1	0.912	1.438	7.29	0.204	4.105	-5.054	0.987	112.48	0.065
Group (c)	0.449	1.005	0.846	10.967	0.53	4.0799	-11.15	0.991	157.63	0.055

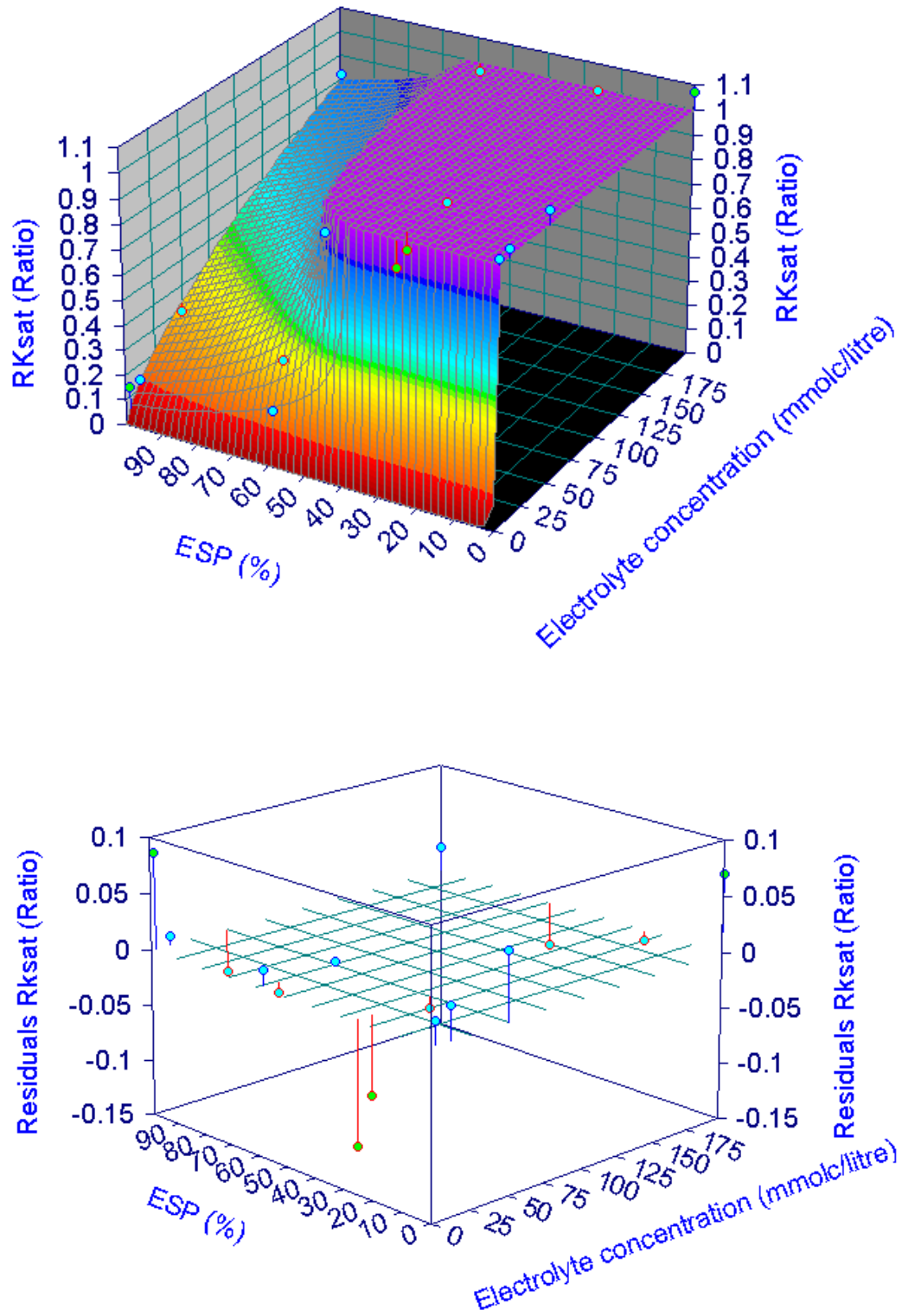


Figure 5.17 Three dimensional surface of best fit and the residuals of RK_{sat} (i.e. between predicted and measured) for the for the group (a) soils

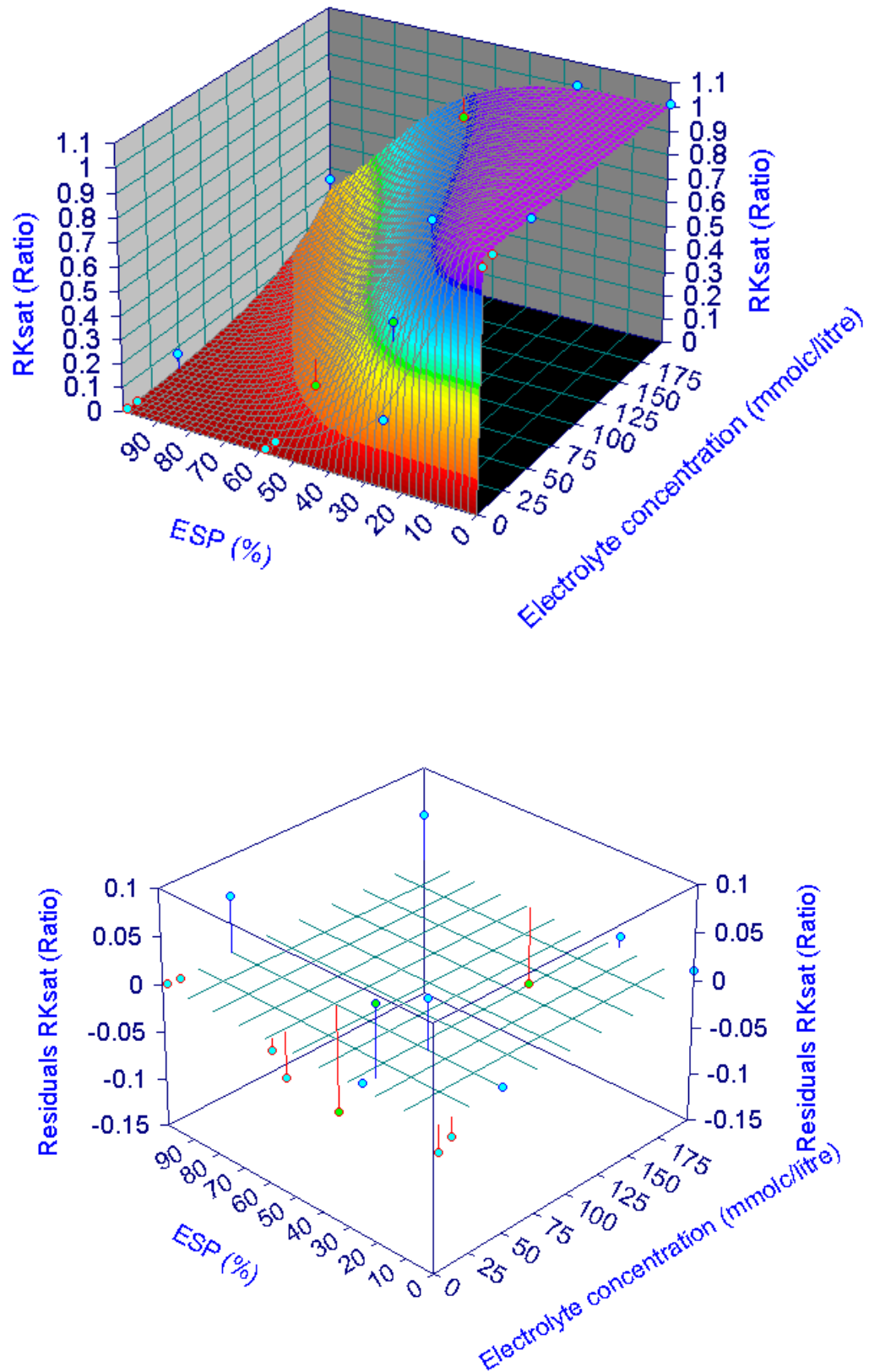


Figure 5.18 Three dimensional surface of best fit and the residuals of RK_{sat} (i.e. between predicted and measured) for the group (b) soils

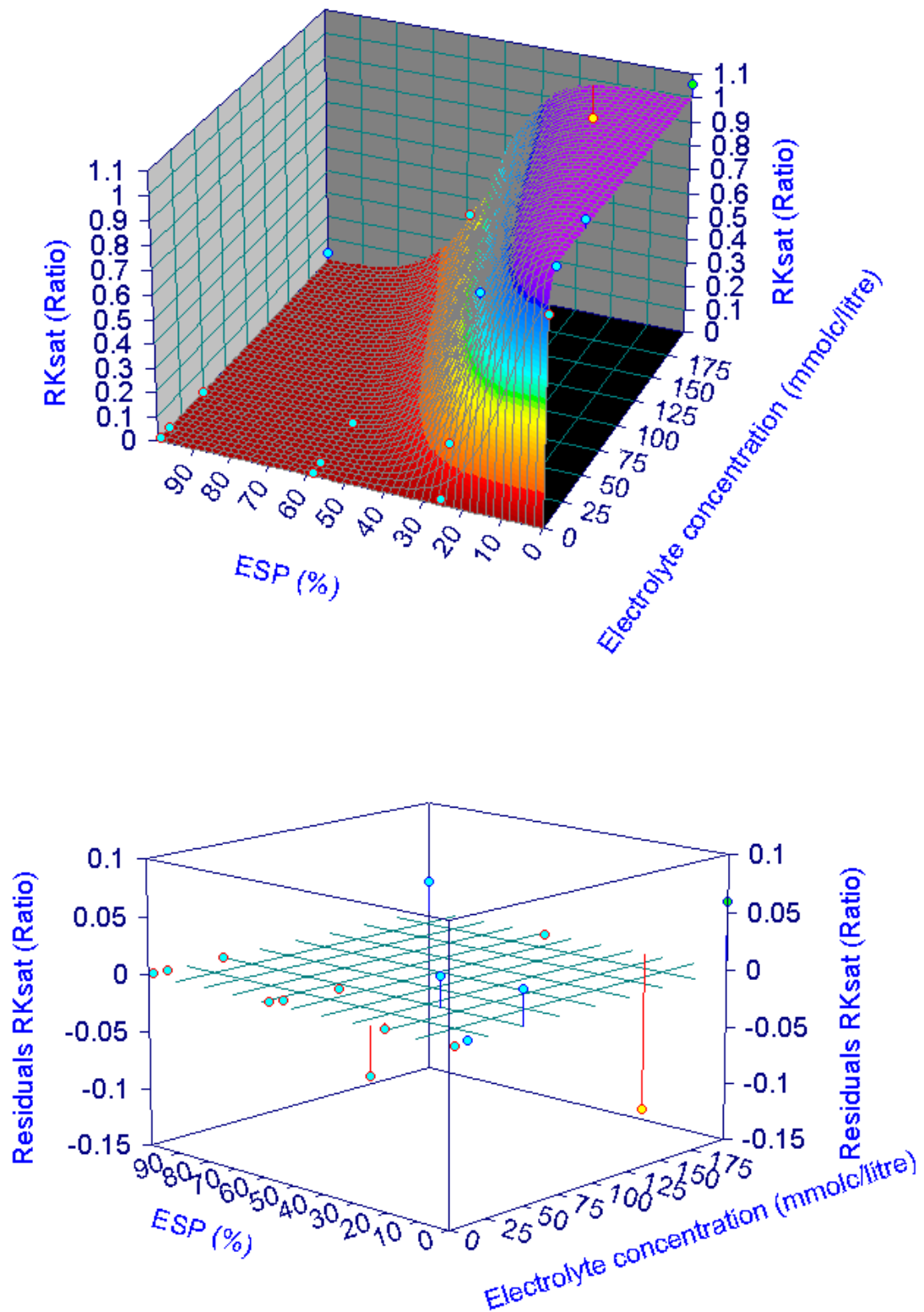


Figure 5.19 Three dimensional surface of best fit and the residuals of RK_{Sat} (i.e. between predicted and measured) for the group (c) soils

5.7 Conclusion

This chapter has shown that the traditional clay swelling model has a number of weak points that may limit its accuracy. It has been shown that the calculation of the adjusted interlayer spacing by McNeal (1968) was misinterpreted. Furthermore it has been also concluded that main weaknesses are the generalised threshold ESP_T incorporated to calculate the swelling factor (x), the uncertainty over the values of n and c , and their relations to sodicity levels. A demonstration of the clay swelling model using the generalised parameters incorporated into UNSATCHEM reveals that the values of n assigned for ranges of ESP are not appropriate and results in ambiguous prediction of the K_{sat} reduction. Furthermore, both n and c are shown to vary continuously with ESP.

The proposed generic clay swelling model includes an adjusted interlayer spacing, an ESP_T function to be determined for the soil, replacing the montmorillonite fraction by a fitted parameter, and substituting the n and c parameters as functions of ESP. The new form of the model contains seven parameters to be determined by fitting the model to experimental data. Calibration of the new form of clay swelling model with the original McNeal et al (1968) data for three soil groups shows a good agreement between predicted and measured RK_{sat} . The new generic form of clay swelling model describes successfully the negative effect of sodicity on soil K_{sat} for the data used. However, further evaluation for a wider range of soils is required.

CHAPTER 6: Applicability of the Generic Clay Swelling Model for a Broader Range of Soils

6.1 Introduction

The McNeal (1968) clay swelling model was modified in chapter 5 to better handle the effect of different water qualities (i.e. different sodicity level and electrolyte concentration) on relative saturated hydraulic conductivity (RK_{Sat}). A new generic clay swelling model (GCSM) was also evaluated with the original RK_{Sat} data from McNeal et al. (1968). The evaluation results showed a good agreement between the estimated and the experimental RK_{Sat} data. However, there is a need to validate the GCSM with more RK_{Sat} data for different soils. Therefore, this chapter provides additional validation of the generic clay swelling model using different RK_{Sat} data for a number of local soils. Data was obtained by both experimental work (conducted during this study) and from published studies. Two different sets of data groups from Australian soils are used to validate the GCSM.

This chapter contains six sections. Section 6.2 presents the summary of the experimental work to obtain RK_{Sat} data. Section 6.3 summarises the RK_{Sat} data obtained from Jayawardane (1977). Section 6.4 provides the methodology used to evaluate the generic clay swelling model. Section 6.5 presents and discusses the results from the non-linear analysis, and section 6.6 presents the conclusions.

6.2 RK_{sat} data for the Sodosol and Vertosol soils

Short column experiments were carried out in the soil laboratory at the University of Southern Queensland. The short column experiments were conducted to measure the change in K_{Sat} under different mixed NaCl-CaCl₂ (i.e. varying in SAR and C_0) solutions for a Sodosol and two Vertosol soils.

6.2.1 Sodosol and Vertosol soils characteristics

Three local soils were used in the short column experiments. The Sodosol and Brown Vertosol were the same soils that were used in the long column experiments (chapter 3). The physical and chemical properties for these soils were presented in chapter 3 (Tables 3.1, 3.2, and 3.3). The third soil was collected from Moree, NSW. This soil is classified as a Grey Vertosol and samples were obtained from the surface 20 cm depth. The soil texture is clayey with about 70% clay content. The chemical properties of this soil are summarised in Table 6.1.

Table 6.1 Selected chemical properties for the Grey Vertosol soil

Chemical Analysis	Results
EC _{se} (dS/m)	0.04
pH	7.79
CEC (mmol _c /kg)	258.4
ESP %	3.3
Exch. Na ⁺ (mmol _c /kg)	8.57
Exch. Ca ⁺² (mmol _c /kg)	153.59
Exch. Mg ⁺² (mmol _c /kg)	90.20
Exch. K ⁺ (mmol _c /kg)	8.4
Cl ⁻ (mmol _c /kg)	1.02

6.2.2 Experimental design

The procedure adopted for the K_{Sat} reduction experiment involved preparing a range of water quality treatments with different solute concentrations and SAR. Each water quality treatment was applied to short soil columns separately. Each soil column was treated as an independent experiment in which the reduction in K_{Sat} was measured for every solution. The SAR of the water applied was used to establish the ESP of the soil using the USSL Staff (1954) relationship (equation 2.13).

The salinity values of greatest interest for agricultural purposes are up to 8 dS/m (i.e. approximately 80 mmol_e/litre), which is the salt tolerance threshold for the most salt tolerant crops such as barley (Maas and Hoffman 1977). However, 120 mmol_e/litre (\approx 12 dS/m) was chosen as the maximum salinity value for this experiment to further clarify the effect of high electrolyte concentrations, and also cover higher salinity levels for the purpose of salinity management at which some yield losses may be acceptable (Maas and Hoffman 1977, van Genuchten 1987, Maas 1990).

The relative saturated hydraulic conductivity (RK_{Sat}) values were obtained by dividing the K_{Sat} produced from application of the saline solution by the K_{Sat}^{Max} obtained from previous application of good quality water (i.e. SAR <1 and C_o about 15 mmol_e/litre).

It is worth noting that replicates were sacrificed to provide broader coverage of the experimental variables, and facilitate evaluation of the magnitude of K_{Sat} at a wide range of SAR and C_o levels.

6.2.3 Saturated K_{Sat} apparatus and soil packing

The K_{Sat} apparatus as described in chapter 3 (Figure 3.1) was used. The K_{Sat} was measured by the direct application of the Darcy law in a vertical soil column using the constant head method (Klute 1965).

Soil columns were prepared in plastic cylinders 10 cm diameter and 5.2 cm high. The soils were packed by filling 236 g for the Sodosol soil, and 215 g for the both Vertosol soils (i.e. Brown and Grey Vertosol) to form soil columns having about 2.6 cm height. Filter papers (Whatman No. 4) were placed at the bottom and the top of the soil columns to prevent any disturbance or loss of the soil. Each soil column was used once to examine the effect on the K_{Sat} of a single solution. The water head at the top of each soil column was measured after applying the solutions, and monitored during the experiment. The data obtained from the experiment was used to calculate the K_{Sat} for both treatments for each soil column.

6.2.4 Water treatments

Pre-treatment applications

The relative K_{Sat} requires having a measurement of K_{Sat} when there is no reduction of K_{Sat} due to sodicity. Therefore, the K_{Sat} was measured for each soil column independently using one litre of good quality water (i.e. about seven times the pore volume in soil column that assumed to bring soil complex to chemical equilibrium with solution added) having SAR less than 1 and C_o above 15 mmol_c/litre. The final values of K_{Sat} were assumed to be the K_{Sat}^{Max} for the particular soil column. The pre-treatment water was prepared by adding calcium chloride ($CaCl_2 \cdot H_2O$) to tap water ($C_o \approx 6$ mmol_c/litre) at the rate of 0.5g /litre to provide C_o about 15 mmol_c /litre.

Water treatment applications

The various water quality solutions were prepared by mixing sodium chloride (NaCl) and calcium chloride ($CaCl_2 \cdot H_2O$) in deionised water. The relative amounts of each salt were calculated based on maximum C_o values and the SAR desired (Appendix D). The C_o values of 120, 60, 30, 15, and 7.5, mmol_c/litre were chosen. The SAR values were chosen arbitrarily, and ranged from about 5 to 168.

A simple procedure was used to prepare the solutions with the desired C_o and SAR values. The first step was preparing the higher C_o solutions (i.e. 120 mmol_c/litre) with different values of the SAR. The lower C_o and SAR solutions were then obtained by diluting the more concentrated solution with deionised water to produce

solutions with C_o of 60, 30, 15, and 7.5 mmol_c/litre. The dilution process formed solutions with different values of SAR. The calculation process is summarized in Appendix I. An example of the C_o and SAR values for the various solutions prepared for the Sodosol and Brown Vertosol are shown in Figure 6.1.

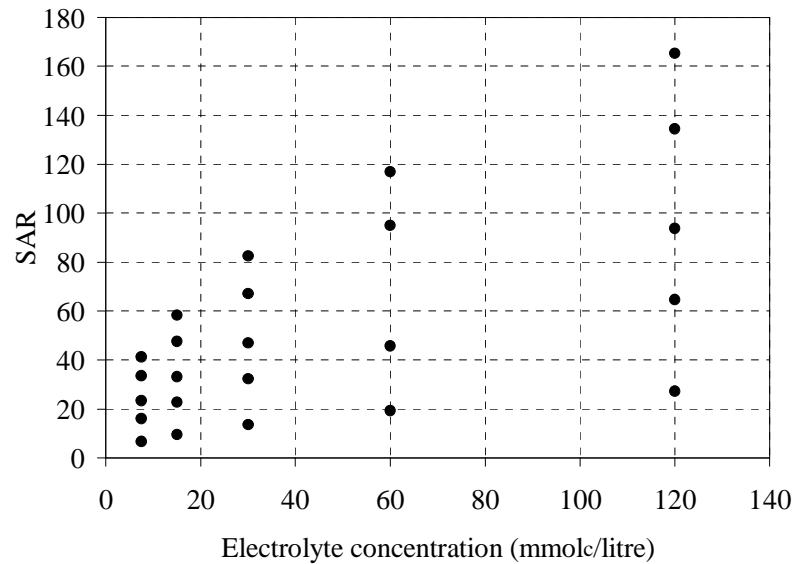


Figure 6.1 Electrolyte concentration and SAR of the water quality treatments applied to the Sodosol and Brown Vertosol

The water treatments for the Grey Vertosol were prepared at lower SAR levels as shown in Figure 6.2, because initial experiments showed that this soil was more sensitive to sodicity.

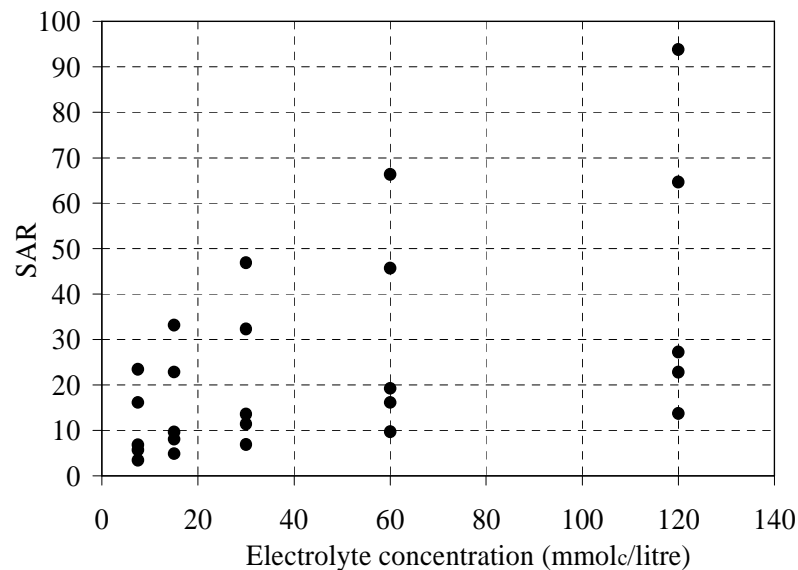


Figure 6.2 Electrolyte concentration and SAR of the water quality treatments applied to the Grey Vertosol

6.2.5 The RK_{sat} for different sodicity and salinity levels for the Sodosol and Vertosol soils

The measured RK_{sat} values for the three soils are presented in Tables 6.2, 6.3 and 6.4. The ESP values at equilibrium were estimated from the SAR of the water added using the empirical relationship proposed by USSSL Staff (1954).

Table 6.2 Saturated hydraulic conductivity RK_{sat} measurements for the Sodosol soil columns at different mixed NaCl-CaCl₂ solutions with different electrolyte concentration

Electrolyte concentration (mmol _e /litre)	Estimated ESP (%)	RK_{sat} (Ratio)
120	70.7	0.58
	66.3	0.72
	57.7	0.96
	48.4	1.00
	27.9	1.00
60	63.0	0.61
	58.1	0.72
	39.7	1.00
	21.3	0.95
30	54.6	0.60
	49.4	0.81
	40.4	0.87
	31.6	0.98
	15.8	0.98
15	45.8	0.59
	40.7	0.85
	24.4	0.93
	32.2	0.93
	11.4	1.00
7.5	37.3	0.58
	32.5	0.79
	24.9	0.91
	18.4	0.98
	8.0	0.94

Table 6.3 Saturated hydraulic conductivity RK_{Sat} measurements for the Brown Vertosol soil columns at different mixed NaCl-CaCl₂ solutions with different electrolyte concentration

Electrolyte concentration (mmol/litre)	Estimated ESP (%)	RK_{Sat} (Ratio)
120	70.7	0.53
	66.3	0.67
	57.7	0.80
	48.4	0.86
	27.9	0.94
60	63.0	0.45
	58.1	0.75
	39.7	0.79
	21.3	0.90
30	54.6	0.54
	49.4	0.75
	40.4	0.83
	31.6	0.86
	15.8	1.00
15	45.8	0.48
	40.7	0.70
	32.2	0.84
	24.4	0.80
	11.4	0.83
7.5	37.3	0.48
	32.5	0.71
	24.9	0.90
	18.4	0.77
	8.0	0.77

Table 6.4 Saturated hydraulic conductivity RK_{Sat} measurements for the Grey Vertosol soil columns at different mixed NaCl-CaCl₂ solutions with different electrolyte concentration

Electrolyte concentration (mmol_e/litre)	Estimated ESP (%)	RK_{Sat} (Ratio)
120	57.7	0.30
	48.4	0.43
	27.9	0.79
	24.4	1.01
	15.9	0.95
60	49.1	0.42
	39.7	0.35
	21.3	0.57
	18.3	0.96
	11.5	0.92
30	40.4	0.38
	31.6	0.42
	15.8	0.54
	13.4	0.88
	8.1	0.99
15	32.2	0.39
	24.4	0.47
	11.4	0.52
	9.6	0.88
	5.6	0.96
7.5	24.9	0.40
	18.4	0.48
	8.0	0.57
	6.7	0.75
	3.7	0.83

6.3 Red brown and Alluvial soils

6.3.1 Characterisation of the soils

RK_{Sat} data were obtained for two Tasmanian soils from work published by Jayawardane (1977). The description of these soils as provided by Jayawardane (1977) is:

- 1) An alluvial soil (Loveday 1957) on a fairly broad alluvial plain near Sorell in south-eastern Tasmania. The soil material was taken from approximately 61 to 91 cm depth has a sandy clay loam texture.
- 2) A red brown soil on basalt near Sorell in south-eastern Tasmania. The soil mapped as Stoneleigh clay loam (Loveday 1957). The soil material was taken from approximately 56 to 86 cm and has a clay loam texture.

The physical and the chemical analyses for both soils are shown in Table 6.5. The Red-brown soil was packed to a bulk density of 1.22 g/cm³. The alluvial soil was packed to a bulk density of 1.13 g/cm³. The solution was prepared by mixing sodium chloride (NaCl) and calcium chloride (CaCl₂·H₂O) in deionised water. Different electrolyte concentrations at each SAR level were applied to the soil column. The soil was leached for 24h with a solution of the same SAR and next highest electrolyte concentration. The saturated conductivity to this solution of lower electrolyte concentration was measured as before. This process was continued until the conductivity for the solution of lowest electrolyte concentration at the same SAR was measured.

Table 6.5 Selected physical and chemical properties of the Alluvial and Red brown soils

		Alluvial soil	Red brown soil
Particle size analysis:	Sand (2.0-0.02 mm)	52.9	32.1
	Silt (0.02-0.002 mm)	9.1	25.6
	Clay (<0.002 mm)	36.9	40.6
Soil pH		7.1	6.9
Cation Exchange capacity (mmol_c/100g)		43.32	24.57
Exchangeable bases (mmol_c/100g)		29.79	23.81

Source: (Jayawardane 1977)

6.3.2 RK_{sat} data

The data for the Red brown and alluvial soils are shown in Tables 6.6 and 6.7. It should be noted that points at high C_o and $ESP = 0$ have been added with $RK_{sat} = 1$. These points were added based on the theoretical knowledge that at high levels of C_o and low ESP sodicity has no effect on RK_{sat} . Hence, this step is consistent with the physical results and is simply intended to enhance the regression fitting process.

Table 6.6 Relative saturated hydraulic conductivity of the Red brown soil for water quality treatments.
Bulk density 1.22 g/cm³

SAR	Estimated ESP	Electrolyte concentration (mmol/litre)	RK_{sat}
40	36.52	640	1.000
		160	0.815
		80	0.260
		40	0.011
		20	0.001
20	21.96	160	1.000
		40	0.528
		20	0.169
		10	0.019
10	11.85	160	1.000
		40	0.882
		10	0.496
		2.5	0.110
0*	0	640	1
		160	1

Source: (Jayawardane 1977)

* SAR at zero level is added to enhance non-linear fitting process

Table 6.7 Relative saturated hydraulic conductivity of the Alluvial soil for different water quality treatments. Bulk density 1.22 g/cm³

SAR	Estimated ESP	Electrolyte concentration (mmol_e/litre)	RK_{Sat}
40	36.52	640	1.000
		160	0.719
		80	0.390
		40	0.104
		20	0.002
20	21.96	160	1
		40	0.401
		20	0.213
		10	0.092
		5	0.087
		2.5	0.007
10	11.85	160	1.000
		40	0.753
		10	0.482
		2.5	0.203
0*	0	640	1
		160	1

Source: (Jayawardane 1977)

* SAR at zero level is added to enhance non-linear fitting process

6.4 Evaluation of the GCSM using the non-linear regression analysis

The calibration of the generic clay swelling model was conducted using a non-linear regression analysis with ordinary least squares method. The model was fitted to the RK_{Sat} experimental data for the five soils. A non-linear surface fit was used as described previously in chapter 5. TableCurve 3D software (version 4.0.01e) was used. The regression analyses were performed to determine the seven parameters in the generic clay swelling model (i.e. a , b , g , m , l , s , and f). The processes of fitting for the five soils are presented in Appendix G (section G.2).

6.5 Results and Discussion

The processes of fitting were conducted for RK_{Sat} data obtained in view of the physical interpretation for decrease of K_{Sat} due to sodicity. As in chapter 5, the initial values for the parameters fitted were altered many times to ensure the best fit. Resultant parameters for the GCSM for different RK_{Sat} data and statistical analyses are shown in Appendix J. Table 6.8 shows the derived GCSM parameters and the main statistical indices.

Table 6.8 Summary of the GCSM surface fit output for the five soils

Soil type	Model parameters							R ²	F-test	Fit Std Error
	<i>a</i>	<i>b</i>	<i>g</i>	<i>m</i>	<i>f</i>	ESP _T parameters				
						<i>s</i>	<i>l</i>			
Sodosol	8.7×10 ⁻⁷	0.526	4.417	7.105	0.061	8.256	0.692	0.895	24.11	0.0586
Brown Vertosol	3.67×10 ⁻⁸	0.024	0.955	4.304	0.107	6.311	-19.343	0.658	5.133	0.101
Grey Vertosol	0.99	0.0715	0.807	5.183	0.234	6.767	-7.983	0.881	22.21	0.098
Red brown	3.9×10 ⁻⁷	0.47	4.52	9.936	0.368	10.398	-31.14	0.975	38.40	0.093
Alluvial	0.786	0.686	0.345	12.67	0.36	31.285	-140.037	0.985	90.20	0.06

The Figures 6.3, 6.4, 6.4, 6.5, and 6.6 present RK_{Sat} surfaces predicted for the entire range of ESP and electrolyte concentration from 0 to 120 mmol_c/litre for the various soils. The Figures also show the residual between experimental and predicted RK_{Sat} . The data fitted is concentrated in only the early stage of RK_{Sat} decrease. However, the model predictions were extended to demonstrate the higher ranges of ESP levels (assuming that SAR-ESP relationship is valid for the entire range of SAR and ESP) at the C_o range of concern in agriculture.

Generally, it can be noted from the residual plots that the GCSM has higher errors at lower electrolyte concentrations. In most cases, the model over-predicted the RK_{Sat} at low salinity ranges (i.e. C_o approaches zero). These results can be interpreted in view of the original domain model. From Figure 5.3, it can be noted that the clay expansion does not follow the domain model (equation 5.6) at lower electrolyte concentrations. The clay expansion was higher than that predicted by the domain model and was inconsistent. However, in most cases the soil solution in general has electrolyte concentrations above that range, except under very intensive leaching.

From Table 6.9, the values for the parameter a obtained for the Sodosol, Vertosol and Red brown soils are very small. Thus, the first term in equation 5.24 is nearly one and n values at different levels of ESP are approximately equal. The n values for the Sodosol, Vertosol and Red brown soils are 1.526, 1.024, and 1.47, respectively. This suggests that the n for these soils are independent of ESP and can be treated as a constant. However, the values of the n for the Grey Vertosol and Alluvial soils are closely related to ESP.

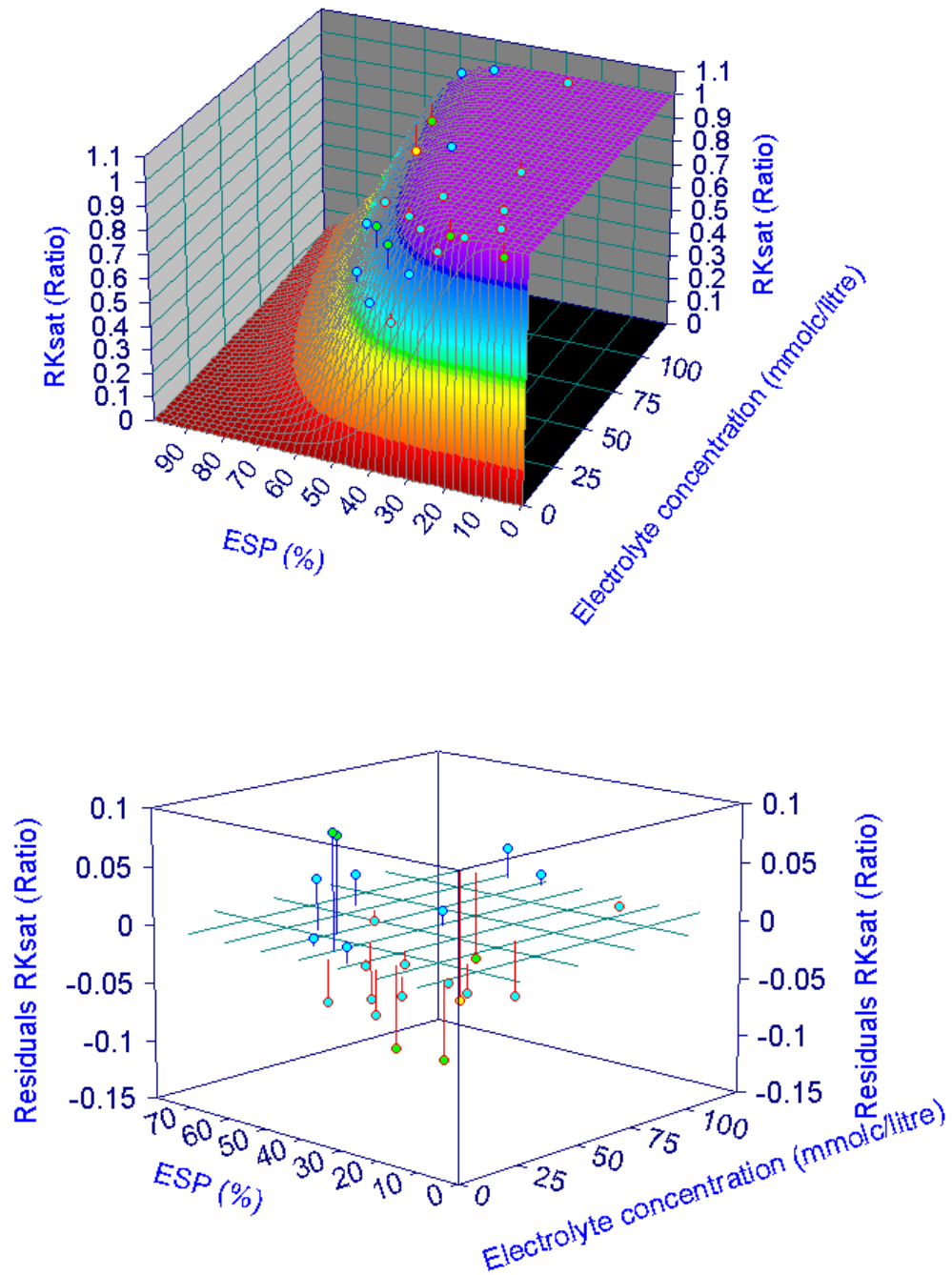


Figure 6.3 Three dimensional surface of best fit and the residuals of RK_{sat} (i.e. between predicted and measured) for the Sodosol soil

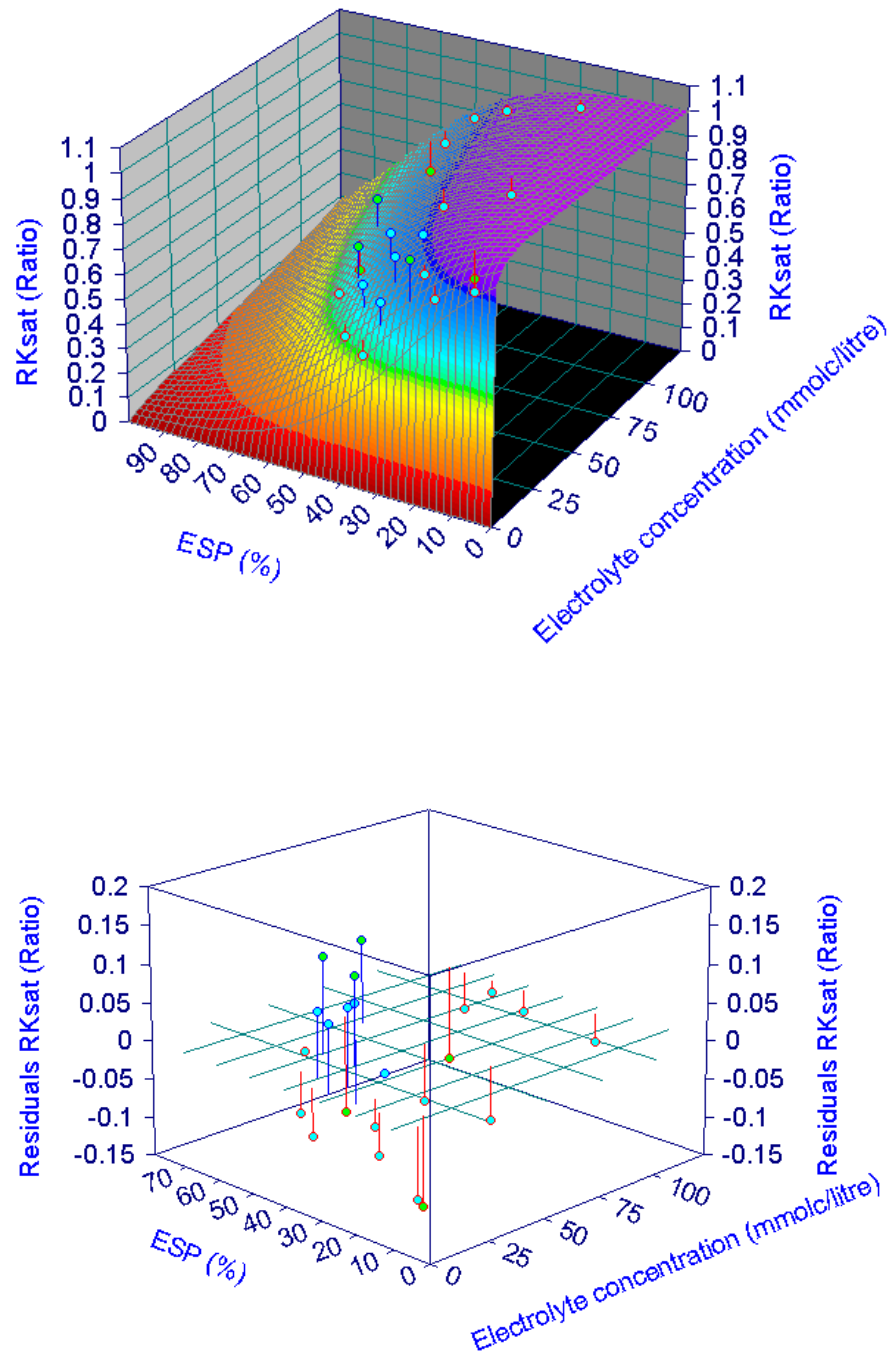


Figure 6.4 Three dimensional surface of best fit and the residuals of RK_{sat} (i.e. between predicted and measured) for the Brown Vertisol soil

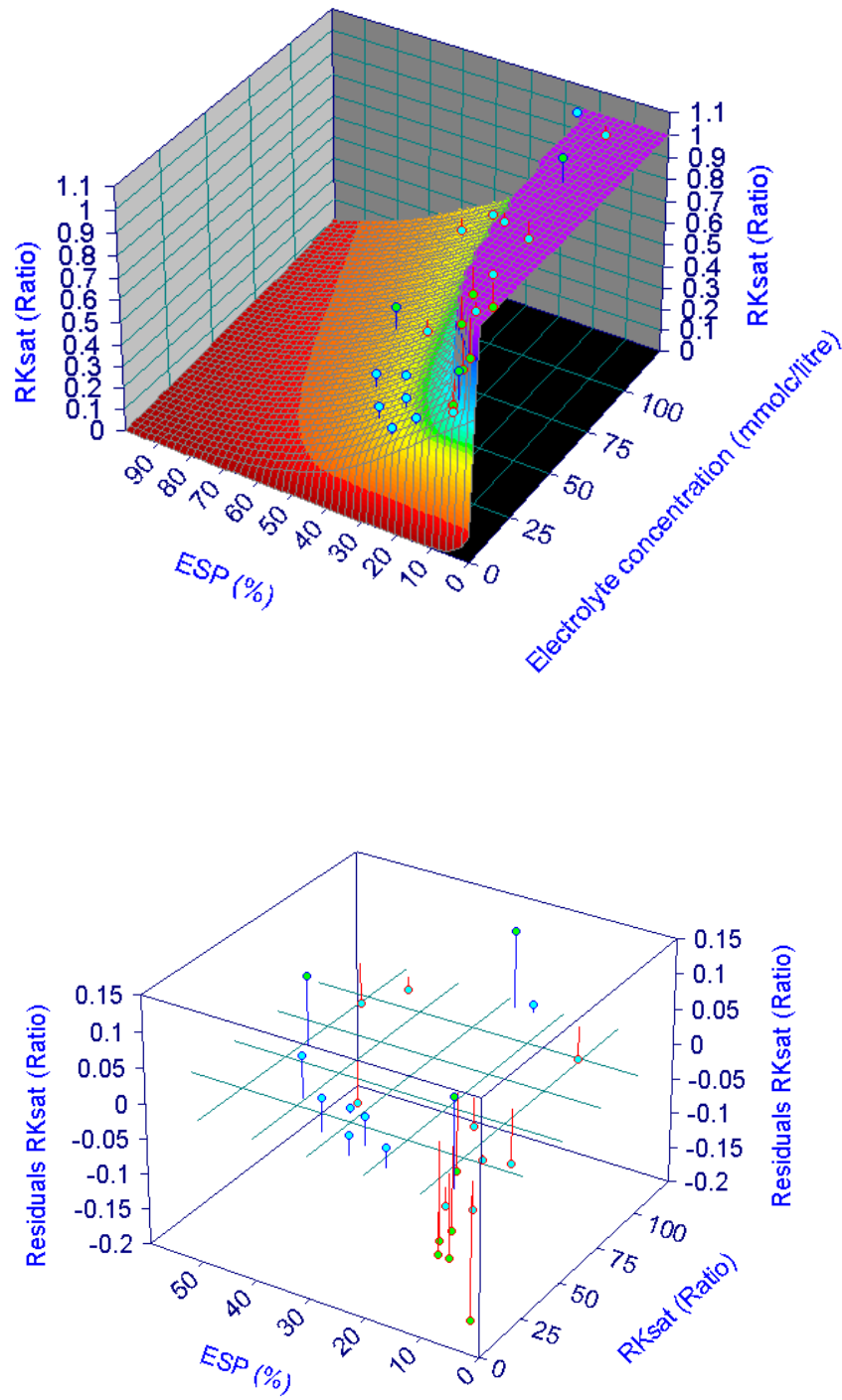


Figure 6.5 Three dimensional surface of best fit and the residuals of RK_{sat} (i.e. between predicted and measured) for the Grey Vertosol soil

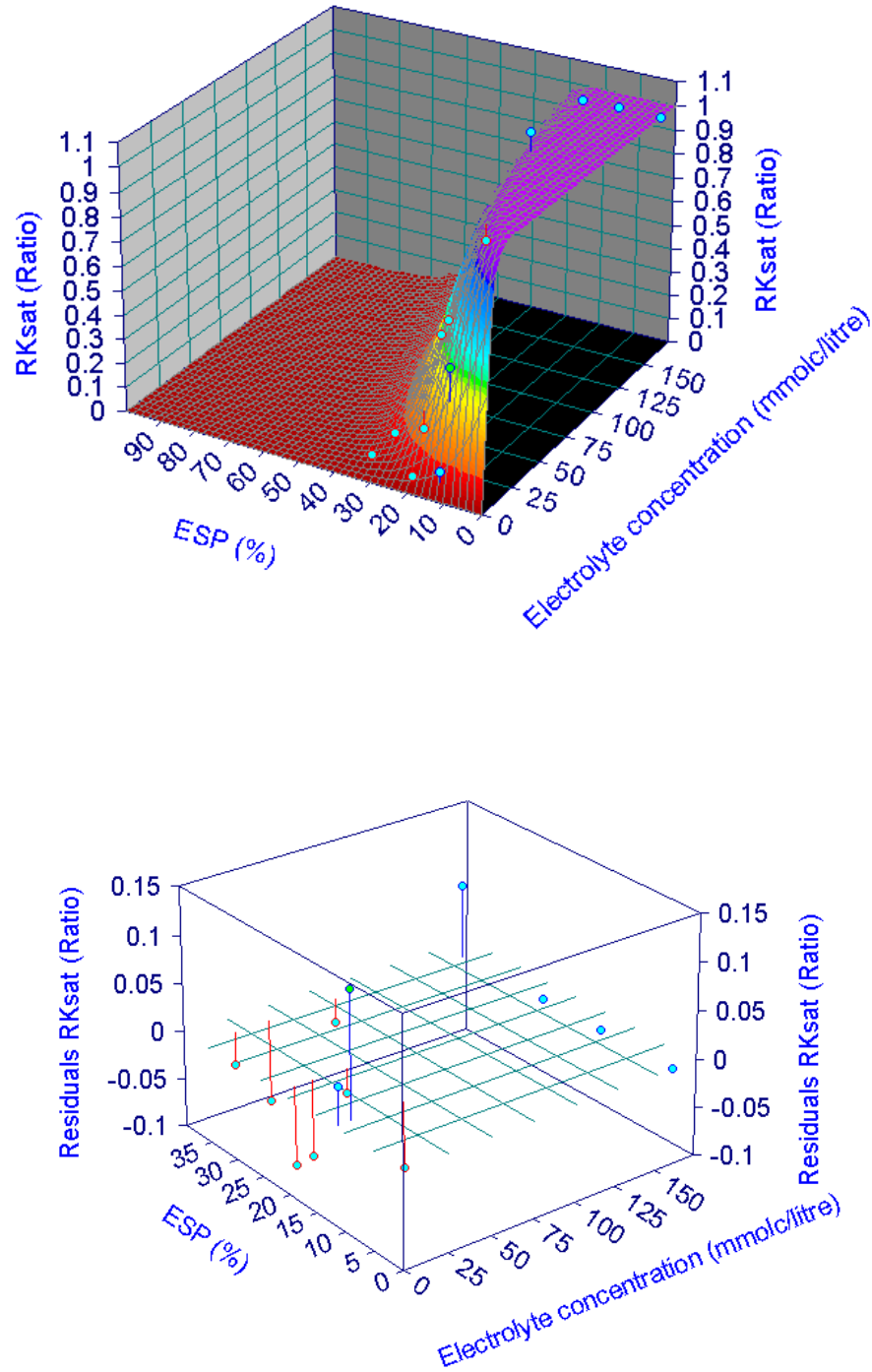


Figure 6.6 Three dimensional surface of best fit and the residuals of RK_{sat} (i.e. between predicted and measured) for the Red brown soil

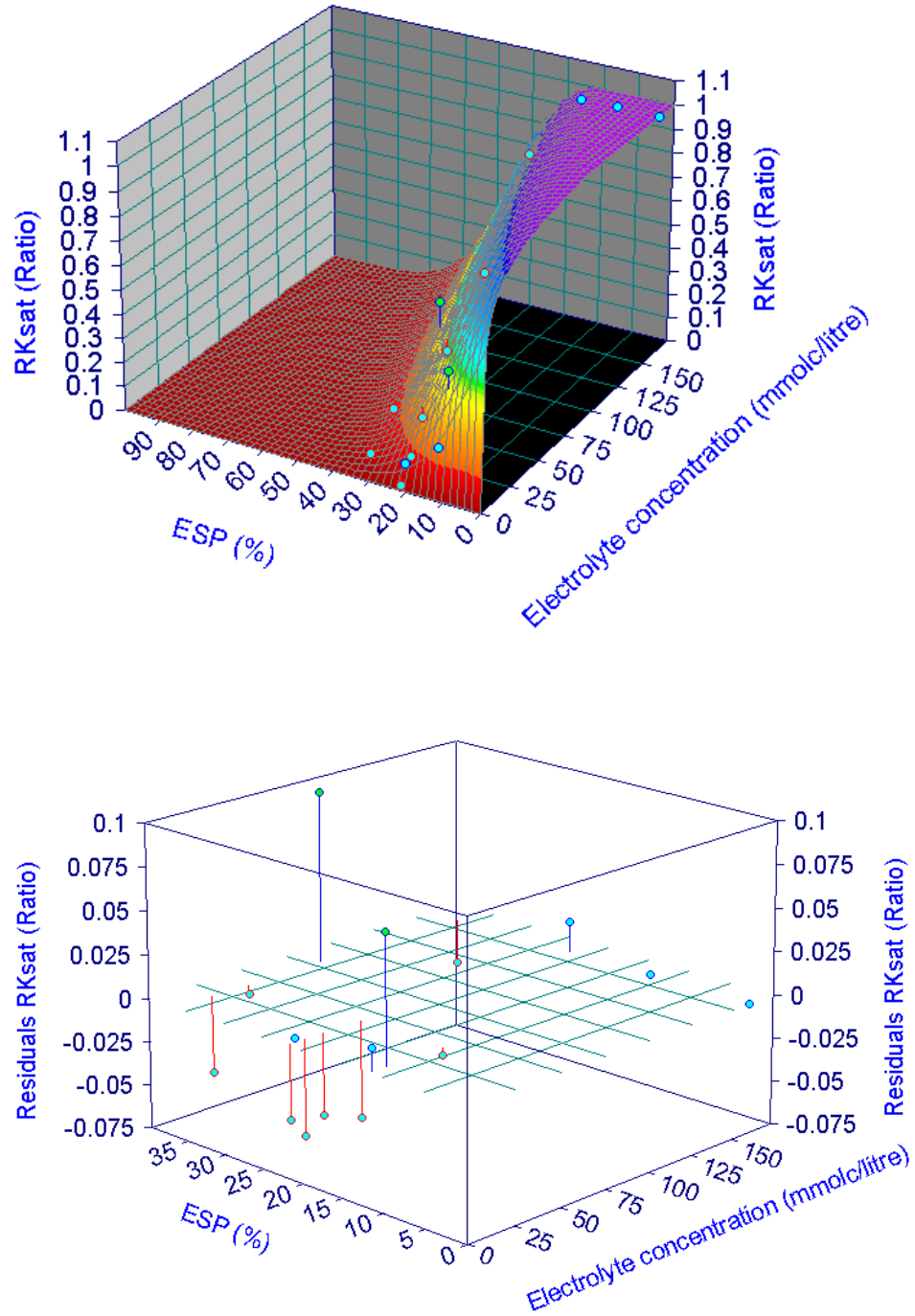


Figure 6.7 Three dimensional surface of best fit and the residuals of RK_{Sat} (i.e. between predicted and measured) for the Alluvial soil

Except for the Brown Vertosol, the results show that the generic clay swelling model is able to describe the overall reduction of RK_{Sat} for the soils tested. In Table 6.8, the significant F-test values produced indicate that the generic clay swelling model is able to describe the change of RK_{Sat} with various water qualities. However, the values of t-test for the single parameters are insignificant, indicating that the parameters are interrelated. This means that a number of sets of parameter values can satisfactorily fit the data. However, the application of the parameters is limited to a particular soil. Once the model can fit the entire data available, the decrease of RK_{Sat} can be calculated at any combined levels of C_o and ESP for this soil irrespective of parameters and their significance.

Having the f as a fitted (empirical) parameter increases the accuracy of the model prediction. However, it should not be given a physical meaning.

The best fit for the Brown Vertosol RK_{Sat} data produced a significant F value (i.e. 5.133). However, the R^2 was low (i.e. 0.658). This low R^2 value compared with other data may be due to inconsistency of the measured RK_{Sat} , as result of the delay in achieving the equilibrium between water added and colloid surface. The short soil columns could also increase the probability of loss of the dispersed clay fraction with water movement leading to an increase in the conductivity.

Values of C_o and SAR that produce the same RK_{Sat} reduction can be presented as contour lines for the soil tested (Figures 6.8, 6.9, 6.10, 6.11 and 6.12). The TEC curves for the soils at which RK_{Sat} reduced by a certain percentage were extracted from these graphs. The distribution of the contour lines reveals that reduction of RK_{Sat} at different sodicity levels varies from soil to soil. For example, the data from the Brown Vertosol indicates that the reduction of RK_{Sat} occurs at lower values of SAR compared with the Sodosol. However, as the SAR increases, the RK_{Sat} reduction in the Sodosol is more rapid compared with the Vertosol.

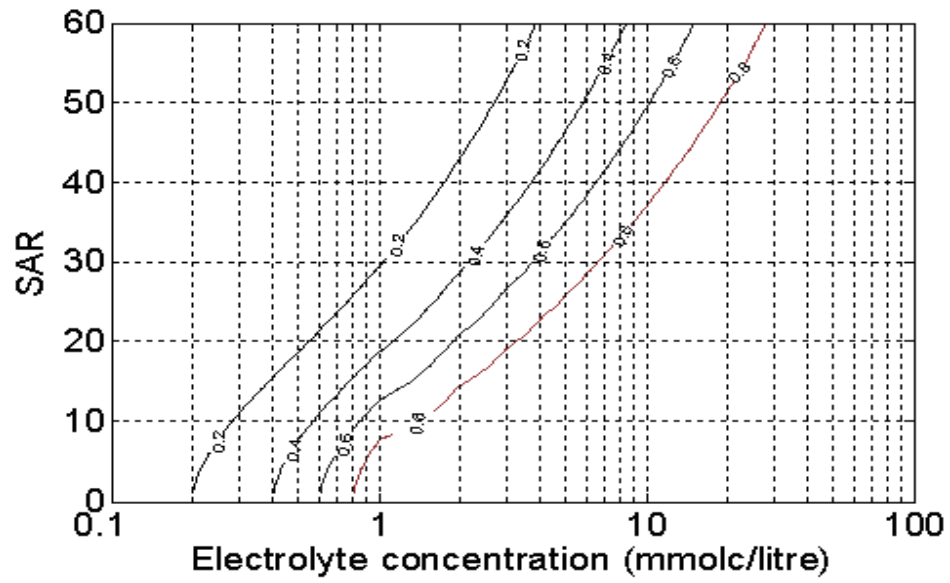


Figure 6.8 Change of RK_{Sat} with electrolyte concentration and SAR for the Sodosol as produced using the GCSM

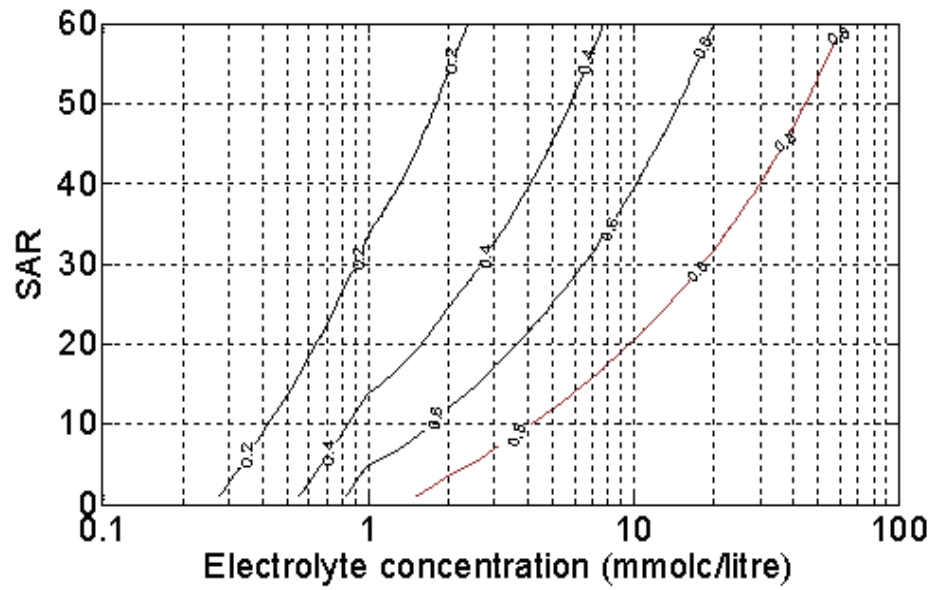


Figure 6.9 Change of RK_{Sat} with electrolyte concentration and SAR for the Brown Vertisol as produced using the GCSM

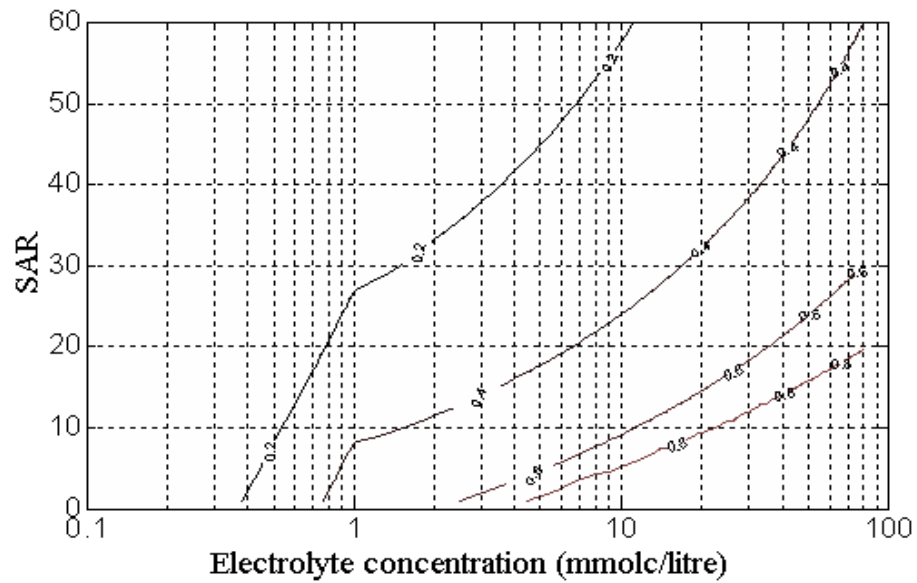


Figure 6.10 Change of RK_{Sat} with electrolyte concentration and SAR for the Grey Vertisol as produced using the GCSM

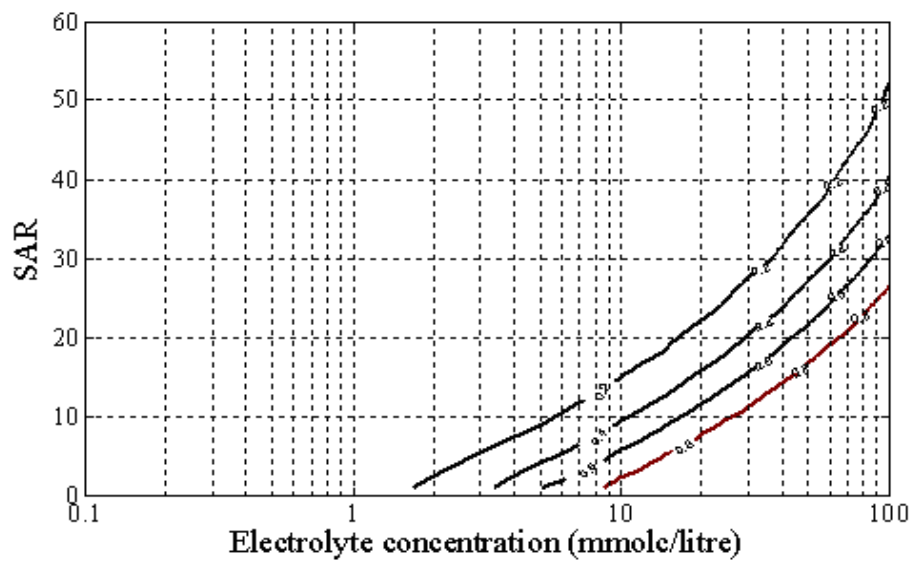


Figure 6.11 Change of RK_{Sat} with electrolyte concentration and SAR for the Red brown soil as produced using the GCSM

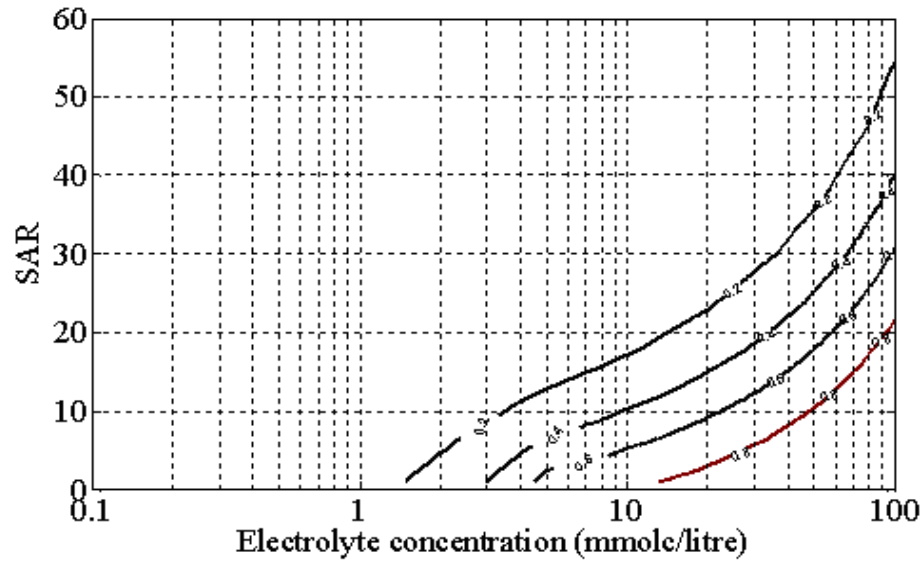


Figure 6.12 Change of RK_{Sat} with electrolyte concentration and SAR for the Alluvial soil as produced using the GCSM

For comparison, the change of RK_{Sat} with electrolyte concentration and SAR produced from the traditional clay swelling model is shown in Figure 6.13. It can be noted that the variation between this prediction and the Sodosol is large. However, the variation between the Vertosol and the McNeal RK_{Sat} values is less, which explains the results from the UNSATCHEM. Figure 6.13 shows also the ambiguous prediction due to switching from $n = 1$ to 2 (particularly in the contour line for 20% RK_{Sat} reduction). This result confirms that the discrete n values used are not appropriate.

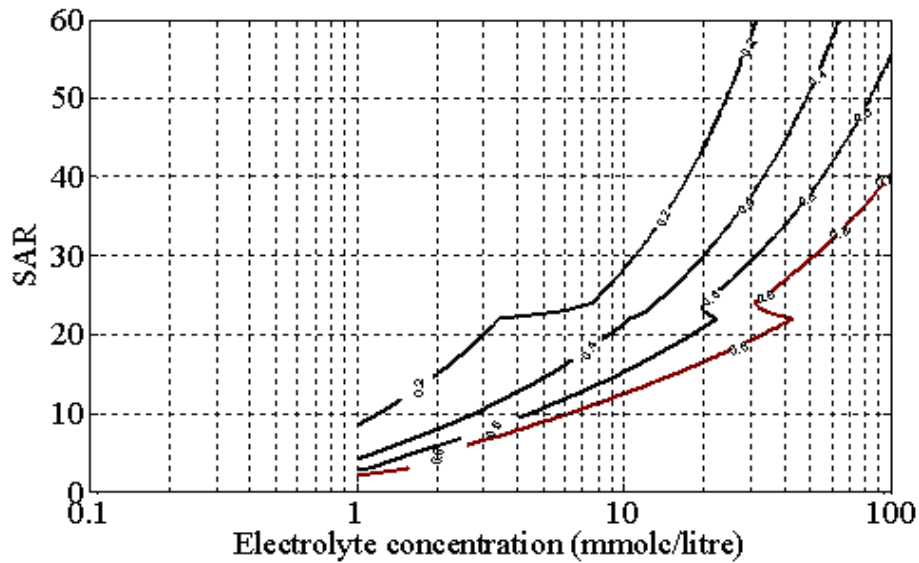


Figure 6.13 Change of RK_{Sat} with electrolyte concentration and SAR as produced from the McNeal (1968) clay swelling model using the parameters incorporated in the UNSATCHEM model for any soil

6.6 Conclusion

It is clear that the generic swelling model is able to describe the reduction of RK_{Sat} for most data fitted. F-test values were significant for all the data fitted which indicates that the generic clay swelling model describes well the RK_{Sat} data. The coefficient of determinations (R^2) values are high except for the Brown Vertosol. The residual plots reveal that at low C_o some experimental values of RK_{Sat} were relatively overestimated. That might be due the limitation of domain model at lower C_o . The buffering in such soils might reduce the effect of sodicity during short term experiments.

Despite the physical meaning for the weighted fraction of montmorillonite in the McNeal model the produced f parameter in the generic model has no physical meaning.

It should be noted that the GCSM parameters can be reduced from seven to six by considering the n function as a constant for a given soil. This result was noted in a number of soils in which the n function was independent of the ESP.

CHAPTER 7: Evaluation of the UNSATCHEM with the Generic Clay Swelling Model Incorporated

7.1 Introduction

The results from chapter 4 showed that there is uncertainty regarding the modelling of water and solute movement under sodic conditions in which soil hydraulic properties are degraded. The limitations were primarily attributed to the hydraulic conductivity reduction function incorporated into the model (i.e. pH- RK_{sat} function (Suarez et al. 1984) and the McNeal clay swelling model). The review of the McNeal clay swelling model (chapter 5) confirms that the traditional clay swelling model has a number of weaknesses that result in an inaccurate in predicting the RK_{sat} . The inaccuracy in RK_{sat} prediction can result in error in simulations of water and solute movement under irrigation with saline-sodic water. A new general form of clay swelling model has been developed. The new form improves the prediction of the RK_{sat} under sodic conditions. The validation of the generic clay swelling model with RK_{sat} data for a number of Australian soils (chapter 6) shows agreement between the model predictions and the experimental data.

This chapter investigates the effect of using the GCSM in a simulation process. The UNSATCHEM was used to simulate the same experiments that were used in chapter 4 for both Sodosol and Vertosol data after the GCSM was incorporated. The simulation results are compared with the results reported in chapter 4.

This chapter contains five sections. Section 7.2 discusses the methodology and includes the process of incorporating the generic clay swelling model. Section 7.3 provides the results. Section 7.4 discusses the results and provides a new approach to improve modelling water and solute movement under sodic conditions. Section 7.5 documents the findings and potential future research in this area.

7.2 Methodology

7.2.1 Incorporating the generic clay swelling model in the UNSATCHEM

The GCSM was integrated in the UNSATCHEM using the code provided by and presented in Appendix K. The values of the GCSM parameters were entered manually into UNSATCHEM using a DOS window (Figure 7.1) prior to running the simulation. The GCSM parameters used were presented previously in Table 6.10. However, it was noted that n is approximately constant over the entire range of ESP for the two soils, with values of 1.526 and 1.024 for the Sodosol and Vertosol, respectively.

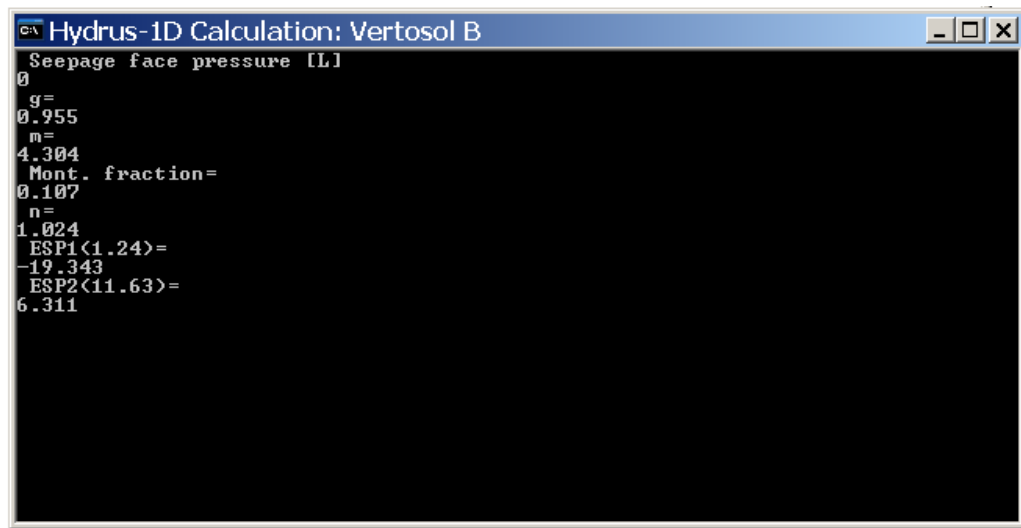


Figure 7.1 DOS window to enter the GCSM parameters into UNSATCHEM (i.e. HYDRUS 1D)

7.2.2 The UNSATCHEM parameters for the Sodosol and Vertosol soils

The UNSATCHEM model with the GCSM was used to re-simulate the column experiments for the Sodosol and Vertosol soils as used in chapter 4. The parameters used are the same parameters presented in Table 4.6. Thus, differences between the simulations reported in chapter 4 and the new results in this chapter represent the effect of the new form of clay swelling model.

7.3 Results

The results from simulations after incorporating the GCSM show that the predictions of the outflow and the saturated hydraulic conductivity are generally improved. However, the differences between the predictions and the experimental data are still high. The results for the outflow and the hydraulic conductivity for the Sodosol are shown in Figures 7.2 and 7.3, respectively. It is clear that the prediction of water movement is enhanced. The predicted hydraulic conductivity especially at the final stage approaches the measured values. However, the predicted hydraulic conductivity values are still low at the initial stage of application of the HSS water.

The estimated outflow and K_{sat} for the Sodosol during the application of the diluted HSS water are shown in Figures 7.4 and 7.5, respectively. It can be noted that the estimated K_{sat} is enhanced but the values are still underestimated. This result suggests that the pH- RK_{sat} relationship incorporated in the hydraulic conductivity reduction function may also not be appropriate and cause significant variations in hydraulic conductivity.

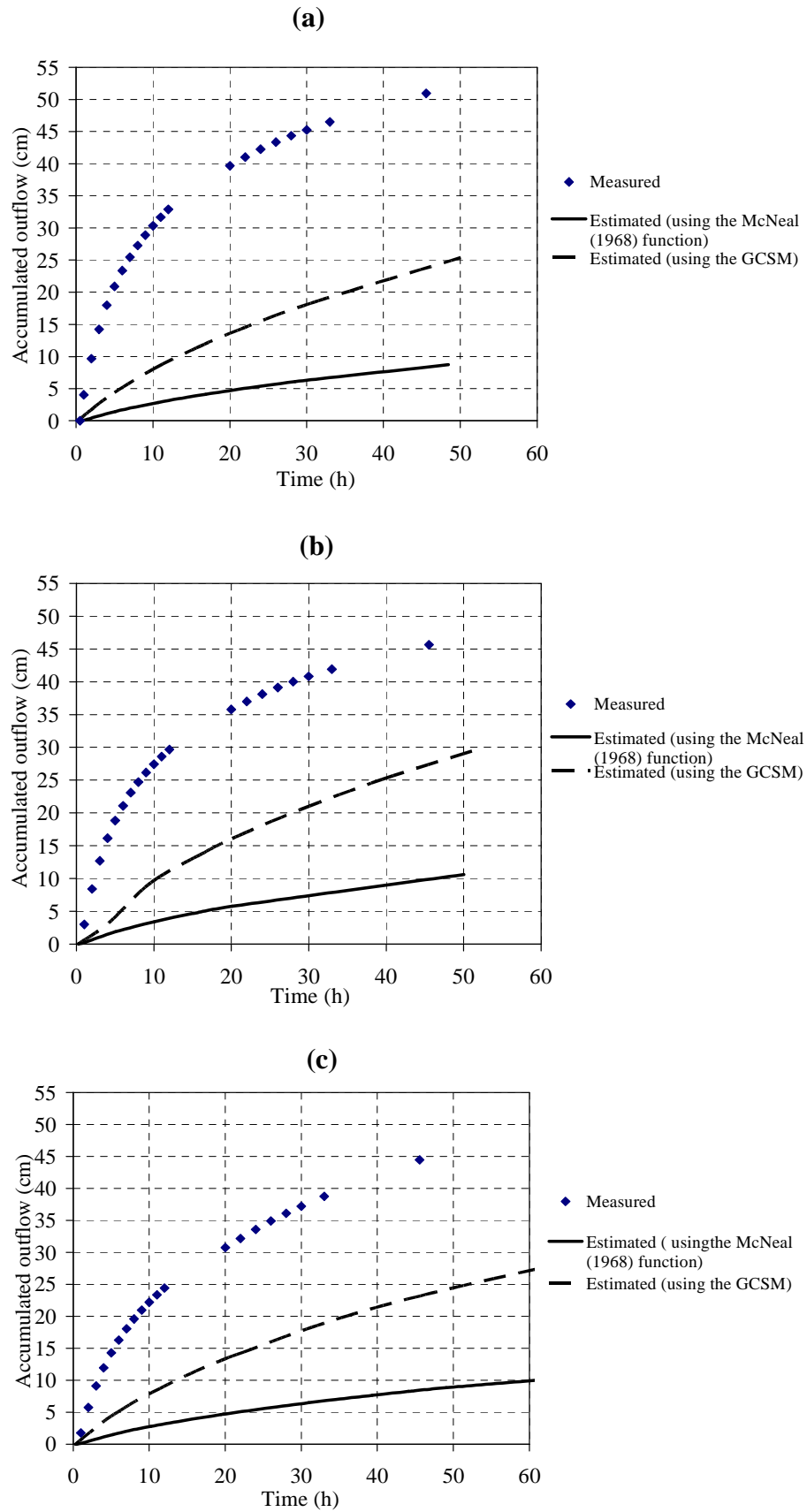


Figure 7.2 The estimated outflow by the UNSATCHEM when the GCSM was used compared with the estimated outflow using the UNSATCHEM that incorporated the McNeal model for the Sodosol soil column during application of HSS water (a) replicate 1, (b) replicate (2), and (c) replicate 3

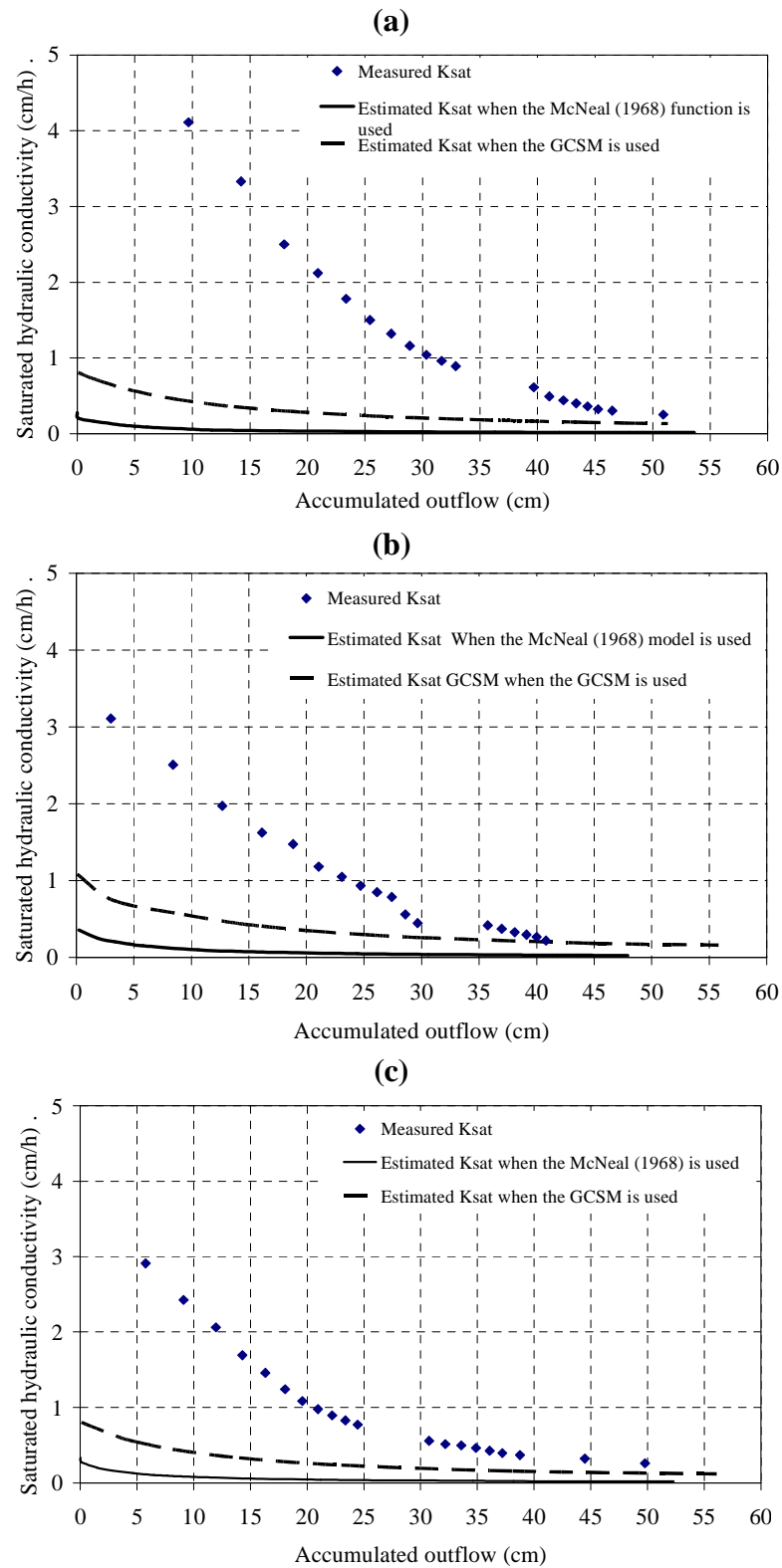


Figure 7.3 The estimated K_{sat} by the UNSATCHEM when the GCSM was used compared with the estimated K_{sat} produced using the UNSATCHEM that incorporated the McNeal model for the Sodosol soil column during application of the HSS water (a) replicate 1, (b) replicate (2), and (c) replicate 3

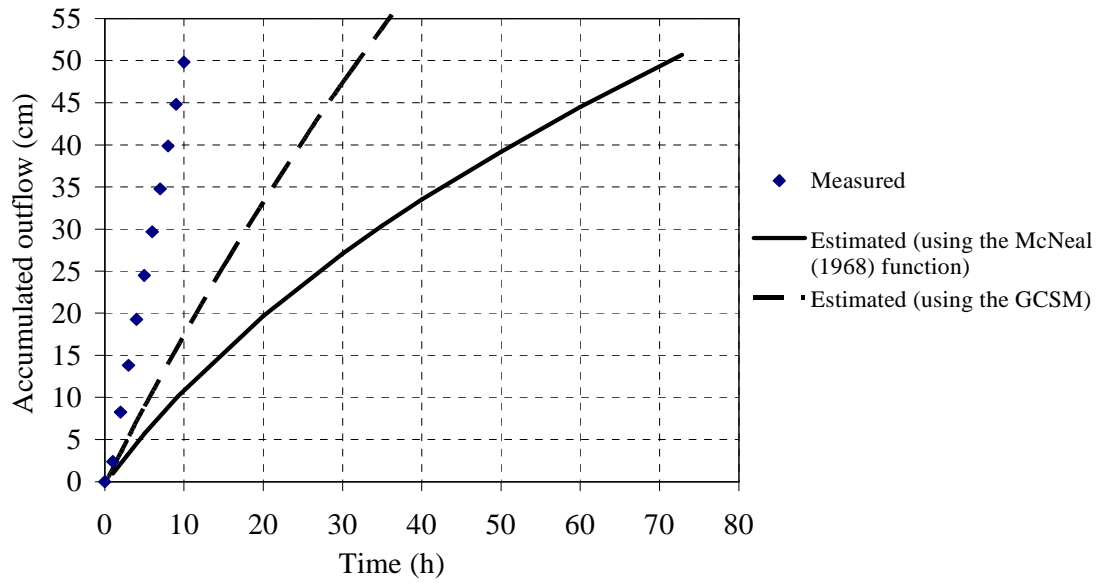


Figure 7.4 The estimated outflow by the UNSATCHEM when the GCSM was used compared with the estimated outflow using the UNSATCHEM that incorporated the McNeal model for the Sodosol soil column during application of diluted HSS water

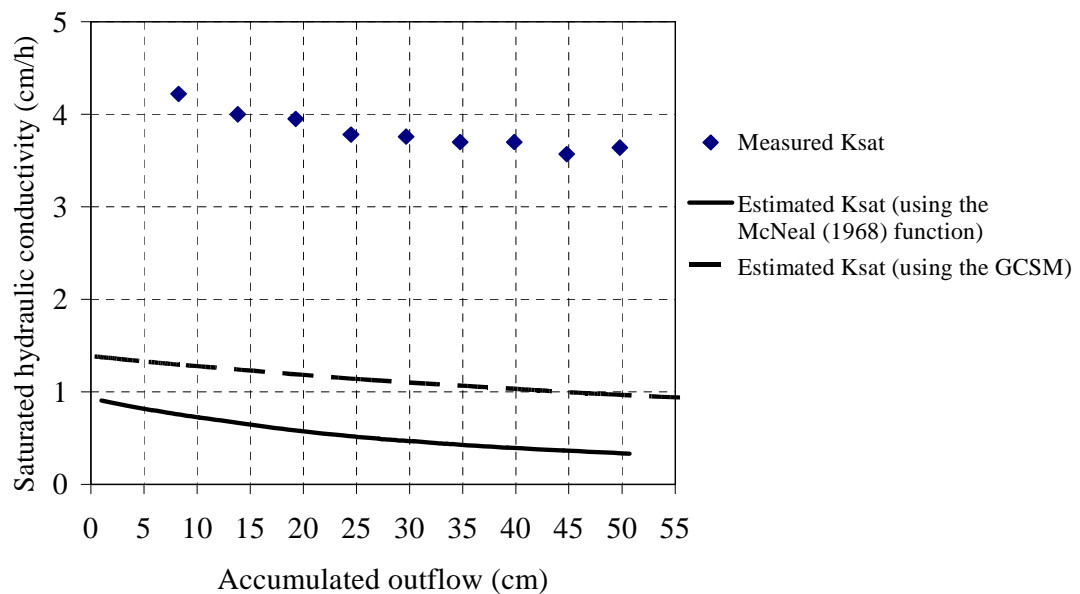


Figure 7.5 The estimated K_{Sat} by the UNSATCHEM when the GCSM was used compared with the estimated K_{Sat} produced using the UNSATCHEM that incorporated the McNeal model for the Sodosol soil column during the applications of diluted HSS water

The estimated outflows and K_{Sat} of the three replicates of the Vertosol during the application of the HSS water are presented in Figures 7.6 and 7.7. The accumulated outflows are further increased compared with the experimental data. The comparison between the estimated and measured K_{Sat} along with the estimated K_{Sat} using the McNeal (1968) model was presented. It can be noted that the predicted K_{Sat} are still low at the initial time, however, the values of estimated K_{Sat} are higher in the last stage. It should be noted that the R^2 for the GCSM was low (about 0.65) for the Vertosol during determination of the model parameters. This indicates that the GCSM did not achieve high accuracy for this soil. However, the discrepancy could be caused due the limitation of the pH- RK_{Sat} relationship that is incorporated in the model. If this is the case, then the Vertosol is highly affected by the increase of pH and the relationship underestimated the influence of the pH on K_{Sat} at higher sodic condition. However, the results from the diluted HSS water shown in Figures 7.8 and 7.9, respectively, for the accumulated outflow with time and the change of conductivity with the outflow are similar to the results noted from the Sodosol. This suggests that the second part of the hydraulic conductivity reduction function that relates the K_{Sat} to the pH needs further consideration

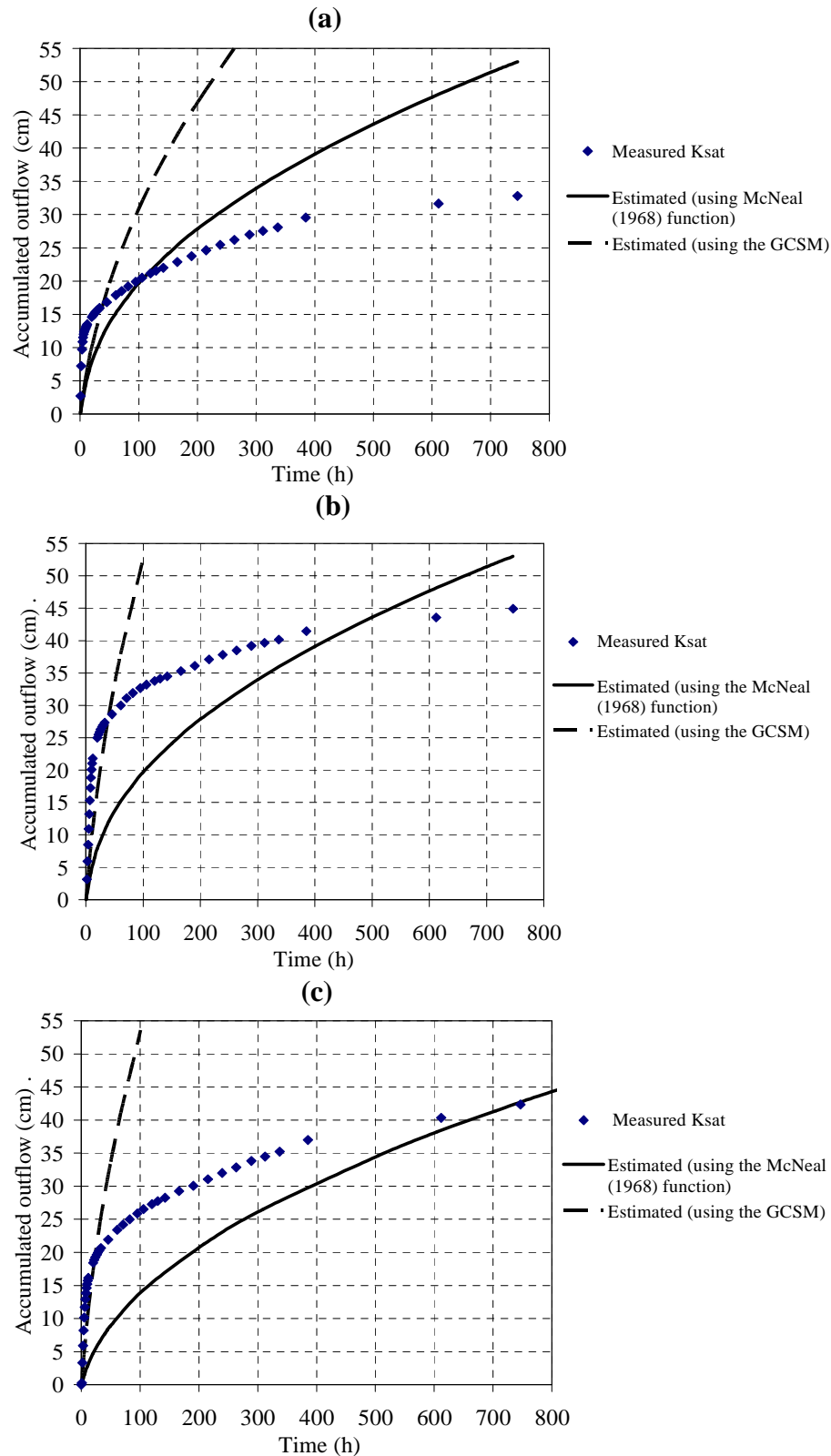


Figure 7.6 The estimated outflow by the UNSATCHEM when the GCSM was used compared with the estimated outflow using the UNSATCHEM that incorporated the McNeal model for the Vertosol soil columns during application of the HSS water (a) replicate 1, (b) replicate (2), and (c) replicate 3

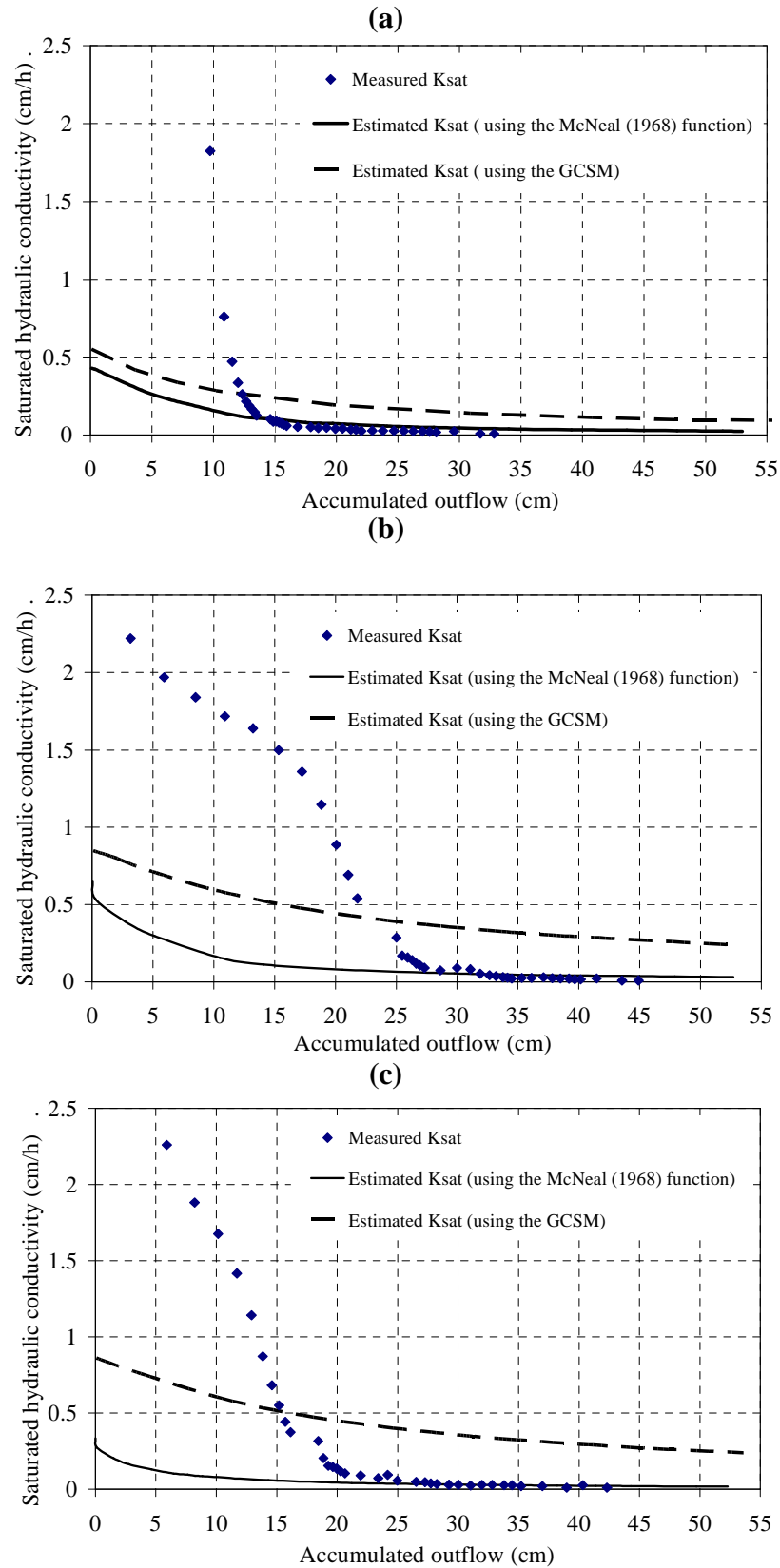


Figure 7.7 The estimated K_{Sat} by the UNSATCHEM when the GCSM was used compared with the estimated K_{Sat} produced using the UNSATCHEM that incorporated the McNeal model for the Vertosol soil columns during application of the HSS water (a) replicate 1, (b) replicate (2), and (c) replicate 3

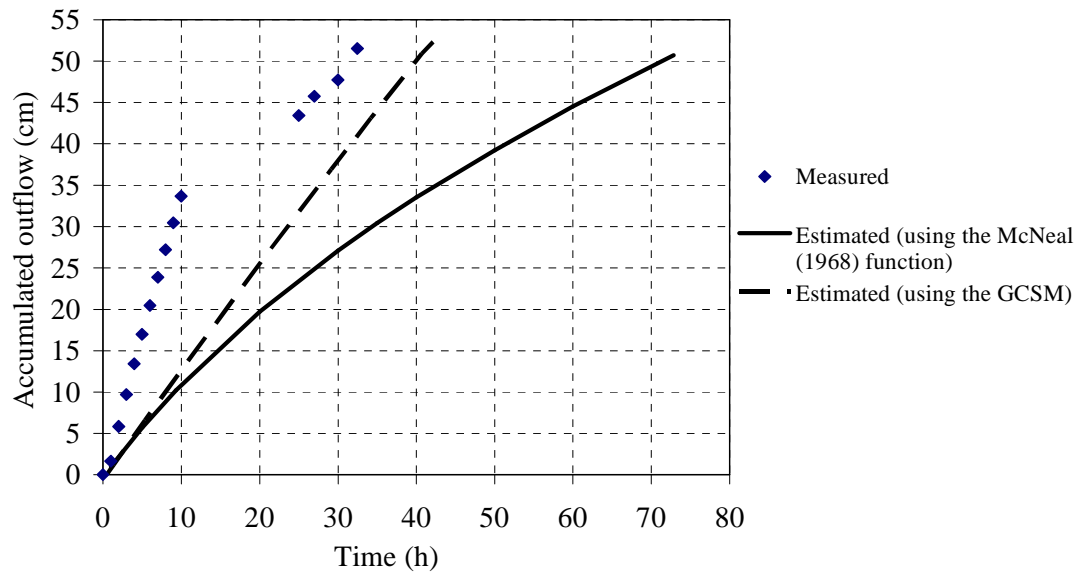


Figure 7.8 The estimated outflow by the UNSATCHEM when the GCSM was used compared with the estimated outflow using the UNSATCHEM that incorporated the McNeal model for the Vertosol soil column during application of diluted HSS water

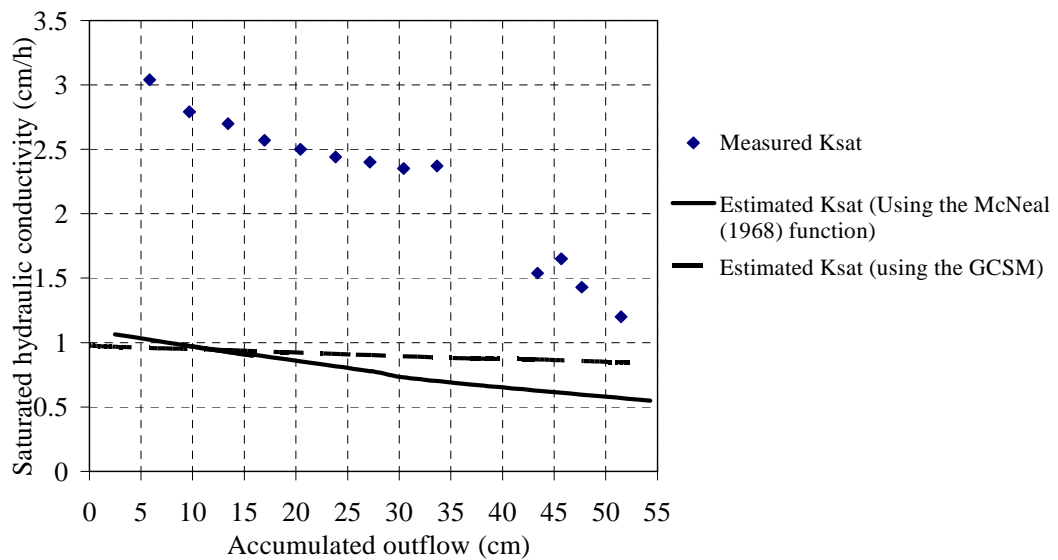


Figure 7.9 The estimated K_{Sat} by the UNSATCHEM when the GCSM was used compared with the estimated K_{Sat} produced using the UNSATCHEM that incorporated the McNeal model for the Vertosol soil column during the applications of diluted HSS water

The results show that the incorporated GCSM does reduce the variation between the estimated and the measured saturated hydraulic conductivity. However, the variation is still significant. The GCSM has been developed and tested with different soil types. The estimated RK_{Sat} using the GCSM was in good agreement especially for the Sodosol (chapter 6). However, the results presented herein show that the variations are still significant.

7.4 Discussion

The results raise questions about the equilibrium chemical reaction model and the second term of the hydraulic conductivity reduction function incorporated into the UNSATCHEM. Marsi and Evangelou (1991) found that the K_{Sat} decreased with increasing pH in two soils different in their clay mineralogy. The magnitude of K reduction varied between the two soils. Bolan et al. (1996) related the change of conductivity due to the change in pH to the change in variable charges initiated on the clay surfaces. They noted that K_{Sat} increases when the pH value increases and approaches the point of zero net charge (PZNC). However, as the pH increases above this point the negative charge increases and conductivity is reduced. Aydin et al. (2004) showed that the pH- K_{Sat} relationship has an S-shape and varies from soil to soil. Furthermore, they stated that the influence of pH on K_{Sat} depends on the clay mineralogy and the increase of variable charge density.

The assumption inherent with the model is that the CEC is pH independent. Many researchers have shown that the CEC increases with increase of soil pH in soils containing variable charge minerals. The change of the CEC is determined by the amount of variable charge minerals and organic matter (Evangelou & McDonald Jr 1999), which depends on the pH. As the pH increases above 7, the exchange surfaces require more cations to neutralise the charged surfaces in the soil. This increase of CEC is very important in relation to the ionic and chemical balance during water and solute movement. Ignoring the effect of pH on CEC most probably result in a soil chemical system that is varied from the actual chemical conditions within the soil profile.

The pH seems to have also an effect on the values of ESP. It has been shown by many researchers (e.g. Khajanchi & Meena 2008; Robbins & Meyer 1990) that when the soil pH increases above 7, the ESP increases rapidly. The ESP increase was attributed to an increase of the preference for the Na^+ cations to be adsorbed. Similarly, early results by Martin et al. (1964) showed that decreasing soil pH (from 8 to 4) reduces the CEC and increases the ESP, causing the hydraulic conductivity to drop sharply. The reason given is that the lower pH decreases the CEC and increases the amount of the sodium adsorbed (i.e. increases the ESP).

The above discussion suggests that the pH influences the hydraulic conductivity and ESP in the opposite manner (i.e. as the pH increases above 7 the ESP increases and K_{Sat} decreases). This suggests that the pH influences the hydraulic conductivity by affecting both the ESP and the CEC. Therefore, the reduction of conductivity could be considered in relation to the change in the ESP that related directly to the soil pH. The clay swelling model should be sufficient to account for the sodicity effect as it relates the hydraulic conductivity to the ESP. This approach simplifies the hydraulic conductivity reduction function by considering the reduction of conductivity regarding the change of ESP only. It also enhances the accuracy of the ionic balance and the performance of the chemical reaction model during the simulation of water and solute movement. However, limited research has been conducted to clarify the effect of pH on the CEC and the ESP. More research is required to quantify the effect of the pH on the ESP and their relation to K_{Sat} .

However, another reason that may contribute to the deficiency of the UNSATCHEM model is that the ESP data used to predict the GCSM parameters values were estimated from the SAR-ESP relationship provided by USSL Staff (1954). This estimation has been showed by many researchers to be unsuitable for different soils. Organic matter also can affect the soil chemistry and cause a variation.

The process of simulation using HSS water rich with bicarbonate is very complicated and requires further research to determine the main factors that affect the soil degradation. Further research is required to determine the role of pH on hydraulic conductivity reduction and soil degradation under different soil conditions.

7.5 Conclusion

The UNSATCHEM module incorporated in HYDRUS 1D has been evaluated using the same data used in chapter 4 after replacing the McNeal (1968) model with the GCSM. The aim of this evaluation was to test the effect of the GCSM on simulation processes of the water and solute movement under highly sodic conditions. The results, in general, show that the outflow and hydraulic conductivity predictions are improved compared with results from the UNSATCHEM with the McNeal (1968) swelling function. However, it failed to describe properly the experimental data and the magnitude of the conductivity reduction and water movement within the soil profile. The variations between the estimated and the measured hydraulic conductivities were high.

It is concluded that UNSATCHEM still has limitations. The limitations are mainly identified in the pH- RK_{Sat} function integrated in the hydraulic conductivity reduction function and chemical reaction model. Many researchers have pointed out that CEC and ESP can be increased by several orders of magnitude with an increase of pH above 7. Therefore, the assumption that the ESP and CEC are independent from pH is not appropriate. The change of CEC and ESP can affect significantly clay stability, the conductivity and the chemical reaction system within the soil profile. Therefore, there is a need for a further research to improve UNSATCHEM for modelling highly sodic conditions before using it for any further management investigation. The modelling processes should consider the effect of pH on ESP and CEC and their influence on K_{Sat} . Thus, further research is required to better quantify the pH effect on the hydraulic conductivity along with the chemical reaction model.

CHAPTER 8: Conclusion and Recommendations

8.1 Introduction

In this chapter, conclusions are drawn from the achievements and outcomes of this research regarding improvement modelling of sodicity effect on soil hydraulic properties and solute movement. This chapter contains four main section provides the achievement of the objectives and the outcome of this research. Section 8.2 provides a review of the research. Section 8.3 concludes the achievement of the main objective of this research. Section 8.4 serves as a general findings, recommendations and potential future research in this area.

8.2 Review of research

The need for food and fibre production necessitates more water to be used in irrigated agriculture. Due to the scarcity of fresh water resources there is a trend to use relatively low water quality, which is relative saline and sodic. Using low quality waters containing significant concentration of Na^+ for irrigation requires appropriate management. The main problem for these waters is the high level of sodicity. Using these waters can cause soil degradation, which could compound the problems associated with waterlogging, erosion, salinity, and crop yield.

The sodicity problem is usually managed using amendments such as gypsum, which is added either to the soil or to the irrigation water. The process of investigating good management to use such water can be done using an appropriate model. However, modelling water and solute movement under highly sodic conditions taking into consideration the soil chemical reaction system and soil structure degradation is limited in the literature. Therefore, this research project focuses on improving the

modelling of water and solute movement under sodic conditions and the main issues that need to be addressed.

This PhD study addressed successfully these issues in chapters 3, 4, 5, and 7 of this dissertation that are focussed on:

- 1) Characterise the soil structural degradation associated with the application of saline sodic water.
- 2) Evaluation of modelling the water and solute movement within a soil profile under sodic conditions and diagnose the problem.
- 3) Evaluation of McNeal (1968) model and proposition of a new generic form as a first step to improve the modelling process.
- 4) Addressing the further needs to improve modelling water and solute movement within the soil profile under sodic conditions.

8.3 General conclusions

8.3.1 Characterise the soil structural degradation associated with the application of highly saline and sodic water

The uncontrolled irrigation using highly saline-sodic water is expected to have a significant effect on soil structural stability. Furthermore, it is expected to produce substantial long term impacts on soil structural properties and sustainability of production of the irrigated areas. The column experiments presented in chapter 3 showed that reducing water pH using sulphuric acid did not have any significant effect on the changes observed in soil structural stability or infiltration rates. Soil infiltration rates were found to decline with increasing volumes of HSS water applied irrespective of its pH. However, HSS water which had been diluted with deionised water and amended with gypsum was found to have no adverse impact on the soil structural stability or infiltration.

The results showed that using sulphuric acid to treat HSS water has no significant effect as long as the relative sodium concentration is high. The results from dilution and gypsum application treatments suggested that it may be possible to develop feasible

strategies by using gypsum and mixing HSS water with good quality water. This can ensure the maintenance of infiltration rates above an acceptable target level. The process of investigation can be done primarily by modelling. However, modelling the effect water and solute movement under sodic conditions in which soil degrades is inherent with uncertainty and still limited and requires further consideration.

8.3.2 Evaluation of modelling water and solute movement within soil profile under sodic conditions and diagnosis of the limitations

The UNSATCHEM model has been used to simulate irrigation under sodic conditions and has the ability to quantify soil degradation due to sodicity. The UNSATCHEM module incorporated in HYDRUS 1D has been evaluated with the experimental data obtained from the soil columns experiments. However, results show that the model overestimates the effect of sodicity. It is concluded that the UNSATCHEM can be used to simulate water and solute movement under sodic condition if the hydraulic conductivity reduction function which relates the decrease of water movement to the estimated soil-water sodicity and salinity is improved.

The model was able to demonstrate the type of the outflow change similar to the experimental data. However, the variation between estimated and actual accumulated outflow was large for the Sodosol soil columns. The estimated hydraulic conductivities for the whole simulation were lower than measured values during the percolation of the water treatments applied. The underestimation of the outflow and conductivity in the Sodosol is attributed mainly to the limitation in the hydraulic conductivity reduction function. The first term is the semi-empirical McNeal (1968) clay swelling model and the second term is the empirical $\text{pH}-RK_{sat}$ relationship proposed by Simunek et al. (1996). The McNeal (1968) clay swelling model was incorporated with a general values for its parameters. Therefore, it was assumed that the simulation of highly saline-sodic water percolation using the UNSATCHEM would be improved if the parameters of the clay swelling model were determined for both Sodosol and Vertosol soils used in this study. A conclusion is made that the clay swelling model and the hydraulic conductivity reduction function required further consideration.

8.3.3 Evaluation of McNeal (1968) model and proposing a new generic form

A review of the McNeal (1968) clay swelling model showed clearly that the model has a number of weak points that may limit its accuracy. It has been shown that a soil's response to the levels of sodicity and salinity varies. The threshold of the exchangeable sodium percentage (ESP_T) incorporated in the McNeal model should not be generalised. In addition, the review showed that the model incorrectly accounts for the weighted fraction of expanding clay and has uncertainty regarding the n and c parameters and their relations to sodicity levels. Based on these findings, new adjustments were involved to provide a new generic form of clay swelling model. The new generic clay swelling model can be used to determine the magnitude of RK_{Sat} reduction at any sodicity and salinity levels for a given soil. The generic clay swelling model has been successfully calibrated and evaluated with the relative saturated hydraulic conductivity RK_{Sat} data obtained for nine soils. These soils include the original McNeal (1968) data and data obtained for local soils.

8.3.4 Improved modelling of water and solute movement within soil profiles under sodic conditions and diagnosis of the problem

The degree of improvement in modelling water and solute movement using the UNSATCHEM module incorporated in HYDRUS 1D was tested in chapter 7. The process of investigation was by substituting the McNeal (1968) clay swelling model (incorporated into the UNSATCHEM) with the generic clay swelling model developed in this research. The UNSATCHEM was used to simulate the same experiment data for both Sodosol and Vertosol that were used in chapter 4.

The UNSATCHEM estimates for the outflow for different soil columns showed slight improvement compared the results from UNSATCHEM with the McNeal (1968) model. However, the variations between the experimental data for both soils varied. This indicates that modelling of water and solute movement under sodic conditions using the UNSATCHEM still has limitations. Further research is required to investigate the role of the pH on the ESP and CEC and its effect on the hydraulic conductivity along with the chemical reaction model.

8.4 Recommendations and further research

The main findings and recommendation of this research are:

- 1) The management of irrigation using highly saline-sodic water requires a thorough evaluation of water quality, soil type and condition, and irrigation management. Management practices should be developed in view of these interrelating factors.
- 2) It has been shown in this research that soils response to the increase of sodicity are significantly different. Thus, considering general guidelines for soils is not appropriate. It is recommended to evaluate the effect of sodicity on a local soil before using saline-sodic waters in irrigation.
- 3) Modelling water and solute movement under highly sodic conditions using UNSATCHEM requires further consideration including the pH effect on the hydraulic conductivity and the chemical reaction model. It is recommended that the generic clay swelling model be used in any further research in this area. However, the chemical reaction processes are complex and require further consideration.
- 4) This research focussed on the clay swelling function. However, more research is required to evaluate the second term of the hydraulic conductivity reduction function (i.e. pH- RK_{sat} relationship). Evidence can be found in the literature that the pH affecting the values of ESP and CEC. This suggests that the pH influences the hydraulic conductivity by increasing the values of the ESP. Therefore; the assumption in UNSATCHEM that the CEC and consequently the ESP are pH independent is not appropriate. It is recommended to investigate the effect of pH on the ESP and CEC and relate that effect to the change of conductivity. This approach can improve modelling the chemical reaction system and simplify the hydraulic conductivity reduction function terms.
- 5) It is worth noting that the results presented in this research are based on laboratory work. Further research is required considering field and crop growth conditions.

List of References

- Abu-Sharar, TM, Bingham, FT & Rhoades, JD 1987, 'Stability of soil aggregates as affected by electrolyte concentration and composition', *Soil Science Society of America Journal*, vol. 51, no. 2, pp. 309-314.
- Alperovitch, N, Shainberg, I, Keren, R & Singer, MJ 1985, 'Effect of clay mineralogy and aluminium and iron oxides on the hydraulic conductivity of clay-sand mixtures', *Clays and Clay Minerals*, vol. 33, no. 5, pp. 443-450.
- Amrhein, C 2000, *Revisiting acid injection into irrigation water*, Golf Course Management, viewed 15 March 2008, <<http://www.gcsaa.org/gcm/2000/dec00/12revisiting.html>>.
- ANZECC & ARMCANZ 2000, *Australian and New Zealand guidelines for fresh and marine water quality*, Department of the Environment and Heritage, Australian Government,, viewed 2 July 2005, <<http://www.deh.gov.au/water/quality/nwqms/volume1.html>>.
- Auerswald, K 1995, 'Percolation stability of aggregates from arable topsoils', *Soil Science*, vol. 159, no. 2, pp. 142-148.
- Aydin, M, Yano, T & Kilic, S 2004, 'Dependence of Zeta Potential and Soil Hydraulic Conductivity on Adsorbed Cation and Aqueous Phase Properties', *Soil Science Society of America Journal*, vol. 68, no. 2, pp. 450-459.
- Ayers, RS & Westcot, DW 1976, *Water Quality for Agriculture*, Irrigation and drainage paper no, 29, Food and Agriculture Organization, Rome.
- Ayers, RS & Westcot, DW 1985, *Water Quality for Agriculture*, Irrigation and drainage, paper 29 Rev 1, Food and Agriculture Organization, Rome.
- Bar-Yosef, B 1999, 'Advances in Fertigation', *Advances in Agronomy*, vol. 65, pp. 1 - 75.
- Barzegar, AR, Nelson, PN, Oades, JM & Rengasamy, P 1997, 'Organic matter, sodicity, and clay Type: Influence on soil aggregation', *Soil Science Society of America Journal*, vol. 61, no. 4, pp. 1131-1137.
- Bernstein, L 1961, 'Osmotic adjustment of plants to saline media I, Steady state', *American Journal botany*, vol. 48, pp. 909-918.
- Bernstein, L 1964, *Salt tolerance of plants*, USDA Agricultural Information Bulletin.
- Bernstein, L & Francois, LE 1973, 'Leaching requirements studies: Sensitivity of alfalfa to salinity of irrigation and drainage waters', *Soil Science Society of America Journal*, vol. 37, no. 2, pp. 931-943.
- Black, CA 1968, *Soil-Plant Relationships*, John Wiley and Sons, New York.

- Bolan, NS, Syers, JK, Adey, MA & Sumner, ME 1996, 'Origin of the effect of pH on the saturated hydraulic conductivity of non-sodic soils', *Communications in Soil Science and Plant Analysis*, vol. 27, no. 9, pp. 2265 - 2278.
- Bouwer, H 1969, 'Salt balance, irrigation efficiency, and drainage design', *Irrigation and Drainage Division*, vol. 95, no. 1, pp. 153-170.
- Brady, NC 1990, *The Nature and Properties of soils*, 10th edn, Macmillan, Inc, New York.
- Brady, NC & Weil, RR 2008, *The Nature and Properties of Soils*, 14th edn, Pearson Education, Inc, Upper Saddle, New Jersey.
- Bresler, E, McNeal, BL & Carter, DL 1982, *Saline and sodic soils: Principle - dynamics - modelling*, vol. 10, Advanced Series in Agricultural Sciences, Springer Verlag, Berlin.
- Bromly, M, Hinz, CL & Aylmore, AG 2007, 'Relation of dispersivity to properties of homogeneous saturated repacked soil columns', *European Journal of Soil Science*, vol. 58, no. 1, pp. 293-301.
- Brooks, RH & Corey, AT 1966, 'Properties of porous media affecting fluid flow', *Journal of the Irrigation and Drainage Division*, vol. 72, no. IR2, pp. 61-88.
- Buckingham, E 1907, *Studies on the movement of soil moisture*, Bulletin. 38, Soils Bulletin, Bureau of soils, US Department of Agriculture, Washington, D. C.
- Burger, F & Celkova, A 2003, 'Salinity and sodicity hazard in water flow processes in the soil', *Plant, Soil and Environment*, vol. 49, no. 7, pp. 314 - 320.
- Burt, CM 1995, *The surface irrigation manual*, Waterman Industries, USA.
- Carman, PH 1937, 'Fluid flow through granular beds', *Transactions Institute of Chemistry and Engineering*, vol. 3, pp. 150-166.
- Carman, PH 1948, 'Some physical aspects of water flow in porous media', *Faraday Society Discussions*, vol. 3, pp. 72-77.
- Cavazza, L 1989, 'Irrigation systems and techniques for saline water', in R Bouchet (ed.), *Reuse of low quality water for irrigation*, CIHEAM - IAMB, Cairo, vol. no.1, pp. 49-57.
- Chartres, CJ 1993, 'Sodic soils - an introduction to their formation and distribution in Australia', *Australian Journal of Soil Research*, vol. 31, no. 6, pp. 751-760.
- Chartres, CJ, Greene, RSB, Ford, GW & Rengasamy, P 1985, 'The effects of gypsum on macroporosity and crusting of two red duplex soils', *Australian Journal of Soil Research*, vol. 23, no. 4, pp. 467-479.

- Childs, EC 1940, 'The use of soil Moisture characteristics in soil studies', *Soil Science*, vol. 50, pp. 239-222.
- Chorom, M & Rengasamy, P 1997, 'Carbonate chemistry, pH, and physical properties of an alkaline sodic soil as affected by various amendments', *Australian Journal of Soil Research*, vol. 35, no. 1, pp. 149-162.
- Churchman, GJ, Skjemstad, JO & Oades, JM 1993, 'Influence of clay minerals and organic matter on effects of sodicity on soils', *Australian Journal of Soil Research*, vol. 31, no. 6, pp. 779-800.
- Cook, FJ, Jayawardane, NS, Rassam, DW, Christen, EW, Hornbuckle, JW, Stirzaker, RJ, Bristow, KL & Biswas, KT 2006, *The state of measuring, diagnosing, amelioration and managing solute effects in irrigated systems*, CRC for Irrigation Futures, Technical Report No. 04/06.
- Cook, GD & Muller, WJ 1997, 'Is exchangeable sodium content a better index of soil sodicity than exchangeable sodium percentage?: A reassessment of published data.' *Soil Science*, vol. 162, no. 5, pp. 343-349.
- Cote, CM, Bristow, KL, Ford, EJ, Verburg, K & Keating, BA 2001, *Measurement of water and solute movement in large 'Undisturbed' soil cores: Analysis of Macknade and Bundaberg data*, CSIRO Land and Water, Townsville, Australia.
- Dane, JH & Hopmans, JW 2002, 'Water retention and storage', in GS Campbell, GC Topp & JH Dane (eds), *Methods of soil analysis, Part 4, Physical methods*, Soil Science Society of America, Madison, Wis., vol. 5, pp. 671-720.
- Dehayr, R & Gordon, I 2005, *Irrigation water quality: Salinity and soil structure stability*, Natural Resource Sciences, Queensland Government, viewed 3 April 2006, <<http://www.nrm.qld.gov.au/factsheets/pdf/water/w55.pdf>>.
- Dennis, HJ 2006, *Precision irrigation in South Africa*, Technical Centre for Agricultural and Rural Cooperation, viewed 14 July 2006, <<http://ageconsearch.umn.edu/bitstream/7023/4/cp02de01.pdf>>.
- Department of Natural Resources 1997, *Salinity Management Handbook*, Department of natural Resource in Queensland.
- Davidson, JL & Quirk, JP 1961, 'Influence of dissolved gypsum on pasture establishment on irrigated sodic clays', *Australian Journal of Agriculture Research*, vol. 12, pp. 100 -114.
- Doneen, LD 1975, 'Water quality for irrigated agriculture', in A Poljakoff-Mayber & J Gale (eds), *Plants in saline environments*, Springer, Berlin Heidelberg, New York, pp. 56-75.
- Dudley, LM 1994, 'Salinity in the soil environment', in M Pessarakli (ed.), *Handbook of Plant and Crop Stress*, Marcel Dekker, Inc, New York, pp. 13-30.

- Emerson, WW & Bakker, AC 1973, 'The comparative effects of exchangeable calcium, magnesium, and sodium on some physical properties of red-brown earth subsoils: II. The spontaneous dispersion of aggregates in water', *Australian Journal of Soil Research*, vol. 11, no. 2, pp. 151-157.
- Emerson, WW & Chi, CL 1977, 'Exchangeable calcium, magnesium and sodium and dispersion of illites in water. II* Dispersion of illites in water', *Australian Journal of Soil Research*, vol. 15, pp. 255-262.
- Evangelou, VP & McDonald Jr, LM 1999, 'Influence of sodium on soils of humid regions', in M Pessarakis (ed.), *Handbook of Plant and crop Stress*, 2 edn, Marcel Dekker, New York, pp. 17 -50.
- Felhendler, R, Shainberg, I & Frenkel, H 1974, 'Dispersion and hydraulic conductivity of soils in mixed solutions.' in *International Congress in Soil Science Transactions 10*, Moscow, vol. 1, pp. 103-112.
- Fetter, CW 1999, *Contaminant Hydrogeology.*, Macmillan, New York.
- Frenkel, H, Goertzen, JO & Rhoades, JD 1978, 'Effects of clay type and content, exchangeable sodium percentage, and electrolyte concentration on clay dispersion and soil hydraulic conductivity', *Soil Science Society of America Journal*, vol. 42, no. 1, pp. 32-39.
- Gale, G, Koenig, R & Barnhill, J 2001, *Managing soil pH in Utah*, Utah State University, viewed 15 March 2008, <<http://extension.usu.edu/files/publications/publication/AG-SO-07.pdf>>.
- Ghafoor, A, Muhammed, S, Ahmed, N & Main, MA 1988, 'Indices for the estimation of ESP from SAR of soil solution', *Pakistan Journal of Science*, vol. 39-40, pp. 89-98.
- Ghassemi, F, Jakeman, AJ & Nix, HA 1995, *Salinisation of land and water resources*, University of New South Wales Press, Sydney.
- Goldberg, S, Suarez, DL & Glaubig, RA 1988, 'Factors affecting clay dispersion and aggregate stability of arid-zone soils', *Soil Science*, vol. 146, pp. 317-325.
- Goldberg, S, Forster, HS & Heick, EL 1991, 'Flocculation of illite/kaolinite and illite/montmorillonite mixtures as affected by sodium adsorption ratio and pH', *Clays and Clay Minerals*, vol. 39, no. 4, pp. 375-380.
- Goncalves, MC, Simunek, J, Ramos, TB, Martins, JC, Neves, MJ & Pires, FP 2006, 'Multicomponent solute transport in soil lysimeters irrigated with waters of different quality', *Water Resource Research*, vol. 42. pp. 1-17.
- Gonçalves, RAB, Folegatti, MV, Gloaguen, TV, Libardi, PL, Montes, CR, Lucas, Y, Dias, CTS & Melfi, AJ 2007, 'Hydraulic conductivity of a soil irrigated with treated sewage effluent', *Geoderma*, vol. 139, no. 1-2, pp. 241-248.

- Greene, RSB & Ford, GW 1985, 'The effect of gypsum on cation exchange in two red duplex soils', *Australian Journal of Soil Research*, vol. 23, no. 1, pp. 61-74.
- Gupta, RK, Bhumbla, DK & Albol, IP 1984, 'Effect of sodicity, pH, organic matter, and calcium carbonate on the dispersion behaviour of soils', *Soil Science*, vol. 137, pp. 245-251.
- Hamdy, A 2002, 'Saline irrigation management for a sustainable use: Ecophysiological and Agronomic Analyses', in N Katerji, A Hamdy, IW Van Hoorn & M Mastroiilli (eds), *Mediterranean Crop Responses to Water and Soil Salinity (Options Méditerranéennes)*, CIHEAM - IAMB, Bari., series B 36, p. 280.
- Hoffman, GJ 1986, 'Guidelines for reclamation of salt- affected soils', *Applied Agricultural Research*, vol. 1, no. 2, pp. 65 -72.
- Hoffman, GJ 2006, *An evaluation of irrigation and salinity research programs along the River Murray, Australia*, Cooperative Research centre for irrigation futures, viewed 25 June 2006,
<<http://www.irrigationfutures.org.au/imagesDB/news/HoffmanWinterZoneReport2006.pdf>>.
- Hoffman, GJ & van Genuchten, MT 1983, 'Soil properties and efficient water use water management for salinity control', in HM Taylor, WR Jordan & TR Sinclair (eds), *Limitations to efficient water use in crop production, Monogr*, American Society of Agronomy, Madison, pp. 73-85.
- Hopmans, JW & Bristow, KL 2002, 'Current capabilities and future needs of root water and nutrient uptake modelling', *Advances in Agronomy*, vol. 77, pp. 104-175.
- Hussain, N, Hassan, G, Arshhadullah, M & Mujeeb, F 2001, 'Evaluation of amendments for the improvement of physical properties of sodic soil', *International Journal of Agriculture and Biology*, vol. 3, no. 3, pp. 319-22.
- Inskip, WP & Bloom, PR 1985, 'An evaluation of rate equations for calcite precipitation kinetics at pCO₂ less than 0.01 atm and pH greater than 8', *Geochimica et Cosmochimica Acta*, vol. 49, no. 10, pp. 2165-2180.
- Isbell, RF 2002, *The Australian soil classification*, 2nd. edn, Australian soil and land survey handbook ; vol. 4, CSIRO Publishing, Collingwood, Victoria.
- Iwata, S, Tabuchi, T & Warkentin, BP 1995, *Soil-Water Interactions*, 2 edn, Marcel Dekker, Inc, New York.
- Jayawardane, NS 1977, 'The effect of salt composition of groundwaters on the rate of salinisation of soils from a water table', PhD Thesis, University of Tasmania.
- Jayawardane, NS 1979, 'An equivalent salt solutions method for predicting hydraulic conductivities of soils for different salt solutions', *Australian Journal of Soil Research*, vol. 17, no. 3, pp. 423-428.

- Jayawardane, NS 1983, 'Further examination of the use of the equivalent salt solutions method for predicting hydraulic conductivity of soils for different salt solutions', *Australian Journal of Soil Research*, vol. 21, no. 1, pp. 105-108.
- Jayawardane, NS 1992, 'Prediction of unsaturated hydraulic conductivity changes of a loamy soil in different salt solutions by using the equivalent salt solutions concept', *Australian Journal of Soil Research*, vol. 30, no. 5, pp. 565-571.
- Jayawardane, NS & Beattie, JA 1978, 'Effect of salt solution composition on moisture release curves of soil', *Australian Journal of Soil Research*, vol. 17, no. 1, pp. 89-99.
- Katerji, N, van Hoorn, JW, Hamdy, A & Mastroianni, M 2003, 'Salinity effect on crop development and yield, analysis of salt tolerance according to several classification methods.' *Agricultural Water Management*, vol. 62, no. 1, pp. 37-66.
- Keren, R 1991, 'Specific effect of magnesium on soil erosion and water infiltration', *Soil Science Society of America Journal*, vol. 55, no. 3, pp. 783-787.
- Keren, R & Singer, MJ 1988, 'Effect of low electrolyte concentration on hydraulic conductivity of sodium/calcium-montmorillonite-sand system', *Soil Science Society of America Journal*, vol. 52, no. 2, pp. 368-3673.
- Kernebone, FE, Muir, JS & Slavich, PG 1986, 'Water run gypsum trial on a crusting soil, paper presented to Conference on Agriculture Engineering, Adelaide.
- Key, BP & Angers, DA 2000, 'Soil structure', in ME Summer (ed.), *Handbook of Soil Science*, CRC Press, Boca Raton, Florida, pp. A229-A269.
- Khajanchi, L & Meena, RL 2008, 'Diagnosis of soil and water for salinity', in L Khajanchi, RL Meena, RK Gupta, DS Bundela, RK Yadav & S Gurbachan (eds), *Conjunctive Use of Canal and Groundwater*, Intech Graphics, Karnal, India, pp. 57-66.
- Khosla, BK 1979, 'Salt leaching and effect of gypsum application in a saline- sodic soil', *Agricultural Water Management*, vol. 2, pp. 193-202.
- Kjellander, R, Marcelia, S & Quirk, JP 1988, 'Attractive double-layer interactions between calcium clay particles', *Journal of Colloid and Interface Science*, vol. 126, no. 1, pp. 194-211.
- Kopittke, PM, So, HB & Menzies, NW 2004, 'Effect of cultivation on soil C contents and saturated hydraulic conductivity', paper presented to The 3rd Australian New Zealand Soils Conference, University of Sydney, Sydney, 5 – 9 December.
- Klute, A 1965, 'Laboratory measurement of hydraulic conductivity of saturated soil', in CA Black (ed.), *Methods of soil analysis part 1*, American Society of Agronomy, Madison, Wis., pp. 210-221.

- Kosugi, K 1996, 'Lognormal distribution model for unsaturated soil hydraulic properties', *Water Resource Research*, vol. 32, no. 9, pp. 2697-2703.
- Lagerwerff, JV, Nakayama, FS & Frere, MH 1969, 'Hydraulic conductivity related to porosity and swelling of soil', *Soil Science Society of America Journal*, vol. 33, no. 1, pp. 3-11.
- Lauchli, A & Epstein, E 1990, 'Plant responses to saline and sodic conditions', in KK Tanji (ed.), *Agricultural salinity assessment and management*, American Society of Civil Engineers, New York, pp. 113-137.
- Levy, GJ 2000, 'Sodicity', in ME Summer (ed.), *Handbook of Soil Science*, CRC Press, Boca Raton, Florida.
- Levy, GJ, Goldstein, D & Mamedov, AI 2005, 'Saturated hydraulic conductivity of semiarid soils: Combined effects of salinity, sodicity, and rate of wetting', *Soil Science Society of America Journal*, vol. 69, no. 3, pp. 653-62.
- Loveday, J 1957, *Soils of Sorell-Carlton-cropping area*, Soil Publication No. 8, CSIRO, Melbourne.
- Maas, EV 1990, 'Crop salt tolerance', in KK Tanji (ed.), *Agriculture salinity assessment and management*, American Society of Civil Engineers, New York, pp. 262-304.
- Maas, EV & Hoffman, M 1977, 'Crop salt tolerance - current assessment', *Journal of Irrigation and drainage*, vol. 103, pp. 115-134.
- Marsi, M & Evangelou, VP 1991, 'Chemical and physical behaviour of two kentucky soils: II. Saturated hydraulic conductivity - exchangeable sodium relationships', *Journal of Environmental Science and Health, Part A: Toxic/Hazardous Substances and Environmental Engineering*, vol. 26, no. 7, pp. 1177 - 1194.
- Martin, JP, Richards, SJ & Pratt, PF 1964, 'Relationship of exchangeable Na percentage at different soil pH levels to hydraulic conductivity', *Soil Science Society of America Journal*, vol. 28, no. 5, pp. 620-622.
- Mater, A, Osaman, Sayegh, A & Boyadgiev, T 1990, *Characteristics of Gypsiferous Soils*, Food and Agriculture Organisation, Rome.
- McIntyre, DS 1979, 'Exchangeable sodium, subplasticity and hydraulic conductivity of some Australian soils', *Australian Journal of Soil Research*, vol. 17, no. 1, pp. 115-120.
- McNeal, BL 1968, 'Prediction of the effect of mixed-salt solutions on soil hydraulic conductivity', *Soil Science Society of America Journal*, vol. 32, no. 2, pp. 190-193.
- McNeal, BL 1974, 'Soil salts and their effects on water movement', in J Van Schilfgaarde (ed.), *Drainage for Agriculture*, American Society of Agronomy, Madison, Wis.

- McNeal, BL & Coleman, NT 1966, 'Effect of solution composition on soil hydraulic conductivity', *Soil Science Society of America Journal*, vol. 30, no. 3, pp. 308-312.
- McNeal, BL, Norvell, WA & Coleman, NT 1966, 'Effect of solution composition on the swelling of extracted soil clays', *Soil Science Society of America Journal*, vol. 30, no. 3, pp. 313-317.
- McNeal, BL, Layfield, DA, Norvell, WA & Rhoades, JD 1968, 'Factors influencing hydraulic conductivity of soils in the presence of mixed-salt solutions', *Soil Science Society of America Journal*, vol. 32, no. 2, pp. 187-190.
- Meiri, A 1984, 'Plant response to salinity: experimental methodology and application to the field', in I Shainberg & J Shalhevet (eds), *Soil Salinity Under Irrigation*, Springer, New York, pp. 284-297.
- Meiri, A & Plaut, Z 1985, 'Crop production and management under saline conditions', *Plant and Soil*, vol. 89, pp. 253-271.
- Mering, J 1946, 'The hydration of montmorillonite', *Faraday Society*, vol. 42B, pp. 205-219.
- Millington, RJ & Quirk, JP 1961, 'Permeability of porous solids', *Transactions of the Faraday Society*, vol. 57, pp. 1200-1207.
- Minhas, PS, Sharma, DR & Khosla, BK 1990, 'Mungbean response to irrigation with waters of different salinities', *Irrigation Science*, vol. 11, no. 1, pp. 57 - 62.
- Miyazaki, T, Hasegawa, S & Kasubuchi, T 1993, *Water Flow in Soils*, Marcel Dekker INC, New York.
- Mmolawa, K & Or, D 2000, 'Root zone solute dynamics under drip irrigation: A review', *Plant and Soil*, vol. 222, no. 1 - 2, pp. 163-190.
- Motulsky, H 1996, *The GraphPad guide to nonlinear regression*, GraphPad Software, Inc, viewed 7 November 2008, <<http://www.graphpad.com/www/nonling1.htm>>.
- Moutier, M, Shainberg, I & Levy, GJ 1998, 'Hydraulic gradient, aging, and water quality effects on hydraulic conductivity of a vertisol', *Soil Science Society of America Journal*, vol. 62, no. 6, pp. 1488-1496.
- Moutier, M, Shainberg, I & Levy, GJ 2000, 'Hydraulic gradient and wetting rate effects on the hydraulic conductivity of two calcium vertisols', *Soil Science Society of America Journal*, vol. 64, no. 4, pp. 1211-1219.
- Mualem, Y 1976, 'A new model for predicting the hydraulic conductivity of unsaturated porous media', *Water Resource Research*, vol. 12, no. 3, pp. 513-522.

- Mustafa, MA & Hamid, KS 1977, 'Comparisons of two models for predicting the relative hydraulic conductivity of salt-affected swelling soils', *Soil Science*, vol. 123, pp. 149-154.
- Nelson, PN, Baldock, A, Oades, JM, Churchman, GJ & Clarke, P 1999, 'Dispersed clay and organic matter in soil: their nature and associations', *Australian Journal of Soil Research*, vol. 37, no. 2, pp. 289-316.
- Norrish, K 1954, 'The swelling of montmorillonite', *Discussions of the Faraday Society*, vol. 18, pp. 120-134.
- Oster, JD & Shainberg, I 2001, 'Soil responses to sodicity and salinity: challenges and opportunities', *Australian Journal of Soil Research*, vol. 39, no. 6, pp. 1219-1224.
- Oster, JD, Shainberg, I & Wood, JD 1980, 'Flocculation value and gel structure of sodium/calcium montmorillonite and illite suspensions', *Soil Science Society of America Journal*, vol. 44, no. 5, pp. 955-9.
- Oster, JD, Hoffman, GJ & Robinson, FE 1984, 'Management alternative: Crop, water and soil', *California Agriculture*, vol. 38, no. 10, pp. 29 - 32.
- Panabokke, CR & Quirk, JP 1957, 'Effect of initial water content on stability of soil aggregates in water', *Soil Science*, vol. 83, pp. 185-95.
- Panabokke, CR (ed.) 1999, *Handbook of Plant and Crop Stress*, 2 edn, Marcel Dekker, Inc, New York.
- Patel, RM, Prasher, SO, Bonnell, RB & Broughton, RS 2002, 'Development of comprehensive soil salinity index', *Journal of Irrigation & Drainage Engineering*, vol. 128, no. 3, pp. 185-8.
- Perry, C 2006, *Variable Rate Irrigation*, University of Georgia, viewed 11 October 2006, <<http://www.nespal.org/PrecAg/vri.asp>>.
- Pitzer, KS 1973, 'Thermodynamics of electrolytes: I. Theoretical basis and general equations', *The Journal of Physical Chemistry*, vol. 77, no. 2, pp. 268-77.
- Plummer, LN, Wigley, TML & Parkhurst, DL 1978, 'The kinetics of calcite dissolution in CO₂-water systems at 5 degrees to 60 degrees C and 0.0 to 1.0 atm CO₂', *American Journal of Science*, vol. 278, no. 2, pp. 179-216.
- Pratt, PF & Suarez, DL 1990, 'Irrigation water quality assessments', in KK Tanji (ed.), *Agricultural Salinity Assessment and Management*, American Society of Civil Engineers, ASCE Manuals Reports On Engineering Practice, pp. 220 - 61. New York.
- Pupisky, H & Shainberg, I 1979, 'Salt effects on the hydraulic conductivity of a sandy soil', *Soil Science Society of America Journal*, vol. 43, no. 3, pp. 429-433.

- Qadir, M & Schubert, S 2002, 'Degradation processes and nutrient constraints in sodic soils', *Land Degradation & Development*, vol. 13, no. 4, pp. 275-294.
- Qadir, M & Oster, JD 2004, 'Crop and irrigation management strategies for saline-sodic soils and waters aimed at environmentally sustainable agriculture', *Science of The Total Environment*, vol. 323, no. 1-3, pp. 1-19.
- Qadir, M, Noble, AD, Schubert, S, Thomas, RJ & Arslan, A 2006, 'Sodicity-induced land degradation and its sustainable management: Problems and prospects', *Land Degradation & Development*, vol. 17, no. 6, pp. 661-676.
- QGC (2009). Application for Beneficial Reuse of a Resource. Document QGC –T-APP- 002. Queensland Gas Company, Brisbane.
- Quirk, JP 1994, 'Interparticle forces: A basis for the interpretation of soil physical behaviour', *Advanced in Agronomy*, vol. 53, pp. 121-128.
- Quirk, JP 2001, 'The significance of the threshold and turbidity concentrations in relation to sodicity and microstructure', *Australian Journal of Soil Research*, vol. 39, no. 6, pp. 1185-1217.
- Quirk, JP & Schofield, RK 1955, 'The effect of electrolyte concentration on soil permeability', *Journal of Soil Science*, vol. 6, no. 2, pp. 163-178.
- Quirk, JP & Murray, RS 1991, 'Towards a model for soil structural behaviour', *Australian Journal of Soil Research*, vol. 29, no. 6, pp. 829-867.
- Raine, S & Loch, RJ 2003, *What is a sodic soil? Identification and management options for construction sites and disturbed lands*, University of Southern Queensland, viewed 14 March 2008, <http://www.usq.edu.au/users/raine/index_files/Raine&Loch_WhatIsASodicSoil_2003.pdf>.
- Raine, SR, Meyer, WS, Rassam, DW, Hutson, JL & Cook, FJ 2005, *Soil-water and salt movement associated with precision irrigation systems- Research investment opportunities*, Final report to the National Program for Sustainable Irrigation. CRCIF report number 3. 13/1, Cooperative Research Centre for Irrigation Futures, Toowoomba.
- Rengasamy, P 1983, 'Clay dispersion in relation to changes in the electrolyte composition of dialysed red-brown earths', *Journal of Soil Science*, vol. 34, pp. 723-732.
- Rengasamy, P, Greene, RSB, Ford, GW & Mehanni, AH 1984, 'Identification of dispersive behaviour and the management of red-brown earths', *Australian Journal of Soil Research*, vol. 22, no. 4, pp. 413-431.
- Rhoades, JD 1974, 'Drainage for salinity control', in JV Schilfgaarde (ed.), *Drainage for Agriculture*, American Society of Agronomy, Madison, pp. 433-461.

- Rhoades, JD 1982, 'Reclamation and management of salt-affected soils after drainage', paper presented to First Annual Western Provincial Conference on Rationalization of water and Soil Research and Management, Lethbridge, Alberta, Canada, 29 November - 2 December.
- Rhoades, JD, Chanduvi, F & Lesch, S 1999, *Soil salinity assessment*, 1 edn, vol. 57, Irrigation and drainage paper, Food and Agriculture Organization of the United Nations, Rome.
- Richards, LA 1931, 'Capillary conduction of liquids through porous mediums', *Physics*, vol. 1, pp. 318-333.
- Robbins, CW & Meyer, WS 1990, 'Calculating pH from EC and SAR values in salinity models and SAR from soil and bore water pH and EC data', *Australian Journal of Soil Research*, vol. 28, no. 6, pp. 1001-1011.
- Robbins, CW, Wagenet, RJ & Jurinak, JJ 1980a, 'A Combined salt transport-chemical equilibrium model for calcareous and gypsiferous soils', *Soil Science Society of America Journal*, vol. 44, no. 6, pp. 1191-1194.
- Robbins, CW, Jurinak, JJ & Wagenet, RJ 1980b, 'Calculating cation exchange in a salt transport model', *Soil Science Society of America Journal*, vol. 44, no. 6, pp. 1195-1200.
- Rose, CW, Dayananda, PWA, Nielson, DR & Biggar, JW 1979, 'Long term solute dynamics and hydrology in irrigated slowly permeable soils', *Irrigation Science*, vol. 1, pp. 77-87.
- Rowell, DL, Payne, D & Ahmed, N 1969, 'The effect of the concentration and movement of solutions on the swelling, dispersion, and movement of clay in saline and alkali soils', *Journal of Soil Science*, vol. 20, pp. 176-188.
- Ruiz-Vera, VM & Wu, L 2006, 'Influence of sodicity, clay mineralogy, prewetting rate, and their interaction on aggregate stability', *Soil Science Society of America Journal*, vol. 70, no. 6, pp. 1825-33.
- Russo, D 1986, 'Simulation of leaching of a gypsiferous-sodic desert soil', *Water Resources Research*, vol. 22, pp. 1341-1349.
- Russo, D & Bresler, E 1977a, 'Effect of mixed Na-Ca solutions on the hydraulic properties of unsaturated soils', *Soil Science Society of America Journal*, vol. 41, no. 4, pp. 713-717.
- Russo, D & Bresler, E 1977b, 'Analysis of the saturated-unsaturated hydraulic conductivity in a mixed sodium-calcium soil system', *Soil Science Society of America Journal*, vol. 41, no. 4, pp. 706-710.
- Rycroft, DW & Amer, MH 1995, *Prospects For the Drainage of Clay Soils*, FAO Irrigation and Drainage, vol. 51, Food and Agriculture Organisation, Rome.

- Schaap, MG, Leij, FJ & van Genuchten, MT 2001, 'A computer program for estimating soil hydraulic parameters with hierarchical pedotransfer functions', *Journal of Hydrology*, vol. 251, no. 3-4, pp. 163-176.
- Scherer, TF, Seelige, B & Franzen, D 1996, *Soil, Water and plant characteristics important to irrigation*, NDSU Extension Service, North Dakota State University, viewed 7 August 2005, <<http://www.ext.nodak.edu/extpubs/ageng/irrigate/eb66w.htm>>.
- Schoups, G, Hopmans, JW & Tanji, KK 2006, 'Evaluation of model complexity and space-time resolution on the prediction of long-term soil salinity dynamics, western San Joaquin Valley, California', *Hydrological Processes*, vol. 20, no. 13, pp. 2647-2668.
- Seetharam, SC, Thomas, HR & Cleall, PJ 2007, 'Coupled thermo /hydro /chemical /mechanical model for unsaturated soils - Numerical algorithm', *International Journal for Numerical Methods in Engineering*, vol. 70, no. 12, pp. 1480-511.
- Shakir, MS, Anwar-ul-Hassan & Razzaq, A 2002, 'Effect of salts on bulk density, particle density and porosity of different soil series', *Asian Journal of Plant Sciences*, vol. 1, no. 1, pp. 5-6.
- Shainberg, I, Levy, GJ, Goldstein, D, Mamedov, AI & Letey, J 2001, 'Prewetting rate and sodicity effects on the hydraulic conductivity of soils', *Australian Journal of Soil Research*, vol. 39, no. 6, pp. 1279-1291.
- Sherard, JL, Dunnigan, LP & Decker, RS 1976, 'Identification and nature of dispersive soils', *Journal of Geotechnical Engineering Division, ASCE*, vol. 102, pp. 287-301.
- Shternina, EB 1960, 'Solubility of gypsum in aqueous solutions of salts', *International Geology Review*, vol. 2, pp. 605 - 616.
- Simunek, J & Suarez, DL 1994, 'Two-dimensional transport model for variably saturated porous media with major ion chemistry', *Water Resource Research*, vol. 30, no. 4, pp. 1115-1133.
- Simunek, J & Suarez, DL 1997, 'Sodic soil reclamation using multicomponent transport modelling', *Journal of Irrigation and Drainage Engineering*, vol. 123, no. 5, pp. 367-376.
- Simunek, J, Suarez, DL & Sejna, M 1996, *The UNSATCHEM Software Package For Simulating One-Dimensional Variably Saturated Water Flow, Heat Transport, Carbon Dioxide Production and Transport, and Multicomponent Solute Transport With Major Ion Equilibrium and Kinetic Chemistry, Version 2.0*, U.S. Salinity Laboratory Agricultural Research Service, Riverside, California.
- Simunek, J, Sejna, M & van Genuchten, MT 1999, *The HYDRUS-2D Software Package for Simulating Two-Dimensional Movement of Water, Heat, And*

- Multiple Solutes in Variable Saturated Media, Version 2*, International Ground Water modelling Center, Colorado.
- Simunek, J, van Genuchten, MT & Sejna, M 2005, *The HYDRUS-1D Software Package for Simulating One-Dimensional Movement of Water, Heat, and Multiple Solutes in Variable Saturated Media, Version 3*, University of California Riverside, Riverside, California.
- Simunek, J, van Genuchten, MT, Sejna, M, Toride, N & Leij, FJ 1999, *Transport in Porous Media Using Analytical Solutions Of Convection-Dispersion Equation*, U.S. Salinity Laboratory, Riverside, California.
- Skene, JKM 1965, 'The diagnosis of alkali soils', *Journal of the Australian Institute of Agricultural Science*, vol. 31, pp. 321-2.
- Slavich, PG & Yang, J 1990, 'Estimation of field scale leaching rates from chloride mass balance and electromagnetic induction measurements', *Irrigation Science*, vol. 11, pp. 7 - 14.
- Smith, GD & McShane, TJ 1981, *Modification and Management of Irrigation Soils in Lower Burdekin valley, Queensland*, 17, Queensland Department of Primary Industries, Toowoomba, QLD.
- Smith, R & Raine, S 2000, *A Prescriptive Future for Precision and Spatially Varied Irrigation*, National Centre for Engineering in Agriculture, viewed 10 July 2008, <http://www.usq.edu.au/users/raine/index_files/IAA2000_Smith&Raine.pdf>.
- Smith, RJ & Hancock, NH 1986, 'Leaching Requirements of irrigated soils', *Agricultural Water Management*, vol. 11, pp. 13-22.
- So, HB & Aylmore, LAG 1993, 'How do sodic soils behave - the effects of sodicity on soil physical behaviour', *Australian Journal of Soil Research*, vol. 31, no. 6, pp. 761-777.
- Sophocleous, M 1979, 'Analysis of water and heat flow in unsaturated-saturated porous media', *Water Resource Research*, vol. 15, no. 5, pp. 1195-206.
- Stevens, R 2002, *Interactions between irrigation, salinity, leaching efficiency, salinity tolerance and sustainability*, The Australian and New Zealand Grapegrower and Winemaker Journal, viewed 20 April 2006, <http://www.sardi.sa.gov.au/pdfserve/hort/viticulture/vineyard_irrigation.pdf>.
- Stumm, W & Morgan, JJ 1981, *Aquatic chemistry: An introduction emphasizing chemical equilibria in natural waters*, John Wiley & Sons, New York.
- Suarez, DL 1977, 'Ion activity products of calcium carbonate in waters below the root zone', *Soil Science Society of America Journal*, vol. 41, no. 2, pp. 310-315.

- Suarez, DL 1981, 'Relation between pH_c and sodium adsorption ratio (SAR) and an alternative method of estimating SAR of soil or drainage Waters', *Soil Science Society of America Journal*, vol. 45, no. 3, pp. 469-475.
- Suarez, DL & Rhoades, JD 1982, 'The apparent solubility of calcium carbonate in soils', *Soil Science Society of America Journal*, vol. 46, no. 4, pp. 716-722.
- Suarez, DL & Simunek, J 1997, 'UNSATCHEM: Unsaturated water and solute transport model with equilibrium and kinetic chemistry' *Soil Science Society of America Journal*, vol. 61, no. 6, pp. 1633-1646.
- Suarez, DL, Rhoades, JD, Lavado, R & Grieve, CM 1984, 'Effect of pH on saturated hydraulic conductivity and soil dispersion', *Soil Science Society of America Journal*, vol. 48, no. 1, pp. 50-55.
- Sumner, ME 1992, 'The electrical double layer and clay dispersion', in ME Summer & BA Stewart (eds), *Soil Crusting: Chemical and Physical processes*, Lewis Publishers, Boca Raton, London.
- Sumner, ME 1993, 'Sodic soils - new perspectives', *Australian Journal of Soil Research*, vol. 31, no. 6, pp. 683-750.
- Surapaneni, A & Olsson, KA 2002, 'Sodification under conjunctive water use in the Shepparton Irrigation Region of northern Victoria: a review', *Australian Journal of Experimental Agriculture*, vol. 42, no. 3, pp. 249-63.
- Sustainable Soils & Management 2005, *Assessment of soil on 'Windibri' for sprinkler irrigation with berwyndale South Coalbed Methane Production Water*, ACN 105 201 581, Warren, NSW.
- Tanji, KK 1990, 'Nature and extent of agriculture salinity', in KK Tanji (ed.), *Agricultural salinity assessment and management*, American Society of Civil Engineers, ASCE Manual and Report on Engineering Practice, New York, , pp. 1 -17.
- Tanji, KK & Kielen, NC 2002, *Agriculture drainage water management in arid and semi-arid areas*, Irrigation and drainage paper n.61, Food and Agriculture Organization, Rome.
- Tisdall, JM 1996, 'Formation of soil aggregates and accumulation of soil organic matter', in MR Carter & BA Stewart (eds), *Structure and Organic Matter Storage in Agricultural Soils*, CRC Press, Inc, Boca Raton, Florida, p. 477.
- Toride, N, Leij, FJ & van Genuchten, MT 1999, *The CXTFIT code for estimating transport parameters from laboratory or field tracer experiments version 2.1*, 137, U.S Salinity Laboratory, Riverside, California.
- Truesdell, AH & Jones, BF 1974, 'WATEQ, A computer program for calculating chemical equilibria of natural waters', *Journal of Research, U.S. Geological Survey*, vol. 2, no. 2, pp. 233-274.

- USSL Staff (ed.) 1954, *Diagnosis and improvement of saline and alkaline soils*, USDA Handbook 60, Salinity Laboratory Staff. California.
- van de Graaff, R & Patterson, RA 2001, 'Explaining the mysteries of salinity, sodicity, SAR and ESP in on-site practice', paper presented to Advancing On-site Wastewater Systems, Armidale.
- van Genuchten, MT 1976, 'Mass transfer studies in sorbing porous media', *Soil Science Society of America Journal*, vol. 40, no. 4, pp. 473 - 480.
- van Genuchten, MT 1980, 'A closed-form equation for predicting the hydraulic conductivity of unsaturated soils', *Soil Science Society of America Journal*, vol. 44, no. 5, pp. 892-898.
- van Genuchten, MT 1987, 'A numerical model for water and solute movement in and below the root zone', *Res. Rep.*
- van Genuchten, MT & Hoffman, GJ 1984, 'Analysis of crop salt tolerance data', in I Shainberg & J Shalhevet (eds), *Soil Salinity Under Irrigation, Processes and Management*, Springer Verlag, New York, pp. 258 - 271.
- van Genuchten, MT & Parker, JC 1984, 'Boundary conditions for displacement experiments through short laboratory soil columns', *Soil Science Society of America Journal*, vol. 48, no. 4, pp. 703-708.
- van Genuchten, MT, Leij, FJ & Yates, SR 1991, *The RETC code for quantifying the hydraulic functions of unsaturated soils*, EPA/600/2-91/065, Robert S. Kerr Environmental Research Laboratory, Ada, Oklahoma.
- van Hoorn, IW & van Alphen, JG 1994, 'Salinity control', in HP Ritzema (ed.), *Soil salinity assessment*, 2nd edn, ILRI Publication, Wageningen, vol. 16, pp. 533 -600.
- Van Hoorn, JW, Katerji, N & Hamdy, A 1997, 'Long-term salinity development in a lysimeter experiment', *Agricultural Water Management*, vol. 34, no. 1, pp. 47-55.
- van Schilfgaarde, J, Bernstein, L, Rhoades, JD & Rawlins, SL 1974, 'Irrigation management for salt control', in JV Schilfgaarde (ed.), *Drainage for Agriculture*, American Society of Agronomy, Madison, vol. 100, pp. 321-338.
- Vogel, T & Cislerova, M 1988, 'On the reliability of unsaturated hydraulic conductivity calculated from the moisture retention curve', *Transport in Porous Media*, vol. 3, no. 1, pp. 1-15.
- Wagenet, RJ & Hutson, JL 1987, *LEACHM: A finite-difference model for simulating water, salt, and pesticide movement in the plant root zone*, *Continuum 2*, New York State Water Resources Institute, Cornell University, Ithaca.
- Wallace, G 2003, *Garden science: Gypsum*, North Pacific Group, INC, viewed 6 November 2008, <http://www.northpacific.com/dept/gypsum/gyp_whitepapers.html>.

- Warrence, NJ, Bauder, JW & Pearson, KE 2003, *The basics of salinity and sodicity effects on soil Physical properties*, Montana State University, viewed 5 September 2005, <http://waterquality.montana.edu/docs/methane/basics_highlights.pdf>.
- Wearing, C 2004, 'Sodicity and Soil Microstructure', PhD Thesis, University of Queensland.
- White, N & Zelazny, LW 1986, 'Charge properties in soil colloids', in DL Sparks (ed.), *Soil Physical Chemistry*, CRC Press, Boca Raten, Florida, pp. 39-81.
- Yaron, B & Thomas, GW 1968, 'Soil hydraulic conductivity as affected by sodic water', *Water Resource Research*, vol. 4, pp. 545-552.
- Yeh, G-T & Tripathi, VS 1991, 'A Model for simulating transport of reactive multispecies components: Model development and demonstration', *Water Resource Research*, vol. 27, pp. 3075-3094.
- Zia, HM, Ghafoor, A, Saifullah & M. Boers, T 2006, 'Comparison of sulfurous acid generator and alternate amendments to improve the quality of saline-sodic water for sustainable rice yields', *Paddy and Water Environment*, vol. 4, pp. 153-162.

Appendix A: Standard Chemical Analysis for HSS Water



CTW.2603022

Certificate of Analysis

SAMPLE NUMBER: 2006009982 **SAMPLE(S) RECEIVED:** 15 June 2006
COMMODITY: Water 15/06/2006 **CERTIFICATE ISSUED:** 03 July 2006
MARKINGS: Ber.South well 38

<u>TEST IDENTITY</u>	<u>RESULT</u>	<u>UNITS</u>	<u>METHOD</u>
Total Dissolved Solids	2958.0	mg/L	TDS001
Fluoride	3.06	mg/L	FLU005
pH	8.6	pH	WAT001
Sodium Adsorption Ratio	118.4		WAT040
Bicarbonate Alkalinity	1500.2	mg CaCO ₃ /L	WAT040
Carbonate Alkalinity	61.6	mg/kg	WAT040
Hydroxide Alkalinity	0.2	mg CaCO ₃ /L	WAT040
Selenium	<0.01	mg/L	MIN002
Aluminium	1.5	mg/L	MIN001
Boron	0.97	mg/L	MIN001
Calcium	4.6	mg/L	MIN001
Iron	0.24	mg/L	MIN001
Potassium	5.0	mg/L	MIN001
Magnesium	1.3	mg/L	MIN001
Sodium	1100	mg/L	MIN001
Sulphate	<1	mg/L	MIN001
Chloride	584	mg/L	SAL003

Note: < is Less Than.

Page 22 of 34

Robert Lascelles
Chief Chemist
For and on behalf of
SGS Australia Pty Ltd

The results apply only to the sample analysed. The sample on which the test was performed was not collected by or on behalf of SGS Agritech. This certificate is discrete and can only be reproduced in full. The analysis was performed between 15/06/2006 and 3/07/2006

Appendix B: Data Obtained From Long Columns Experiments

B.1 Introduction

The saturated hydraulic conductivity (K_{sat}) is a most important soil parameter that has been used widely to diagnose soil structure degradation under sodic condition. The K_{sat} can be defined as a Darcian flux through a saturated soil at a hydraulic gradient equals to unity. The K_{sat} can be expressed by rearrangement of Darcy's law as:

$$K_{sat} = \frac{q}{A} \frac{dl}{dh} \quad (A.1)$$

Where q is Darcy flux (L/T), dl designated to the length of the soil (L), and dh is the hydraulic gradient weight unit (i.e. water head (L)).

Measuring K_{sat} in laboratory

The K_{sat} can be measured by two different ways which are constant head core and falling head core. The constant head core method can be carried out by saturating a known length of soil column (could be disturbed or intact soil) and maintaining constant water head at the top of the soil column. The water is drained and collected at the bottom of the soil column at time increments (Figure A.1). The K_{sat} can be calculated by a direct application of Darcy's law (equation A.1).

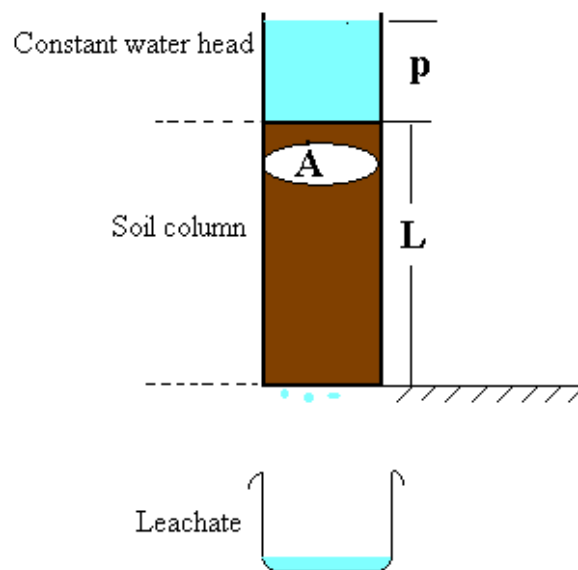


Figure A.1 Graphical description of constant head method for measuring K_{sat}

Appendix B: Data Obtained From Long Columns Experiments

The falling head method can be carried out by saturating the soil column and applying a variable water head (in a tiny tube) at the top of the soil column (Figure A.2). The decrease of the water head at different time increments is recorded. At a given time (t_1), the water head is at h_1 , and at t_2 the water head is decreased as the water moves within the soil column to be h_2 . Assuming that the flow in the soil column is equal to the reduction of the water head, conservation mass equation can be written as:

$$dt h a = AK_{sat} \frac{dh}{L} \quad (A.2)$$

Where a is the across section area of the tiny tube above the soil column, L soil length, t time, and A is the cross section area of the soil column.

The resultant integration of equation (A.2) between t_1 and t_2 is:

$$K_{sat} = \frac{aL}{A\Delta t} \ln\left(\frac{h_1}{h_2}\right) \quad (A.3)$$

The falling head method is recommended for fine texture soils that have low permeability because the measurement requires only the change of water head in the tiny tube above the soil column (Figure A.2).

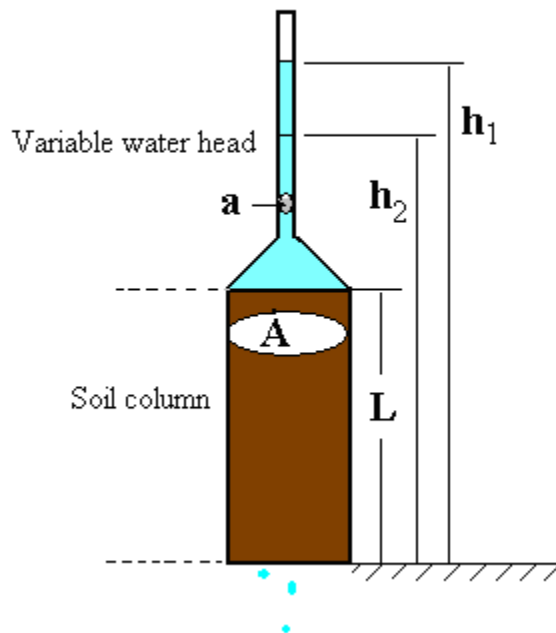


Figure A.2 Graphical description of falling head method for measuring K_{sat}

It should be noted that measuring K_{sat} is inherent with difficulties in the laboratory. The packaging of the soil and water movement can cause a discrepancy of measured K_{sat} due to movement of finer particles with percolated water, which could result in variation of the K_{sat} values measured for the same soil.

Long column experiments data

Leachate (i.e. outflow) volume was determined at increment time for each experiment. EC of each leachate volume collected was measured unless the water volume was not enough to conduct EC measurement. Geometry information needed to calculate K_{sat} such as water head at the top soil column were also measured. The data collected were transferred to spreadsheets to calculate K_{sat} . It should be noted that the water treatments have been added incrementally because of difficulties associated with monitoring the columns for more than 10 hours. Therefore, the time increments were reset each time at which the experiment started again for each replicate.

In addition, the replicates were flexible and might be exposed to different conditions. In the first two replicates only the average final K_{sat} under treatment were reported. However, the changes of K_{sat} with applied treatments were recorded in the following two replicates. In replicate four, HSS water treatments were applied at longer time to determine the minimum K_{sat} .

The following Tables contain the K_{sat} calculated and EC measured at increment time and water head applied. The processes of calculation have been not reported. The first part is the four replicates of each water treatment for the Sodosol soil and the second part is the data obtained for Grey Vertosol. It is worth noting that when the time is reset to zero indicates that the measurements resumed again after pausing for view hours:

B.2 Part I: Sodosol columns experiment results

Table B.1 K_{sat} measured with time for replicate 1 (Sodosol), tap water amended with gypsum treatment (EC = 1.3 dS/m) during applying water with EC = 0.4 dS/m. The Average K_{sat} measured at the final stage of water treatment for this replicate was 3.84 cm/h.

Time (h)	Water head (cm)	EC in leachate (dS/m)	K_{sat} (cm/h)	Accumulated leachate (cm)
0	9.1			0.00
0.25	9.1		3.48	1.27
0.5	9.2		3.79	2.66
0.75	9.2		3.74	4.04
1	9.2		3.81	5.44
1.25	9.1		3.80	6.83
1.5	9.1		3.69	8.18
1.75	9.1		3.65	9.52
2	9.1		3.67	10.86
2.25	9.1		3.69	12.21
2.5	9.1		3.67	13.56
2.75	8.6		3.76	14.91
3	8.6		3.67	16.23
3.25	8.6		3.61	17.53
3.5	8.6		3.63	18.83
3.75	8.6		3.58	20.12
4	8.6		3.54	21.39
4.25	8.5		3.55	22.67
4.5	8.5		3.53	23.93
4.75	8.5		3.55	25.21
5	8.5		3.46	26.45
5.25	8.5		3.51	27.70
0	9			
0.25	9		2.95	35.08
0.5	9.2		3.32	36.30
0.75	9.2		3.34	37.53
1	9.2		3.23	38.72
1.25	9.2		3.25	39.91
1.5	8.9		3.29	41.11
1.75	8.9		3.26	42.29
2	8.9		3.26	43.48
2.25	8.8		3.32	44.68
2.5	8.8		3.28	45.87
2.75	8.8		3.21	47.03
3	8.8		3.86	48.43
3.25	8.8		2.58	49.37
3.5	8.8		3.21	50.53
3.75	8.8		3.19	51.68
4	8.8		3.21	52.85
4.257	8.8		3.23	54.05

Table B.2 K_{sat} measured with time for replicate 1(Sodosol), tap water amended with gypsum treatment ($EC \approx 1.3$ dS/m) during applying water with $EC = 0.1$ dS/m after applying water with $EC=0.4$.

Time (h)	Water head (cm)	EC in drained water (dS/m)	K_{sat} (cm/h)	Accumulated leachate (cm)
0	7.9			0.00
0.25	7.9			0.80
0.5	7.9		2.76	1.77
0.75	7.9	0.566	2.83	2.76
1	7.9		2.74	3.72
1.25	7.9		2.78	4.69
1.5	7.9		2.78	5.67
1.75	7.9		2.78	6.64
2	7.9	0.391	2.78	7.62
2.25	7.9		2.76	8.58
2.5	7.9	0.234	2.69	9.53
2.75	7.9		2.72	10.48
3	7.9		2.72	11.43
3.25	7.9		2.69	12.37
3.5	7.9	0.1589	2.67	13.31
3.75	7.9		2.69	14.25
4	7.9		2.65	15.18
4.25	7.9		2.65	16.10
4.5	7.9	0.1381	2.65	17.03
4.75	7.9		2.60	17.94
5	7.9		2.65	18.87
5.25	7.9		2.65	19.80
5.5	7.9	0.1323	2.67	20.73
5.75	7.9		2.65	21.66
6	7.9		2.65	22.59
6.25	7.9		2.60	23.50
6.5	7.9	0.127	2.65	24.43
6.75	7.9		2.60	25.34
7	7.9		2.60	26.25
7.25				
7.5	7.9	0.1239	2.63	28.09
7.75	7.9		2.60	29.00
8	7.9		2.56	29.90
8.25	7.9		2.58	30.80
8.5	7.9	0.1218	2.60	31.71
8.75	7.9		2.58	32.62
9	7.9		2.58	33.52
9.25	7.9		2.60	34.43
9.5	7.9	0.1192	2.58	35.34
9.75	7.9		2.60	36.25
10	7.9	0.1194	2.65	37.18

Table B.3 K_{sat} measured with time for replicate 2 (Sodosol), tap water amended with gypsum treatment (EC \approx 1.3 dS/m) during applying water with EC = 0.4 dS/m. The Average K_{sat} measured at the final stage of water treatment for this replicate was 3.07 cm/h.

Time (h)	Water head (cm)	EC in leachate (dS/m)	K_{sat} (cm/h)	Accumulated leachate (cm)
0	9.6			0.00
0.25	9.6	1.522		0.68
0.5	9.6	1.613	1.95	1.40
0.75	9.6	1.669	1.95	2.12
1	9.6	1.672	2.03	2.88
1.25	9.6	1.670	1.95	3.60
1.5	9.6	1.710	1.99	4.34
1.75	9.6	1.715	1.99	5.08
2	9.6	1.590	1.86	5.77
2.25	9.6	1.345	1.91	6.48
2.5	8.9	1.095	2.04	7.22
2.75	8.9	0.908	2.08	7.97
3	8.9	0.789	2.04	8.71
3.25	8.9		2.00	9.43
3.5	8.9		2.04	10.17
3.75	8.8		2.07	10.92
4	8.9	0.549	2.00	11.64
5	8.9	0.472	2.00	14.53
6	8.9	0.433	2.01	17.44
7	8.9	0.398	2.01	20.36
8	8.9	0.390	2.00	23.25
0	8.8			0.00
0.25	8.8	0.434		26.48
0.5	8.8	0.465	1.61	27.06
0.75	8.8	0.473	1.83	27.72
1	8.8	0.480	1.78	28.36
1.25	8.8	0.480	1.81	29.02
1.5	8.8	0.487	1.78	29.66
1.75	8.8	0.500	1.87	30.34
2	8.8	0.497	1.96	31.05
2.25	8.8	0.491	1.65	31.64
2.5	8.8	0.491	1.83	32.30
3	8.8	0.464	1.83	33.62
4	8.8	0.439	1.80	36.22
5	8.8	0.398	1.83	38.86
6	8.8	0.380	1.78	41.44
7	8.8	0.386	1.82	44.06
8	8.8	0.387	1.83	46.71
9	8.8	0.383	1.82	49.33

Table B.4 K_{sat} measured with time for replicate 2 (Sodosol), tap water amended with gypsum treatment (EC \approx 1.3 dS/m) during applying water with EC = 0.1 dS/m after applying water with EC=0.4.

Time (h)	Water head (cm)	EC in drained water (dS/m)	K_{sat} (cm/h)	Accumulated leachate (cm)
0	8.1			0.00
0.25	8.1	0.382		0.42
0.5	8.1	0.454	1.65	1.01
0.75	8.1	0.454	1.61	1.57
1	8.1	0.467	1.61	2.14
2	8.1	0.471	1.57	4.35
3	8.1	0.385	1.58	6.59
4	8.2	0.264	1.62	8.88
5	8.2	0.200	1.56	11.08
6	8.2	0.161	1.57	13.30
7	8.2	0.142	1.52	15.44
8	8.2	0.131	1.53	17.61
9	8.2	0.126	1.52	19.77
10	8.2	0.123	1.51	21.90
0				
0.5	8.4	0.465		1.07
1	8.4	0.480	1.57	1.12
2	8.4	0.497	1.48	3.22
3	8.4	0.464	1.55	5.43
4	8.1	0.439	1.52	7.57
5	8.1	0.398	1.50	9.68
6	8.1	0.380	1.48	11.77
7	8.1	0.386	1.49	13.88
8	8.1	0.387	1.48	15.96
9	8.1	0.383	1.48	18.05
10	8.1	0.378	1.51	20.18

Table B.5 K_{sat} measured with time for replicate 3 (Sodosol), tap water amended with gypsum treatment (EC \approx 1.3 dS/m), during applying water treatment.

Time (h)	Water head (cm)	EC in leachate (dS/m)	K_{sat} (cm/h)	Accumulated leachate (cm)
0	7.8			0.00
1	7.8	2.639		3.13
2	7.8	1.451	4.09	8.82
3	7.8	1.29	3.81	14.12
4	8.1	1.251	3.71	19.33
5	8.1	1.24	3.68	24.51
6	8.1	1.192	3.61	29.58
7	7.7	1.172	3.61	34.59
8	7.7	1.133	3.55	39.51
9	7.7	1.109	3.54	44.41
10	7.35	1.069	3.57	49.30

Table B.6 K_{sat} measured with time for replicate 3 (Sodosol), tap water amended with gypsum treatment (EC \approx 1.3 dS/m), during applying water with EC = 0.4 dS/m.

Time (h)	Water head (cm)	EC in drained water (dS/m)	K_{sat} (cm/h)	Accumulated leachate (cm)
0	7.3			0.00
1	7.3	1.136		2.89
2	7.3	1.137	2.24	5.95
3	7.8	0.72	2.22	9.03
5.5	7.8	0.42	2.20	16.68
6	7.8	0.36	2.19	18.20
7	7.8	0.356	2.23	21.31
8	7.8	0.351	2.17	24.33
9	7.8	0.338	2.03	27.15
10	4.8	0.33	1.98	29.61
0	0		0.00	0.00
1	6.9	0.405	2.33	34.54
2	6.9	0.41	2.49	37.89
3	7.1	0.376	2.51	41.29
4.02	7.1	0.34	2.50	44.74
6	7.1	0.339	2.43	51.26
7	7.1	0.355	2.52	54.67
8	6.2	0.328	2.47	57.91
9	3.75	0.323	2.38	60.74

Appendix B: Data Obtained From Long Columns Experiments Part I: Sodosol

Table B.7 K_{sat} measured with time for replicate 3 (Sodosol), tap water amended with gypsum treatment (EC \approx 1.3 dS/m) during applying water with EC = 0.1 dS/m.

Time (h)	Water head (cm)	EC in drained water (dS/m)	K_{sat} (cm/h)	Accumulated leachate (cm)
0	4.4			0.00
1.01	7.4	0.389		3.51
2.1667	7.4	0.33	2.57	7.59
3	7.7	0.1884	2.56	10.55
4.007	7.7	0.1451	2.49	14.01
6.6667	7.7	0.1201	2.39	22.80
8	7.6	0.12	2.36	27.14
9.03	7.6	0.1207	2.37	30.50
10	7.6	0.1054	2.31	33.60
11	7.6	0.1157	2.31	36.79
0	0		0.00	0.00
1	7.7	0.2205	2.36	50.52
2	7.7	0.214	2.45	53.92
3	6.9	0.1229	2.45	57.21

Table B.8 K_{sat} measured with time for replicate 4 (Sodosol), tap water amended with gypsum treatment (EC \approx 1.3 dS/m), during applying water treatment.

Time (h)	Water head (cm)	EC in drained water (dS/m)	K_{sat} (cm/h)	Accumulated leachate (cm)
0	8			0.00
1	8	2.941		2.00
2	8	1.594	3.13	6.38
3	8	1.292	2.91	10.46
4	8	1.192	2.80	14.38
5	7.5	1.17	2.81	18.23
6	7.5	1.22	2.73	21.99
7	7.5	1.228	2.74	25.76
8.5	7.5	1.145	2.71	31.36
10	0	1.202	3.71	36.92
1	7	1.214	1.24	44.23
2	7	1.183	2.46	47.56
3.083	7	1.193	2.45	51.13

Table B.9 K_{sat} measured with time for replicate 4 (Sodosol), tap water amended with gypsum treatment (EC \approx 1.3 dS/m), during applying water with EC = 0.4 dS/m.

Time (h)	Water head (cm)	EC in drained water (dS/m)	K_{sat} (cm/h)	Accumulated leachate (cm)
0	7.7			0.00
0.5	7.7	1.313		0.79
2	7.7	1.2	1.34	3.57
3	7.7	1.18	1.32	5.40
4	7.7	0.916	1.32	7.22
5	7.6	0.661	1.34	9.08
6	7.6	0.475	1.34	10.93
7	7.6	0.448	1.41	12.88
1	7.4	0.44	1.29	24.62
2	7.4	0.671	1.35	26.47
3	7.4	0.473	1.37	28.35
4	7.4	0.43	1.35	30.20
5	7.6	0.386	1.33	32.04
6	7.6	0.375	1.33	33.87
7	7.6	0.366	1.33	35.70
8	7.6	0.366	1.29	37.47
9	7.6	0.345	1.29	39.25
17.25	4.5	0.339	1.31	52.50

Table B.10 K_{sat} measured with time for replicate 4 (Sodosol), tap water amended with gypsum treatment (EC \approx 1.3 dS/m), during applying water with EC = 0.1 dS/m.

Time (h)	Water head (cm)	EC in drained water (dS/m)	K_{sat} (cm/h)	Accumulated leachate (cm)
0	7.9			0.00
1.01	7.9	0.36		1.71
2	7.9	0.363	1.23	3.42
3	7.9	0.335	1.21	5.11
5	8.2	0.265	1.16	8.39
6	8.2	0.1771	1.11	9.97
1	7.7		0.86	31.93
2	7.7		0.86	33.12
5	7.7		0.82	36.52
6	7.7		0.78	37.60
0	8.2		0.00	0.00
0.5	8.2		0.71	47.06
1	8.2		0.80	47.63

Table B.11 K_{sat} measured with time for replicate 1 (Sodosol), Diluted HSS water and amended with gypsum treatment during applying water with EC = 0.4 dS/m. The Average K_{sat} measured at the final stage of water treatment for this replicate was 2.86 cm/h.

Time (h)	Water head (cm)	EC in leachate (dS/m)	K_{sat} (cm/h)	Accumulated leachate (cm)
0	9.4			0.00
0.25	9.4			1.16
0.5	9.3		3.67	2.52
0.75	9.3		3.63	3.85
1	9.3		3.55	5.16
1.25	9.4		3.53	6.46
1.5	9.4		3.53	7.77
1.75	9.4		3.62	9.10
2	9.2		3.60	10.42
2.25	9.2		3.60	11.74
2.5	9.2		3.51	13.03
2.75	8.8		3.59	14.33
3	8.8		3.50	15.59
3.25	8.8		3.43	16.84
3.5	9		3.39	18.07
3.75	9		3.37	19.30
4	9		3.41	20.54
4.25	9		3.43	21.79
4.5	8.9		3.38	23.01
4.75	8.9		3.42	24.25
5	8.9		3.38	25.48
5.25	8.9		3.38	26.71
0	8.3			
0.25	8.3		3.43	34.35
0.5	8.2		3.62	35.63
0.75	8.2		3.68	36.93
1	8.2		3.46	38.16
1.25	8.5		3.51	39.42
1.5	8.5		3.54	40.68
1.75	8.5		3.47	41.92
2.25	8.2		3.49	43.16
2.5	8.2		3.49	44.39
2.75	8.2		3.46	45.62
3.05	8		3.50	47.09
3.25	8		3.47	48.07
3.5	8		3.42	49.27
3.75	8		3.44	50.48
4	8		3.44	51.69

Table B.12 K_{sat} measured with time for replicate 1 (Sodosol), Diluted HSS water and amended with gypsum treatment ($EC \approx 1.3$ dS/m) during applying water with $EC = 0.1$ dS/m after applying water with $EC=0.4$.

Time (h)	Water head (cm)	EC in drained water (dS/m)	K_{sat} (cm/h)	Accumulated leachate (cm)
0	7.8			0.00
0.25	7.8			0.90
0.5	7.8		2.93	1.93
0.75	7.8	0.577	2.75	2.88
1	7.8		2.93	3.91
1.25	7.8		2.95	4.94
1.5	7.8		2.95	5.97
1.75	7.8	0.4	2.93	6.99
2	8.2		2.89	8.01
2.25	8.2		2.84	9.01
2.5	8.2	0.2423	2.89	10.04
2.75	8.2		2.89	11.06
3	8.2		2.84	12.06
3.25	8.2		2.80	13.05
3.5	8.2	0.1657	2.80	14.04
3.75	8.2		2.84	15.05
4	8.2		2.80	16.04
4.25	8.2		2.82	17.04
4.5	8.2	0.1419	2.77	18.02
4.75	8.2		2.77	19.00
5	8.2		2.75	19.98
5.25	8.2		2.75	20.95
5.5	8.2	0.1334	2.77	21.94
5.75	7.9		2.80	22.92
6	7.9		2.74	23.88
6.25	7.9		2.76	24.84
6.5	7.9	0.1294	2.76	25.81
6.75	7.9		2.74	26.77
7	7.9		2.74	27.73
7.5	7.9	0.1267	2.72	29.63
7.75	7.9		2.74	30.59
8	7.9		2.69	31.53
8.25	7.9		2.76	32.50
8.5	7.9	0.1245	2.74	33.46
8.75	7.9		2.72	34.41
9	7.9		2.74	35.37
9.25	7.9		2.72	36.32
9.5	7.9	0.1214	2.74	37.28
9.75	7.9		2.74	38.24
10	8.4	0.1216	2.69	39.20

Table B.13 K_{sat} measured with time for replicate 2 (Sodosol), Diluted HSS water and amended with gypsum treatment during applying water with EC = 0.4 dS/m. The Average K_{sat} measured at the final stage of water treatment for this replicate was 2.78 cm/h.

Time (h)	Water head (cm)	EC in leachate (dS/m)	K_{sat} (cm/h)	Accumulated leachate (cm)
0	8.9			0.00
0.25	8.9	1.738		1.01
0.5	8.9	1.954	3.13	2.14
0.7517	8.9	2.026	3.07	3.25
1	8.9	2.039	3.15	4.39
1.25	8.9	2.009	3.05	5.49
1.5	8.9	1.697	3.09	6.60
1.75	8.9	1.255	3.07	7.71
2	8	0.925	2.92	8.73
2.25	8.9	0.726	3.22	9.90
2.5	8.9	0.619	2.96	10.96
2.75	8.9	0.550	3.00	12.05
3	8.9	0.512	2.96	13.12
3.25	8.9		3.00	14.20
3.5	8.9		2.92	15.26
3.7523	8.9		2.93	16.32
4	8.9	0.440	2.90	17.36
5	8.9	0.425	2.94	21.61
6	7.5	0.409	3.01	25.75
7	7.5	0.395	3.04	29.93
8	7.5	0.380	3.06	34.14
0	7.9			
0.2527	7.9	0.490		39.25
0.5	7.9	0.506	2.60	40.15
0.75	7.9	0.488	2.75	41.11
1	7.9	0.482	2.75	42.06
1.25	7.9	0.485	2.79	43.04
1.5	7.9	0.497	2.79	44.01
1.7525	7.9	0.495	2.81	45.00
2	7.9	0.483	2.96	46.03
2.25	7.9	0.456	2.70	46.97
2.5	7.9	0.440	2.70	47.91

Appendix B: Data Obtained From Long Columns Experiments Part I: Sodosol

Table B.14 K_{sat} measured with time for replicate 2 (Sodosol), Diluted HSS water and amended with gypsum treatment ($EC \approx 1.3$ dS/m) during applying water with $EC = 0.1$ dS/m after applying water with $EC=0.4$.

Time (h)	Water head (cm)	EC in drained water (dS/m)	K_{sat} (cm/h)	Accumulated leachate (cm)
0	7.7			0.00
0.25	7.7	0.463		0.63
0.5	7.7	0.478	2.13	1.37
0.75	7.7	0.477	2.13	2.11
1	7.7	0.475	2.09	2.83
2	7.7	0.469	2.11	5.75
3	7.1	0.338	2.14	8.65
4	8	0.217	2.07	11.55
5	8	0.164	2.07	14.44
6	8	0.143	2.08	17.35
7	8	0.132	2.03	20.18
8	8	0.126	2.03	23.03
9	8	0.124	2.05	25.90
0				
0.5	7.4	0.139		30.14
1	7.4	0.129	2.16	31.62
2	7.4	0.129	2.13	34.54
3	7.4	0.126	2.09	37.41
4	6	0.125	2.10	40.14

Table B.15 K_{sat} measured with time for replicate 3 (Sodosol), Diluted HSS water and amended with gypsum treatment during applying water treatment.

Time (h)	Water head (cm)	EC in leachate (dS/m)	K_{sat} (cm/h)	Accumulated leachate (cm)
0	7.8			0.00
1	7.8	3.05		2.39
2	7.8	1.709	4.22	8.25
3	7.8	1.531	4.00	13.82
4	7.6	1.56	3.95	19.27
5	7.6	1.568	3.78	24.48
6	7.6	1.565	3.76	29.67
7	7.6	1.519	3.70	34.77
8	7.6	1.565	3.70	39.87
9	7.7	1.565	3.57	44.81
10	7.35	1.549	3.64	49.80

Table B.16 K_{sat} measured with time for replicate 3 (Sodosol), Diluted HSS water and amended with gypsum treatment during applying water with EC = 0.4 dS/m.

Time (h)	Water head (cm)	EC in drained water (dS/m)	K_{sat} (cm/h)	Accumulated leachate (cm)
0	7.2			0.00
1	7.2	1.617		2.96
2	7.2	1.5	2.25	6.02
3	7.6	0.893	2.19	9.05
5.5	7.6	0.469	1.90	15.59
6	7.6	0.406	2.11	17.04
7	7.6	0.395	2.17	20.03
0	0		0.00	0.00
1	7.5	0.453	2.30	32.83
2	7.5	0.451	2.55	36.33
3	7.5	0.366	2.47	39.73
4.02	7.5	0.357	2.33	43.00
6	7.5	0.367	2.37	49.46
7	7.5	0.363	2.34	52.68
8	6.3	0.351	2.38	55.81

Table B.17 K_{sat} measured with time for replicate 3 (Sodosol), Diluted HSS water and amended with gypsum treatment (EC \approx 1.3 dS/m) during applying water with EC = 0.1 dS/m after applying water with EC=0.4.

Time (h)	Water head (cm)	EC in drained water (dS/m)	K_{sat} (cm/h)	Accumulated leachate (cm)
0	7.3			0.00
1.01	7.3	0.391		3.69
2.167	7.8	0.322	2.64	7.93
3	7.8	0.1879	2.73	11.09
4	7.8	0.1462	2.66	14.79
6.667	7.4	0.1186	2.63	24.40
8	7.4	0.1185	3.37	29.01
9.03	7.4	0.1139	2.51	32.55
10	7.4	0.1137	2.47	35.83
0				
1	7.8	0.145	2.39	50.76
2	7.8	0.1287	2.57	54.32

Table B.18 K_{sat} measured with time for replicate 4 (Sodosol), Diluted HSS water and amended with gypsum treatment during applying water treatment.

Time (h)	Water head (cm)	EC in leachate (dS/m)	K_{sat} (cm/h)	Accumulated leachate (cm)
0	7.7			0.00
1	7.7	2.634		2.72
2	7.7	1.580	3.50	7.56
3	7.7	1.458	3.27	12.09
4	7.7	1.436	3.14	16.44
5	7.9	1.452	2.98	20.60
6	7.9	1.461	3.00	24.79
7	7.9	1.472	2.96	28.92
0				
0.5	7	1.559		41.97
1	7	1.652	2.38	43.57
2	7	1.674	2.37	46.77
3.083	7	1.582	2.34	50.19

Table B.19 K_{sat} measured with time for replicate 4 (Sodosol), Diluted HSS water and amended with gypsum treatment during applying water with EC = 0.4 dS/m.

Time (h)	Water head (cm)	EC in drained water (dS/m)	K_{sat} (cm/h)	Accumulated leachate (cm)
0	7.3			0.00
0.5	7.3	1.751		1.07
2	7.3	1.491	2.03	5.23
3	7.3	0.996	1.96	7.91
4	7.1	0.714	1.86	10.42
5	7.1	0.520	1.89	12.98
6	7.1	0.454	1.78	15.40
7	7.1	0.423	1.79	17.82
0				
1	7.8	0.526	1.09	32.04
2	7.8	0.537	1.12	33.60
3	7.8	0.546	1.11	35.14
4	7.8	0.522	1.10	36.67
5	7.8	0.477	1.07	38.17
6	7.8	0.425	1.05	39.62
7	7.8	0.414	1.04	41.07
8	7.8	0.394	1.02	42.48
9	7.8	0.386	1.01	43.88
17.25	7.5	0.374	0.97	54.93

Table B.20 K_{sat} measured with time for replicate 4 (Sodosol), Diluted HSS water and amended with gypsum treatment ($EC \approx 1.3$ dS/m) during applying water with $EC = 0.1$ dS/m after applying water with $EC=0.4$.

Time (h)	Water head (cm)	EC in drained water (dS/m)	K_{sat} (cm/h)	Accumulated leachate (cm)
0	7.9			0.00
1.01	7.9	0.480		1.62
2	7.9	0.387	1.17	3.23
3	7.9	0.345	1.13	4.80
5	8.2	0.279	1.04	7.73
6	8.2	0.214	0.96	9.09
0				
1	7.7	0.126		27.73
2	7.7	0.124	0.64	28.61
5	7.7	0.130	0.62	31.18
6	7.7	0.133	0.60	32.01
0				
0.5	8.200			46.75
1	8.2		0.49	47.09

Table B.21 K_{sat} measured with time for replicate 1 (Sodosol), HSS water amended with sulphuric acid to reduce pH at 5 treatment during applying water with $EC = 0.4$ dS/m. The Average K_{sat} measured at the final stage of water treatment for this replicate was 0.24 cm/h.

Time (h)	Water head (cm)	EC in drained water (dS/m)	K_{sat} (cm/h)	Accumulated leachate (cm)
0	7.1			0.00
1	7.1		0.03	0.04
2	7.1		0.03	0.08
3	7.1		0.02	0.10
5	7.1		0.02	0.17
7	7.1		0.01	0.20
10	7.1		0.01	0.25
23	7.1		0.01	0.35
33	7.1		0.00	0.39
48	7.1		0.00	0.42
80	7.1		0.00	0.42

Table B.22 K_{sat} measured with time for replicate 2 (Sodosol), HSS water amended with sulphuric acid to reduce pH at 5 treatment during applying water with EC = 0.4 dS/m. The Average K_{sat} measured at the final stage of water treatment for this replicate was 0.25 cm/h.

Time (h)	Water head (cm)	EC in drained water (dS/m)	K_{sat} (cm/h)	Accumulated leachate (cm)
0	8.1			0.00
14.5	8.1			0.12
17.5	8.1		0.01	0.15
20.5	8.1		0.00	0.16
24.5	8.1		0.00	0.17
34.5	8.1		0.00	0.20
Water with EC = 0.4 added HSS water pH= 5 treatment (falling head method)				
Time (h)	K_{sat} (cm/h)			
0				
2	0.00352			
4	0.00289			
6	0.00280			
8	0.00302			
23	0.00213			

Table B.23 K_{sat} measured with time for replicate 3 (Sodosol), HSS water amended with sulphuric acid to reduce pH at 5 treatment during applying water treatment.

Time (h)	Water head (cm)	EC in leachate (dS/m)	K_{sat} (cm/h)	Accumulated leachate (cm)
0	7.4			0.00
1	7.4	4.91		4.04
2	7.4	4.35	4.11	9.67
3	7.4	4.3	3.33	14.23
4	10	4.38	2.50	17.98
5	7.7	4.23	2.12	20.91
6	7.7	4.32	1.78	23.37
7	7.7	4.27	1.50	25.45
8	7.7	4.27	1.32	27.28
9	7.7	4.25	1.16	28.89
10	7.7	4.31	1.04	30.34
11	7.7		0.96	31.67
12	7.7		0.89	32.90
20	7.8		0.61	39.68
22	7.8		0.49	41.03
24	7.8		0.44	42.26
26	7.8		0.40	43.36
28	7.8		0.36	44.36
30	7.8		0.32	45.26
33	7.8		0.30	46.51
45.55	7.8		0.25	50.94

Table B.24 K_{sat} measured with time for replicate 3 (Sodosol), HSS water amended with sulphuric acid to reduce pH at 5 treatment during applying water with EC = 0.4 dS/m.

Time (h)	Water head (cm)	EC in leachate (dS/m)	K_{sat} (cm/h)	Accumulated leachate (cm)
0	8.1	EC in whole drained water 5.29		0.00
2	8.1		0.03300	0.09
6	8.1		0.01762	0.19
10	8.1		0.00559	0.22
22	8.1		0.00140	0.25
46	8.1		0.00224	0.32
70	8.1		0.00098	0.36
96	8.1		0.00120	0.40
144	8.1		0.00112	0.47
169	8.1		0.00116	0.52
Water with EC = 0.4 added HSS water pH= 5 treatment (falling head method)				
Time (h)	K_{sat} (cm/h)			
0	0			
4	0.025913736			
23	0.022320104			
27.6	0.018792304			
48	0.022883204			
96	0.007729955			

Table B.25 K_{sat} measured with time for replicate 4 (Sodosol), HSS water amended with sulphuric acid to reduce pH at 5 treatment during applying water treatment.

Time (h)	Water head (cm)	EC in drained water (dS/m)	K_{sat} (cm/h)	Accumulated leachate (cm)
0	7.6			0.00
1	7.6	5.440		2.09
2	7.6	4.180	3.20645	6.52
3	7.6	4.130	2.85334	10.45
4	7.6	4.120	2.58566	14.02
5	7.6	4.040	2.32368	17.23
6	7.5	4.150	2.11492	20.14
7	7.5	3.970	1.89771	22.75
8.5	7.5	4.160	1.67669	26.20
10	7.5	4.160	1.51284	29.32
0				
1	7			39.96
2	7		0.06637	40.05
3	7		0.07685	40.15
9	7	4.310	0.06889	40.71
22	7	4.400	0.06091	41.78
30	7	4.550	0.06841	42.52
198	7	4.780	0.02367	47.89
332	7.3	4.790	0.01018	49.75
500	7.3	4.850	0.00679	51.31

Appendix B: Data Obtained From Long Columns Experiments Part I: Sodosol

Table B.26 K_{sat} measured with time for replicate 1 (Sodosol), HSS water amended with sulphuric acid to reduce pH at 7 treatment during applying water with EC = 0.4 dS/m. The Average K_{sat} measured at the final stage of water treatment for this soil replicate was 0.27 cm/h.

Time (h)	Water head (cm)	EC in drained water (dS/m)	K_{sat} (cm/h)	Accumulated leachate (cm)
0	8.1			0.00
1	8.1		0.01678	0.02
2	8.1		0.02238	0.06
3	8.1		0.02238	0.09
5	8.1		0.02517	0.16
7	8.1		0.01678	0.20
10	8.1		0.01305	0.26
23	8.1		0.00688	0.39
33	8.1		0.00392	0.44
48	8.1		0.00224	0.49
80	8.1		0.00052	0.51

Table B.27 K_{sat} measured with time for replicate 2 (Sodosol), HSS water amended with sulphuric acid to reduce pH at 7 treatment during applying water with EC = 0.4 dS/m. The Average K_{sat} measured at the final stage of water treatment for this replicate was 0.24 cm/h.

Time (h)	Water head (cm)	EC in drained water (dS/m)	K_{sat} (cm/h)	Accumulated leachate (cm)
0	8.1			0.00
14.5	8.1		0.00331	0.06
17.5	8.1		0.00892	0.10
20.5	8.1		0.00707	0.13
24.5	8.1		0.00614	0.17
34.5	8.1		0.00469	0.23
Water with EC = 0.4 added HSS water pH= 5 treatment (falling head method)				
Time (h)	K_{sat} (cm/h)			
0				
2	0.00466			
4	0.00414			
6	0.00438			
8	0.00281			

Table B.28 K_{sat} measured with time for replicate 3 (Sodosol), HSS water amended with sulphuric acid to reduce pH at 7 treatment during applying water treatment.

Time (h)	Water head (cm)	EC in leachate (dS/m)	K_{sat} (cm/h)	Accumulated leachate (cm)
0	7.5			0.00
1	7.5	4.48		3.01
2	7.5	3.92	3.927	8.41
3	7.5	3.79	3.110	12.69
4	7.5	4.04	2.509	16.14
5	7.4	4.02	1.973	18.84
6	7.4	3.98	1.624	21.06
7	7.4	4	1.474	23.08
8	7.4	3.98	1.182	24.70
9	7.4	4.04	1.050	26.14
10	7.4	4.04	0.935	27.42
11	7.4		0.849	28.59
12	7.4	3.99	0.786	29.66
20	7.2	3.98	0.561	35.76
22	7.2	4.06	0.445	36.97
24	7.2	4.08	0.416	38.10
26	7.2	4.06	0.373	39.12
28	7.2	4.08	0.329	40.01
30	7.2	4.06	0.295	40.81
33	7.2	4.12	0.266	41.90
45.55	7.2	4.02	0.218	45.62

Table B.29 K_{sat} measured with time for replicate 3 (Sodosol), HSS water amended with sulphuric acid to reduce pH at 7 treatment during applying water with EC = 0.4 dS/m.

Time (h)	Water head (cm)	EC in leachate (dS/m)	K_{sat} (cm/h)	Accumulated leachate (cm)
0	8.1			0.00
2	8.1		0.03133	0.09
6	8.1		0.02238	0.21
10	8.1		0.00727	0.25
22	8.1		0.00158	0.28
46	8.1		0.00247	0.36
70	8.1		0.00135	0.41
96	8.1		0.00069	0.44
144	8.1		0.00082	0.49
169	8.1		0.00112	0.53
Water with EC = 0.4 added HSS water pH= 7 treatment (falling head method)				
Time (h)	K_{sat} (cm/h)	Accumulated leachate (cm)		
0	0.00000	0.00		
4	0.00119	0.01		
23	0.00089	0.04		
27.6	0.00091	0.01		
48	0.00086	0.04		
96	0.00017	0.02		

Table B.30 K_{sat} measured with time for replicate 4 (Sodosol), HSS water amended with sulphuric acid to reduce pH at 7 treatment during applying water treatment.

Time (h)	Water head (cm)	EC in leachate (dS/m)	K_{sat} (cm/h)	Accumulated leachate (cm)
0	7.5			0.00
1	7.5	5.050		1.86
2	7.5	3.790	3.0466	6.05
3	7.5	3.860	2.7208	9.79
4	7.5	3.790	2.4750	13.20
5	7.5	3.790	2.2121	16.24
6	7.6	3.880	1.9649	18.95
7	7.6	3.860	1.7542	21.37
8.5	7.6	3.910	1.4998	24.47
10	7.6	3.740	1.3099	27.19
0				
1	7.6			36.19
2	7.6			36.19
3	7.6		0.0296	36.23
9	7.6		0.0256	36.44
22	7.6		0.0215	36.82
30	7.6		0.0164	37.00
198	7.6	4.550	0.0096	39.22
332	7.6	4.680	0.0065	40.42
634	7.6	5.260	0.0029	41.62

Table B.31 K_{sat} measured with time for replicate 1 (Sodosol), natural HSS water having pH 8.36 treatment during applying water with EC = 0.4 dS/m. The Average K_{sat} measured at the final stage of water treatment for this soil replicate was 0.34 cm/h.

Time (h)	Water head (cm)	EC in drained water (dS/m)	K_{sat} (cm/h)	Accumulated leachate (cm)
0	8			0.00
1	8		0.04478	0.06
2	8		0.05598	0.14
3	8		0.04478	0.20
5	8		0.03359	0.30
7	8		0.02239	0.36
10	8		0.01493	0.42
23	8		0.00689	0.55
33	8		0.00392	0.61
48	8		0.00299	0.67
80	8		0.00175	0.75

Table B.32 K_{sat} measured with time for replicate 2 (Sodosol), natural HSS water having pH 8.36 treatment during applying water with EC = 0.4 dS/m. The Average K_{sat} measured at the final stage of water treatment for this soil replicate was 0.30 cm/h.

Time (h)	Water head (cm)	EC in drained water (dS/m)	K_{sat} (cm/h)	Accumulated leachate (cm)
0	8			0.00
14.5	8		0.02325	0.44
17.5	8		0.01345	0.50
20.5	8		0.01345	0.55
24.5	8		0.00589	0.59
34.5	8		0.00460	0.65

Falling head method	
Water with EC = 0.4 added HSS water pH= 5 treatment (falling head method)	
Time (h)	K_{sat} (cm/h)
0	
2	0.00478
4	0.00487
6	0.00403
8	0.00435

Appendix B: Data Obtained From Long Columns Experiments Part I: Sodosol

Table B.33 K_{sat} measured with time for replicate 3 (Sodosol), natural HSS water having pH = 8.6 treatment during applying water treatment.

Time (h)	Water head (cm)	EC in leachate (dS/m)	K_{sat} (cm/h)	Accumulated leachate (cm)
0	7.6			0.00
1	7.6			1.74
2	7.6	3.32	2.910	5.76
3	7.6	3.43	2.426	9.11
4	7.6	3.49	2.062	11.95
5	7.6	3.56	1.692	14.29
6	7.6	3.48	1.458	16.30
7	8.1	3.43	1.242	18.05
8	8.1	3.59	1.085	19.57
9	8.1	3.62	0.979	20.95
10	8.1	3.57	0.895	22.20
11	8.1	3.64	0.828	23.37
12	8.1	3.63	0.772	24.45
20	8.1	3.71	0.559	30.74
22	8.1	3.68	0.515	32.18
24	8.1	3.71	0.498	33.58
26	8.1	3.8	0.464	34.89
28	8.1	3.85	0.428	36.09
30	8.1	3.85	0.397	37.21
33	8.1	3.79	0.369	38.76
45.55	8.1	3.98	0.324	44.48
61	6.3	3.75	0.261	49.78

Table B.34 K_{sat} measured with time for replicate 3 (Sodosol), natural HSS water having pH = 8.6 treatment during applying water with EC = 0.4 dS/m.

Time (h)	Water head (cm)	EC in leachate (dS/m)	K_{sat} (cm/h)	Accumulated leachate (cm)
0	7.8			0.00
2	7.8		0.06785	0.19
6	7.8		0.03336	0.37
10	7.8		0.01244	0.44
22	7.8		0.00377	0.51
46	7.8		0.00339	0.62
70	7.8		0.00198	0.69
96	7.8		0.00178	0.75
144	7.8		0.00151	0.85
169	7.8		0.00154	0.90
Water with EC = 0.4 added natural HSS water pH=8.6 treatment (falling head method)				
Time (h)	K_{sat} (cm/h)		Accumulated leachate (cm)	
0	0.00000		0.00	
4	0.00133		0.01	
23	0.00118		0.05	
27.6	0.00108		0.01	
48	0.00124		0.05	
96	0.00041		0.05	

Table B.35 K_{sat} measured with time for replicate 4 (Sodosol), natural HSS water having pH = 8.6 treatment during applying water treatment.

Time (h)	Water head (cm)	EC in leachate (dS/m)	K_{sat} (cm/h)	Accumulated leachate (cm)
0	8.4			0.00
1	8.4	4.330		2.39
2	8.4	3.170	2.95562	6.59
3	8.4	3.230	2.66780	10.37
4	8.4	3.310	2.38553	13.76
5	8.4	3.330	2.10878	16.76
6	8.7	3.520	1.87314	19.44
7	8.7	3.430	1.70883	21.90
8.5	8.7	3.480	1.52991	25.19
10	8.7	3.480	1.38386	28.17
0				
1	8.6			37.76
2	8.6		0.09673	37.90
3	8.6		0.11212	38.06
9	8.6	3.740	0.08794	38.82
22	8.6	3.820	0.09470	40.58
30	8.6	3.940	0.10718	41.80
198	0	4.080	0.02901	46.68
0				
134	8.5	4.150	0.03927	54.18
302	8.5	4.310	0.03526	62.62

B.3 Part II: Vertosol columns experiment results

Table B.36 K_{sat} measured with time for replicate 1(Vertosol), tap water amended with gypsum treatment (EC = 1.3 dS/m) during applying water with EC = 0.4 dS/m. The Average K_{sat} measured at the final stage of water treatment for this soil column (this replicate) was 3.84 cm/h.

Time (h)	Water head (cm)	EC in leachate (dS/m)	K_{sat} (cm/h)	Accumulated leachate (cm)
0	9.1			0.00
0.25	9.1		3.11	1.13
0.5	9.1		2.33	1.98
0.75	8.6		2.40	2.84
1	8.6		2.29	3.65
1.25	8.6		2.22	4.45
1.5	8.6		2.15	5.22
1.75	8.6		2.15	5.99
2	8.6		2.11	6.74
2.25	8.6		2.11	7.50
2.5	8.6		2.11	8.25
2.75	8.6		2.15	9.02
3	8.6		2.11	9.78
3.25	8.6		2.07	10.52
3.5	8.7		2.13	11.28
3.75	8.7		2.08	12.03
4	8.7		2.08	12.77
4.25	8.7		2.08	13.52
4.5	8.7		2.04	14.25
4.75	8.8		2.07	15.00
5	8.8		2.10	15.75
5.25	8.8		2.07	16.50
5.5	8.8		2.03	17.23
5.75	8.8		2.01	17.95
6	8.8		2.03	18.68
6.25	8.8		2.05	19.42
0.000	8.7			
0.250	8.7		1.77	21.41
0.500	8.7		2.10	22.16
0.750	8.7		2.06	22.90
1.000	8.7		1.97	23.61
1.250	8.9		1.94	24.31
1.500	8.9		1.94	25.01
1.750	8.9		1.94	25.71
2.250	8.9		1.91	26.40
2.500	8.9		1.89	27.08
2.750	8.9		1.89	27.77
3.050	8.9		1.85	28.57
3.250	8.9		1.88	29.11
3.500	8.9		1.85	29.78
3.750	8.9		1.83	30.44
4.000	8.9		1.81	31.09
4.257	9.2		1.80	31.77

Appendix B: Data Obtained From Long Columns Experiments Part II: Vertosol

Continue in Table B.36

Time (h)	Water head (cm)	EC in leachate (dS/m)	K_{sat} (cm/h)	Accumulated leachate (cm)
4.500	9.2		1.86	32.43
4.750	9.2		1.81	33.09
5.000	9.2		1.81	33.75
5.250	9.2		1.81	34.41
5.500	9.2		1.79	35.06
5.750	8.7		1.82	35.71
6.000	8.7		1.77	36.35
6.255	8.7		1.76	36.99
6.513	8.7		1.76	37.65
6.750	8.7		1.73	38.24
7.000	8.7		1.75	38.87
7.250	8.7		1.77	39.50
7.500	8.7		1.75	40.13
7.750	8.7		1.75	40.76
8.000	8.7		1.73	41.38
8.250	8.7		1.75	42.01
8.500	8.7		1.71	42.62
8.750	8.6		1.74	43.24
9.000	8.6		1.71	43.86
9.250	8.6		1.71	44.47

Table B.37 K_{sat} measured with time for replicate 1 (Vertosol), tap water amended with gypsum treatment (EC ≈ 1.3 dS/m) during applying water with EC = 0.1 dS/m after applying water with EC=0.4.

Time (h)	Water head (cm)	EC in drained water (dS/m)	K_{sat} (cm/h)	Accumulated leachate (cm)
0	8.2			0.00
0.25	8.2		1.71	0.61
0.5	8.2		1.60	1.17
0.75	8.2	0.488	1.63	1.74
1	8.2		1.60	2.31
1.25	8.2		1.60	2.88
1.5	8.2		1.60	3.44
1.75	8.2	0.573	1.58	4.00
2	8.2		1.60	4.57
2.25	8.2		1.58	5.12
2.5	8.2	0.53	1.60	5.69
2.75	8.2		1.56	6.24
3	8.2		1.56	6.79
3.25	8.2		1.56	7.34
3.5	8.2	0.42	1.54	7.88
3.75	8.2		1.56	8.43
4	8.2		1.56	8.98
4.25	8.2		1.54	9.53
4.5	8.2	0.337	1.51	10.06
4.75	8.2		1.54	10.60
5	8.2		1.54	11.14
5.25	8.2		1.54	11.69

Appendix B: Data Obtained From Long Columns Experiments Part II: Vertosol

Continue in Table B37

Time (h)	Water head (cm)	EC in drained water (dS/m)	K_{sat} (cm/h)	Accumulated leachate (cm)
5.5	8.2	0.288	1.54	12.23
5.75	8.2		1.51	12.76
6	8.2		1.51	13.30
6.25	8.2		1.47	13.82
6.5	8.2	0.257	1.49	14.34
6.75	8.2		1.47	14.86
7	8.2		1.49	15.39
7.5	8.2	0.2453	1.47	16.43
7.75	8.2		1.47	16.95
8	8.2		1.45	17.46
8.25	8.2		1.45	17.97
8.5	8.2	0.2317	1.45	18.48
8.75	8.2		1.42	18.98
9	8.2		1.42	19.48
9.25	8.2	0.225	1.42	19.99
9.5	8.2		1.45	20.50
9.75	8.2		1.45	21.01
10	8.2	0.2209	1.45	21.52
0.00	8.1			
0.25	8.1		1.27	21.97
0.50	8.1	0.2452	1.30	22.42
0.75	8.1	0.2353	1.39	22.91
1.00	8.1		1.34	23.38
1.25	8.1		1.34	23.85
1.50	8.1	0.2291	1.36	24.33
1.75	8.1		1.36	24.81
2.00	8.1		1.34	25.28
2.25	8.1		1.39	25.77
2.50	8.1	0.2293	1.34	26.24
2.75	8.1		1.34	26.71
3.00	8.1		1.36	27.19
3.25	8.1		1.34	27.67
3.50	8.1	0.2217	1.36	28.14
3.75	8.1		1.34	28.62
4.00	8.1		1.34	29.09
4.50	8.3	0.2175	1.31	30.02
4.75	8.3		1.33	30.49
5.00	8.3	0.2155	1.33	30.96
5.25	8.3		1.31	31.42
5.50	8.3	0.2117	1.31	31.89
5.75	8.3		1.33	32.36
6.00	8.3		1.31	32.82
6.25		0.2032		
6.50	8.3		1.29	33.73
7.50	8.3	0.1993	1.30	35.57
8.70	8.3	0.1942	1.26	37.71
9.00	8.3	0.1903	1.33	38.28
9.25	8.3		1.24	38.72

Appendix B: Data Obtained From Long Columns Experiments Part II: Vertosol

Table B.38 K_{sat} measured with time for replicate 2 (Vertosol), tap water amended with gypsum treatment (EC ≈ 1.3 dS/m), during applying water with EC = 0.4 dS/m. The Average K_{sat} measured at the final stage of water treatment for this replicate was 3.84 cm/h.

Time (h)	Water head (cm)	EC in leachate (dS/m)	K_{sat} (cm/h)	Accumulated leachate (cm)
0	9.5			0.00
0.25	9.5	1.593		0.61
0.5	9.5	1.731	1.83	1.29
0.75	9.5	1.740	1.83	1.96
1	9.5	1.717	1.90	2.66
1.25	9.5	1.755	1.81	3.33
1.5	9.5	1.738	1.83	4.01
1.75	9.5	1.761	1.83	4.68
2	9.5	1.716	1.79	5.34
2.25	9.5	1.702	1.79	6.00
2.5	9.5	1.607	1.83	6.68
2.75	9	1.443	1.91	7.37
3	9	1.286	1.86	8.05
3.25	9		1.89	8.73
3.5	9		1.86	9.41
3.7523	9		1.89	10.10
4	9	0.800	1.84	10.76
5	9	0.659	1.87	13.47
6	9	0.538	1.88	16.19
7	9	0.504	1.87	18.90
8	9	0.474	1.83	21.56
9	9	0.462	1.83	24.21
0	8.6			
0.2527	8.6	0.551		24.79
0.5	8.6	0.590	1.62	25.36
0.75	8.6	0.572	1.67	25.96
1	8.6	0.574	1.67	26.56
1.25	8.6	0.556	1.69	27.16
1.5	8.6	0.563	1.69	27.77
1.7525	8.6	0.560	1.65	28.36
2.017	8.6	0.563	1.70	29.01
2.25	8.6	0.567	1.70	29.58
2.5	8.6	0.574	1.69	30.18
3	8.6	0.580	1.67	31.38
4	8.6	0.548	1.66	33.75
5	8.6	0.489	1.68	36.15
7	8.6	0.446	1.68	40.94
8	8.6	0.442	1.67	43.33
9	8.6	0.437	1.70	45.76

Appendix B: Data Obtained From Long Columns Experiments Part II: Vertosol

Table B.39 K_{sat} measured with time for replicate 2 (Vertosol), tap water amended with gypsum treatment (EC ≈ 1.3 dS/m), during applying water with EC = 0.1 dS/m after applying water with EC=0.4.

Time (h)	Water head (cm)	EC in drained water (dS/m)	K_{sat} (cm/h)	Accumulated leachate (cm)
0	8.5			0.00
0.25	8.5	0.478		0.42
0.5	8.5	0.553	1.43	0.93
0.75	8.5		1.41	1.43
1	8.5	0.526	1.39	1.93
2	8.5	0.540	1.36	3.87
3	8.5	0.500	1.38	5.83
4	9	0.418	1.34	7.78
5	9	0.343	1.34	9.73
6	9	0.283	1.34	11.67
7	9	0.250	1.33	13.60
8	9	0.226	1.33	15.54
9	9	0.216	1.32	17.46
0				
0.5	8.7	0.216		20.38
1	8.7	0.204	1.40	21.39
2	8.7	0.196	1.45	23.46
3	8.7	0.196	1.41	25.49
4	8.5	0.194	1.42	27.52
5	8.5	0.186	1.41	29.53
6	8.5	0.179	1.41	31.54
7	8.5	0.186	1.43	33.58
8	8.5	0.171	1.41	35.59
9	8.5	0.170	1.42	37.61
10	8.5	0.164	1.42	39.64

Appendix B: Data Obtained From Long Columns Experiments Part II: Vertosol

Table B.40 K_{sat} measured with time for replicate 3 (Vertosol), tap water amended with gypsum treatment (EC ≈ 1.3 dS/m), during applying water treatment.

Time (h)	Water head (cm)	EC in leachate (dS/m)	K_{sat} (cm/h)	Accumulated leachate (cm)
0	7.6			0.00
1	7.4	2.101		1.90
2	7.4	1.391	3.28	6.40
3	7.4	1.255	3.04	10.56
4	7.4	1.201	2.98	14.65
5	7.7	1.186	2.84	18.58
6	7.7	1.168	2.88	22.56
7	7.7	1.167	2.85	26.51
8	7.7	1.177	2.84	30.44
9	7.7	1.169	2.79	34.30
10	7.7	1.147	2.63	37.94
11	7.7	1.162	2.72	41.71

Table B.41 K_{sat} measured with time for replicate 3 (Vertosol), tap water amended with gypsum treatment (EC ≈ 1.3 dS/m), during applying water with EC = 0.4 dS/m.

Time (h)	Water head (cm)	EC in drained water (dS/m)	K_{sat} (cm/h)	Accumulated leachate (cm)
0	7.4			0.00
1	7.4	1.269		2.29
2	7.4	1.237	1.86	4.84
3	7.4	1.118	1.88	7.42
5.5	7.4	0.634	1.72	13.30
6	7.4	0.481	1.84	14.56
7	7.4	0.455	1.87	17.12
8	7.4	0.432	1.82	19.62
9	7.4	0.414	1.80	22.08
10	6.95	0.392	1.79	24.49
11	5.3	0.392	1.75	26.71
0				
1	6.9	0.409	1.62	32.59
2	6.9	0.484	1.74	34.93
3	7.1	0.5	1.74	37.29
4.02	7.1	0.463	1.76	39.71
6	7.1	0.421	1.80	44.56
7	7.1	0.406	1.78	46.97
8	5.3	0.393	1.91	49.39

Appendix B: Data Obtained From Long Columns Experiments Part II: Vertosol

Table B.42 K_{sat} measured with time for replicate 3 (Vertosol), tap water amended with gypsum treatment (EC \approx 1.3 dS/m) during applying water with EC = 0.1 dS/m.

Time (h)	Water head (cm)	EC in drained water (dS/m)	K_{sat} (cm/h)	Accumulated leachate (cm)
0	7.7			0.00
1	7.7	0.461	2.01	2.79
2.167	7.7	0.441	1.98	6.00
3	7.8	0.346	1.97	8.28
4.001	7.8	0.288	1.93	10.96
6.6667	7.8	0.2391	1.89	17.97
8	7.8	0.2069	1.68	21.08
9.03	7.8	0.1954	1.81	23.67
10	7.8	0.1871	1.78	26.08
0	0		0.00	0.00
1	8.1	0.202	1.61	44.39
2	8.1	0.198	1.82	46.95
3	8.1	0.179	1.81	49.50

Table B.43 K_{sat} measured with time for replicate 4 (Vertosol), tap water amended with gypsum treatment (EC \approx 1.3 dS/m), during applying water treatment.

Time (h)	Water head (cm)	EC in leachate (dS/m)	K_{sat} (cm/h)	Accumulated leachate (cm)
0	7.9			0.00
1	7.9	2.357		0.92
2	7.9	1.459	2.30	4.13
3	7.9	1.232	2.06	6.99
4	7.9	1.198	1.94	9.71
5	7.9	1.171	1.90	12.36
6	7.9	1.152	1.87	14.96
7	8.1	1.142	1.82	17.53
8.5	8.1	1.157	1.80	21.33
10	8.1	1.105	1.81	25.14
0				
1	7.6	1.473	0.72	41.90
2	7.6	1.491	1.42	43.86
3.083	7.6	1.487	1.42	45.99
5.333	7.6	1.424	1.41	50.36

Appendix B: Data Obtained From Long Columns Experiments Part II: Vertosol

Table B.44 K_{sat} measured with time for replicate 4 (Vertosol), tap water amended with gypsum treatment (EC ≈ 1.3 dS/m), during applying water with EC = 0.4 dS/m.

Time (h)	Water head (cm)	EC in drained water (dS/m)	K_{sat} (cm/h)	Accumulated leachate (cm)
0	7.7			0.00
0.5	7.7			0.55
2	7.7	1.442	1.18	3.01
3	7.7	1.434	1.16	4.62
4	7.7	1.292	1.13	6.19
5	7.6	1.088	1.14	7.77
6	7.5	0.900	1.07	9.25
7	7.5	0.736	1.10	10.76
0				
1	7.5	0.650	1.02	31.41
2	7.5	0.641	1.14	32.99
3	7.5	0.653	1.14	34.56
4	7.5	0.634	1.14	36.13
5	7.5	0.606	1.14	37.69
6	7.7	0.559	1.12	39.25
7	7.7	0.509	1.13	40.82
8	7.7	0.490	1.10	42.35
9	7.7	0.462	1.11	43.89
17.25	6.65	0.431	1.11	56.11

Table B.45 K_{sat} measured with time for replicate 4 (Vertosol), tap water amended with gypsum treatment (EC ≈ 1.3 dS/m) during applying water with EC = 0.1 dS/m.

Time (h)	Water head (cm)	EC in drained water (dS/m)	K_{sat} (cm/h)	Accumulated leachate (cm)
0	7.5			0.00
1.01	7.5	0.585		1.55
2	7.5	0.485	1.20	3.18
3	7.5	0.479	1.17	4.79
5	7.4	0.403	1.16	7.99
6	7.4	0.319	1.12	9.53
1	7.3	0.194	0.90	32.40
2	7.3	0.186	0.92	33.66
5	7.3	0.191	0.92	37.43
6	7.3	0.190	0.90	38.66
0	7.3			
0.5	7.300	0.266	0.88	47.36
1	7.3	0.259	0.99	48.04

Appendix B: Data Obtained From Long Columns Experiments Part II: Vertosol

Table B.46 K_{sat} measured with time for replicate 1 (Vertosol), Diluted HSS water and amended with gypsum treatment during applying water with EC = 0.4 dS/m. The Average K_{sat} measured at the final stage of water treatment for this soil s replicate was 2.11 cm/h.

Time (h)	Water head (cm)	EC in leachate (dS/m)	K_{sat} (cm/h)	Accumulated leachate (cm)
0	9.5			0.00
0.25	9.5			0.65
0.50	9.5		2.13	1.44
0.75	9.5		2.09	2.21
1.00	9.4		2.14	2.99
1.25	9.4		2.05	3.75
1.50	9.4		2.03	4.50
1.75	9.4		2.03	5.24
2.00	9.4		1.92	5.95
2.25	9.4		1.99	6.68
2.50	9.4		1.97	7.40
2.75	9.4		1.95	8.12
3.00	9.4		1.90	8.82
3.25	9.4		1.90	9.52
3.50	9.4		1.88	10.21
3.75	8.9		1.91	10.90
4.00	8.9		1.89	11.58
4.25	8.9		1.89	12.27
4.50	8.9		1.85	12.94
4.75	8.9		1.85	13.60
5.00	8.9		1.83	14.26
5.25	8.9		1.81	14.92
5.50	8.9		1.83	15.58
5.75	8.9		1.81	16.23
6.00	8.9		1.83	16.89
6.25	8.9		1.81	17.54
0	8.9			
0.25	8.9		1.47	19.33
0.5	8.9		1.78	19.98
0.75	8.9		1.78	20.62
1	8.9		1.73	21.25
1.25	9.2		1.69	21.87
1.5	9.2		1.74	22.51
1.75	9.2		1.67	23.12
2	9.2		1.69	23.74
2.25	9.2		1.69	24.36
2.5	9.2		1.65	24.97
2.75	9.2		1.61	25.56
3	9.1		1.94	26.27
3.25	9.1		1.31	26.75
3.5	9.1		1.63	27.34
3.75	9.1		1.57	27.92
4	9.1		1.57	28.49
4.25	9.1		1.59	29.07

Appendix B: Data Obtained From Long Columns Experiments Part II: Vertosol

Continue in Table 46

Time (h)	Water head (cm)	EC in leachate (dS/m)	K_{sat} (cm/h)	Accumulated leachate (cm)
4.5	9.1		1.46	29.61
4.75	9.1		1.55	30.17
5	9.1		1.55	30.74
5.25	9.1		1.55	31.30
5.5	9.1		1.53	31.86
5.75	9.1		1.51	32.41
6	9.4		1.51	32.97
6.25	9.4		1.53	33.54
6.5	9.4		1.53	34.10
6.75	9.4		1.38	34.61
7	9.4		1.49	35.16
7.25	9.4		1.49	35.71
7.5	9.4		1.45	36.25
7.75	9.4		1.45	36.78
8	8.9		1.47	37.32
8.25	8.9		1.47	37.85
8.5	8.9		1.47	38.39
8.75	8.9		1.47	38.92
9	8.9		1.47	39.45
9.25	8.9		1.43	39.97
10	8.9			41.64

Table B.47 K_{sat} measured with time for replicate 1 (Vertosol), Diluted HSS water and amended with gypsum treatment (EC \approx 1.3 dS/m) during applying water with EC = 0.1 dS/m after applying water with EC=0.4.

Time (h)	Water head (cm)	EC in drained water (dS/m)	K_{sat} (cm/h)	Accumulated leachate (cm)
0	7.7			0.00
0.25	7.7			0.38
0.5	7.7		1.41	0.86
0.75	7.7	0.465	1.41	1.35
1	7.7		1.41	1.84
1.25	7.7		1.41	2.33
1.5	7.7		1.41	2.81
1.75	7.7	0.567	1.38	3.29
2	7.7		1.36	3.76
2.25	7.7		1.38	4.24
2.5	7.7	0.522	1.41	4.73
2.75	7.7		1.36	5.20
3	7.7		1.38	5.68
3.25	7.7		1.36	6.15
3.5	7.7	0.464	1.36	6.63
3.75	7.7		1.36	7.10
4	7.7		1.31	7.55
4.25	7.7		1.34	8.02

Appendix B: Data Obtained From Long Columns Experiments Part II: Vertosol

Continue in table B.47

Time (h)	Water head (cm)	EC in drained water (dS/m)	K_{sat} (cm/h)	Accumulated leachate (cm)
4.5	8	0.38	1.35	8.49
4.75	8		1.32	8.95
5	8		1.26	9.39
5.25	8		1.28	9.84
5.5	8	0.327	1.30	10.30
5.75	8		1.30	10.75
6	8		1.28	11.20
6.25	8		1.26	11.64
6.5	8	0.29	1.30	12.10
6.75	8		1.26	12.54
7	8		1.28	12.98
7.5	8	0.275	1.26	13.86
7.75	8		1.28	14.31
8	8		1.23	14.74
8.25	8		1.26	15.18
8.5	8	0.253	1.23	15.62
8.75	8		1.23	16.05
9	8		1.21	16.47
9.25	8		1.23	16.91
9.5	8	0.2404	1.21	17.33
9.75	8		1.21	17.75
10	8	0.2367	1.23	18.19
0	8.1			
0.25	8.1	0.2293	1.21	18.61
0.5	8.1		1.25	19.05
0.75	8.1		1.23	19.48
1	8.1	0.2345	1.23	19.92
1.25	8.1		1.21	20.34
1.5	8.1		1.21	20.76
1.75	8.1		1.21	21.19
2	8.1	0.2234	1.21	21.61
2.25	8.1		1.18	22.03
2.5	8.1		1.21	22.45
2.75	8.1		1.18	22.87
3	8.1	0.1979	1.21	23.30
3.25	8.1		1.18	23.71
3.5	8.1		1.18	24.13
4	8.1	0.2189	1.17	24.95
4.25	8.1		1.18	25.37
4.5	8.1		1.18	25.79
4.75	8.1		1.18	26.20
5	8.1	0.213	1.14	26.60
5.25	7.9		1.15	27.01
5.5	7.9		1.19	27.42
6	7.9	0.2075	1.18	28.25
7	7.9	0.2035	1.26	30.01
8.2	7.9	0.201	1.13	31.91
8.5	7.9	0.196.2	1.22	32.42
8.75	7.9		1.10	32.81

Appendix B: Data Obtained From Long Columns Experiments Part II: Vertosol

Table B.48 K_{sat} measured with time for replicate 2 (Vertosol), Diluted HSS water and amended with gypsum treatment during applying water with EC = 0.4 dS/m. The Average K_{sat} measured at the final stage of water treatment for this replicate was 2.33 cm/h.

Time (h)	Water head (cm)	EC in leachate (dS/m)	K_{sat} (cm/h)	Accumulated leachate (cm)
0	8.9			0.00
0.25	8.9	1.666		0.44
0.5	8.9	1.975	1.63	1.03
0.75	8.9	1.958	1.69	1.64
1	8.9	2.021	1.65	2.24
1.25	8.9	2.027	1.65	2.84
1.5	8.9	2.026	1.63	3.43
1.75	8.9	2.039	1.63	4.02
2	8.9	2.033	1.52	4.57
2.25	8.9	2.067	1.74	5.20
2.5	8.9	2.034	1.61	5.78
2.75	8.9	1.971	1.63	6.37
3	8.3	1.811	1.69	6.96
3.25	8.3		1.69	7.56
3.5	8.3		1.69	8.16
3.7523	8.3		1.63	8.74
4	8.3	1.135	1.57	9.29
5	8.3	0.857	1.62	11.58
6	8.3	0.671	1.59	13.84
7	8.3	0.590	1.59	16.10
8	8.3	0.546	1.57	18.32
9	8.3	0.514	1.55	20.52
0				
0.2527	8.2	0.601	1.32	20.99
0.5	8.2	0.622	1.42	21.49
0.75	8.2	0.610	1.47	22.01
1	8.2	0.615	1.42	22.51
1.25	8.2	0.601	1.49	23.04
1.5	8.2	0.607	1.45	23.55
1.7525	8.2	0.608	1.45	24.07
2.017	8.2	0.599	1.45	24.61
2.25	8.2	0.593	1.46	25.09
2.5	8.2	0.602	1.42	25.59
3	8.2	0.601	1.45	26.61
4	8.2	0.567	1.48	28.70
5	7.05	0.522	1.47	30.70
7	8.2	0.465	1.47	34.82
8	8.2	0.462	1.49	36.92
9	8.2	0.449	1.48	39.01
10	8.2	0.440	1.50	41.14
11	8.2	0.436	1.49	43.24
12.017	8.2	0.429	1.48	45.37

Appendix B: Data Obtained From Long Columns Experiments Part II: Vertosol

Table B.49 K_{sat} measured with time for replicate 2 (Vertosol), Diluted HSS water and amended with gypsum treatment ($EC \approx 1.3$ dS/m) during applying water with $EC = 0.1$ dS/m after applying water with $EC=0.4$.

Time (h)	Water head (cm)	EC in drained water (dS/m)	K_{sat} (cm/h)	Accumulated leachate (cm)
0	8.2			0.00
0.25	8.2	0.536		0.39
0.5	8.2	0.587	1.42	0.90
0.75	8.2	0.567	1.42	1.40
1	8.2		1.40	1.89
2	8.2	0.570	1.40	3.87
3	8.2	0.530	1.40	5.85
4	8.2	0.437	1.39	7.81
5	8.2	0.360	1.45	9.86
6	8.2	0.303	1.45	11.90
7	8.2	0.263	1.42	13.90
8	8.2	0.240	1.40	15.88
9	8.2	0.225	1.44	17.91
10	8.2	0.214	1.40	19.88
0				
0.5	8	0.228	1.44	20.89
1	8	0.212	1.78	22.14
2	8	0.205	1.52	24.28
3	8	0.197	1.51	26.40
4	8	0.193	1.52	28.54
5	8	0.189	1.52	30.68
6	8	0.182	1.52	32.81
7	8	0.193	1.55	34.98
8	8	0.171	1.56	37.17
9	8	0.183	1.56	39.36
10	8	0.164	1.55	41.54

Appendix B: Data Obtained From Long Columns Experiments Part II: Vertosol

Table B.50 K_{sat} measured with time for replicate 3 (Vertosol), Diluted HSS water and amended with gypsum treatment during applying water treatment.

Time (h)	Water head (cm)	EC in leachate (dS/m)	K_{sat} (cm/h)	Accumulated leachate (cm)
0	7.5			0.00
1	7.6	2.369		1.63
2	7.6	1.614	3.04	5.83
3	7.6	1.549	2.79	9.68
4	7.6	1.561	2.70	13.41
5	7.6	1.557	2.57	16.96
6	7.8	1.576	2.50	20.43
7	7.8	1.537	2.44	23.83
8	7.8	1.572	2.40	27.16
9	7.8	1.587	2.35	30.42
10	7.25	1.582	2.37	33.65
0	7.9			
1	7.9	1.591	1.54	43.39
2	7.9	1.657	1.65	45.69
3	7.9	1.581	1.43	47.68
5.5	5.4	1.667	1.20	51.48

Table B.51 K_{sat} measured with time for replicate 3 (Vertosol), Diluted HSS water and amended with gypsum treatment during applying water with EC = 0.4 dS/m.

Time (h)	Water head (cm)	EC in drained water (dS/m)	K_{sat} (cm/h)	Accumulated leachate (cm)
0	7.7			0.00
1	7.7	1.583		2.17
2	7.7	1.597	1.65	4.45
3	7.7	1.48	1.62	6.70
4	7.8	1.03	1.60	8.92
6	7.8	0.651	1.53	13.18
7	7.8	0.538	1.51	15.28
8	7.8	0.527	1.47	17.32
9	7.8	0.484	1.48	19.37
10	0	0.475	2.02	21.39
11	0	0.46	2.00	23.39
1	8.1	0.555	1.68	31.92
2	8.1	0.544	1.97	34.69
3	8.1	0.517	2.00	37.51
4.02	7.8	0.463	1.66	39.86
6.6667	10		1.55	46.03
8	7.8	0.393	1.62	49.04
9	7.8	0.389	1.66	51.35

Appendix B: Data Obtained From Long Columns Experiments Part II: Vertosol

Table B.52 K_{sat} measured with time for replicate 3 (Vertosol), Diluted HSS water and amended with gypsum treatment ($EC \approx 1.3$ dS/m) during applying water with $EC = 0.1$ dS/m after applying water with $EC=0.4$.

Time (h)	Water head (cm)	EC in drained water (dS/m)	K_{sat} (cm/h)	Accumulated leachate (cm)
0	8.9			0.00
1	8.9	0.489		2.34
2	8.9	0.402	1.86	5.03
3	9.1	0.405	1.77	7.61
4	9.1	0.369	1.74	10.14
5.0167	9.1	0.287	1.68	12.63
7.5	9.1	0.265	1.70	18.77
8	9.1		1.60	19.93
9	9.1	0.2414	1.59	23.41
10	9.1	0.1894	1.57	25.68
1	7.8	0.443	1.63	33.45
2	7.8	0.437	1.76	35.90
3	7.8	0.378	1.72	38.29
4.0256	7.8	0.3	1.64	40.63
5	7.8		1.58	42.78
6	7.6	0.2434	1.57	44.95
8	7.6	0.2234	1.53	49.17
9.5	7.6	0.2142	1.49	52.25

Table B.53 K_{sat} measured with time for replicate 4 (Vertosol), Diluted HSS water and amended with gypsum treatment during applying water treatment.

Time (h)	Water head (cm)	EC in leachate (dS/m)	K_{sat} (cm/h)	Accumulated leachate (cm)
0	7.5			0.00
1	7.5			0.27
2	7.7	1.802	2.09	3.16
3	7.7	1.542	1.85	5.72
4	7.7	1.485	1.75	8.14
5	7.7	1.437	1.69	10.48
6	7.7	1.497	1.63	12.75
7	7.7	1.474	1.61	14.98
0				
1	7	1.626	0.68	25.97
2	7	1.627	1.34	27.78
3.083	7	1.663	1.33	29.72
5.333	7	1.695	1.31	33.72
0				
1	2.5	1.520	1.26	41.22
2	2.5	1.674	1.28	42.66
3	2.5	1.628	1.31	44.13

Appendix B: Data Obtained From Long Columns Experiments Part II: Vertosol

Table B.54 K_{sat} measured with time for replicate 4 (Vertosol), Diluted HSS water and amended with gypsum treatment during applying water with EC = 0.4 dS/m.

Time (h)	Water head (cm)	EC in drained water (dS/m)	K_{sat} (cm/h)	Accumulated leachate (cm)
0	7.3			0.00
0.5	7.3	1.528		0.41
2	7.3	1.743	0.92	2.29
3	7.3	1.780	0.88	3.50
4	7.3	1.778	0.88	4.69
5	7.3	1.655	0.88	5.89
6	7.3	1.411	0.85	7.04
7	7.3	1.106	0.86	8.21
0				
1	7.8	0.759	0.71	16.01
2	7.8	0.863	0.77	17.09
3	7.8	0.825	0.79	18.19
4	7.8	0.810	0.80	19.30
5	7.8	0.786	0.78	20.38
6	7.8		0.77	21.46
7	7.8	0.686	0.78	22.54
8	7.8	0.638	0.75	23.58
9	7.8	0.605	0.75	24.62
17.25	7.8	0.512	0.73	32.98

Table B.55 K_{sat} measured with time for replicate 4 (Vertosol), Diluted HSS water and amended with gypsum treatment (EC \approx 1.3 dS/m) during applying water with EC = 0.1 dS/m after applying water with EC=0.4.

Time (h)	Water head (cm)	EC in drained water (dS/m)	K_{sat} (cm/h)	Accumulated leachate (cm)
0	7.3			0.00
1	7.3	0.562		1.15
2	7.3	0.513	0.96	2.45
3	7.3	0.503	0.94	3.74
5	7.3	0.450	0.91	6.23
6	7.3	0.376	0.90	7.46
0				
1	7.7	0.214	0.76	27.07
2	7.7	0.208	0.82	28.20
5	7.7	0.213	0.81	31.56
6	7.7	0.258	0.79	32.66
0	6.6			
0.5	6.600	0.284	0.76	38.82
1	6.6	0.259	0.80	39.35

Appendix B: Data Obtained From Long Columns Experiments Part II: Vertosol

Table B.56 K_{sat} measured with time for replicate 1 (Vertosol), HSS water amended with sulphuric acid to reduce pH at 5 treatment during applying water with EC = 0.4 dS/m. The Average K_{sat} measured at the final stage of water treatment for this soil replicate was 0.09 cm/h.

Time (h)	Water head (cm)	EC in drained water (dS/m)	K_{sat} (cm/h)	Accumulated leachate (cm)
0	7.1			0.00
1	7.1		0.03498	0.05
2	7.1		0.02332	0.08
3	7.1		0.01166	0.09
5	7.1		0.01166	0.13
7	7.1		0.00875	0.15
10	7.1		0.00389	0.17
23	7.1		0.00224	0.19
33	7.1		0.00292	0.23
48	7.1		0.00078	0.24
80	7.1			0.24

Table B.57 K_{sat} measured with time for replicate 2 (Vertosol), HSS water amended with sulphuric acid to reduce pH at 5 treatment during applying water with EC = 0.4 dS/m. The Average K_{sat} measured at the final stage of water treatment for this soil replicate was 0.07 cm/h.

Time (h)	Water head (cm)	EC in drained water (dS/m)	K_{sat} (cm/h)	Accumulated leachate (cm)
0	7.8			0.00
14.5	7.8		0.000105001	0.01
17.5	7.8		0.000107101	0.01
20.5	7.8		7.56009E-05	0.00
24.5	7.8		4.25255E-05	0.00
34.5	7.8		2.45703E-05	0.00
Falling head method				
Water with EC = 0.4 added HSS water pH= 5 treatment (falling head method)				
Time (h)	K_{sat} (cm/h)			
0				
2	0.002761607			
4	0.002666679			
6	0.002758879			
8	0.002856769			

Appendix B: Data Obtained From Long Columns Experiments Part II: Vertosol

Table B.58 K_{sat} measured with time for replicate 3 (Vertosol), HSS water amended with sulphuric acid to reduce pH at 5 treatment during applying water treatment.

Time (h)	Water head (cm)	EC in leachate (dS/m)	K_{sat} (cm/h)	Accumulated leachate (cm)
0	7.4			0
1	7.4	4.17		
2	7.4	4.14		7.23
3	7.4	4.1	1.82432	9.73
4	10	4.08	0.75975	10.87
5	7.7	4.14	0.47100	11.52
6	7.7	4.1	0.33481	11.99
7	7.7		0.26104	12.35
8	7.7	4.08	0.21564	12.65
9	7.7		0.18727	12.91
10	7.7	4	0.16457	13.13
11	7.7		0.14754	13.34
12	7.7		0.12484	13.51
20	7.8	4.21	0.10107	14.63
22	7.8	0	0.08481	14.87
24	7.8	4.26	0.08764	15.11
26	7.8		0.07916	15.33
28	7.8	4.14	0.07351	15.54
30	7.8		0.06502	15.72
33	7.8		0.05843	15.96
45.55	7.8	4.3	0.05136	16.86
61	7.8	4.31	0.04977	17.93
71	7.8	4.31	0.04354	18.53
82	7.8	4.39	0.04523	19.22
95	7.8	4.5	0.03915	19.93
105.67	7.8	4.36	0.03974	20.52
120	7.8	4.5	0.03354	21.19
129.67	7.8		0.03158	21.61
142	7.8		0.02476	22.04
166	7.8	4.32	0.02686	22.93
190	7.8	4.32	0.02592	23.80
215	7.8	4.37	0.02578	24.69
239	7.8	4.47	0.02427	25.50
263	7.8	4.67	0.02262	26.26
289	7.8	4.65	0.02131	27.03
312	7.8	4.37	0.01795	27.60
337	7.8	4.46	0.01515	28.13
385	7.8	4.31	0.02191	29.59
611.5	8.2	4.84	0.00662	31.71
746	8.2	4.77	0.00605	32.85
Water with EC = 0.4 added HSS water pH= 7 treatment (falling head method)				
Time (h)	K_{sat} (cm/h)			
0				
1.5	0.010531505			
3	0.009706586			
4	0.007371487			

Appendix B: Data Obtained From Long Columns Experiments Part II: Vertosol

Table B.59 K_{sat} measured with time for replicate 4 (Vertosol), HSS water amended with sulphuric acid to reduce pH at 5 treatment during applying water treatment.

Time (h)	Water head (cm)	EC in drained water (dS/m)	K_{sat} (cm/h)	Accumulated leachate (cm)
0	7.5			0.00
1	7.5	4.920		0.42
2	7.4	4.040	1.98495	3.14
3	7.4	3.840	1.84153	5.66
4	7.4	3.670	1.73827	8.04
5	7.4	3.790	1.58337	10.21
6	7.4	3.980	1.58911	12.39
7	7.4	3.850	1.50306	14.45
8.5	7.4	3.920	1.36537	17.25
10	7.4	3.860	1.15885	19.63
0				
22	7.7		0.00384	24.49
30	7.7		0.00837	24.58
198	7.7	5.010	0.00402	25.52
332	7.7	5.000	0.00288	26.05
500	7.7	5.270	0.00284	26.71

Table B.60 K_{sat} measured with time for replicate 1 (Vertosol), HSS water amended with sulphuric acid to reduce pH at 7 treatment during applying water with EC = 0.4 dS/m. The Average K_{sat} measured at the final stage of water treatment for this soil replicate was 0.09 cm/h.

Time (h)	Water head (cm)	EC in drained water (dS/m)	K_{sat} (cm/h)	Accumulated leachate (cm)
0	9.5			0.00
1	9.5		0.02669	0.04
2	9.5		0.02135	0.07
3	9.5		0.02135	0.10
5	9.5		0.01868	0.16
7	9.5		0.01601	0.20
10	9.5		0.01067	0.25
23	9.5		0.00657	0.38
33	9.5		0.00480	0.45
48	9.5		0.00178	0.49
80	9.5		0.00100	0.53

Appendix B: Data Obtained From Long Columns Experiments Part II: Vertosol

Table B.61 K_{sat} measured with time for replicate 2 (Vertosol), HSS water amended with sulphuric acid to reduce pH at 7 treatment during applying water with EC = 0.4 dS/m. The Average K_{sat} measured at the final stage of water treatment for this soil replicate was 0.09 cm/h.

Time (h)	Water head (cm)	EC in drained water (dS/m)	K_{sat} (cm/h)	Accumulated leachate (cm)
0	8			0.00
14.5	8		0.01001	0.20
17.5	8		0.00938	0.24
20.5	8		0.00751	0.28
24.5	8		0.00563	0.31
34.5	8		0.00608	0.39
Falling head method				
Water with EC = 0.4 added HSS water pH= 5 treatment (falling head method)				
Time (h)	K_{sat} (cm/h)			
0				
2	0.007101904			
4	0.007037996			
6	0.013537403			
8	0.010456379			

Appendix B: Data Obtained From Long Columns Experiments Part II: Vertosol

Table B.62 K_{sat} measured with time for replicate 3 (Vertosol), HSS water amended with sulphuric acid to reduce pH at 7 treatment during applying water treatment.

Time (h)	Water head (cm)	EC in leachate (dS/m)	K_{sat} (cm/h)	Accumulated leachate (cm)
0	7.6			0.00
1	7.6			0.04
2	8.1	3.89	2.22080	3.16
3	8.1	3.82	1.96907	5.93
4	8.1	3.84	1.84041	8.51
5	8.1	3.86	1.71734	10.93
6	8.1	3.92	1.63903	13.23
7	8.1	3.94	1.49918	15.34
8	8.1	3.95	1.35933	17.25
9	8	3.98	1.14524	18.85
10	8	3.92	0.88700	20.09
11	8	3.97	0.69051	21.06
12	8	3.98	0.53894	21.81
20	8	4.02	0.28631	25.02
22	8	3.86	0.16842	25.49
24	8	3.89	0.15719	25.93
26	8		0.14035	26.32
28	8		0.11789	26.65
30	8	3.85	0.10666	26.95
33	8	0	0.08982	27.33
45.55	8	3.87	0.07336	28.62
61	0	3.75	0.08851	29.99
71	8	3.94	0.07972	31.10
82	8	3.87	0.05155	31.90
95	8	3.94	0.04189	32.66
105.67	8	3.85	0.03630	33.20
120	8	3.74	0.02899	33.78
129.67	8		0.02671	34.14
142	8	3.6	0.02003	34.49
166	8	3.8	0.02479	35.32
190	8	3.68	0.02386	36.12
215	8	3.83	0.02785	37.10
239	7.8	4.47	0.02167	37.82
263	7.8	4.67	0.02026	38.50
289	7.8	4.65	0.01936	39.20
312	7.8	4.37	0.01475	39.67
337	7.8	4.46	0.01425	40.16
385	7.8	4.31	0.01955	41.47
611.5	8.4	4.84	0.00650	43.56
746	8.4	4.77	0.00700	44.90
Water with EC = 0.4 added HSS water pH= 7 treatment (falling head method)				
Time (h)	K_{sat} (cm/h)	Accumulated leachate (cm)		
0				
1.5	0.007127825	0		
3	0.009070902	0.02357851		
4	0.007044049	0.02986611		

Appendix B: Data Obtained From Long Columns Experiments Part II: Vertosol

Table B.63 K_{sat} measured with time for replicate 4 (Vertosol), HSS water amended with sulphuric acid to reduce pH at 7 treatment during applying water treatment.

Time (h)	Water head (cm)	EC in leachate (dS/m)	K_{sat} (cm/h)	Accumulated leachate (cm)
0	8.4			0.00
1	8.4	4.460		0.60
2	8.4	3.700	2.31357	3.88
3	8.4	3.660	1.97595	6.69
4	8.4	3.620	1.80436	9.25
5	8.4	3.840	1.67706	11.63
6	8.4	3.860	1.58297	13.88
7	8.4	3.790	1.46674	15.96
8.5	8.4	3.820	1.28778	18.71
10	8.4	3.820	1.20291	21.27
0				
22	8.3		0.00402	24.67
30	8.3		0.01041	24.79
198	8.3	4.120	0.00575	26.16
332	8.3	5.170	0.00464	27.04
500	8.3	4.460	0.00410	28.01

Table B.64 K_{sat} measured with time for replicate 1 (Vertosol), natural HSS water treatment having pH=8.6 during applying water with EC = 0.4 dS/m. The Average K_{sat} measured at the final stage of water treatment for this soil replicate was 0.1 cm/h.

Time (h)	Water head (cm)	EC in drained water (dS/m)	K_{sat} (cm/h)	Accumulated leachate (cm)
0	9.6			0.00
1	9.6		0.05310	0.08
2	9.6		0.04248	0.14
3	9.6		0.01593	0.17
5	9.6		0.01859	0.22
7	9.6		0.01328	0.26
10	9.6		0.01062	0.31
23	9.6		0.00531	0.41
33	9.6		0.00478	0.48
48	9.6		0.00177	0.52
80	9.6		0.00166	0.60

Appendix B: Data Obtained From Long Columns Experiments Part II: Vertosol

Table B.65 K_{sat} measured with time for replicate 2, natural HSS water treatment having pH=8.6 during applying water with EC = 0.4 dS/m. The Average K_{sat} measured at the final stage of water treatment for this soil replicate was 0.09 cm/h.

Time (h)	Water head (cm)	EC in drained water (dS/m)	K_{sat} (cm/h)	Accumulated leachate (cm)
0	8			0.00
1	8		0.01126	0.02
14.5	8		0.01251	0.25
17.5	8		0.00938	0.29
20.5	8		0.00901	0.33
24.5	8		0.00479	0.36
34.5	8		0.00417	0.41
Falling head method				
Water with EC = 0.4 added HSS water pH= 5 treatment (falling head method)				
Time (h)	K_{sat} (cm/h)			
0				
2	0.00434			
4	0.00394			
6	0.00393			
8	0.00467			

Appendix B: Data Obtained From Long Columns Experiments Part II: Vertosol

Table B.66 K_{sat} measured with time for replicate 3, natural HSS water (having pH =8.6) treatment during applying water treatment.

Time (h)	Water head (cm)	EC in leachate (dS/m)	K_{sat} (cm/h)	Accumulated leachate (cm)
0	7.5			0.00
1	7.5			0.24
2	7.4	3.43	2.26032	3.33
3	7.4	3.45	1.88169	5.91
4	7.4	3.46	1.67516	8.21
5	7.4	3.46	1.41701	10.15
6	7.4	3.4	1.14164	11.71
7	7.4	3.51	0.87200	12.91
8	7.4	3.56	0.68269	13.84
9	7.4	3.49	0.55074	14.60
10	7.4	3.45	0.44174	15.20
11	7.4	3.48	0.37290	15.71
12	7.4	3.32	0.31553	16.14
20	8	3.46	0.20421	18.43
22	8	3.4	0.15438	18.86
24	8	3.28	0.14596	19.27
26	8		0.13473	19.65
28	8	3.31	0.11789	19.98
30	8		0.10386	20.27
33	8	3.23	0.08982	20.65
45.55	8	3.28	0.07336	21.94
61	0	3.23	0.09462	23.40
71	8	3.29	0.05670	24.19
82	8	3.31		24.98
95	8	3.26	0.04837	25.86
105.67	8	3.28	0.04525	26.53
120	8	3.23	0.03722	27.28
129.67	8	3.08	0.03483	27.75
142	8	3.02	0.02914	28.25
166	8	3.16	0.02947	29.25
190	8	3.22	0.02386	30.05
215	8	3.24	0.02874	31.05
239	8	4.47	0.02737	31.97
263	8	4.67	0.02596	32.84
289	8	4.65	0.02656	33.81
312	8	4.37	0.02075	34.48
337	8	4.46	0.02111	35.22
385	8	4.31	0.02620	36.98
611.5	7.6	4.84	0.01071	40.33
746	7.6	4.77	0.01080	42.33
Water with EC = 0.4 added HSS water pH= 7 treatment (falling head method)				
Time (h)	K_{sat} (cm/h)	Accumulated leachate (cm)		
0	0.00000	0.00		
1.5	0.01084	0.04		
3	0.01474	0.04		
4	0.01065	0.02		

Appendix B: Data Obtained From Long Columns Experiments Part II: Vertosol

Table B.67 K_{sat} measured with time for replicate 4 (Vertosol), natural HSS water (having pH = 8.6) treatment during applying water treatment.

Time (h)	Water head (cm)	EC in leachate (dS/m)	K_{sat} (cm/h)	Accumulated leachate (cm)
0	7.4			0.00
1	7.4	3.660		1.28
2	7.6	3.310	2.64262	4.93
3	7.6	3.260	2.31798	8.13
4	7.6	3.360	2.14713	11.09
5	7.6	3.310	2.02183	13.88
6	7.6	3.510	1.87945	16.47
7	7.6	3.330	1.75415	18.89
8.5	7.6	3.360	1.60228	22.21
10	7.6	3.940	1.47318	25.26
0				
2	8.3		0.01111	34.79
3	8.3		0.00889	34.80
22	8.3		0.00316	34.88
30	8.3		0.00889	34.98
198	8.3	3.570	0.00522	36.23
332	8.3	3.780	0.00398	36.98
500	8.3	3.540	0.00357	37.83

Appendix C: the UNSATCHEM Sub-Models

This Appendix provides a review of the sub-models incorporated into the UNSATCHEM model. It also provides details about the soil physical and chemical functions used and methods to estimate their parameters.

C.1 Water movement sub-model

The water movement sub-model numerically solves the Richards equation for variably saturated water flow at specific initial and boundary conditions. Plant water uptake is included as a sink term. The decrease in water flow due to sodicity is included in the Richards equation through the hydraulic conductivity reduction function (r). The r represents the relative reduction (as a ratio) in unsaturated hydraulic conductivity (K_{Unsat}) due to the increase in sodicity. It accounts for the effect of salinity and sodicity as influenced by both soil solution pH and clay swelling. The Richards equation describing vertical one dimensional flow in UNSATCHEM is:

$$\frac{\partial \theta_w}{\partial t} = \frac{\partial}{\partial z} \left(r K_g \frac{\partial h}{\partial z} + r K_g \right) - S \quad (C.1)$$

where h is the soil-water pressure head, θ_w is volumetric soil-water content, K_g is the hydraulic conductivity, t is time, z is soil depth (positive upward), and S defines the root water uptake term.

The main input data needed to solve the Richards equation are bulk density, K_{sat} and the soil-water characteristic curve (SWCC). The SWCC is needed to calculate soil-water content and K_{Unsat} change corresponding to the soil-water matric potential. UNSATCHEM permits the use of four different non-linear analytical models for describing the hydraulic properties. These functions are Brooks and Corey (1966), van Genuchten (1980), modified van Genuchten and van Genuchten-Mualem with air-entry value of -2 cm (Vogel & Cislerova 1988).

The Brooks and Corey (1966) function is a simple function having four parameters to be determined from experimental volumetric soil-water content - matric potential data.

However, the main limitation of the Brooks and Corey (1966) function is its failure to describe SWCC at water contents near saturation. van Genuchten (1980) used the statistical pore-size distribution model of Mualem (1976) to obtain predictive functions for the soil-water characteristic curve and the related K_{Unsat} in the range between saturated volumetric soil-water content (θ_{sw}) to residual volumetric soil-water content (θ_{sw}). It has five parameters that need to be determined. However, Simunek et al. (2005) indicated that this equation does not describe properly the K_{Unsat} at higher water contents in very fine texture soils.

Vogel and Cislérova (1988) modified the equations of van Genuchten (1980) to add flexibility for description of the hydraulic properties near saturation. In this approach, the θ_{sw} parameter in the van Genuchten retention function was replaced by an extrapolated volumetric soil-water content which is slightly higher than the saturation. In addition, the θ_{sw} is replaced by a lower extrapolated water content. Simunek et al. (2005) indicated that this change has no effect on the soil-water characteristic curve, but it has a positive effect on the shape and value of the hydraulic conductivity function, especially for fine-textured soils. The approach maintains the physical meaning of θ_{sw} and θ_{sw} as measurable quantities. This model contains nine unknown parameters. Simunek et al. (2005) simplified the Vogel and Cislérova (1988) model in which extrapolated water content higher than θ_{sw} calculated at air entry equal to -2 cm. The Vogel and Cislérova (1988) model is incorporated into the UNSATCHEM under the “van Genuchten-Mualem with air-entry value of -2 cm” option. Simunek et al. (2005) recommended using this model for simulation of water flow in heavy clay soils.

The parameters required for each soil hydraulic functions discussed above can be determined from an experimental SWCC data for the range of suction from 0 to 15 bars. Non-linear regression analysis programs are usually used to obtain the parameters, such as the RETC software (van Genuchten et al. 1991). Furthermore, the UNSATCHEM incorporates a neural network (Schaap et al. 2001) that can be used to predict such parameters from the main soil physical properties (based on the American textural classification system). However, it is not recommended to use this neural network prediction for local soil as long as the SWCC data are available.

The Richards equation requires specification of the initial condition in terms of the pressure head distribution within the soil profile. The initial condition could be also specified in term of

moisture content distribution. The software has an initial condition option which allows specifying either initial pressure head or volumetric soil-water content at any soil depth. In addition, the software offers a variety of user defined boundary conditions that specify different soil conditions at both the top and bottom of the soil profile.

Simunek et al. (2005) categorised the boundary conditions in the UNSATCHEM for the water movement within the flow domain in two groups. The first group are independent boundary conditions that must be specified at the soil surface or at the bottom of the soil profile. The main boundaries in this group are the prescribed values of the pressure head and/or the soil-water flux. The second group are dependent boundary conditions which cannot be defined prior to simulation. Rather, they are defined based on the water flow condition during simulation at each space and time. An example of these boundary conditions is the seepage face at the bottom of the finite soil column in which water can leave the bottom. This type of boundary condition assumes that a zero-flux boundary condition applies as long as the local pressure head at the bottom of the soil column is negative. However, a zero pressure head indicates that the bottom of the profile becomes saturated and water comes out as seepage.

The UNSATCHEM permits the change of the boundary conditions and input variables with time via time variable boundary conditions option, which allows some variable inputs to be accounted, such as rainfall, evaporation, and water salinity along the period of simulation.

C.2 Solute movement sub-model

The transport of solute ions are described individually using convection-dispersion type equations. The UNSATCHEM considers the transport of seven major ions, namely Ca^{2+} , Mg^{2+} , Na^+ , K^+ , HCO_3^- , SO_4^{2-} , and Cl^- . Transport of each ion is simulated in one dimensional flow with the advection–dispersion equation, which can be expressed in general form as (Simunek et al. 2005):

$$\frac{\partial \theta_w C_k}{\partial t} + \rho \frac{\partial \bar{C}_k}{\partial t} + \rho \frac{\partial \hat{C}_k}{\partial t} = \frac{\partial}{\partial z} \left[\theta_w D \frac{\partial C_k}{\partial z} - q_w C_k \right] \quad k = 1, 2, \dots, N_c \quad (\text{C.2})$$

where θ_w is volumetric soil-water content, C_k is the total dissolved concentration of the aqueous species k , \bar{C}_k is the total surface species concentration of the aqueous component k , \hat{C}_k is the total solid phase concentration of aqueous component k , ρ is the soil bulk density, D is the dispersion

coefficient, q_w is the volumetric flux calculated by Buckingham- Darcy law, and N_c is the number of primary aqueous species. The second and the third terms on the left side of equation C.2 are zero for non-exchangeable ions. However, these terms are determined by solving the reaction system for species that go through ion exchange or precipitation/dissolution processes.

The dispersion coefficient D in equation C.2 represents the combined effect of molecular diffusion and mechanical dispersion on solute convection transport. The D is given by:

$$\theta_w D = D_L |q_w| + \theta_w D_w \tau_w \quad (C.3)$$

where D_w is the molecular diffusion coefficient in free water, τ_w is a tortuosity factor in the liquid phase, $|q_w|$ is the absolute value of the Darcian water flux density and D_L is the longitudinal dispersivity . The tortuosity factor is evaluated in the UNSATCHEM as a function of the water content using the relationship of Millington and Quirk (1961):

$$\tau_w = \frac{\theta_w^{7/3}}{\theta_s^2} \quad (C.4)$$

where θ_s is the saturation moisture content. While the molecular diffusion values can be found in the literature, the longitudinal dispersivity can be determined from analysing break through curves for the aqueous species.

Solute movement boundary condition

The UNSATCHEM permits specifying three types of solute concentration boundary conditions (BC) which are concentration flux BC, concentration BC, and stagnant BC for volatile solutes. Concentration flux BC (a third-type BC) prescribes the solute flux (not the concentration) at the boundary, while constant concentration BC (a first-type BC) prescribes the concentration at the boundary (not the flux into the domain). Concentration BC is not physical and does not conserve mass (van Genuchten & Parker 1984). Therefore, Simunek et al. (2005) recommended using the concentration flux BC as it is more physically realistic. Soil surface BC is incorporated into the UNSATCHEM for volatile solutes, when they are present in both liquid and gas phases. This BC is a third-type boundary condition with an additional term to account for gaseous diffusion through a boundary of stagnant layer on the soil surface.

CDE solute parameters

Solute parameters are usually determined by fitting an analytical solution of CDE under appropriate initial conditions to experimental data. This can be conducted using a measurement of the solute concentrations at a certain depth with time or at a given time with different soil depth. The main parameters that can be determined are the dispersion coefficient, average pore velocity, retardation and production coefficients (in the case of solute chemically reacts with soil surfaces).

The deterministic equilibrium CDE for steady state one dimensional transport of reactive solute subject to adsorption, first order degradation and zero order production, in a homogeneous soil can be written as (Toride et al. 1999):

$$R_f \frac{\partial C_r}{\partial t} = D \frac{\partial^2 C_r}{\partial z^2} - v \frac{\partial C_r}{\partial z} - \mu C_r + \gamma(z) \quad (C.5)$$

where C_r is the volume averaged or resident concentration in liquid phase, D is the dispersion coefficient, v is average pore water velocity, t is time, μ is the combined first order decay coefficients for degradation of the solute in the liquid and adsorbed phase, R_f is the retardation factor, and $\gamma(z)$ is combined zero order production coefficients in liquid phase as a function of soil depth.

Equation C.5 could be modified in dimensionless parameters for non-reactive solute transport and without solute sink source (Cote et al. 2001):

$$\frac{\partial \tilde{C}_r}{\partial T} = \frac{\partial^2 \tilde{C}_r}{P \partial \bar{z}^2} - \frac{\partial \tilde{C}_r}{\partial \bar{z}} \quad (C.6)$$

Where \tilde{C}_r is a characteristic solute concentration($\frac{C_r}{C_o}$), T is the pore volume and represents the amount of water passed through the soil according to the total amount of water present in soil, \bar{z} is the relative soil depth according to the entire soil column length. P is the peclet number (i.e. the ratio between the convective and dispersive transport terms). P indicates which solute transport type is predominant in relation to increment travel distance within soil profile. The peclet number is expressed as:

$$P = \frac{vz}{D} \quad (C.7)$$

where z is the length of soil column.

Assuming that solute reaction during movement is negligible, the non-reactive solute transport equation (equation C.6) incorporated in CXTFIT program (Toride et al. 1999) can be used to obtain the solute parameters. The analytical solution for equation C.5 is based on third type boundary conditions. The initial condition could be expressed for solute third type boundary condition as (Toride et al. 1999):

$$C_r(0, T) - \frac{1}{P} \frac{\partial C_r(0, T)}{\partial z} = C_o(T) \quad (C.8)$$

The flux-averaged concentrations boundary condition used usually to describe the solute inflow. The outflow (bottom of the soil column) boundary condition which is often used for a finite soil column is the zero concentration gradient (Toride et al. 1999). The zero concentration gradient can be expressed as (Toride et al. 1999):

$$\frac{\partial C_r}{\partial z}(1, T) = 0 \quad (C.9)$$

It is worth noting that the description of the solute movement in the previous equations is based on an average residual concentration (i.e. concentration in soil-water). The average flux concentrations could be obtained from residual solute concentration as (Toride et al. 1999):

$$C_f = C_r - \frac{1}{P} \frac{\partial C_r}{\partial z} \quad (C.10)$$

C.3 The CO₂ production and transport sub-model

Carbon dioxide (CO₂) has a significant role in dissolution/ precipitation reactions for a number of soil components (e.g. gypsum and calcite). These reactions have a direct impact on soil sodicity and salinity levels. The concentrations of CO₂ in soil solution depend on its concentration in soil air. The concentration of CO₂ in atmosphere is about 0.035% (Simunek et al. 1996). However, CO₂

concentration in soils may be much higher due to its production mainly from biological reaction (Simunek et al. 1996). The biological production of CO_2 is by soil microbes and plant roots. The increase of CO_2 concentration in soil air increases the amount of diluted CO_2 in soil solution which forms carbonic dioxide acid (H_2CO_3). Carbonic dioxide acid involves in a series of dissolve/precipitate reactions within soil profile.

The CO_2 sub-model into the UNSATCHEM considers only the biological production. Simunek et al. (2005) assumed that the individual CO_2 production processes are a sum of the production by the soil micro-organisms (γ_s) and the production by plant roots (γ_r) as:

$$P_{\text{CO}_2} = \gamma_s + \gamma_r \quad (\text{C.11})$$

Simunek et al. (1996) explained that the production of CO_2 , in both terms is affected by many factors such as soil depth, temperature, water content, soil-water salinity, availability of oxygen in soil (i.e. oxygen stress), nutrient status of the soil. These factors are changing with time. The effects of these factors were incorporated as a ratio (i.e. production coefficients) in the optimum CO_2 production for both micro-organisms and root production as (Simunek et al. 2005):

$$\gamma_s = \gamma_{s0} \prod_i f_{si} \quad \gamma_r = \gamma_{r0} \prod_i f_{ri} \quad (\text{C.12})$$

$$\prod f_i = f(z) f(h) f(T) f(c_{\text{CO}_2}) f(h_\phi) f(t) \quad (\text{C.13})$$

Where γ_{s0} is the optimum CO_2 production from micro-organisms, γ_{r0} is the optimum CO_2 production from plant roots, $f(z)$ the reduction coefficient of the soil depth, $f(h)$ the reduction coefficient of pressure head (soil-water content), $f(T)$ is temperature coefficient which could be more than one at temperature above 20°C , $f(c_{\text{CO}_2})$ is the reduction coefficient of oxygen (O_2) gas concentration, $f(h_\phi)$ is the reduction coefficient of osmotic effect. The actual CO_2 production rate is obtained by integrating the CO_2 production for the entire soil profile depth as:

$$P_{\text{CO}_2} = \int_0^z P_{\text{CO}_2} dz \quad (\text{C.14})$$

The total CO₂ production needs to be specified. Furthermore, the UNSATCHEM assumes that the CO₂ produced from plant root is about 40% of the total CO₂ produced.

CO₂ in soil solution defined into the UNSATCHEM as the sum of diluted CO₂ in soil solution and HCO₂, and is related to the CO₂ in soil air as (Sturnm & Morgan 1981):

$$Cw_{CO_2} = K_{CO_2} R T C a_{CO_2} \quad (C.15)$$

where K_{CO_2} Henry law constant, R is the universal gas constant which is 8.314 kg×m² / s. × K× mol, K^0 is the absolute temperature.

The UNSATCHEM assumes that the main transport of CO₂ for gaseous and liquid phase occurs by diffusion and dispersion. Therefore, the CO₂ transport in both phases is described by the convection-dispersion type equation. The one-dimensional CO₂ transport is described by the following mass balance equation (Simunek et al. 2005):

$$\frac{\partial(Ca_{CO_2}\theta_a + Cw_{CO_2}\theta_w)}{\partial t} = \left(\theta_a D_a \frac{\partial Ca_{CO_2}}{\partial z} - \frac{\partial(q_a Ca_{CO_2})}{\partial z} \right) + \left(\theta_w D_{wCO_2} \frac{\partial Cw_{CO_2}}{\partial z} - \frac{\partial(q_w Cw_{CO_2})}{\partial z} \right) - SCw + P_{CO_2} \quad (C.16)$$

where Ca_{CO_2} is the volumetric concentration of CO₂ in the gaseous phase, Cw_{CO_2} is the CO₂ concentration in the liquid phase, θ_{sw} is the soil air content, θ_{sw} is the volumetric soil-water content, D_a is the diffusivity of the CO₂ in soil air, D_{wCO_2} is the CO₂ diffusivity in soil solution, SCw is the dissolved CO₂ removed from soil by root water uptake and P_{CO_2} is the CO₂ production term as defined in equation C.14.

C.4 Chemical reactions sub-model

The chemical reactions sub-model incorporated into the UNSATCHEM includes ion complexation, cation exchange, and mineral precipitation-dissolution reactions for 37 species (Table C.1). The species include seven primary dissolved ions (Ca^{2+} , Mg^{2+} , Na^+ , K^+ , SO_4^{2-} , Cl^- , and NO_3^-). Simunek et al. (1996) explained that about 36 or 35 equilibrium chemical reaction equations are needed to solve the chemical system. However, they stated that dolomite dissolution is treated as kinetic reaction and not included in the equilibrium system. Furthermore, the UNSATCHEM allows excluding calcite from the equilibrium system to be treated as a kinetic precipitation-dissolution reaction.

The kinetic calcite precipitation/dissolution reactions are described in UNSATCHEM using the model of Plummer et al. (1978) in the pH range between 2 to 8, while the Inskeep and Bloom (1985) expression is used at the range of pH above 8. In the kinetic reactions models the rate of reactions is determined by the surface area of calcite and set as input parameter. Suarez and Simunek (1997) indicated that the kinetic calcite precipitation/dissolution model produces values closer to the field measurements. This result was demonstrated in a number of published data (e.g. Suarez, 1977; Suarez and Rhoades, 1982).

Table C.1 Chemical species considered in the chemical reaction sub-model

1	Aqueous components	7	Ca^{2+} , Mg^{2+} , Na^+ , K^+ , SO_4^{2-} , Cl^- , NO_3^-
2	Complexed species	10	CaCO_3^0 , CaHCO_3^+ , CaSO_4^0 , MgCO_3^0 , MgHCO_3^+ , MgSO_4^0 , NaCO_3^- , NaHCO_3^0 , NaSO_4^- , KSO_4^-
3	Precipitated species	6	CaCO_3 , $\text{CaSO}_4 \cdot 2\text{H}_2\text{O}$, $\text{MgCO}_3 \cdot 3\text{H}_2\text{O}$, $\text{Mg}_5(\text{CO}_3)_4(\text{OH})_2 \cdot 4\text{H}_2\text{O}$, $\text{Mg}_2\text{Si}_3\text{O}_{7.5}(\text{OH}) \cdot 3\text{H}_2\text{O}$, $\text{CaMg}(\text{CO}_3)_2$
4	Sorbed species	4	Ca, Mg, Na, K
5	CO₂-H₂O species	7	P_{CO_2} , H_2CO_3 , CO_3^{2-} , HCO_3^- , H^+ , OH^- , H_2O
6	Silica species	3	H_4SiO_4 , H_3SiO_4^- , $\text{H}_2\text{SiO}_4^{2-}$

Source: (Simunek et al. 2005)

UNSATCHEM uses modified Debye-Huckel equation (Truesdell & Jones 1974) to calculate single ion activities at solute concentration less than a critical value, which is defined by the user. The recommended critical concentration by Simunek et al. (2005) is 0.5M. For concentration more the critical solution and up to 16M it uses an equation based on Pitzer theory (Pitzer 1973).

The major ions (i.e. Ca^{2+} , Mg^{2+} , Na^+ , K^+ , SO_4^{2-} , Cl^- , and NO_3^-) are assumed to be in instantaneous equilibrium with exchangeable surfaces at which the total net negative charge of the clay minerals and organic matter are balanced. Thus, the cation exchange capacity (CEC) of the soil is calculated as:

$$\text{CEC} = \text{Ca}^{2+} + \text{Mg}^{2+} + \text{Na}^+ + \text{K}^+ \quad (\text{C.17})$$

It should be noted that the ionic exchange between soil solution and exchangeable surface reported in (Simunek et al. 2005; Suarez & Simunek 1997) is described by adjusted Gapon equation (White & Zelazny 1986) as:

$$K_{Gij} = \frac{\text{EXN}_i^{y+} (C_j^{x+})^{1/x}}{\text{EXN}_j^{x+} (C_i^{y+})^{1/y}} \quad (\text{C.18})$$

where EXN is denoted to adsorbed species concentration in units ($\text{mol}_\text{c}/\text{kg}$), and C is designated to an ion concentration in soil solution in units ($\text{mol}_\text{c}/\text{litre}$). The subscripts y and x are valence of species i and j , respectively, K_{Gij} is the Gapon selectivity coefficient for species i and j .

The exchange reaction govern by equation C.18 is assumed to be reversible. Thus, the UNSATCHEM considers the exchange reaction between Na^+ and Ca^{2+} species as following:

$$K_{\text{GCa-Na}} = \frac{\text{Ca}^{2+}}{\text{Na}^{x+}} \frac{(Na^+)}{(Ca^{2+})^{1/2}} \quad (\text{C.19})$$

From equation C.12, it can be noted that the value of $K_{\text{GCa-Na}}$ is inverse of the value of Gapon selectivity coefficient that can be found in many literature. The adjusted Gapon equation requires determining the Gapon selectivity coefficients for Ca-Na, Mg-Ca- Mg, and Ca-K exchange equations.

The exchangeable sodium percentage (ESP) is determined as in equation 2.4 (in chapter 2). It is worth noting that the ESP could be varied with soil pH (Khajanchi & Meena 2008) as discussed in section 2.3.3. However, the UNSATCHEM assumes that the ESP is independent from soil pH.

C.5 Heat transport sub-model

The UNSATCHEM considers the effect of the temperature change and heat transport in water and solute movement, chemical reaction system and evaporation process within soil profile. The heat transport in the UNSATCHEM is described by a one-dimensional convection-dispersion type equation assuming that the effect of water vapour diffusion on transport is negligible. The equation is expressed as (Sophocleous 1979):

$$C_p(\theta_w) \frac{\partial T}{\partial t} = \frac{\partial}{\partial z} \left[\lambda(\theta_w) \frac{\partial T}{\partial z} \right] - C_w q_w \frac{\partial T}{\partial z} \quad (\text{C.20})$$

where T is the absolute temperature, q_w is Darcy flux density, $\lambda(\theta_w)$ is the coefficient of the apparent thermal conductivity of the soil, $C_p(\theta)$ and C_w are the volumetric heat capacities of the soil system and water, respectively. The first term on the right-hand side of equation C.20 represents heat flow due to conduction, the second term represents the heat transported by flowing water, and the third term represents the energy uptake by plant roots associated with root water uptake.

Appendix D: Determination of the Dispersivity Coefficient and Longitudinal Dispersivity for the Sodosol and Vertosol Soils

The CXTFIT program (Toride et al. 1999) incorporated into STANMOD (Simunek et al. 1999) was used to estimate the solute parameters (mainly the dispersion coefficient) for both Sodosol and Vertosol soils. Assuming that solute is non-reactive, the solute parameters were determined by fitting the EC measurements in outflow with time to an appropriate analytical solution (included in CXTFIT program) for the CDE (i.e. steady one-dimensional flow and solute transport). The inverse problem is solved in CXTFIT using non-linear regression based on least-squares inversion method (Levenberg and Marquardt method).the process of determine dispersion coefficient and longitudinal dispersivity are as following.

CXTFIT graphic interface inputs

The data of column experiments for normal tap water and amended with gypsum treatment followed by normal water with EC 0.4 and then 0.1 dS /m were used. The applications of either water with 0.4 or 0.1 dS/m were used as an independent experiment. The processes of analysing data selected using STANMOD software, CXTFIT module is as following: For every set of EC versus time data, a new file was created. In the first window, the option inverse solution was specified. An assumption was made that the solute transport is in equilibrium state, the deterministic equilibrium CDE button was chosen in second window. The third window permits to determine the type of the data for the indirect problem. Since the experimental data is the EC measured in the outflow with time, assumption was made that the electrolyte concentration passes the bottom of the soil column is equal to that in outflow. Thus, the time and concentration button at specified depth of the soil column (i.e. 20 cm) was chosen. In fourth window, the units for the length and time were specified as cm and hours while the solute concentration is left dimensionless. In the fifth window, the boundary condition at the top of the soil column was specified as a flux average concentration.

In the following windows, no constraint was set for the parameter values with maximum alteration about 20. Assumption was made that no chemical reaction can cause change of the solute balance during water and solute percolation. Therefore, only parameters need to be optimised are dispersion coefficient (D) and average soil pore velocity (v). The retardation (R_f) and production coefficient (μ) can be used only if the solute percolated involves in chemical reaction within soil profile. The

Appendix D: Determination of the Dispersivity coefficient and the Longitudinal Dispersivity

experimental data represent one side solute leaching that has been added prior to apply lower concentration solution. Thus, the step input was chosen with input concentration equal to added water treatment concentration. However, the input concentration was assumed to be unknown. It is assumed that the initial concentration within the soil column is equal to first EC measurement in outflow at the beginning of the experiment. The button zero production was chosen (i.e. added water is the sole source of solute).

The optimised values of the parameters were evaluated in term of statistical parameters (i.e. F-values, t-values and coefficient of determination (R^2)). The initial values of the parameters were alerted many time and refitted with the experimental data until the sum of squares was minimised and come closer to the best fit.

The obtained solute parameters

The values of the parameters produced and statistical indicators for both soils are shown in Table D.1. The higher t-values indicate that the values of D and v estimated for all the data analysed are significant. The D values ranged from 4 to 12 cm^2/h . The R^2 values indicate that the model used for non-linear fitting is an appropriate model.

Table D.1 Solute parameters produced from analysing solute data for three selected replicates for the Sodosol and Vertosol soils

Soil Type	Replicate number	D (cm^2/h)	Fit Std Error	V (cm/h)	Fit Std Error	R^2
Sodosol	Replicate 1 (input EC=0.1dS/m)	6.36	1.26	9.11	0.118	0.996
	Replicate 2 (input EC=0.4dS/m)	4.28	0.83	7.56	0.12	0.99
	Replicate 2 (input EC=0.1dS/m)	6	0.647	5.03	0.077	0.998
	Replicate 3 (input EC=0.4dS/m)	11.82	1.789	6.94	0.177	0.996
	Replicate 3 (input EC=0.1dS/m)	4.88	1	7.45	0.153	0.994
Vertosol	Replicate 1 (input EC=0.1dS/m)	7.83	0.719	4.89	0.081	0.998
	Replicate 2 (input EC=0.4dS/m)	6.03	0.811	5.31	0.117	0.991
	Replicate 2 (input EC=0.1dS/m)	7.06	1.339	4.08	0.193	0.995
	Replicate 3 (input EC=0.4dS/m)	6.00	0.986	4.46	0.133	0.996
	Replicate 3 (input EC=0.1dS/m)	11.28	4.997	5.28	0.54	0.974

Determination of longitudinal dispersivity

The input for the UNSATCHEM requires both diffusion coefficient and longitudinal dispersivity as separate input parameters. This option allows for instant calculation of D , which is useful at higher sodicity level as the Darcy flux is changing due to the decrease of hydraulic conductivity. The longitudinal dispersivity could be predicted from dispersion coefficient by rearrangement of Equation 4.3 (in chapter 4) as:

$$D_L = \frac{D}{v} - \frac{D_w \tau_w}{v} \quad (\text{D.1})$$

The second term in the right hand side represents the effect of water diffusion. This value is small and can be neglected. Thus, Equation D.1 can be approximated as:

$$D_L = \frac{D}{v} \quad (\text{D.2})$$

Equation D.2 was used to calculate longitudinal dispersivity for different replicates. The longitudinal dispersivity calculated is shown in Table D.2. However, it is noted that equation D.2 does not hold for low pore-water velocities where diffusion cannot be assumed to be negligible (Bromly et al. 2007). Therefore, the value of water diffusion was set at value $0.00001 \text{ cm}^2 / \text{S}$ (Fetter 1999) during modelling of HSS water treatments.

Table D.2 Longitudinal dispersivity (cm) calculated for the three replicates for both soils based on equation D.2

Replicate number	Sodosol	Vertosol
Replicate 1 (input EC=0.1dS/m)	0.7	1.60
Replicate 2 (input EC=0.4dS/m)	0.57	1.14
Replicate 2 (input EC=0.1dS/m)	1.19	1.73
Replicate 3 (input EC=0.4dS/m)	1.70	1.35
Replicate 3 (input EC=0.1dS/m)	0.66	2.14
Average	0.964	1.592

Appendix E: Evaluation of the SAR-ESP Relationship and Calculating the Gapon Selectivity Coefficients Values for the Sodosol and Vertosol

E.1 Background

The SAR-ESP relationship developed by USSL Staff (1954) was based on a linear correlation between the experimental measurements of Exchangeable Sodium Ratio (i.e. $ESR = EXNa/(CEC-EXNa)$) and ESP for 51 American soils. The linear relationships produced ($R^2=0.923$) was:

$$ESR = -0.0126 + 0.01475SAR \quad (E.1)$$

The relationship can be rewritten in general form as:

$$ESR = a_i + b_i SAR \quad (E.2)$$

Where a_i and b_i are fitted parameters. The ESP can be calculated from ESR as:

$$ESP = 100 \times \left(\frac{ESR}{1 + ESR} \right) \quad (E.3)$$

And, the ESR can be calculated from ESP as:

$$ESR = \frac{ESP}{100 - ESP} \quad (E.4)$$

The Gapon equation is widely used to describe the exchange reaction between soil solution and exchange complex in the soil. The Gapon equation as described by white and zaliniy (1986) is:

$$\frac{EXNa^+}{EXCa^{2+}} = K_G \frac{[Na^+]}{[Ca^{2+}]^{\frac{1}{2}}} \quad (E.5)$$

where $EXNa^+$ and $EXCa^{2+}$ are the amounts of Na^+ and Ca^{2+} balancing the charge of the soil's exchange complex commonly in units (mmol_c/Kg), K_G is the Gapon selectivity coefficient units (mol_c/litre)^{0.5}. The Na and Ca concentrations in solution are expressed in mol_c/litre.

If there is only Ca and Na in equilibrium solution then the exchange complex will be saturated by Ca and Na and the ESR can be calculated as:

$$ESR = \frac{Na^+}{Ca^{2+}} \times 100 \quad (E.6)$$

And the SAR for the soil water can be calculated as:

$$SAR = \frac{Na^+}{\sqrt{\frac{Ca^{2+}}{2}}} \quad (E.7)$$

Substituting equation E.6 and E.7 in equation E.1 provides the relationship between ESR and SAR for a Na-Ca solution (Quirk 2008):

$$ESR = K_G \times SAR \quad (E.8)$$

Hence, if the SAR and corresponding ESR data are available for a given soil, the Gapon selectivity coefficient can be determined. The Gapon selectivity coefficient may be calculated by fitting different values of SAR and ESR to equation E.7. In addition, the empirical SAR-ESP relationship (similar to that described by USSL Staff (1954)) can be obtained (assuming equilibrium between exchange surfaces and soil solution).

E.2 Material and methods

E.2.1 SAR- ESP Data

The SAR- ESP data for both soils under two different conditions (i.e. cultivated non-cultivated from Sodosol and Vertosol samples taken from depth from 5 to 10 cm) were obtained from Kopittke et al. (2004). The soil columns were leached with a solution (having 50 mol/Litre of a mixed sodium chloride (NaCl) and calcium chloride (CaCl₂.H₂O) in deionised water) with different SAR values and solutions until equilibration and chemical analyses were conducted to determine the ESP of the soil samples.

E.2.2 Data analyses

The ESP data was used to calculate the ESR based on equation E.3. The data obtained by Kopittke et al. (2004) and the calculated ESR values are presented in Table E.1. The ESR and SAR relationship was established to evaluate the validity of using the SAR-ESP (USSL staff 1954) relationship for the Vertosol and Sodosol soils. The KG_{Na-Ca} values were also determined by fitting equation E.8.

Table E.1 Effect of equilibrating solution sodium adsorption ratio (SAR) on the soil exchangeable Na percentage (ESP) for cultivated/non-cultivated soils (from Kopittke et al. (2004))

SAR (mmol _c L ⁻¹) ^{0.5})	Sodosol				Vertosol			
	Cultivated		Non-cultivated		Cultivated		Non-cultivated	
	ESP (%)	ESR (c/c)	ESP (%)	ESR (c/c)	ESP (%)	ESR (c/c)	ESP (%)	ESR (c/c)
3	9.2	0.1013	5.5	0.0582	3.3	0.0341	3.0	0.0309
6	14	0.1628	7.7	0.0834	6.6	0.0707	5.4	0.0571
12	18	0.2195	11	0.1236	11	0.1236	11	0.1236
18	20	0.25	14	0.1628	16	0.1905	16	0.1905
24	28	0.3889	19	0.2346	21	0.2658	20	0.2500

E.3 SAR-ESP relationship for the Sodosol and Vertosol compared with the USSL Staff (1954) relationship

Equation E.2 was fitted to the SAR and ESR data to obtain the parameters for both soils under cultivation and non cultivation. Equation E.8 was also fitted to obtain the KG values. The resultant graphs are shown in Figure E.1 and E.2:

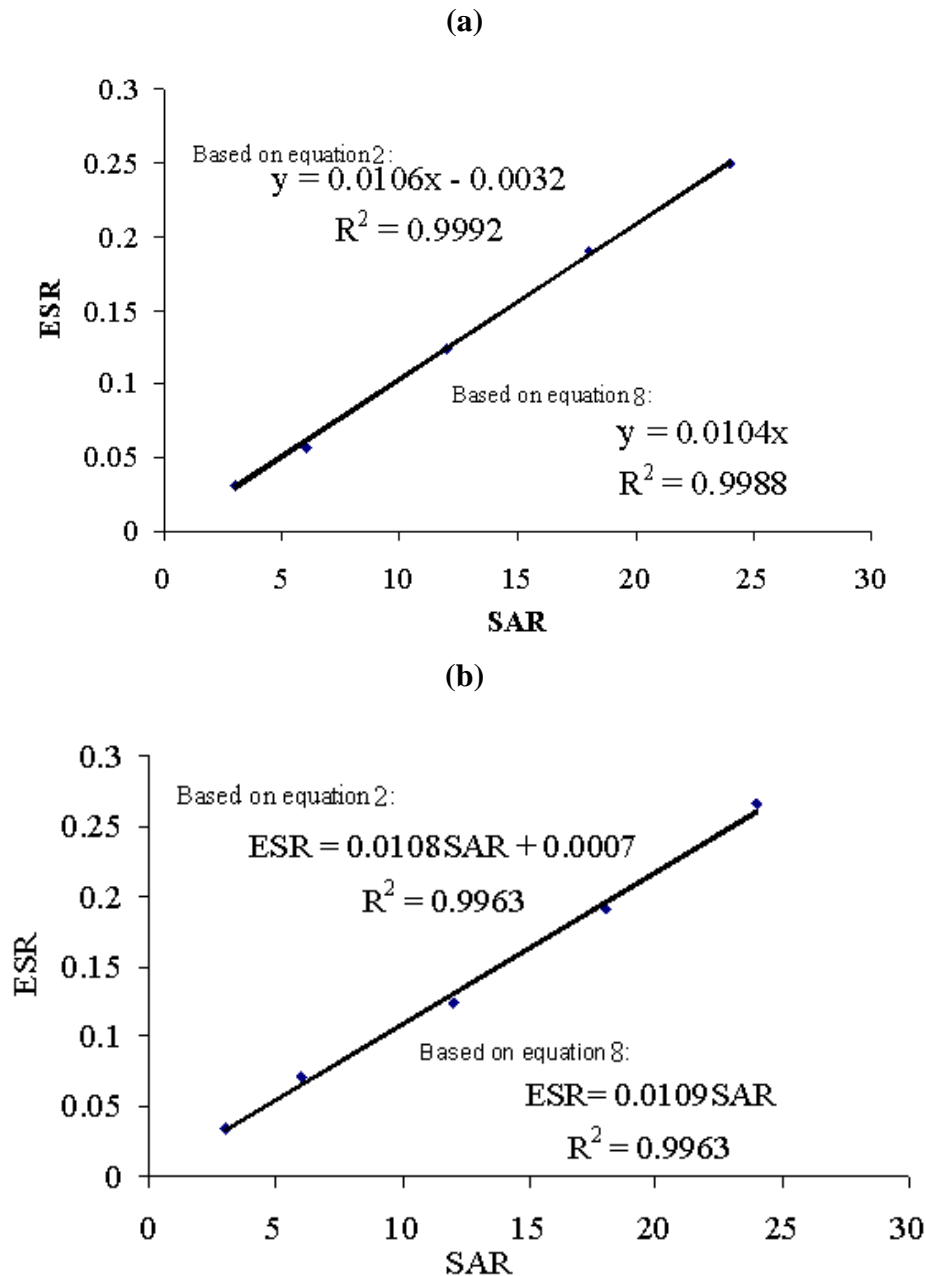


Figure E.1 Relationship between SAR and ESR for Vertosol, (a) is non- Cultivated, and (b) is cultivated Vertosol samples.

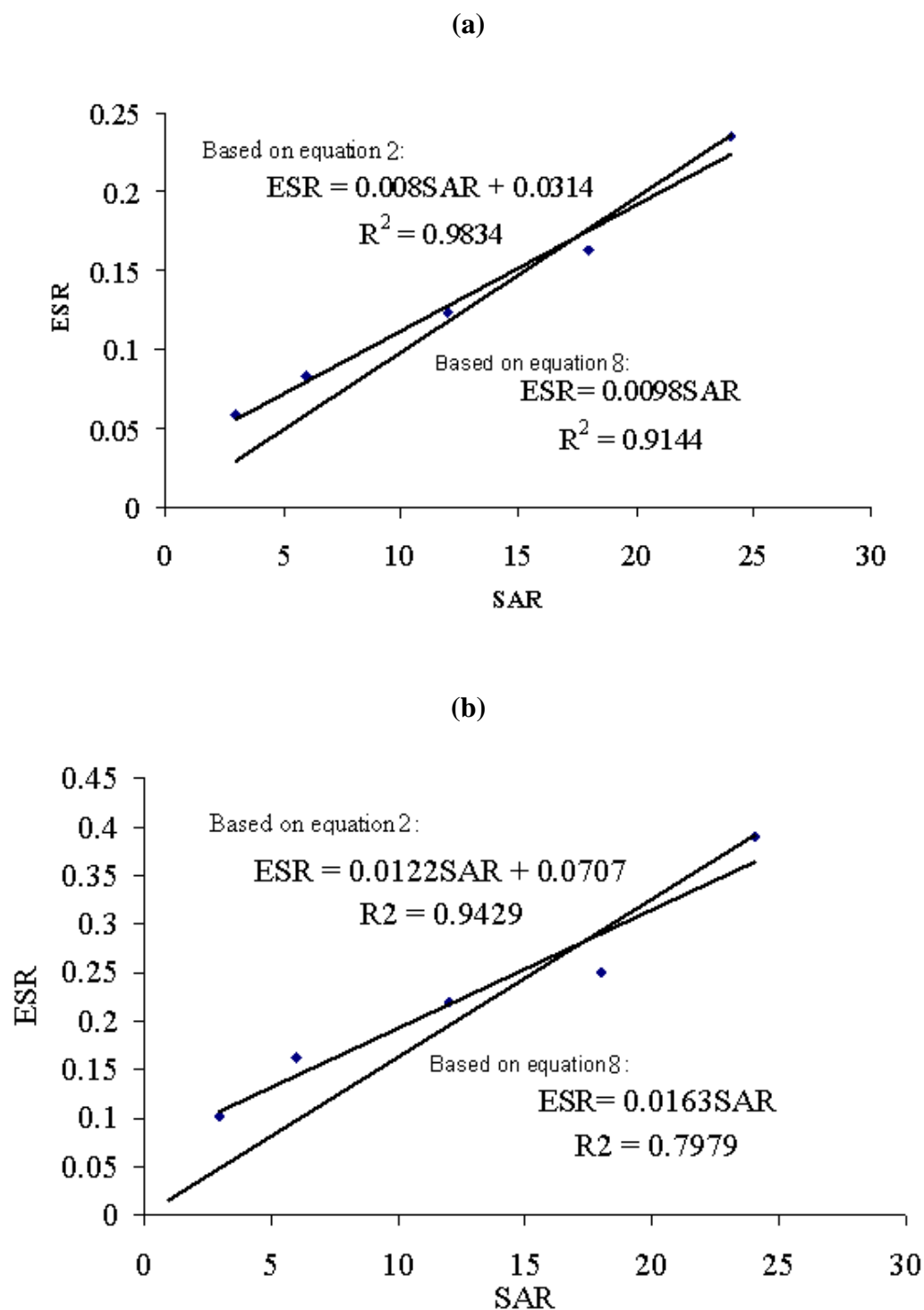


Figure E.2 Relationships between SAR and ESR for Sodosol (a) is non- Cultivated, and (b) is cultivated Vertosol samples

SAR-ESP relationship parameters are varied from USSL staff (1954). The validity of the new parameters up to SAR and ESP about 24 and 19 respectively: the equation for Vertosol non-cultivated is:

$$ESP = \frac{100(-0.0032 + 0.0106SAR)}{1 + (-0.0032 + 0.0106SAR)} \quad (E.11)$$

And for cultivated Vertosol is:

$$ESP = \frac{100(0.0007 + 0.0108SAR)}{1 + (0.0007 + 0.0108SAR)} \quad (E.12)$$

The equation for Sodosol soil in the range of SAR and ESP up to 24 and 20 for non-cultivated soil is:

$$ESP = \frac{100(0.0314 + 0.008SAR)}{1 + (0.0314 + 0.008SAR)} \quad (E.13)$$

And for cultivated condition is:

$$ESP = \frac{100(0.0707 + 0.0122SAR)}{1 + (0.0707 + 0.0122SAR)} \quad (E.14)$$

A comparison between the USSL staff (1954) and both equation obtained for non-cultivated Vertosol and Sodosol is shown in Figure E.3. It was assumed that equations of USSL staff (1954), Vertosol and Sodosol are valid for higher values of ESP and SAR. Figure E.3 shows also that the ESP predicted using USSL staff (1954) equation could overestimate the ESP. But the variation did not exceed a 12% in the whole range of SAR ESP. However, the validity of the new equations is limited to $ESP = 20\%$.

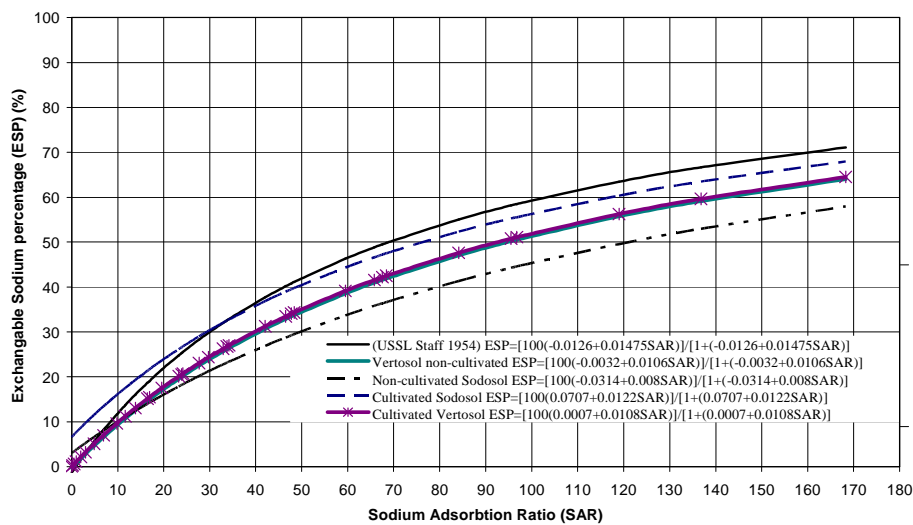


Figure E. 3 Comparison of different SAR- ESP relationships for Vertosol, Sodosol and USSL Staff (1954) at wide range of SAR (0-169)

E.4 Determine the Gapon selectivity coefficients

The exchangeable concentrations of sodium were estimated by multiplying the measured ECEC for the soil by the ESP and conversion with the appropriate units (mmol_c/Kg).

Since the applied solutions were prepared using NaCl and CaCl₂·2H₂O, an assumption was made that the remaining charged surface is neutralised by the Ca cations. This allows estimation of the exchangeable concentration of Ca by subtracting the Na concentration from the ECEC values for each soil.

The concentration of the solution applied was 50 mmol /L. Thus the total solute concentration can be expressed as:

$$\text{Na} + \text{Ca}/2 = 50 \text{ mmol/L} \quad (\text{E. 9})$$

Rearranging equations E.7 and E.9 and considering them as simultaneous equations results in serious of equations that allow determining the Ca and Na concentrations that used to prepare the solutions. To determine the $K_{\text{GNa-Ca}}$ based on equation E.5 a linear regression was conducted between the terms of the $\text{Na}_{\text{ads}}/\text{Ca}_{\text{ads}}$ and $\text{Na}/(\text{Ca})^{0.5}$ as described by white and zaliniy (1986). The resultant regression is shown in the Figures E.4, and E.5.

It should be noted that UNSATCHEM consider reverse exchange reaction between Na and Ca. Thus the KG is considered as Ca-Na, and KG input required is $\text{KG}_{\text{Ca-Na}}$.

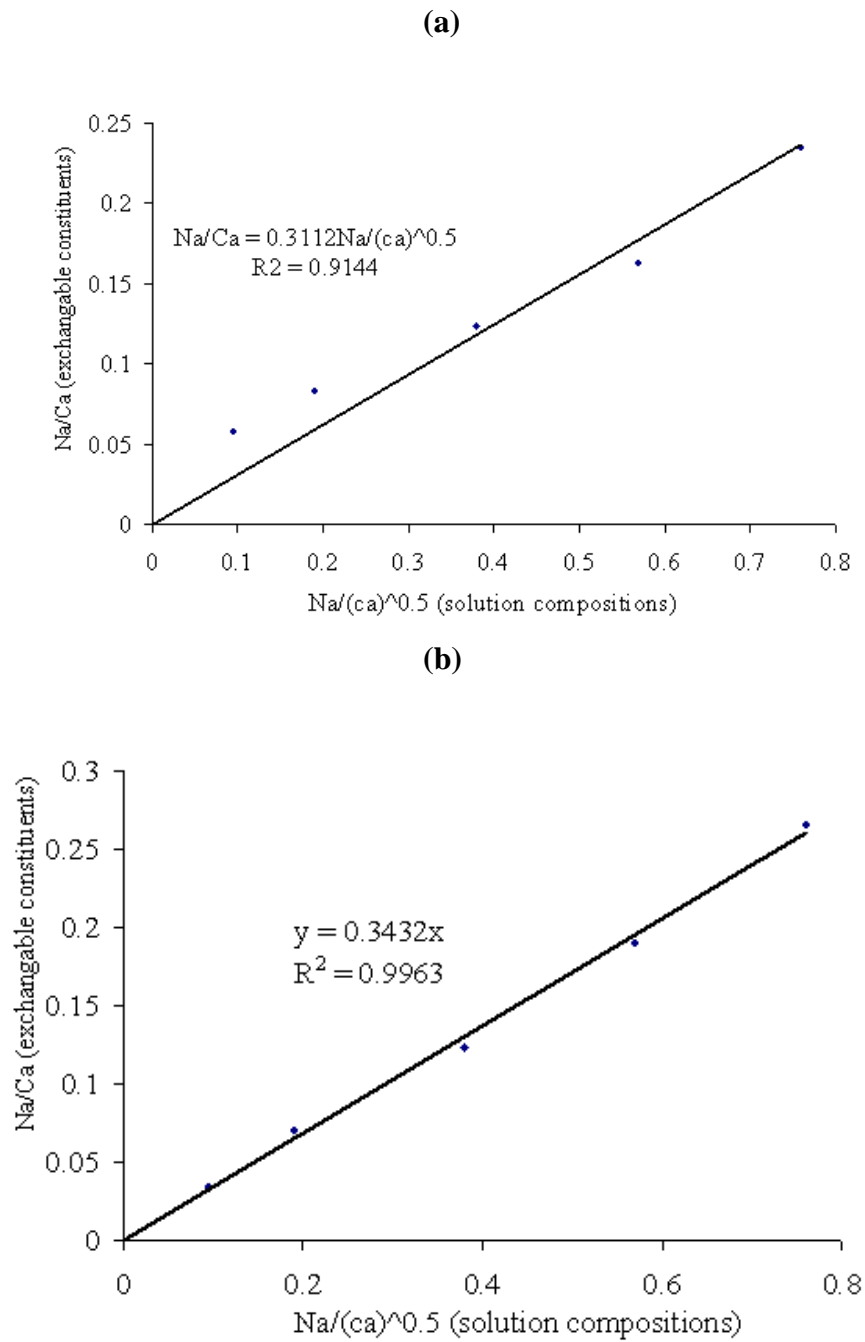


Figure E.4 Determine $K_{\text{GNa-Ca}}$ using the White and Zelazny (1986) equation for (a) non-cultivated Vertosol and (b) cultivated Vertosol.

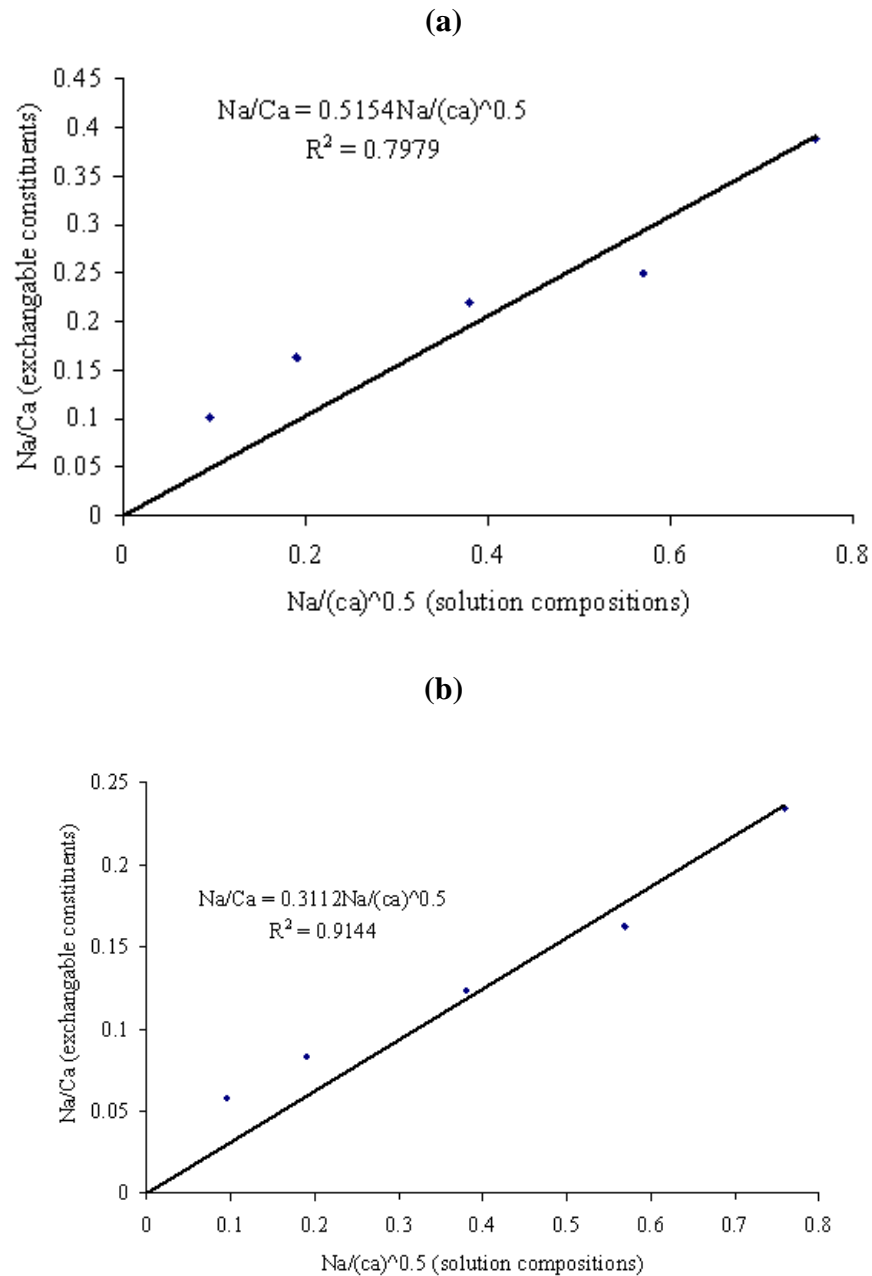


Figure E.5 Determine K_{Na-Ca} using the White and Zelazny (1986) method for (a) non-cultivated Sodosol and (b) cultivated Sodosol.

The resultant KG_{Na-Ca} values are:

Non-cultivated Vertosol $KG_{Na-Ca} = 0.3112 \text{ l}/(\text{mol})^{0.5}$

Cultivated Vertosol $KG_{Na-Ca} = 0.3432 \text{ l}/(\text{mol})^{0.5}$

Non-cultivated Sodosol $KG_{Na-Ca} = 0.5154 \text{ l}/(\text{mol})^{0.5}$

Cultivated Sodosol $KG_{Na-Ca} = 0.03112 \text{ l}/(\text{mol})^{0.5}$

The KG_{Ca-Na} value is inverse to KG_{Na-Ca} , thus the KG_{Ca-Na} values should be used in UNSATCHEM are:

- Non-cultivated Vertosol $KG_{Ca-Na} = 2.91 \text{ l}/(\text{mol})^{0.5}$
- Cultivated Vertosol $KG_{Ca-Na} = 3.03 \text{ l}/(\text{mol})^{0.5}$
- Non-cultivated Sodosol $KG_{Ca-Na} = 1.96 \text{ l}/(\text{mol})^{0.5}$
- Sodosol $KG_{Ca-Na} = 3.22 \text{ l}/(\text{mol})^{0.5}$

The Gapon selectivity coefficient adopted in simulation the column trials using the UNSATCHEM are within is in the average of the range values obtained for different conditions for each soil.

Appendix F: The MATLAB Code to Demonstrate the Three Surface of McNeal (1968) Function

```
% this script loads three parameters and performs 2-D interpolation to the
% result
close all
clear all
[FileName,PathName,FilterIndex] = uigetfile('*.csv','Open Data');
%uiopen('*.csv');

FullFileName=strcat(PathName,FileName);
ArrayData=load(FullFileName,'*.csv');

[vlength,vwidth]=size(ArrayData);

x_ele=ArrayData(1,2:vwidth);
y_ESP=ArrayData(2:vlength,1);
z_ksat=ArrayData(2:vlength,2:vwidth);

for k=2:1:vwidth
    for i=2:1:vlength
        if z_ksat(i-1,k-1)<-1
            z_ksat(i-1,k-1)=-1;
        end
    end
end
% asksat for the minimum and maximum values for x and y
iminx=min(x_ele);
imaxx=max(x_ele);
iminy=min(y_ESP);
imaxy=max(y_ESP);

minx = inputdlg(strcat('Enter the minimum ele value: (actual min=',num2str(iminx),'),','minimum x'));
maxx = inputdlg(strcat('Enter the maximum ele value: (actual max=',num2str(imaxx),'),','maximum x'));
miny = inputdlg(strcat('Enter the minimum ESP value: (actual min=',num2str(iminy),'),','minimum y'));
maxy = inputdlg(strcat('Enter the maximum ESP value: (actual max=',num2str(imaxy),'),','maximum y'));

minx=str2double(minx);
maxx=str2double(maxx);
miny=str2double(miny);
maxy=str2double(maxy);

xi=minx:1:maxx;
yi=miny:1:maxy;
xi=xi';
% creates a grid of X and Y
[I_ELE,I_ESP]=meshgrid(xi,yi);
choosetype='linear';
choosetype=inputdlg('Choose the type of interpolation: linear/spline/cubic','Interpolation Method');
% interpolates using the desired scheme
if strcmp(choosetype,'linear')
    I_KSat=interp2(x_ele,y_ESP,z_ksat,xi,yi,'linear');
else
    if strcmp(choosetype,'spline')
```

```
I_KSat=interp2(x_ele,y_ESP,z_ksat,xi,yi,'spline');
else
    if strcmp(choosetype,'cubic')
        I_KSat=interp2(x_ele,y_ESP,z_ksat,xi,yi,'cubic');
    else
        return;
    end
end
end
%remove all negative values
[vlength,vwidth]=size(I_KSat);
for k=1:1:vwidth
    for i=1:1:vlength
        if I_KSat(i,k)<0
            I_KSat(i,k)=0;
        end
    end
end
%plots the surface
surf(I_ELE,I_ESP,I_KSat)
xlabel('Electrolyte concentration')
ylabel('ESP')
zlabel('Ksat')
colormap('cool')
figure
% plots the contour plot
[C,h]=contourf(I_ELE,I_ESP,I_KSat)
xlabel('Electrolyte concentration')
ylabel('ESP')
zlabel('Ksat')
clabel(C,h)
colormap('cool')
figure
% plots a higher resolution contour plot
min_ksat=min(min(I_KSat));
max_ksat=max(max(I_KSat));
min_ksat=(floor(min_ksat*10))/10;
v=min_ksat:0.1:max_ksat;
[C,h]=contour(I_ELE,I_ESP,I_KSat,v);
xlabel('Electrolyte concentration (mmolc/litre)')
ylabel('ESP (%)')
zlabel('RKsat (Ratio)')
clabel(C,h)
```

Appendix G: Calibration of the Generic Clay Swelling Model Using the Non-linear Regression (TableCurve 3D package)

G.1 The McNeal et al. (1968) RK_{sat} Data

The process of calibration of the generic clay swelling model was carried out using A non-linear surface regression (ordinary least squares method). The model was fitted to the original experimental data from McNeal et al. (1966). The data for higher electrolyte concentrations were excluded as those levels of salinity were not applicable in the model.

The TableCurve 3D software version 4.0.01e was used for the surface fit purpose. The software uses for the fitting process Levenberg and Marquardt method to minimise the sum of squares. The program starts the iteration process using the initial values for the parameters estimated by the user and calculates the sum of squares. The program then goes through a series of iterations to minimise the sum of squares around those initial values and fit the surface closer to the experimental points. During the non-linear fit, the program is likely to counter more than one false minimum (Figure G.1).

To minimise this problem, different initial values need to be tried until the user is certain that the real minimum has been located (Motulsky 1996).

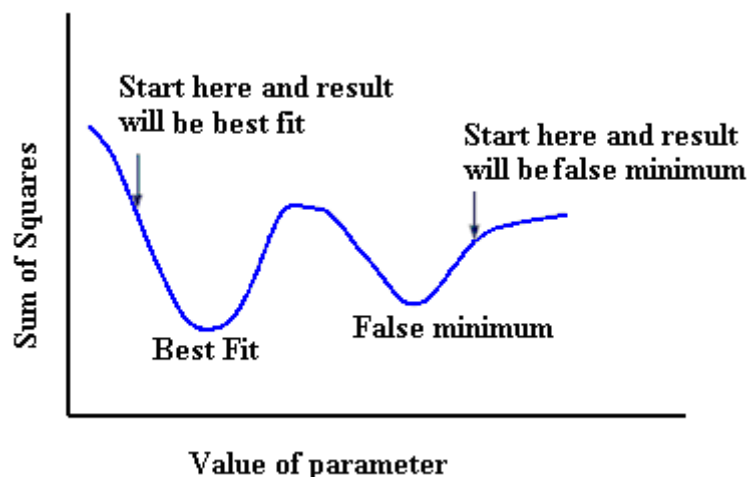


Figure G.1 Demonstration of best fit and false minimum could occur under non-linear regression, Source: (Motulsky 1996)

The initial parameter values were set based on the physical knowledge of the effect of SAR or ESP and salinity on the behaviour of the K_{Sat} and the basic assumption of the domain clay swelling described by McNeal (1968).

The parameters of n and c functions

The proposed n function of ESP (equation 5.24) is allowed to less rapid increase of n with increase of estimated ESP to fall in the range proposed by McNeal (1968) between 1 and 3. Thus, the parameter for a is limited between 0 to 1. This range gives more flexibility to the model to handle different data fitted as n increases with the increase of ESP level. The shape of in n function at b equal zero is demonstrated in Figure G.2. The parameter b is the intercept and account for the minimum n values and set to be between 0 and 2. The intensive fitting process for the entire data available revealed that the best initial values for a and b parameters are 0.3 and 0.7 respectively.

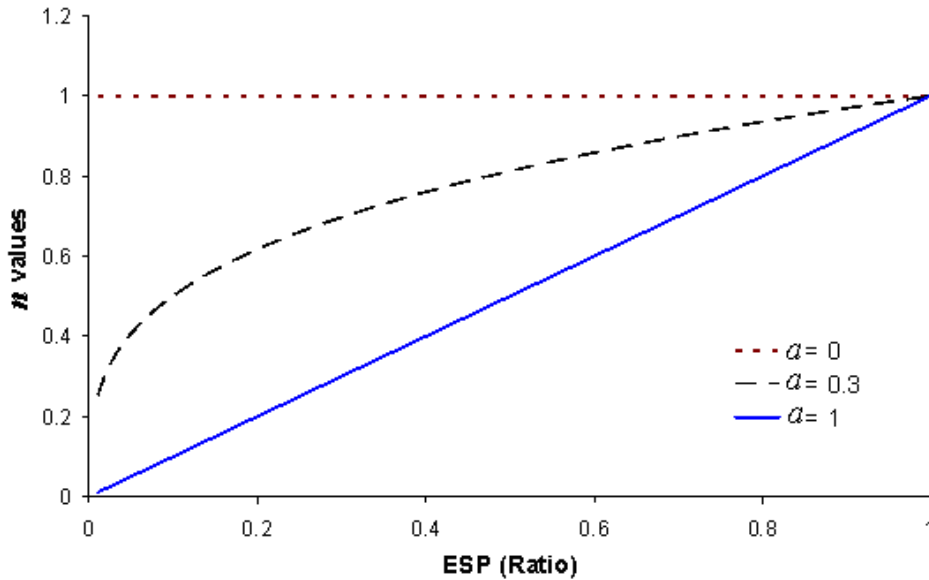


Figure G.2 Demonstration of n function at different values of a parameter at b parameter equal zero

The parameters g and m in the c equation were left with higher range and adjusted during the fitting process. However, it is recommended to set 5 for both parameters as initial values.

Effective weighted fraction of montmorillonite parameter

Despite the physical meaning of the weighted fraction of montmorillonite clay, the difficulties associated with determining montmorillonite ratio and its impact on K_{Sat} are very high in the soil system (consists of different clay types). The preferred way to solve this problem is considering the f_{amount} as a fitting parameter (f) with an initial value equal to the

actual weighted fraction of montmorillonite clay (i.e. f_{amount}). The range of f must be more than 0, and less than 1 in very pure clayey soil. The initial f values for the soil tested were estimated based on general information available about the montmorillonite content.

Initial ESP_T curve parameters

A manipulation of the interpolated ESP_T curve at which K_{sat} reduced by 10% were used as an initial estimation of ESP_T function parameters. The parameters of the interpolated ESP_T functions for soil group a, b, and c obtained from the RK_{sat} data (Figures 5.10, 5.11, and 5.12) were used as initial values for ESP_T parameters. It should be noted that the estimated ESP_T parameters produced from the surface fit represent the estimated critical ESP_T values at which the K_{sat} begin to decline. In addition, the acceptable ESP_T values for irrigation application accept some reduction in K_{sat} which can be calculated from the model using the produced parameters.

Clay swelling model and TableCurve software

“Tablecurve 3D v4.0.01” software allows any model to be entered as a user defined function. The program has the capability to test the defined function statistically and warn for any mistakes. It runs also parameters test for the range that defined for every parameter. As precaution process, the generic clay swelling model was defined in a number of steps. The steps are set as following:

$$F1=(Y/100)^{A0+A1}.$$

$$F2=A2*EXP((Y/100)*A3)$$

$$F3=Y-(A4*LN(X)+A5)$$

$$F4=356.4/((X)^{0.5})-20.5767$$

$$F5=A6*3.6*10^{(-4)}$$

$$F6=IF((F3*F4*F5)>0,F3*F4*F5,0)$$

$$F7=(F2*F6^F1)/(1+F2*F6^F1)$$

$$Z=1-F7$$

where X is designated to electrolyte concentration (mmol/litre), Y is designated to Exchangeable sodium percentage (ESP), and Z is designated to RK_{sat} , $A0$ and $A1$ is the parameters a and b in n function (equation 5.6), $A2$ and $A3$ is g and m respectively in c function (equation 5.7), $A4$ and $A5$ are the parameters for the ESP_T function (equation 5.31), and $A6$ is effective weighted fraction of montmorillonite parameter (f).

G.2. The Sodosol, Vertosols, Red brown, and Alluvial soils

The processes of the GCSM fitting described in section E1 were used in chapter 6 soils. Determining the initial parameters for the ESP_T function and the non-linear regression analyses are described briefly herein.

Determine the initial parameters of the ESP_T

The ESP_T in the GCSM determines the estimated boundary between the flocculation and deflocculation condition under different water quality added in clay swelling model. However, the ESP_T represents the expectable reduction percentage of K_{Sat} as a boundary between the flocculation and deflocculation condition under sodic condition. In chapter 5 and also herein, assumption is made that the initial ESP_T is about 10% reduction of K_{Sat} .

ESP_T curve were determined by fitting different points at different C_o and estimated ESP_T values to a logarithmic function (equation 5.21). The points were estimated by simple interpolation between two experimental values of RK_{Sat} values at each C_o level. The obtained ESP_T equations were summarised in Table G.1 for the entire RK_{Sat} data obtained. However, this calculation is rough prediction and depends on the accuracy of these points only. The parameters obtained are used only as initial values in non-linear regression step.

Table G.1 ESP_T equations determined from experimental data at 10% K_{Sat} reduction for the soil tested

Soil type	ESP_T Estimated	Coefficient of determination (R^2)
Sodosol	$ESP_T = 11.539 \ln(C_o) - 1.779$	0.958
Brown Vertosol	$ESP_T = 11.798 \ln(C_o) - 21.468$	0.897
Grey Vertosol	$ESP_T = 7.321 \ln(C_o) - 10.238$	0.978
Red Brown	$ESP_T = 12.397 \ln(C_o) - 36.514$	0.962
Alluvial	$ESP_T = 15.466 \ln(C_o) - 58.038$	0.928

The GCSM user defined function in TableCurve 3D program

Tablecurve 3D software version 4.01 was used for a surface fit for the data obtained as described in section E.1. In this process, the parameters a , b , g , m , s , l and f were estimated for the data obtained. It is worth noting that n should be at the range from 0 to 3. Thus, the parameter a was set at the range from 0 to 1, while parameter b between 0 and 2. In addition the parameter f related to the weighted fraction of montmorillonite clay and has the range from 0 to less than 1. The process of identifying the GCSM as a user function in TableCurve 3D program and fitting is similar to that discussed in detail in section G.1.

Appendix H: Results of Non-linear Regression for Soils (a), (b), and (c) from McNeal et al. (1968)

Group (a) Soils

Data Description:

X Variable: Electrolyte concentration (mmolc/litre)

Xmin:	3.13	Xmax:	200	Xrange:	196.87
Xmean:	66.4075	Xstd:	81.692468319		

Y Variable: ESP (%)

Ymin:	0	Ymax:	100	Yrange:	100
Ymean:	46.3725	Ystd:	38.646331693		

Z Variable: Rksat (Ratio)

Zmin:	0.14	Zmax:	1.07	Zrange:	0.93
Zmean:	0.73	Zstd:	0.36		

Initial value for the parameters:

Parameter	Value
<i>a</i>	0.3
<i>b</i>	0.7
<i>g</i>	5
<i>m</i>	5
<i>s</i>	12.186
<i>l</i>	2.7863
<i>f</i>	0.01

Non-linear regression output:

Procedure	Minimization	Iterations
Lev-Marq	Least Squares	30

r ² Coef Det	DF Adj r ²	Fit Std Err
0.9803274426	0.9631139549	0.0651864433

Source	Sum of Squares	DF	Mean Square	F Statistic	P>F
Regr	1.9057565	6	0.31762609	74.7483	0.00000
Error	0.038243452	9	0.0042492724		
Total	1.944	15			

Parameters produced:

Parm	Value	Std Error	t-value	95.00% Confidence Limits		P> t
<i>a</i>	0.648824698	18.71485338	0.03466897	-41.6871149	42.9847643	0.97310
<i>b</i>	0.00028293	7.419605069	3.81327e-05	-16.7840298	16.78459567	0.99997
<i>g</i>	8.837082547	1.31339e+07	6.72846e-07	-2.9711e+07	2.97109e+07	1.00000
<i>m</i>	4.045954505	3.57445e+06	1.13191e-06	-8.086e+06	8.08597e+06	1.00000
<i>s</i>	6.356358691	308.3642704	0.020613149	-691.212084	703.9248014	0.98400
<i>l</i>	30.8180756	1383.329387	0.02227819	-3098.49041	3160.126556	0.98271
<i>f</i>	0.00847054	42854.17061	1.9766e-07	-96942.8605	96942.87743	1.00000

Model precision :

XYZ *	X Value	Y Value	Z Value	Z Predict	Residual	Residual %	Weights
1	200	100	0.82	0.7984728	0.0215272	2.6252683	1
2	200	59.3	0.96	1	-0.04	-4.166667	1
3	200	26.19	0.99	1	-0.01	-1.010101	1
4	200	0	1.07	1	0.07	6.5420561	1
5	50	100	0.29	0.3297096	-0.03971	-13.69295	1
6	50	59.3	0.76	0.7572782	0.0027218	0.358129	1
7	50	26.19	0.99	1	-0.01	-1.010101	1
8	50	0	1.06	1	0.06	5.6603774	1
9	12.5	100	0.14	0.1323099	0.0076901	5.492911	1
10	12.5	59.3	0.38	0.3899826	-0.009983	-2.62699	1
11	12.5	26.19	0.93	1	-0.07	-7.526882	1
12	12.5	0	1.03	1	0.03	2.9126214	1
13	3.13	100	0.14	0.0548277	0.0851723	60.837331	1
14	3.13	59.3	0.21	0.1964844	0.0135156	6.4359882	1
15	3.13	26.19	0.89	1	-0.11	-12.35955	1
16	3.13	0	1.02	1	0.02	1.9607843	1

Group (b) Soils

Data Description:

X Variable: Electrolyte concentration (mmolc/litre)

Xmin: 3.13 Xmax: 200 Xrange: 196.87
Xmean: 66.4075 Xstd: 81.692468319

Y Variable: ESP (%)

Ymin: 0 Ymax: 100 Yrange: 100
Ymean: 46.3725 Ystd: 38.646331693

Z Variable: Rksat (ratio)

Zmin: 0 Zmax: 1.01 Zrange: 1.01
Zmean: 0.5 Zstd: 0.4369591896

Initial values:

Parameter	Value
<i>a</i>	0.3
<i>b</i>	0.7
<i>g</i>	5
<i>m</i>	5
<i>s</i>	9.5
<i>l</i>	-12.122
<i>f</i>	0.16

Non-linear regression output:

Procedure	Minimization	Iterations
Lev-Marq	Least Squares	34

r^2 Coef Det	DF Adj r^2	Fit Std Err	F Statistic	P>F
0.9734175722	0.9501579478	0.0919734704	112.480386	0.00000

Parameters produced:

Parm	Value	Std Error	t-value	95.00% Confidence Limits		P> t
<i>a</i>	0.999813404	10.04779242	0.099505778	-21.7298722	23.72949899	0.92292
<i>b</i>	0.912408903	3.02125467	0.301996688	-5.92214399	7.746961792	0.76952
<i>g</i>	1.437852328	271336.2874	5.29915e-06	-613803.888	613806.7637	1.00000
<i>m</i>	7.289829926	206808.5764	3.52492e-05	-467826.212	467840.7921	0.99997
<i>s</i>	4.105146401	8.638823667	0.475197383	-15.4372304	23.64752323	0.64597
<i>l</i>	-5.05432685	10.58238171	-0.47761714	-28.9933374	18.88468373	0.64431
<i>f</i>	0.204620785	42317.78166	4.83534e-06	-95729.2682	95729.67748	1.00000

Model precision:

XYZ *	X Value	Y Value	Z Value	Z Predict	Residual	Residual %	Weights
1	200	100	0.35	0.301377	0.048623	13.892298	1
2	200	59.3	0.76	0.8437137	-0.083714	-11.01495	1
3	200	26.19	1	0.9885863	0.0114137	1.1413719	1
4	200	0	1.01	1	0.01	0.990099	1
5	50	100	0.07	0.0106463	0.0593537	84.790964	1
6	50	59.3	0.1	0.212687	-0.112687	-112.687	1
7	50	26.19	0.9	0.8482445	0.0517555	5.7506092	1
8	50	0	1	1	0	0	1
9	12.5	100	0	0.0014385	-0.001439	0	1
10	12.5	59.3	0	0.0489778	-0.048978	0	1
11	12.5	26.19	0.62	0.5461334	0.0738666	11.913973	1
12	12.5	0	0.98	1	-0.02	-2.040816	1
13	3.13	100	0	0.0002722	-0.000272	0	1
14	3.13	59.3	0	0.0128599	-0.01286	0	1
15	3.13	26.19	0.26	0.2587605	0.0012395	0.4767441	1
16	3.13	0	0.96	0.9888317	-0.028832	-3.003305	1

Group (c) Soils

Data Description:

X Variable: Electrolyte concentration (mmolc/litre)

Xmin: 3.13 Xmax: 200 Xrange: 196.87
Xmean: 66.4075 Xstd: 81.692468319

Y Variable: ESP (%)

Ymin: 0 Ymax: 100 Yrange: 100
Ymean: 46.3725 Ystd: 38.646331693

Z Variable: Rksat (Ratio)

Zmin: 0 Zmax: 1.06 Zrange: 1.06
Zmean: 0.375 Zstd: 0.4405602494

Initial values for the parameters:

Parameter	Value
<i>a</i>	0.3
<i>b</i>	0.7
<i>g</i>	5
<i>m</i>	5
<i>s</i>	4.2986
<i>l</i>	-12.122
<i>f</i>	0.3

Non-linear regression output:

Procedure	Minimization	Iterations			
Lev-Marq	Least Squares	41			
r ² Coef Det	DF Adj r ²	Fit Std Err			
0.9905737341	0.9823257514	0.0552203974			
Source	Sum of Squares	DF	Mean Square	F Statistic	P>F
Regr	2.8839564	6	0.48065939	157.63	0.00000
Error	0.027443631	9	0.0030492923		
Total	2.9114	15			

Parameters produced:

Parm	Value	Std Error	t-value	95.00% Confidence Limits		P> t
<i>a</i>	0.448931242	13.64075598	0.032911024	-30.4086026	31.30646508	0.97446
<i>b</i>	1.005100513	5.199347603	0.193312813	-10.7566409	12.76684193	0.85101
<i>g</i>	0.845982082	35.88124581	0.023577277	-80.3230351	82.01499927	0.98170
<i>m</i>	10.96712218	41.07702119	0.266989228	-81.9555555	103.8897998	0.79549
<i>s</i>	4.079853846	79.30112491	0.051447616	-175.311754	183.4714615	0.96009
<i>l</i>	-11.1472102	225.5609393	-0.04941995	-521.401505	499.1070842	0.96166
<i>f</i>	0.53488594	15.97466906	0.033483382	-35.6023261	36.67209796	0.97402

Model precision:

XYZ *	X Value	Y Value	Z Value	Z Predict	Residual	Residual %	Weights
1	200	100	0.03	0.0032408	0.0267592	89.19733	1
2	200	59.3	0.33	0.3306681	-0.000668	-0.202461	1
3	200	26.19	0.84	0.9806354	-0.140635	-16.74231	1
4	200	0	1.06	1	0.06	5.6603774	1
5	50	100	0	6.847e-05	-6.85e-05	0	1
6	50	59.3	0.01	0.0140677	-0.004068	-40.67686	1
7	50	26.19	0.66	0.6347136	0.0252864	3.8312689	1
8	50	0	1.03	1	0.03	2.9126214	1
9	12.5	100	0	8.387e-06	-8.39e-06	0	1
10	12.5	59.3	0	0.0020168	-0.002017	0	1
11	12.5	26.19	0.2	0.206053	-0.006053	-3.026488	1
12	12.5	0	0.99	0.9893437	0.0006563	0.0662974	1
13	3.13	100	0	1.473e-06	-1.47e-06	0	1
14	3.13	59.3	0	0.0003993	-0.000399	0	1
15	3.13	26.19	0.01	0.0518494	-0.041849	-418.4937	1
16	3.13	0	0.84	0.8404515	-0.000452	-0.053752	1

Appendix I: Calculations of EC and SAR for the Standard Solutions Used in Soil Stability Indicator Experiments

Number of solution	Na ⁺ (mmol _c /L)	Ca ²⁺ (mmol _c /L)	Na (mg) ⁽¹⁾	Ca (mg) ⁽²⁾	NaCl (mg) ⁽³⁾	CaCl ₂ .H ₂ O (mg) ⁽⁴⁾	SAR ⁽⁵⁾ (mmol _c /L) ^{0.5}	EC ⁽⁶⁾ (dS/m)
1	116.96	1.00	2689.00	20.06	6835.36	73.60	165.3	12
2	58.48	0.50	1344.50	10.03	3417.68	36.80	116.9	6
3	29.24	0.25	672.25	5.02	1708.84	18.40	82.7	3
4	14.62	0.13	336.12	2.51	854.42	9.20	58.4	1.5
5	7.31	0.06	168.06	1.25	427.21	4.60	41.3	0.75
6	116.47	1.50	2677.70	30.10	6806.64	110.40	134.4	12
7	58.24	0.75	1338.85	15.05	3403.32	55.20	95.0	6
8	29.12	0.38	669.42	7.52	1701.66	27.60	67.2	3
9	14.56	0.19	334.71	3.76	850.83	13.80	47.5	1.5
10	7.28	0.09	167.36	1.88	425.42	6.90	33.6	0.75
11	115.00	3.00	2643.80	60.19	6720.48	220.80	93.8	12
12	57.50	1.50	1321.90	30.10	3360.24	110.40	66.4	6
13	28.75	0.75	660.95	15.05	1680.12	55.20	46.9	3
14	14.37	0.38	330.48	7.52	840.06	27.60	33.2	1.5
15	7.19	0.19	165.24	3.76	420.03	13.80	23.5	0.75
16	112.05	6.01	2576.01	120.39	6548.16	441.60	64.7	12
17	56.02	3.00	1288.01	60.19	3274.08	220.80	45.7	6
18	28.01	1.50	644.00	30.10	1637.04	110.40	32.3	3
19	14.01	0.75	322.00	15.05	818.52	55.20	22.9	1.5
20	7.00	0.38	161.00	7.52	409.26	27.60	16.2	0.75
21	94.36	24.03	2169.27	481.55	5514.24	1766.40	27.2219	12
22	47.18	12.01	1084.64	240.77	2757.12	883.20	19.2488	6
23	23.59	6.01	542.32	120.39	1378.56	441.60	13.611	3
24	11.79	3.00	271.16	60.19	689.28	220.80	9.62441	1.5
25	5.90	1.50	135.58	30.10	344.64	110.40	6.80549	0.75

(1) Na weight calculated as Na = mmol_c/L of Na⁺ × 22.99.

(2) Ca weight calculated as Ca = mmol_c/L of Ca × 20.04.

(3) Weight of NaCl salt calculated as NaCl = Na (mg)* 58.44/22.99.

(4) Weight of CaCl₂.H₂O calculated as = Ca (mg)* 147.02/20.04.

(5) SAR is calculated as: $SAR = Na^+ / \sqrt{Ca^{2+} / 2}$

(6) EC values were calculated from the empirical relationship (USSS Staff 1954):
EC ≈ total cation concentrations (mmol_c/L)/10.

Appendix J: The Results of Non-linear Regression for Local Soils

Sodosol Soil

Data Description:

X Variable: Electrolyte concentration (mmolc/litre)

Xmin:	7.5	Xmax:	120	Xrange:	112.5
Xmean:	45.9375	Xstd:	42.559501187		

Y Variable: ESP (%)

Ymin:	8.0341377281	Ymax:	70.737217285	Yrange:	62.703079557
Ymean:	38.359348483	Ystd:	17.693907933		

Z Variable: Rksat (Ratio)

Zmin:	0.577	Zmax:	1.002	Zrange:	0.425
Zmean:	0.8444166667	Zstd:	0.1552828882		

Initial parameters:

Parameter	Value
<i>a</i>	0.3
<i>b</i>	0.7
<i>g</i>	5
<i>m</i>	5
<i>s</i>	11.539
<i>l</i>	-1.779
<i>f</i>	0.07

Non-linear regression output:

Procedure	Minimization	Iterations			
Lev-Marq	Least Squares	58			
r ² Coef Det	DF Adj r ²	Fit Std Err			
0.8948466626	0.8488420775	0.0585699142			
Source	Sum of Squares	DF	Mean Square	F Statistic	P>F
Regr	0.49627644	6	0.08271274	24.1114	0.00000
Error	0.058317392	17	0.0034304349		
Total	0.55459383	23			

Parameters produced:

Parm	Value	Std Error	t-value	95.00% Confidence Limits		P> t
<i>a</i>	8.70892e-07	1.580524707	5.51015e-07	-3.33461478	3.33461652	1.00000
<i>b</i>	0.525707277	1.358596233	0.38694887	-2.34068022	3.392094775	0.70360
<i>g</i>	4.41708186	3.59375e+07	1.2291e-07	-7.5822e+07	7.58216e+07	1.00000
<i>m</i>	7.104965059	9.767865831	0.727381516	-13.5034304	27.71336056	0.47689
<i>s</i>	8.256050043	5.933424567	1.391447713	-4.26238154	20.77448163	0.18203
<i>l</i>	0.69223825	29.09750457	0.023790296	-60.6981302	62.08260668	0.98130
<i>f</i>	0.061322697	327011.5768	1.87525e-07	-689934.058	689934.1805	1.00000

Model precision:

XYZ *	X Value	Y Value	Z Value	Z Predict	Residual	Residual %	Weights
1	120	70.737217	0.577	0.6994092	-0.122409	-21.21476	1
2	120	66.251333	0.723	0.8030965	-0.080097	-11.07836	1
3	120	57.739217	0.959	0.9317998	0.0272002	2.836307	1
4	120	48.413456	0.998	0.9883017	0.0096983	0.9717732	1
5	120	27.91442	0.995	1	-0.005	-0.502513	1
6	60	63.042763	0.612	0.5845858	0.0274142	4.4794386	1
7	60	58.051932	0.719	0.7289705	-0.009971	-1.386718	1
8	60	39.729627	1.002	0.9899106	0.0120894	1.2065264	1
9	60	21.237516	0.953	1	-0.047	-4.931794	1
10	30	54.609208	0.602	0.5596755	0.0423245	7.0306552	1
11	30	49.373241	0.805	0.7225983	0.0824017	10.236235	1
12	30	40.363662	0.874	0.9223658	-0.048366	-5.533848	1
13	30	31.610371	0.982	0.994748	-0.012748	-1.298171	1
14	30	15.776707	0.975	1	-0.025	-2.564103	1
15	15	45.825297	0.589	0.5826752	0.0063248	1.0738151	1
16	15	40.675704	0.846	0.7485152	0.0974848	11.52303	1
17	15	32.223608	0.93	0.9362885	-0.006288	-0.676178	1
18	15	24.47301	0.929	0.9977205	-0.06872	-7.397252	1
19	15	11.388367	0.995	1	-0.005	-0.502513	1
20	7.5	37.284808	0.583	0.620045	-0.037045	-6.354201	1
21	7.5	32.492642	0.79	0.7771562	0.0128438	1.6257945	1
22	7.5	24.972803	0.907	0.9441918	-0.037192	-4.100526	1
23	7.5	18.403316	0.981	0.998143	-0.017143	-1.747505	1
24	7.5	8.0341377	0.94	1	-0.06	-6.382979	1

Brown Vertosol

Data Description:

X Variable: Electrolyte concentration (mmolc /litre)

Xmin: 7.5 Xmax: 120 Xrange: 112.5
Xmean: 46.630434783 Xstd: 43.377365639

Y Variable: ESP (%)

Ymin: 8.0341377281 Ymax: 70.737217285 Yrange: 62.703079557
Ymean: 39.341202452 Ystd: 17.410240129

Z Variable: Rksat (Ratio)

Zmin: 0.445 Zmax: 0.94 Zrange: 0.495
Zmean: 0.7393043478 Zstd: 0.1478323482

Initial parameters:

Parameter	Value
<i>a</i>	0.3
<i>b</i>	0.7
<i>g</i>	5
<i>m</i>	5
<i>s</i>	11.798
<i>l</i>	-21.468
<i>f</i>	0.7

Non-linear regression output:

Procedure	Minimization	Iterations			
Lev-Marq	Least Squares	73			
r ² Coef Det	DF Adj r ²	Fit Std Err			
0.6581122208	0.4985645904	0.101359069			
Source	Sum of Squares	DF	Mean Square	F Statistic	P>F
Regr	0.3164183	6	0.052736383	5.13316	0.00408
Error	0.16437857	16	0.010273661		
Total	0.48079687	22			

Parameter produced:

Parm	Value	Std Error	t-value	95.00% Confidence Limits		P> t
<i>a</i>	3.66271e-08	1.823764811	2.00833e-08	-3.86620865	3.866208726	1.00000
<i>b</i>	0.024029719	0.964663056	0.024909961	-2.02096461	2.069024044	0.98043
<i>g</i>	0.954920914	2.17712e+08	4.38617e-09	-4.6153e+08	4.61529e+08	1.00000
<i>m</i>	4.304250223	5.670889672	0.759007929	-7.71749885	16.3259993	0.45888
<i>s</i>	6.310675997	51.37648227	0.122831999	-102.602601	115.2239531	0.90377
<i>l</i>	-19.3432205	307.1051597	-0.06298566	-670.377076	631.6906352	0.95056
<i>f</i>	0.107352095	2.39008e+07	4.49156e-09	-5.0667e+07	5.06675e+07	1.00000

Model precision:

XYZ *	X Value	Y Value	Z Value	Z Predict	Residual	Residual %	Weights
1	120	70.737217	0.534	0.6626504	-0.12865	-24.09184	1
2	120	66.251333	0.668	0.7207064	-0.052706	-7.89018	1
3	120	57.739217	0.798	0.8153627	-0.017363	-2.175775	1
4	120	48.413456	0.864	0.8922403	-0.02824	-3.268556	1
5	120	27.91442	0.94	0.9782209	-0.038221	-4.066051	1
6	60	63.042763	0.445	0.5724637	-0.127464	-28.64354	1
7	60	58.051932	0.753	0.6459645	0.1070355	14.214546	1
8	60	39.729627	0.788	0.8629048	-0.074905	-9.50569	1
9	60	21.237516	0.899	0.9697623	-0.070762	-7.871218	1
10	30	54.609208	0.536	0.5395498	-0.00355	-0.662281	1
11	30	49.373241	0.746	0.6204627	0.1255373	16.828059	1
12	30	40.363662	0.829	0.7494981	0.0795019	9.5900974	1
13	30	31.610371	0.855	0.8505429	0.0044571	0.5212968	1
14	15	45.825297	0.48	0.5353124	-0.055312	-11.52341	1
15	15	40.675704	0.701	0.6175465	0.0834535	11.904918	1
16	15	32.223608	0.844	0.7441158	0.0998842	11.834622	1
17	15	24.47301	0.804	0.8404841	-0.036484	-4.537823	1
18	15	11.388367	0.834	0.9485195	-0.11452	-13.73136	1
19	7.5	37.284808	0.478	0.540927	-0.062927	-13.16465	1
20	7.5	32.492642	0.706	0.6197943	0.0862057	12.21044	1
21	7.5	24.972803	0.895	0.7370993	0.1579007	17.642535	1
22	7.5	18.403316	0.771	0.8252558	-0.054256	-7.037065	1
23	7.5	8.0341377	0.836	0.9273314	-0.091331	-10.92481	1

Gray Vertosol soil

Data Description:

X Variable: Electrolyte concentration (mmolc/litre)

Xmin: 7.5 Xmax: 120 Xrange: 112.5
Xmean: 46.5 Xstd: 41.758232721

Y Variable: ESP (%)

Ymin: 3.6551948739 Ymax: 57.749192246 Yrange: 54.093997372
Ymean: 22.743498551 Ystd: 14.970107303

Z Variable: RKsat (Ratio)

Zmin: 0.3005642361 Zmax: 1.0105029586 Zrange: 0.7099387225
Zmean: 0.6461765989 Zstd: 0.2450446477

Initial parameters:

Parameter	Value
<i>a</i>	0.3
<i>b</i>	0.7
<i>g</i>	5
<i>m</i>	5
<i>s</i>	7.321
<i>l</i>	-10.238
<i>f</i>	0.7

Non-linear regression output:

Lev-Marq	Least Squares	51			
r ² Coef Det	DF Adj r ²	Fit Std Err			
0.8809904645	0.8319865381	0.0976125075			
Source	Sum of Squares	DF	Mean Square	F Statistic	P>F
Regr	1.2696175	6	0.21160291	22.2081	0.00000
Error	0.17150763	18	0.0095282016		
Total	1.4411251	24			

Parameter produced:

Parm	Value	Std Error	t-value	95.00% Confidence Limits		P> t
<i>a</i>	0.9897425	6.45841736	0.153248458	-12.5788889	14.55837388	0.87991
<i>b</i>	0.071494063	2.104802953	0.033967105	-4.35053285	4.493520979	0.97328
<i>g</i>	0.806778205	120.1870139	0.00671269	-251.696768	253.3103247	0.99472
<i>m</i>	5.183495497	1992.907354	0.002600972	-4181.75949	4192.126481	0.99795
<i>s</i>	6.766511955	6.569180888	1.030038915	-7.03482496	20.56784887	0.31663
<i>l</i>	-7.98327265	23.82781217	-0.3350401	-58.0436484	42.07710311	0.74147
<i>f</i>	0.23447671	467.1483535	0.000501932	-981.207796	981.676749	0.99961

Model precision:

XYZ	X Value	Y Value	Z Value	Z Predict	Residual	Residual %	Weights
1	120	57.749192	0.3005642	0.3620482	-0.061484	-20.45617	1
2	120	48.394718	0.4261879	0.4468133	-0.020625	-4.839508	1
3	120	27.931178	0.7909499	0.6826943	0.1082556	13.686789	1
4	120	24.411155	1.010503	1	0.010503	1.0393793	1
5	120	15.934931	0.95006	1	-0.04994	-5.256513	1
6	60	49.052278	0.4168644	0.3177867	0.0990777	23.767377	1
7	60	39.738143	0.3518073	0.4115372	-0.05973	-16.97801	1
8	60	21.282012	0.5651163	0.6794211	-0.114305	-20.22678	1
9	60	18.345165	0.9573171	1	-0.042683	-4.458599	1
10	60	11.531433	0.9207337	1	-0.079266	-8.609035	1
11	30	40.373595	0.3786693	0.3205067	0.0581626	15.359745	1
12	30	31.628282	0.422953	0.4162602	0.0066928	1.5824007	1
13	30	15.788147	0.5402362	0.681086	-0.14085	-26.0719	1
14	30	13.432899	0.8804348	1	-0.119565	-13.58025	1
15	30	8.1285441	0.991338	1	-0.008662	-0.873768	1
16	15	32.207901	0.3893908	0.3430286	0.0463621	11.906321	1
17	15	24.437755	0.474776	0.434219	0.0405571	8.5423552	1
18	15	11.416534	0.5214326	0.6390404	-0.117608	-22.55475	1
19	15	9.5868344	0.8825391	1	-0.117461	-13.30943	1
20	15	5.5599224	0.9593076	1	-0.040692	-4.241848	1
21	7.5	24.939276	0.3996248	0.3731542	0.0264706	6.6238654	1
22	7.5	18.367116	0.4797636	0.4540549	0.0257087	5.3586101	1
23	7.5	8.0409579	0.5673553	0.5950709	-0.027716	-4.885051	1
24	7.5	6.6543004	0.7510761	0.6282037	0.1228724	16.35951	1
25	7.5	3.6551949	0.8254141	1	-0.174586	-21.15131	1

Red brown soil

Data description:

X Variable: Electrolyte concentration (mmolc/litre)

Xmin: 2.5 Xmax: 640 Xrange: 637.5
Xmean: 145.5 Xstd: 209.80475618

Y Variable: ESP (%)

Ymin: 0 Ymax: 36.524057382 Yrange: 36.524057382
Ymean: 21.190160098 Ystd: 13.161602385

Z Variable: RKsat (Ratio)

Zmin: 0.001 Zmax: 1 Zrange: 0.999
Zmean: 0.5527333333 Zstd: 0.421983491

Initial parameters:

Parameter	Value
<i>a</i>	0.3
<i>b</i>	0.7
<i>g</i>	5
<i>m</i>	5
<i>s</i>	12.397
<i>l</i>	-36.514
<i>f</i>	0.4

Non-linear regression output:

Procedure	Minimization	Iterations			
Lev-Marq	Least Squares	35			
r ² Coef Det	DF Adj r ²	Fit Std Err			
0.9746223159	0.9390935581	0.092691716			
Source	Sum of Squares	DF	Mean Square	F Statistic	P>F
Regr	1.9797824	6	0.32996373	38.4047	0.00016
Error	0.051550525	6	0.0085917542		
Total	2.0313329	12			

Parameter produced:

Parm	Value	Std Error	t-value	95.00% Confidence Limits		P> t
<i>a</i>	3.85517e-05	2.663828549	1.44723e-05	-6.51811509	6.518192195	0.99999
<i>b</i>	0.470427166	5.261354139	0.089411804	-12.4036426	13.34449695	0.93166
<i>g</i>	4.52435445	911388.8857	4.96424e-06	-2.2301e+06	2.23009e+06	1.00000
<i>m</i>	9.935846919	24.72957339	0.401779956	-50.5752393	70.44693309	0.70177
<i>s</i>	10.3979415	50.29427241	0.20674206	-112.66771	133.4635926	0.84305
<i>l</i>	-31.1359509	211.5325156	-0.14719227	-548.73737	486.4654681	0.88780
<i>f</i>	0.368743153	50517.8163	7.29927e-06	-123612.275	123613.0121	0.99999

Model precision:

XYZ	X Value	Y Value	Z Value	Z Predict	Residual	Residual %	Weights
1	160	36.524057	0.815	0.7378568	0.0771432	9.4654236	1
2	160	21.960356	1	0.9996982	0.0003018	0.0301779	1
3	160	11.847673	1	1	0	0	1
4	160	0	1	1	0	0	1
5	80	36.524057	0.26	0.286212	-0.026212	-10.08154	1
6	40	36.524057	0.011	0.0963304	-0.08533	-775.7306	1
7	40	21.960356	0.528	0.5544563	-0.026456	-5.010661	1
8	40	11.847673	0.882	0.9491666	-0.067167	-7.615262	1
9	20	36.524057	0.001	0.0355525	-0.034553	-3455.253	1
10	20	21.960356	0.169	0.2487749	-0.079775	-47.20408	1
11	10	21.960356	0.019	0.1020148	-0.083015	-436.9202	1
12	10	11.847673	0.496	0.3672705	0.1287295	25.953535	1
13	2.5	11.847673	0.11	0.0725959	0.0374041	34.003699	1

Alluvial Soil

Data Description:

X Variable: Electrolyte concentration (mmolc/litre)

Xmin: 2.5 Xmax: 640 Xrange: 637.5
Xmean: 128.82352941 Xstd: 201.82200862

Y Variable: ESP (%)

Ymin: 0 Ymax: 36.524057382 Yrange: 36.524057382
Ymean: 21.280771364 Ystd: 12.314208534

Z Variable: RKsat (Ratio)

Zmin: 0.002 Zmax: 1 Zrange: 0.998
Zmean: 0.4972352941 Zstd: 0.3983987527

Initial values for the parameters:

Parameter	Value
<i>a</i>	0.3
<i>b</i>	0.7
<i>g</i>	5
<i>m</i>	5
<i>s</i>	15.466
<i>l</i>	-58.038
<i>f</i>	0.3

Non-linear regression output:

Procedure	Minimization	Iterations			
Lev-Marq	Least Squares	70			
r ² Coef Det	DF Adj r ²	Fit Std Err			
0.9854333923	0.9708667846	0.0598400046			
Source	Sum of Squares	DF	Mean Square	F Statistic	P>F
Regr	1.9379478	6	0.3229913	90.2002	0.00000
Error	0.028646609	8	0.0035808261		
Total	1.9665944	14			

Parameters produced:

Parm	Value	Std Error	t-value	95.00% Confidence Limits		P> t
<i>a</i>	0.78597796	5.069202977	0.155049613	-10.9036251	12.47558097	0.88062
<i>b</i>	0.685527547	2.144418018	0.319679997	-4.25950926	5.630564357	0.75740
<i>g</i>	0.344604321	9.07655386	0.037966427	-20.5859664	21.27517503	0.97064
<i>m</i>	12.66964553	39.35630372	0.321921632	-78.0861535	103.4254445	0.75576
<i>s</i>	31.2852856	34.27308418	0.912823761	-47.7485881	110.3191593	0.38802
<i>l</i>	-140.036775	182.4669325	-0.76746385	-560.806275	280.7327256	0.46485
<i>f</i>	0.349753398	12.6451174	0.027659166	-28.8099396	29.50944637	0.97861

Model precision:

XYZ	X Value	Y Value	Z Value	Z Predict	Residual	Residual %	Weights
1	160	36.524057	0.719	0.7457926	-0.026793	-3.726368	1
2	160	21.960356	1	0.9820847	0.0179153	1.79153	1
3	160	11.847673	1	1	0	0	1
4	160	0	1	1	0	0	1
5	80	36.524057	0.39	0.290903	0.099097	25.409498	1
6	40	36.524057	0.104	0.1096741	-0.005674	-5.455863	1
7	40	21.960356	0.401	0.4570199	-0.05602	-13.97005	1
8	40	11.847673	0.753	0.7577039	-0.004704	-0.624682	1
9	20	36.524057	0.002	0.0469067	-0.044907	-2245.334	1
10	20	21.960356	0.213	0.2597425	-0.046742	-21.94481	1
11	10	21.960356	0.092	0.1469051	-0.054905	-59.67941	1
12	10	11.847673	0.482	0.4088263	0.0731737	15.181257	1
13	5	21.960356	0.087	0.0848434	0.0021566	2.4788003	1
14	2.5	21.960356	0.007	0.0502684	-0.043268	-618.1201	1
15	2.5	11.847673	0.203	0.1908422	0.0121578	5.9890658	1

Appendix K: The new GCSM Function Code Incorporated Manually into UNSATCHEM

On **Wed, 27/5/09**, **Jiri Simunek** <Jiri.Simunek@ucr.edu> wrote:

From: Jiri Simunek <Jiri.Simunek@ucr.edu>
Subject: RE: RE: from Younes Ezlit (Toowoomba)
To: "younes ezlit" <yezlit@yahoo.com>
Received: Wednesday, 27 May, 2009, 11:21 AM

Younes,

I have modified the code based on your suggestions. I have commented out the old code. Thus at present I have the following:

At the input:

```
lYounes=.true.
if(lYounes.and.iScreenInput.eq.1) then
  write(*,*) "g="
  read(*,*) RedKPar(1)
  write(*,*) "m="
  read(*,*) RedKPar(2)
c   write(*,*) "c1="
c   read(*,*) RedKPar(1)
c   write(*,*) "c2="
c   read(*,*) RedKPar(2)
c   write(*,*) "c3="
c   read(*,*) RedKPar(3)
  write(*,*) "Mont. fraction="
  read(*,*) RedKPar(4)
  write(*,*) "n="
  read(*,*) RedKPar(5)
c   write(*,*) "n1="
c   read(*,*) RedKPar(5)
c   write(*,*) "n2="
c   read(*,*) RedKPar(6)
c   write(*,*) "n3="
c   read(*,*) RedKPar(7)
  write(*,*) "ESP1(1.24)="
  read(*,*) RedKPar(8)
  write(*,*) "ESP2(11.63)="
  read(*,*) RedKPar(9)
c   write(*,*) "ESP Lipit 1 (25.)="
c   read(*,*) RedKPar(10)
  RedKPar(10)=100.
c   write(*,*) "ESP Limit 2 (50.)="
c   read(*,*) RedKPar(11)
end if
```

And in the calculation module:

```
*   Hydraulic conductivity reduction
if(ChPar(4,M).le.0.) lKRed=.false.
if(lKRed) then
  ssConc=Conc(1,i)+Conc(2,i)+Conc(3,i)+Conc(4,i)
  ESP=0.
  if(ChPar(4,M).gt.0.) ESP=XConc(3,i)/ChPar(4,M)*100.
```

```

Clay=.1
ESP1=1.24
ESP2=11.63
if(ESP.le.25.) then
  c=35.
  an=1.
else if(ESP.gt.25..and.ESP.lt.50.) then
  c=932.
  an=2.
else if(ESP.ge.50.) then
  c=25000.
  an=3.
end if
AESP=amax1(ESP-(ESP1+ESP2*log10(ssConc)),0.01)
d=0.
if(ssConc.lt.300.) d=356.4*ssConc**(-0.5)+1.2
if(ssConc.eq.0.) d=1.e10
if(lYounes) then
  Clay=RedKPar(4)
  ESP1=RedKPar(8)
  ESP2=RedKPar(9)
  ESP3=RedKPar(10)
c   ESP4=RedKPar(11)
  an=RedKPar(5)
  if(ESP.le.ESP3) then
    g1=RedKPar(1)
    xml=RedKPar(2)
    c=g1*exp(xml*(ESP/100.))
  end if
c   if(ESP.le.ESP3) then
c     c=RedKPar(1)
c     an=RedKPar(5)
c   else if(ESP.gt.ESP3.and.ESP.lt.ESP4) then
c     c=RedKPar(2)
c     an=RedKPar(6)
c   else if(ESP.ge.ESP3) then
c     c=RedKPar(3)
c     an=RedKPar(7)
c   end if
  AESP=amax1(ESP-(ESP1+ESP2*log(ssConc)),0.01)
  d=0.
  if(ssConc.lt.300.) d=356.4*ssConc**(-0.5)-20.5767
  if(ssConc.eq.0.) d=1.e10
end if
xx=Clay*3.6e-4*AESP*d
xpH=1.
if(pH.gt.6.83) xpH=3.46-0.36*pH
if(pH.gt.9.33) xpH=0.1
red(i)=amax1((1.-c*xx**an)/(1.+c*xx**an))*xpH,0.00001)
red(i)=amin1(1.,red(i))
if(red(i).lt.xRed) xRed=red(i)    ! Only for print
end if

```